UNIVERSITÀ DELLA CALABRIA

Facoltà di Farmacia e Scienze della Nutrizione e della Salute
Dipartimento Farmaco-Biologico
Dottorato di Ricerca in:
"Biochimica Cellulare ed Attività dei Farmaci in Oncologia"
Campo di Ricerca MED/04-PATOLOGIA GENERALE
XXII Ciclo

Farnesoid X Receptor, through the binding with Steroidogenic Factor 1 Responsive Element, inhibits aromatase expression in tumor Leydig cells.

Docente Tutor

Ch.mo Prof. Sebastiano ANDO'

Coordinatore

Ch.mo Prof. Diego SISCI

Dottorando

Dott. Rocco MALIVINDI

ANNO ACCADEMICO 2008-2009

INDEX

SUMMARY

Nuclear receptors (NRs) are ligand-activated transcription factors that have central roles in nearly every aspect of development and adult physiology [1]. This family contains 48 members in humans. Because of the importance of NR functions in different metabolic pathways, they have become attractive targets for drug discovery. The Farnesoid X Receptor (FXR) is a member of the nuclear receptor superfamily that regulates bile acid homeostasis. It is expressed in the liver and the gastrointestinal tract, but also in several non-enterohepatic tissues including testis. Recently, FXR was identified as a negative modulator of the androgen-estrogen-converting aromatase enzyme in human breast cancer cells.

In the present study we detected the expression of FXR in Leydig normal and tumor cell lines and in rat testes tissue. We found, in rat Leydig tumor cells, R2C, that FXR activation by the primary bile acid chenodeoxycholic acid (CDCA) or a synthetic agonist GW4064, through a SHP-independent mechanism, down-regulates aromatase expression in terms of mRNA, protein levels and its enzymatic activity. Transient transfection experiment, using vector containing rat aromatase promoter PII, evidenced that CDCA reduces basal aromatase promoter activity. Mutagenesis studies, electrophoretic mobility shift and chromatin immunoprecipitation analysis reveal that FXR is able to compete with SF-1 in binding to a common sequence present in the aromatase promoter region interfering negatively with its activity. Finally, the FXR activator CDCA exerts anti-proliferative effects on tumor Leydig cells at least in part through an inhibition of estrogen-dependent cell growth.

In conclusion our findings demonstrate that FXR ligands as aromatase inhibitors may represent a promising new therapeutic approach for Leydig cell tumors.

INTRODUCTION

In 1995, Forman et al. [1] and Seol et al. [2] isolated a novel cDNA that encoded an 'orphan' nuclear receptor. At the time it was named the farnesoid X receptor (FXR) on the basis of its weak activation by farnesol and juvenile hormone III [1], and it has been subsequently classified as NR1H4. There are two known FXR genes, which are commonly referred to as FXRα and FXRβ.

FXRα is conserved from humans to fish (teleost fish, *Fugu rubripes*) [3]. The single FXRα gene in humans and mice encodes four FXRα isoforms (FXRα1, FXRα2, FXRα3 and FXRα4) as a result of the use of different promoters and alternative splicing of the RNA [4,5] (Figure 1A, B).

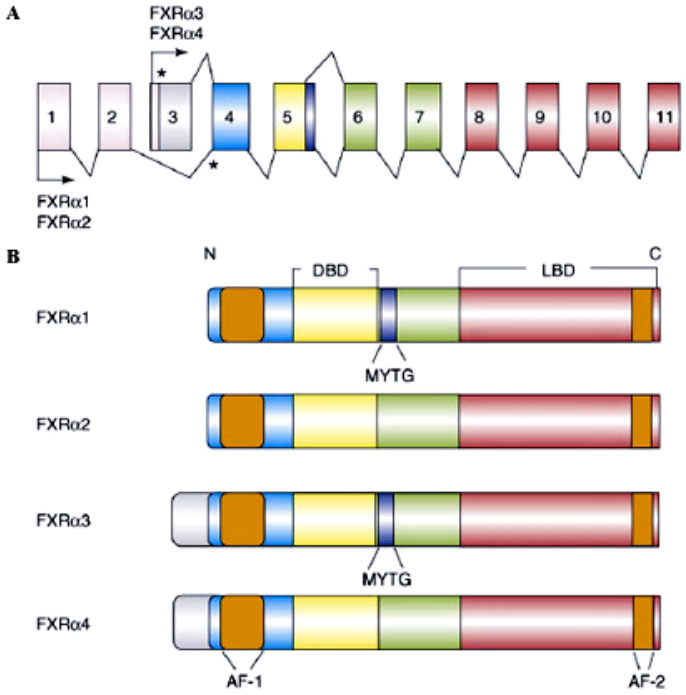

Figure 1. *Genomic organization and protein isoforms of FXRα. (A) Structure of the FXRα gene. The 11 exons of the mouse and human FXRα genes are indicated, along with the two functional promoters that initiate transcription at exons 1 or 3. Alternative splicing of the initial RNAs produces four mRNAs. The alternative splicing of the 12 bp at the 3 end of exon 5, which encodes the MYTG motif, is indicated by the dark blue box. Asterisks indicate the translational start sites (ATG). (B) The four FXR protein isoforms with the different domains color-coded. Abbreviations: AF, activation function; DBD, DNA-*

binding domain; LBD, ligand-binding domain. (Lee, F. Y.et al. (2006) Trends Biochem Sci 31,572-580)

FXRα3 and FXRα4 possess an estende N terminus, which encompasses the poorly defined 'Activation Function 1 domain' (AF-1). In addition, FXRα1 and FXRα3 have an insert of four amino acids (MYTG) immediately adjacent to the DNA-binding domain in a region referred to as the 'hinge domain' (Figure 1 B).

The second FXR gene, FXRβ, encodes a functional member of the nuclear receptor family in rodents, rabbits and dogs, but is a pseudogene in human and primates [6]. FXRβ has been proposed to be a lanosterol sensor, although its physiological function remains unclear.

FXRα is espresse mainly in the liver, intestine, kidney and adrenal gland, with much lower levels in adipose tissue [1,4,5]. Like many other non-steroid hormone nuclear receptors, regulates the expression of a wide variety of target genes involved in bile acid, lipid and glucose metabolism by binding either as monomer or as a heterodimer with the Retinoid X Receptor (RXR) to FXR response element (FXREs) (Figure 2) [7-9].

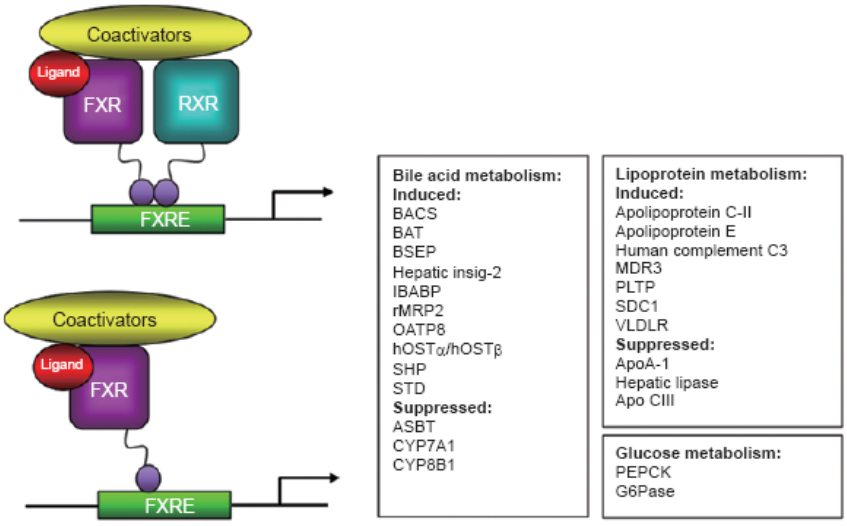

Figure 2 *FXR regulates a large number of target genes involved in bile acid, lipoprotein and glucose metabolisms. FXR binds to DNA either as a heterodimer with RXR or as a monomer to regulate the expression of various genes. (Wang, Y. D. et al. (2008) Cell Research* ***18****, 1087-1095)*

Typical FXREs consist of an inverted repeat (IR) of the canonical AGGTCA hexanucleotide core motif spaced by 0 bp (IR-0) [10] or 1 bp (IR-1) [8, 9].

IR-1 is the primary binding sequence for FXR. FXR regulates human intestinal bile acid binding protein (IBABP), small heterodimer partner (SHP), bile salt export pump (BSEP), BA-CoA:amino acid *N*-acetyltransferase (BAT) [11] and phospholipid transfer protein (PLTP) via IR-1 elements in the promoters of these genes [12-15]. Besides IR-1, other FXREs include IR-0, direct repeat (DR), everted repeat [16] of the core motif separated by eight nucleotides (ER-8) and monomeric binding sites [10, 17-20] (Table 1). In summary, FXR can bind to a variety of FXREs with varied affinities.

Table 1 Summary of related FXR information

Gene	NR1H4 12q23.3
Expression	Liver Small intestine Kidney Adrenals Vascular smooth muscle Adipose tissue Breast cancer
Natural agonists	**Primary bile acid:** CA, CDCA **Secondary bile acid:** LCA, DCA **Polyunsaturated fatty acids:** arachidonic acid; docosahexaenoic acid, and linolenic acid (endogenous and selective bile acid receptor modulators that specifically regulate expression of certain FXR targets) **Bile acid metabolites:** 26- or 25-hydroxylated bile alcohols **Oxysterols:** oxysterol 22(R)-hydroxysholesterol **Androsterone** (very weak activity) **The order of potency of these ligands:** 26- or 25-hydroxylated bile alcohols=CDCA>LCA=DCA>CA
Synthetic agonists	GW4064 (high-affinity agonist), 6ECDCA (semisynthetic bile acid), AGN29 **The potency of these ligands:** GW4064 and 6ECDCA are more potent than the bile acids AGN29 and AGN31 are FXR-selective ligands and 25-fold more potent than naturally occurring ligands
Antagonists	Guggulsterone, lithocholate, AGN34
Response elements	**IR-1:** GAGTTAaTGACCT GGGTGAaTAACCT GGGACAtTGATCCT AGGTCAaGTGCCT GGGTCAgTGACCC **DR-1:** AGAGCAnAGGGGA **ER-8:** TGAACTcttaaccaAGTTCA **Monomer binding site:** GATCCTTGAACTCT TGAACT

*(Wang, Y. D. et al. (2008) Cell Research **18**, 1087-1095)*

By binding to FXREs, FXR regulates many genes belonging to different metabolic pathways (Figure 2). Activation of FXR alters the expression of different groups of genes involved in BA homoeostasis, lipid metabolism,and glucose balance. FXR is the primary sensor of BAs. FXR activates the expression of short heterodimer partner (SHP) which interacts with other nuclear receptors preventing their activation [13, 20, 21].

Recently, new functions of FXR beyond its roles in metabolism were discovered in several nonenterohepatic tissues, including its control in regulating cell growth and carcinogenesis [23-26]. For instance, it has been demonstrated that FXR activation inhibits breast cancer cell proliferation and negatively regulates

aromatase activity reducing local estrogen production which sustains tumor growth and progression [25].

Estrogen dependency is also a feature of testicular tumor which is the most frequent solid malignant tumour diagnosed in young men (20- 40 years old) accounting for up to 20% of all malignancies diagnosed at this age. Ninety-five percent of all human testicular neoplasms arise from germinal cells whereas Leydig cell tumors are the most common tumors of the gonadal stroma [27]. The molecular basis of testicular cell malignant transformation is poorly defined. It has been reported that estrogen serum levels are elevated in patients with testicular germ cell cancer as a consequence of increased local estrogen production reflecting an higher aromatase activity present in Sertoli and Leydig cells [28]. Several studies on both rodents and humans indicate that prenatal, early post-natal and adult exposure to an excess of estrogens might have a central role in the mechanism leading to male reproductive tract malformations such as testicular and prostatic tumors [29]. The biological significance of estrogen-induced testicular tumorogenesis has been suggested by transgenic mice overexpressing aromatase and exhibiting enhancement of 17β-estradiol (E2) circulating levels [30]. About half of these male mice were infertile and/or had enlarged testis and showed Leydig cell hyperplasia and Leydig cell tumors [30]. Recently, we demonstrated aromatase and ERs expression in testis from patients affected by Leydigioma in which high estradiol levels in the presence of ERα could significantly contribute to tumor cell growth and progression [31]. Besides, we also reported that one of the molecular mechanisms determining Leydig cell

tumorogenesis is an excessive estrogen production that stimulates a short autocrine loop determining cell proliferation [32].

Aromatase activity is regulated primarly at the level of gene expression by tissue-specific promoters and is present in testicular somatic cells and along the maturative phases of male germ cells [33, 34]. A promoter proximal to the translation start site, called promoter II (PII) regulates aromatase expression in fetal and adult testis, R2C and H540 rat Leydig tumor cells, and in purified preparations of rat Leydig, Sertoli, and germ cells [35, 36]. Specific sequences seem to be mainly involved in aromatase expression: cyclic AMP (cAMP)-responsive element (CRE)-like sequences binding CREB/ATF protein families [37, 38] and a sequence containing an half-site binding nuclear receptors (AGGTCA) in position -90 binding steroidogenic factor 1 (SF-1) [39] which is essential for sex differentiation and development of gonads [40].

On the basis of all these observations, in this study we investigated in rat tumor Leydig cells, R2C whether FXR activation by specific ligand chenodeoxycholic acid (CDCA) or a synthetic agonist GW4064 may modulate aromatase expression and antagonize estrogen signalling, inhibiting testicular tumor growth and progression. We, for the first time, demonstrated that the molecular mechanism by which FXR ligands inhibit aromatase gene expression in R2C cells is mediated by a direct binding of FXR to SF-1 response element present in the aromatase promoter region.

MATERIALS AND METHODS

Reagents

Nutrient Mixture F-10 Ham, Dulbecco's Modified Eagle's Medium/Nutrient Mixture F-12 Ham (DMEM/F12), Dulbecco's Modified Eagle's Medium (DMEM), L-glutamine, penicillin, streptomycin, fetal bovine serum (FBS), horse serum (HS), phosphate-buffered saline, aprotinin, leupeptin, phenylmethylsulfonyl fluoride (PMSF), bovine serum albumin (BSA) and sodium orthovanadate were purchased by Sigma (Milan, Italy). TRIzol, Lipofectamine 2000 by Invitrogen (Carlsbad, CA, USA) and FuGENE 6 by Roche Applied Science (Indianapolis, IN, USA). TaqDNA polymerase, RETROscript kit, 100-bp DNA ladder, Dual Luciferase kit, TNT master mix, ImProm-II Reverse transcription system kit and TK Renilla luciferase plasmid were provided by Promega (Madison, WI, USA). SYBR Green Universa PCR Master Mix were provided by Bio-Rad, TaqMan rRNA Reagent kit by Applied Biosystems.

Antibodies against FXR, β-actin, GAPDH, Cyclin D1, Cyclin E and Lamin B by Santa Cruz Biotechnology (Santa Cruz, CA, USA), antibody against Aromatase by Serotec (Raleigh, NC, USA) and antibody against SF-1 kindly provided from Dr. K. Morohashi (National Institute Basic Biology, Myodaiji-cho, Okazaki, Japan). ECL system and Sephadex G-50 spin columns from Amersham Biosciences (Buckinghamshire, UK). [1β-^{3}H]androst-4-ene-3,17-dione, [γ^{32}P]ATP, and [^{3}H]thymidine from PerkinElmer (Wellesley, MA, USA). Salmon sperm DNA/protein A agarose by UBI (Chicago, IL, USA).

Plasmids

The plasmids containing different segments of the rat aromatase PII sequence ligated to a luciferase reporter gene [-1037/+94 (p-1037), -688/+94 (p-688), -688/+94 mut (p-688m) (SF-1 site mutant), -475/+94 (p-475) and -183/+94 (p-183)] were previously described [39]. FXR responsive reporter gene (FXRE-IR1) and FXR-DN (dominant negative) expression plasmids were provided from Dr. T.A. Kocarek (Institute of Environmental Health Sciences, Wayne State University, USA) [41]. FXR expression plasmid was provided from Dr. D.J. Mangelsdorf (Southwestern Medical Center, TX, USA). SF-1 expression plasmid and hCYP17 gene reporter were obtained from Dr. W. E. Rainey (Medical College of Georgia, USA). XETL plasmid is a construct containing an estrogen-responsive element from the *Xenopus* vitellogenin promoter, driving expression of the luciferase gene.

Cell Cultures and animals

Rat Leydig tumor cells (R2C) were cultured in Ham/F-10 supplemented with 15% HS, 2.5% FBS, and antibiotics. Mouse Leydig cells (TM3) were cultured in DMEM/F-12 supplemented with 5% HS, 2.5% FBS, and antibiotics. Human Cervix tumor cells (HeLa) and Hepatoma cells (HepG2) were cultured in DMEM supplemented with 10% FBS, 1% L-glutamine and antibiotics. The cells were starved in serum free medium (SFM) 24 hours before treatments. Male Fisher 344 rats (a generous gift of Sgma-Tau), 6 (FRN) and 24 (FRT) months of age, were used for studies. Twenty-four-month-old animals presented spontaneously developed Leydig cell tumors, which were absent in younger animals. Testes of

all animals were surgically removed by qualified, specialized animal care staff in accordance with the Guide for Care and Use of Laboratory Animals (NIH) and used for experiments.

Aromatase Activity Assay

The aromatase activity in subconfluent R2C cells culture medium was measured by the tritiated water release assay using 0.5 μM [1β-^{3}H]androst-4-ene-3,17-dione as substrate [42]. The incubations were performed at 37°C for 2 h under an air/CO2 (5%) atmosphere. The results obtained were expressed as pmol/h and normalized to mg of protein (pmol/h/mg protein).

Total RNA extraction and reverse transcription PCR assay

Total RNA was extracted from R2C and TM3 cells using TRIzol reagent and the evaluation of genes expression was performer by the reverse transcription-PCR method using a RETROscript kit. The cDNAs obtained were amplified by PCR using the following primers:

P450 aromatase	Forward	5'-AGCTATACTGAAGGAATCCACACTGT-3'
	Reverse	5'-AATCGTTTCAAAAGTGTAACCAGGA-3'
FXR	Forward	5'-TTTCTACCCGCAACAACCGGAA-3'
	Reverse	5'-GTGACAAAGAAGCCGCGAATGG-3'
rat-SHP	Forward	5'-CAGCCACCAGACCCACCACAA-3'
	Reverse	5'-GAGGCACCGGACCCCATTCTA-3'
mouse-SHP	Forward	5'-CGTCCGACTATTCTGTATGC-3'
	Reverse	5'-CTTCCTCTAGCAGGATCTTC-3'
L19	Forward	5'-GAAATCGCCAATGCCAACTC-3'
	Reverse	5'-ACCTTCAGGTACAGGCTGTG -3'

The PCR was performed for 25 cycles for P450 aromatase (94°C 1 min, 58°C 1 min, 72°C 2 min), 35 cycles for FXR (94°C 1 min, 65°C 1 min, 72°C 2 min), 28 cycles for SHP (94°C 1 min, 65°C 1 min, 72°C 2 min) and 25 cycles for L19 (94°C 1 min, 60°C 1 min, and 72°C 2 min) in the presence of 1µl of first strand cDNA, 1 µM each of the primers, 0.5 mM dNTP, *Taq* DNA polymerase (2 units/tube) and 2.2 mM magnesium chloride in a final volume of 25 µl. DNA quantity in each lane was analyzed by scanning densitometry.

Immunoblot analysis

R2C, TM3, HepG2 cells or total tissue of FRNT and FRTT were lysed in 500 µl of 50 mM Tris-HCl, 150 mM NaCl, 1% NP-40, 0.5% sodium deoxycholate, 2 mM sodium fluoride, 2 mM EDTA, 0.1% SDS, containing a mixture of protease inhibitors (aprotinin, PMSF, sodium ortho-vanadate) for protein extraction. Nuclear extracts were prepared as previously described [43]. Equal amount of proteins were resolved on 11% SDSpolyacrylamide gel, transferred to a nitrocellulose membrane and probed with FXR, Aromatase, Cyclin D1 and Cyclin E antibodies. To ensure equal loading all membranes were stripped and incubated with anti Lamin B antibody for nuclear extracts or anti-GADPH and anti-β-actin antibodies for total extracts. The antigen-antibody complex was detected by incubation of the membranes with peroxidasecoupled goat anti-mouse, goat anti-rabbit, or donkey anti-goat IgG and revealed using the ECL System. The bands of interest were quantified by Scion Image laser densitometry scanning program.

Immunofluorescence

R2C cells seeded on glass coverslips were treated with CDCA 50 and 100 μM for 24 h, washed with PBS and then fixed with 4% paraformaldehyde in PBS for 20 min at room temperature. Next, cells were permeabilized with 0.2% Triton X-100 in PBS for 5 min, blocked with 5% BSA for 30 min, and incubated overnight with anti-aromatase antibody (1:100) in PBS overnight at 4°C. The day after the cells were washed three times with PBS and incubated with the secondary antibody anti-mouse IgG-FITC (1:200) for 1 h at room temperature. To check the specificity of the immunolabelling the primary antibody was replaced by normal mouse serum (negative control). Immunofluorescence analysis was carried out on a OLYMPUS BX51 microscope using a 40x objective.

Transient transfection assay

R2C cells were transiently transfected using the FuGENE 6 reagent with FXR reporter gene (FXRE-IR1) in the presence or absence of FXR-DN or XETL plasmid. A set of experiments was performed transfecting rat aromatase PII constructs p-1037, p-688, p-475, p-183 and p-688m. HeLa cells were transiently cotransfected with CYP17 gene promoter and FXR or SF-1 expression plasmids. After transfection, R2C and Hela cells were treated with CDCA 50 μM for 24 h. Empty vectors were used to ensure that DNA concentrations were constant in each transfection. TK Renilla luciferase plasmid was used to normalize the efficiency of the transfection. Firefly and Renilla luciferase activities were measured by Dual Luciferase kit. The firefly luciferase data for each sample were

normalized based on the transfection efficiency measured by Renilla luciferase activity.

RNA interference (RNAi)

R2C cells were transfected with RNA duplex of stealth RNAi targeted rat SHP mRNA sequence 5'-ACUGAACUGCUUGAAGACAUGCUUU-3' (Invitrogen, Carlsbad, CA, USA), with RNA duplex of stealth RNAi targeted rat FXR mRNAsequence 5- UCUGCAAGAUCUACCAGCCCGAGAA-3 (Ambion), with RNA duplex of validate RNAi targeted rat aromatase mRNA sequence 5 GCUCAUCUUCCAUAACCAGGtt-3 (Invitrogen, Carlsbad, CA, USA) or with a stealth RNAi control to a final concentration of 50nM using Lipofectamine 2000 as recommended by the manufacturer. After 5 h the transfection medium was changed with SFM and 24 after transfection the cells were exposed to CDCA 50μM and 100μM or GW 3 μM for further 24 h. These transfected cells were used to examine the effects of silencing SHP and FXR gene expression on the aromatase mRNA and protein content and the effects of FXR and aromatase specific knock-down on cellular proliferation by [^{3}H]thymidine incorporation.

Electrophoretic mobility shift assay (EMSA)

Nuclear extracts from R2C cells were prepared as previously described [43]. The probe was generated by annealing single-stranded oligonucleotides, labeled with [γ^{32}P] ATP using T4 polynucleotide kinase, and purified using Sephadex G50 spin columns. The DNA sequences used as probe or as cold competitors are the following (nucleotide motifs of interest are underlined and mutations are shown as

lowercase letters):

SF-1 -AGGACCTGAGTCTCCCAAGGTCATCCTTGTTTGACTTGTA-

mutated SF-1 -TCTCCCAAtaTCATCCTTGT-

In vitro transcribed and translated SF-1 and FXR proteins were synthesized using the T7 polymerase in the rabbit reticulocyte lysate system. The protein-binding reactions were carried out in 20μL of buffer [20 mmol/L HEPES (pH 8), 1 mmol/L EDTA, 50 mmol/L KCl, 10 mmol/L DTT, 10% glycerol, 1 mg/mL BSA, 50 μg/mL poly(dI/dC)] with 50,000 cpm of labeled probe, 20 μg of R2C nuclear protein or an appropriate amount of SF-1 or FXR proteins and 5 μg of poly (dI-dC). The misture were incubated at room temperature for 20 min in the presence or absence of unlabeled competitor oligonucleotides. For experiments involving anti-SF-1 and anti-FXR antibodies, the reaction mixture was incubated with these antibodies at 4°C for 12 h before addition of labeled probe. The entire reaction mixture was electrophoresed through a 6% polyacrylamide gel in 0.25x Tris borate-EDTA for 3 h at 150 V.

Chromatin immunoprecipitation (ChIP) and ReChIP assays

R2C cells were treated with CDCA 50 μM for 1 h and then cross-linked with 1% formaldehyde and sonicated. Supernatants were immunocleared with salmon sperm DNA/protein A agarose for 1 h at 4°C. The precleared chromatin was immunoprecipitated with specific anti FXR or anti polymerase II antibodies and re-immunoprecipitated with anti SF-1 antibody. A normal mouse serum IgG was used as negative control. Pellets were washed as reported, eluted with elution buffer (1% SDS, 0.1 M NaHCO3) and digested with proteinase K. DNA was

obtained by phenol/chloroform/isoamyl alcohol (25:24:1) extractions and precipitated with ethanol; 3 μl of each sample were used for PCR amplification with the following primers flanking SF-1 sequence present in the P450arom PII promoter region: 5'- ATGCACGTCACTCTACCCACTCAA -3' and 5'- TAGCACGCAAAGCAGTAGTTTGGC -3'; upstream of the SF-1 site 5-TGATAACGACTCCAGCGTCTTCA-3 and 5-CAGAGGAGAACAGGAAGAGTGC-3. The amplification products were analyzed in a 2% agarose gel and visualized by ethidium bromide staining. Moreover, 5μl volume of each sample and input were used for real time PCR. PCR reactions were performed in the iCycler iQ Detection System (Biorad Hercules, CA, USA), using 0.1 μM of each primer, in a total volume of 50 μL reaction mixture following the manufacturer's recommendations. SYBR Green Universal PCR Master Mix (Biorad Hercules, CA, USA), with the dissociation protocol, was used for gene amplification. Negative controls contained water instead of DNA. Final results were calculated using the ΔΔCt method as explained above, using input Ct values instead of the 18S. The basal sample was used as calibrator.

[^{3}H]thymidine in corporation

R2C cells were treated with CDCA 50 and 100 μM for 24h and 48 h. For the last 6 hours, [^{3}H]thymidine (1μCi/ml) was added to the culture medium. After rinsing with PBS, the cells were washed once with 10% and three times with 5% trichloroacetic acid, lysed by adding 0.1 N NaOH and then incubated for 30 min at 37 °C. Thymidine incorporation was determined by scintillation counting. In a

set of experiment R2C cells were transiently transfected with FXR-DN expression plasmid 24 h before starting with the same treatments mentioned above.

Anchorage-independent soft agar growth assays

R2C cells were plated in 4 ml of Ham/F-10 with 0.5% agarose and 5% charcoal-stripped FBS, in 0.7% agarose base in six-well plates. Two days after plating, media containing hormonal treatments (androst-4-ene-3,17-dione, CDCA), was added to the top layer, and the appropriate media was replaced every two days. After 14 days, 150 µl of MTT was added to each well and allowed to incubate at 37° for 4 h. Plates were then placed at 4°C overnight and colonies > 50 µm diameter from triplicate assays were counted. Data are the mean colony number of three plates and representative of two independent experiments.

Statistical Analysis

Each datum point represents the mean ± S.D. of three different experiments. Statistical analysis was performed using ANOVA followed by Newman-Keuls testing to determine differences in means. $P<0.05$ was considered as statistically significant.

RESULTS

- ***FXR expression in normal and tumor testicular cells.***

We first aimed to evaluate, by Western Blotting analysis, the expression of FXR receptor in Leydig normal (TM3) and tumor (R2C) cell lines and in testes tissue from younger (FRNT) and older (FRTT) Fisher rats.

The latter group have a high incidence of spontaneous Leydig cell neoplasma [44, 45], a phenomenon not observed in younger animals.

Immunoblot analysis revealed the presence of a FXR-immunoreactive protein band at ~ 60kDa in all samples examined, particularly, FXR receptor seems to be more expressed in R2C cells with respect to TM3 and in FRTT with respect to its control FRNT (Figure 3).

Figure 3. *FXR expression in different cells lines. Western blot analysis of FXR was done on 50 μg of total proteins extracted from normal (TM3), tumor Leydig cells (R2C) and human hepatocytes cells (HepG2) or from tissues of normal (FRNT) and tumor (FRTT) Fisher rat testes. β-actin was used as a loading control.*

Human hepatocyte cells (HepG2) were used as a positive control for FXR expression. In R2C cells, incubation for 24 h with CDCA 50 and 100 μM, a natural ligand of FXR, increased the level of the receptor at both mRNA and protein levels. Because CDCA may also exert FXR-independent effects [46], the influence of GW4064, a synthetic FXR agonist, was also investigated. We observed that GW4064 (3μM) increased FXR mRNA and protein levels to a similar order of magnitude as CDCA (Figs 4 A & B).

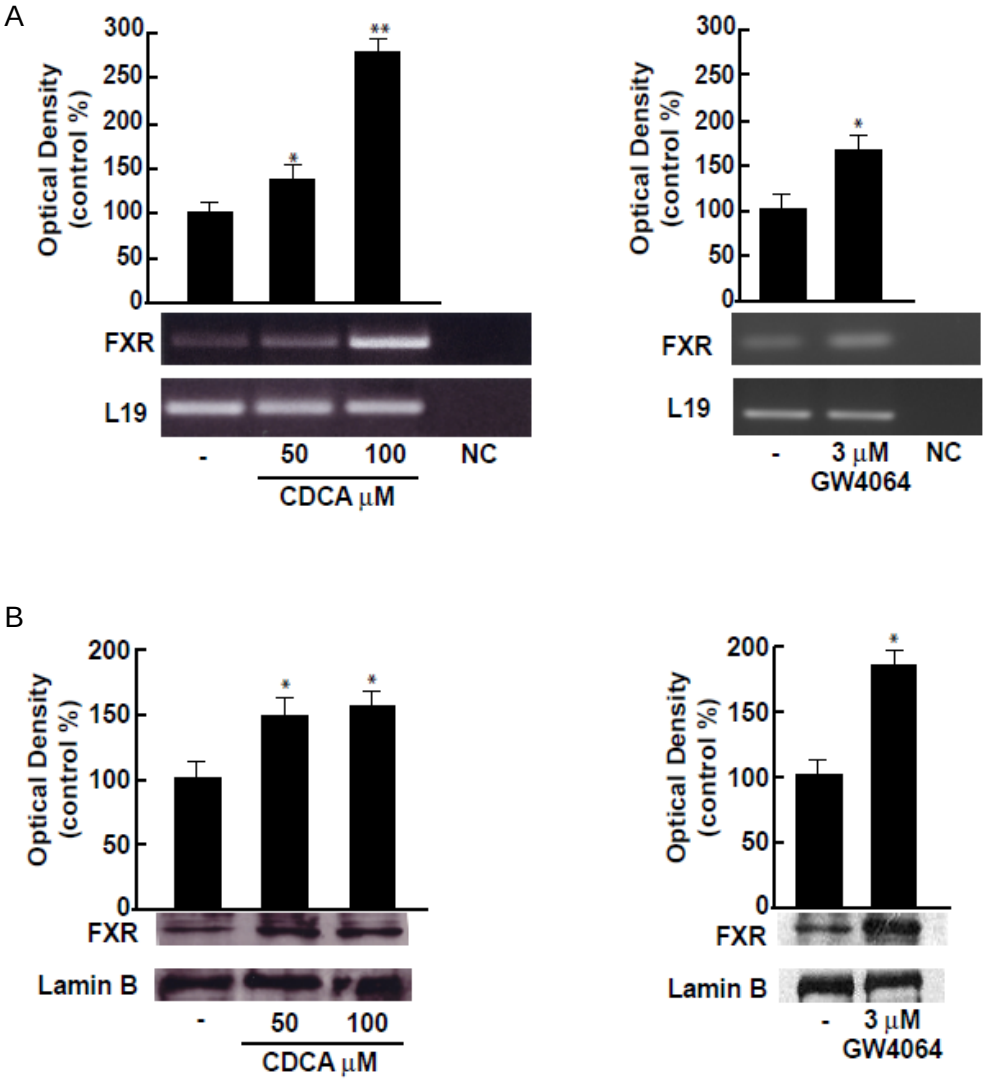

Figure 4. *FXR activation in R2C cells.* ***A****, Total RNA was extracted from R2C cells treated with vehicle (-) or CDCA 50 and 100 μM or GW4064 3 μM for 24 h and reverse transcribed. cDNA was subjected to PCR using primers specific for FXR or L19 (ribosomal protein). NC: negative control, RNA sample without the addition of reverse transcriptase. The histograms represent the means ± S.D. of three separate experiments in which band intensities were evaluated in terms of optical density arbitrary units and expressed as percentages of the control, which was assumed to be 100%. *p<0.05, **p<0.01 compared to vehicle.* ***B****, Nuclear proteins were extracted from R2C cells treated with vehicle (-) or CDCA 50 and 100 μM or GW4064 3 μM for 24 h and then western blotting analysis was performed using anti-FXR antibody. Lamin B was used as loading control. The histograms represent the means ± S.D. of three separate experiments in which band intensities were evaluated in terms of optical density arbitrary units and expressed as percentages of the control, which was assumed to be 100%. *p<0.05 compared to vehicle.*

Moreover, to assess the ability of CDCA and GW4064 to transactivate endogenous FXR, we transiently transfected R2C cells with FXR responsive

reporter gene (FXRE-IR1). As reported in Figure 5, CDCA and GW4064 induced a significant enhancement in transcriptional activation of the reporter plasmid even though to a higher extent under GW treatment, these data were completely reversed in the presence of FXR dominant negative plasmid FXR-DN.

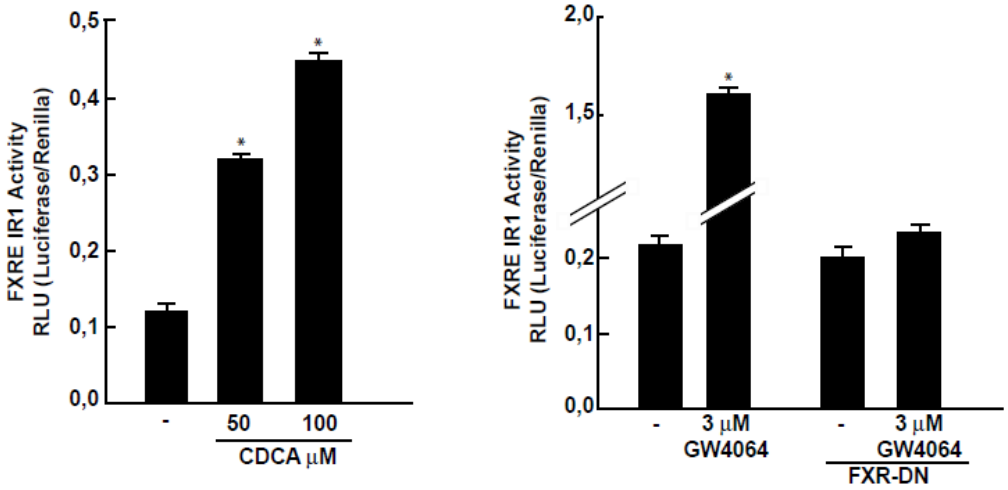

Figure 5. *CDCA and GW 4064 enhances FXR transactivation in R2C cells. R2C cells were transiently transfected with FXR reporter gene (FXRE-IR1) and treated with vehicle (-) or CDCA 50 µM, 100 µM and GW4064 3µM for 24 h or co-trasfected with FXR dominant negative FXR-DN and treated with vehicle(-) or GW4064 3µM . The values represent the means ± S.D. of three different experiments performed in triplicate. * p<0.01 compared to vehicle.*

➢ ***Inhibitory effects of FXR agonists on aromatase expression in R2C cells.***

Starting from previous findings showing that FXR activation represses aromatase expression in breast cancer cells [25] we investigated the ability of FXR agonists to modulate aromatase enzyme in R2C cells which have been shown to have high aromatase expression and activity [39]. Treatment with CDCA 50 and 100 μM for 24 h showed a down-regulation of aromatase mRNA and protein content in a dose related manner. Similar results were observed upon treatment with GW4064 (3μM) for 24 h (Figs. 6 A & 2B).

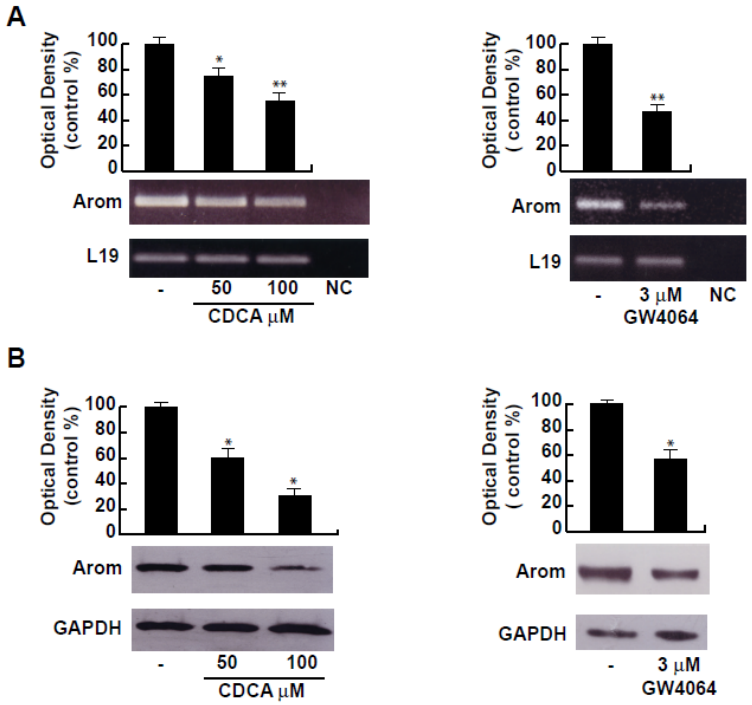

Figure 6. *Effects of CDCA on aromatase expression in R2C cells. **A**, Total RNA was extracted from R2C cells treated with vehicle (-), CDCA 50 and 100 μM or GW4064 3 μM for 24 h and reverse transcribed. cDNA was subjected to PCR using primers specific for P450 aromatase or L19. NC: negative control, RNA sample without the addition of reverse transcriptase. The histograms represent the means ± S.D. of three separate experiments in which band intensities were evaluated in terms of optical density arbitrary units and expressed as percentages of the control which was assumed to be 100%. *p<0.05, **p<0.01 compared to vehicle. **B**, Total proteins extracted from R2C cells treated with vehicle (-), CDCA 50 and 100 μM or GW4064 3 μM for 24 h were used for immunoblot analysis of aromatase. GAPDH was used as a loading control. The histograms representthe means ± S.D. of three separate experiments in which band intensities were evaluated in terms of optical density arbitrary units and*

*expressed as percentages of the control which was assumed to be 100%. *p<0.01 compared to vehicle.*

The down-regulatory effects of CDCA on the expression of aromatase was further confirmed by immunofluorescence analysis. The strong P450 aromatase immunoreactivity was detected in the cytoplasm as well as in the perinuclear region of untreated R2C cells and it was drastically decreased upon CDCA at the doses of 50 and 100 μM for 24 h (Figure 7).

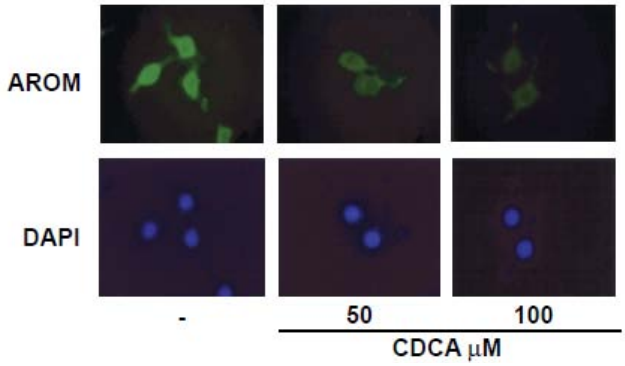

Figure 7 *Down-regulatory effects of CDCA on the expression of aromatase. R2C cells were treated with vehicle (-) or CDCA 50 and 100 μM for 24 h and aromatase expression was determined by immunofluorescence analysis. DAPI staining was used to visualized the cell nucleus. Each experiment is representative of at last 4 tests.*

Next, we evaluated the effects of CDCA on aromatase enzymatic activity by tritiated water release assay. As reported in Figure 8, exposure to CDCA 50 and 100 μM for 24 h reduced enzymatic activity in a dose dependent manner in R2C cells.

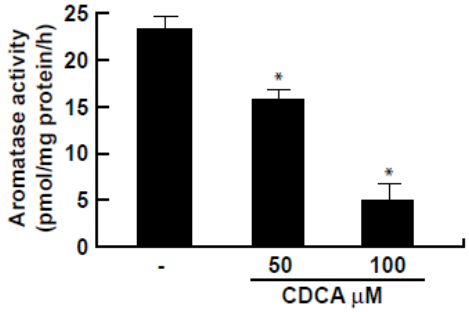

Figure 8. *Effects of CDCA on aromatase activity in R2C cells. R2C were cultured in the presence of vehicle (-) or 50 and 100 μM of CDCA for 24 h. Aromatase activity was performed as described in Materials and Methods. The results obtained were expressed as pmol [^{3}H]*

*H2O/h release and were normalized for mg protein (pmol/mg proteins/h). The values represent the means ± S.D. of three different experiments each performed with triplicate samples. *p<0.01 compared to vehicle.*

- ***SHP is not involved in the downregulatory effects induced by FXR ligand on aromatase.***

Induction of SHP expression is considered one of the canonical features of FXR transactivation. SHP has been shown to be expressed in the interstitial compartment of the adult testis, including steroidogenic Leydig cells [47].

We evidenced that SHP mRNA expression was significantly higher in R2C cells compared with very low levels detected in TM3 cell line, but administration of CDCA or GW4064 did not induce an increase of SHP mRNA in both cell lines. However, to explore the role of SHP in CDCA-mediated repression of aromatase gene, we knocked SHP by siRNA. SHP mRNA expression was effectively silenced as revealed by RT-PCR after 24, 48 and 72 h of siRNA transfection (Fig. 9 A). As shown in Figure 9B and 9C, silencing of the SHP gene failed to reverse the inhibition of aromatase expression induced by the specific FXR ligand in R2C cells ruling out any SHP involvement in the inhibitory effects of CDCA on aromatase expression.

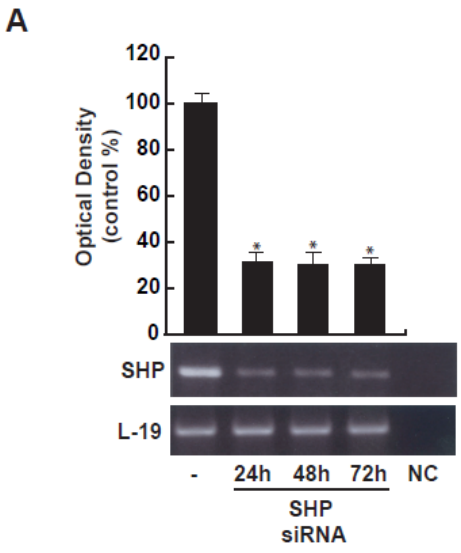

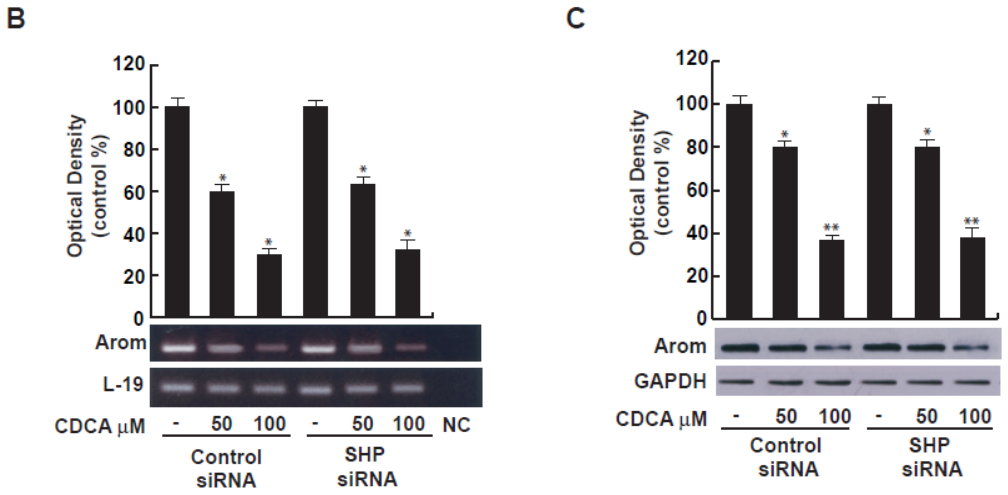

Figure 9. *SHP is not involved in CDCA-mediated down-regulation of aromatase. **A**, SHP mRNA expression in R2C cells which were not transfected (–) or transfected with RNA interference (RNAi) targeted rat SHP mRNA sequence as reported in Materials and Methods for 24, 48 and 72 h. L19 was used as loading control. NC: negative control, RNA sample without the addition of reverse transcriptase. The histograms represent the means ± S.D. of three separate experiments in which band intensities were evaluated in terms of optical density arbitrary units and expressed as percentages of the control, which was assumed to be 100%. *p<0.01 compared to vehicle. **B**, R2C cells were transfected with control siRNA or SHP siRNA for 24 h, and then treated with vehicle (-) or CDCA 50 and 100 μM for 24 h. Total RNA was extracted and RT-PCR analysis was performed to evaluate the expression of aromatase. L19 was used as loading control. NC: negative control, RNA sample without the addition of reverse transcriptase. The histograms represent the means ± S.D. of three separate experiments in which band intensities were evaluated in terms of optical density arbitrary units and expressed as percentages of the control, which was assumed to be 100%. *p<0.01 compared to vehicle. **C**, In the same experimental condition of B, total proteins were extracted and western blotting analysis was performed. GAPDH was used as loading control. The histograms represent the means ± S.D. of three separate experiments in which band intensities were evaluated in terms of optical density arbitrary units and expressed as percentages of the control which was assumed to be 100%. * p<0.05, ** p<0.01 compared to vehicle.*

➢ ***CDCA down-regulates aromatase promoter activity through SF-1 site.***

The aforementioned observations led us to ascertain if the down-regulatory effects of CDCA on aromatase expression were due to its direct inhibitory influence in regulating aromatase gene transcriptional activity. Thus, we transiently transfected in R2C cells plasmids containing different segments of rat PII aromatase (Fig. 10A). A significant reduction of promoter activity was observed in cells transfected with p-1037 and p-688, p-475 and p-183 exposed to CDCA 50 μM for 24 h. It is worth to note that construct p-688m bearing SF-1 mutated site displays significantly lower basal activity compared with the p-688 plasmid while no inhibitory effects were noticeable upon CDCA treatment (Fig. 10B).

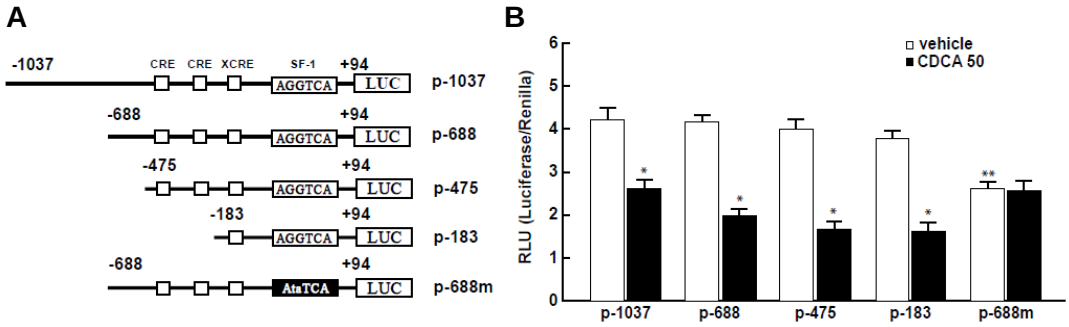

Figure 10. *Functional interaction between FXR and SF-1 site. **A**, Schematic map of the P450arom proximal promoter PII constructs used in this study. All of the promoter constructs contain the same 3' boundary (+94). The 5' boundaries of the promoter fragments varied from -1037 to -183. Three putative CRE motifs (5'-CRE at -335; 3'-CRE at -231; XCRE at -169) are indicated as square. The AGGTCA site (SF-1 RE at-90) is indicated as rectangle. A mutated SF-1 binding site (SF-1 mut) is present in p-688m (black rectangle). **B**, Aromatase transcriptional activity of R2C cells transfected with promoter constructs are shown. After transfection, cells were treated in the presence of vehicle (-) or CDCA 50 μM for 24h. These results represent the means ± S.D. of three different experiments performed in triplicate. *p<0.01 with respect to the vehicle, **p<0.01 with respect to the the control of p688.*

This latter result highlights the importance of the SF-1 binding site in the regulation of aromatase expression in the R2C cells and suggests that the inhibitory effect of CDCA requires AGGTCA sequence motif. SF-1 is closely

related to Liver Receptor Homologue-1 (LRH-1) and both proteins recognize the same canonical DNA motif [48]. However since LRH-1 is not expressed in R2C cells (Figure 11) we focused our attention on SF-1.

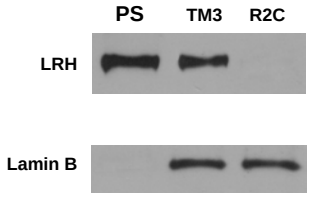

Figure 11. *Western Blotting of LRH-1 in nuclear extracts of TM3 and R2C cells. Transcribed and translated in vitro LRH- protein (lane 1) was used as positive control. Lamin B was used as loading control.*

To further demonstrate the functional interaction of FXR with SF-1 binding site, we transiently cotransfected Hela cells which do not express significant levels of SF-1 [49] with hCYP17 promoter construct containing multiple SF-1 response elements [50] with or without SF-1 plasmid in the presence of increasing amount of FXR expression plasmid. SF-1 expression vector strongly increased the CYP17 promoter activity, which was progressively reduced by FXR overexpression (Figure 12). We observed a similar results also in HeLa cells overexpressing FXR and treated with CDCA. These data support the competitive role of FXR in binding SF-1 site.

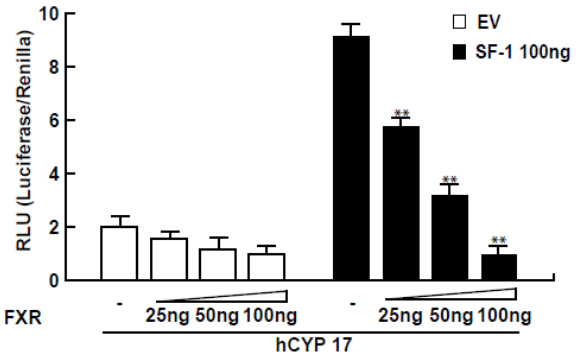

Figure 12.. *HeLa cells were transiently cotransfected with CYP17 promoter and with SF-1 plasmid or empty vector (EV) in the presence of increasing amount of FXR expression plasmid. These results represent the means ± S.D. of three different experiments*

*performed in triplicate. In each experiment, the activities of the transfected plasmids were assayed in triplicate transfections., **p<0.01 with respect to the SF-1 alone.*

- ***FXR protein binds to SF-1 RE in vitro and in vivo.***

On the basis of the evidence that the inhibitory effect of CDCA on aromatase requires the crucial presence of SF-1 RE, EMSA experiments were performed using the SF-1 motif present in aromatase promoter as probe. We observed the formation of a complex in nuclear extract from R2C cells (Figure 13A, lane 1), which was abrogated by 100 fold molar excess of unlabeled probe (Figure 13A, lane 2) demonstrating the specificity of the DNA binding complex. This inhibition was not longer observed when mutated oligodeoxyribonucleotide was used as competitor (Figure 13A, lane 3). CDCA 50 μM for 6 h induced an increase in DNA binding complex compared with control samples (Figure 13 A, lane 4). The inclusion of anti-SF-1 and anti-FXR antibodies in the reactions attenuated the specific bands suggesting the presence of SF-1 and FXR proteins in the complex (Figure 13A, lane 5 and 6). Using SF-1 and FXR proteins transcribed and translated in vitro, we obtained complexes migrating at the same level as that of R2C nuclear extracts (Figure 13A, lane 7 and 8). Competition binding studies revealed that both transcribed and translated SF-1 and FXR DNA binding complex (Figure 13B, lane 1 and 6) were abrogated by 100-fold molar excess of unlabeled probe (Figure 13B, lane 2 and 7). Finally the specificity of these bands was proved by the drastically attenuation of the complex in the presence of anti-SF-1 antibody, while the inclusion of anti-FXR antibody completely immunodepleted the binding (Figure 13B, lane 3 and 8). IgG did not affect either SF-1 or FXR complex formation (Figure 13B, lane 4 and 9).

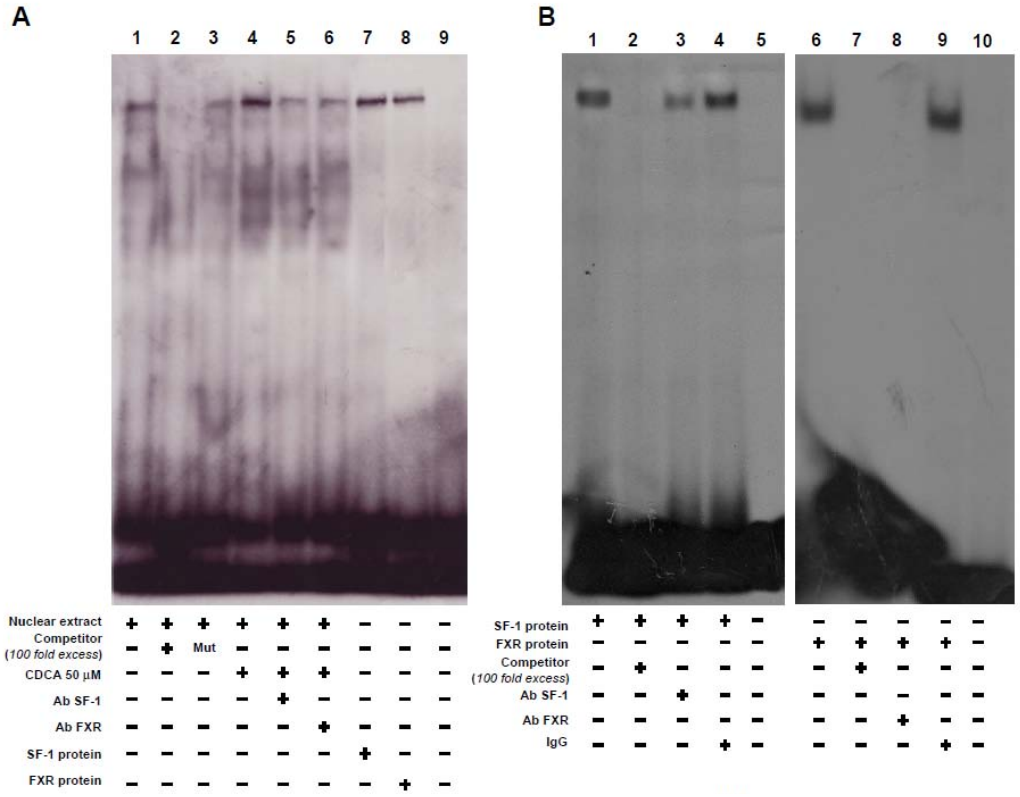

Figure 13. *FXR binds, in vitro, to SF-1site within aromatase promoter region.* ***A****, Nuclear extract from R2C cells were incubated with a double-stranded SF-1-specific sequence probe labeled with [γ32P]ATP and subjected to electrophoresis in a 6% polyacrylamide gel (lane 1). Competition experiments were performed adding as competitor a 100-fold molar excess of unlabeled probe (lane 2) or a 100-fold molar excess of unlabeled oligonucleotide containing a mutated SF-1 RE (lane 3). Lane 4, nuclear extracts from CDCA (50 µM) treated R2C cells. Lanes 5 and 6, CDCA-treated nuclear extracts were incubated with anti-SF-1 or anti-FXR antibodies respectively. We used as positive controls transcribed and translated in vitro SF-1 (lane 7) and FXR (lane 8) proteins. Lane 9 contains probe alone.* ***B****, SF-1 protein (1 µl) (lane 1)and FXR protein (1 µl) (lane 6) was incubated with a double-stranded SF-1 sequence probe labeled with [γ 32P] and subjected to electrophoresis in a 6% polyacrylamide gel. Competition experiments were performed adding as competitor a 100-fold molar excess of unlabeled probe (lane 2 & 7). SF-1 and for FXR proteins were incubated with anti-SF-1 antibody (lane 3) or anti-FXR antibody (lane 8) or IgG (lane 4 &9). Lanes 5 and 10 contain probe alone*

The interaction of FXR with the aromatase gene promoter was further investigated by ChIP assay. Using specific antibody against FXR and RNA-POL II, formaldehyde cross-linked protein-chromatin complexes were immunoprecipitated from R2C cells cultured with or without CDCA 50 and 100 µM. The resulting genomic DNA precipitated by using anti-FXR was then

reprecipitated with the anti SF-1 antibody. The results analyzed by PCR indicated that FXR was weakly constitutively bound to the aromatase promoter in untreated cells and this recruitment was increased upon CDCA treatment, which was correlated with a reduced association of RNA polymerase II. Interestingly, by Re-ChIP assay, we observed upon CDCA stimulation a significant reduction in SF-1 recruitment to the aromatase promoter. Next, the anti-FXR antibody did not immunoprecipitate a region upstream the SF-1 site located within the aromatase promoter gene (Figure 14 A). ChIP assay was quantified by real-time PCR as shown in Figure 14B.

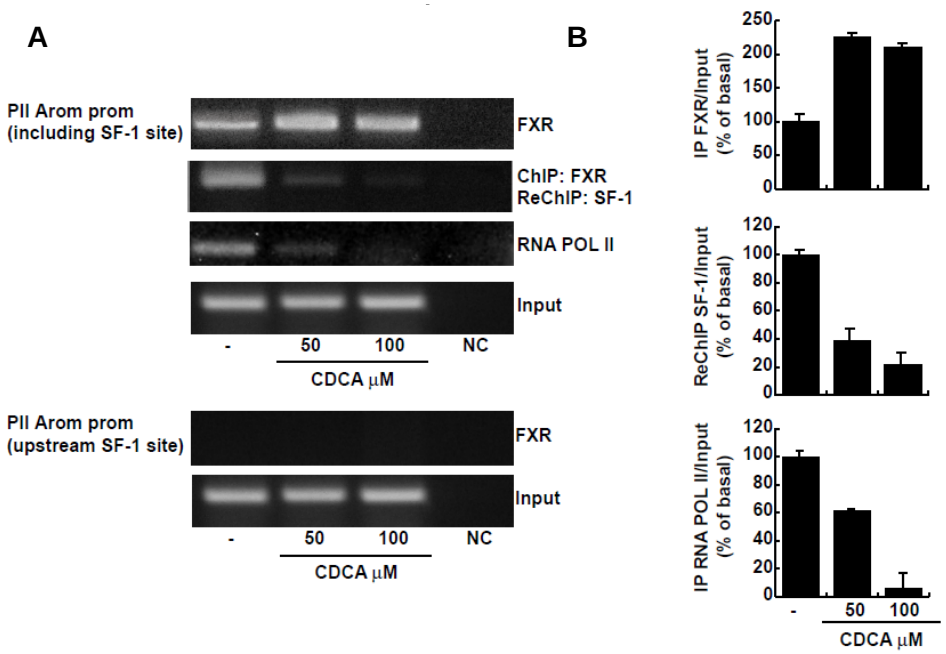

Figure 14. *FXR binds, in vivo, to SF-1 site within aromatase promoter region. **A**, R2C cells were treated in the presence of vehicle (-) or CDCA 50 and 100 μM for 1 hour, then crosslinked with formaldehyde, and lysed. The precleared chromatin was immunoprecipitated with anti-FXR, anti-RNA Pol II antibodies and normal mouse serum (NC) as negative control. Chromatinimmunoprecipitated with the anti-FXR antibody was re-immunoprecipitated with anti-SF-1 antibody. The PII promoter (prom) sequence including the SF-1 site and that located upstream the SF-1 site were detected by PCR with specific primers, as described in Materials and Methods and **B**, 5μl volume of each sample and input were used for real time PCR.*
To control input DNA, PII promoter was amplified from 30 μl initial preparations of soluble chromatin before immunoprecipitations. Similar results were obtained in multiple independent experiments.

➢ ***CDCA inhibits R2C cell proliferation through FXR activation.***

Finally, we evaluated the effect of CDCA on the growth of R2C cells by measuring changes in the rate of DNA synthesis (^{3}H thymidine incorporation). As shown in Figure 15 A, treatment with CDCA for 24 and 48 h reduced R2C cells proliferation in a dose and time dependent manner. The specific involvement of FXR in the antiproliferative response of R2C cells to CDCA was demonstrated by the evidence that such inhibitory effects were completely reversed in the presence of FXR dominant negative plasmid (Figure 15B) as well as after knocking down FXR with a specific siRNA (Figure 15C).

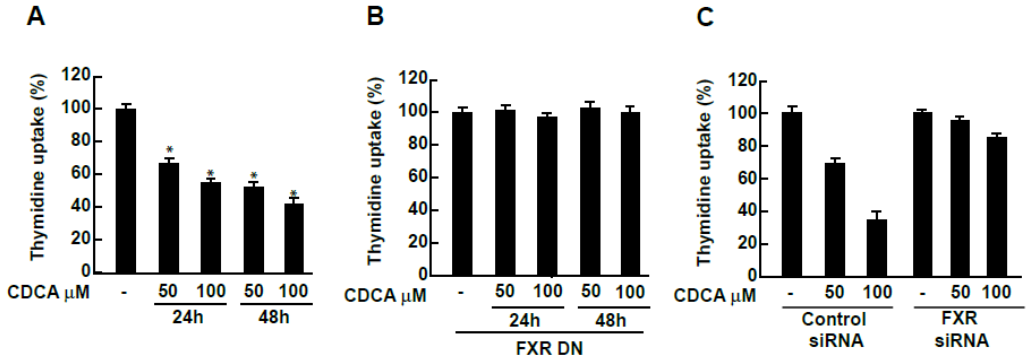

Figure 15. *CDCA effects on R2C cell proliferation.* ***A****, R2C cells were treated with vehicle(-) or CDCA 50 and 100 μM for 24 and 48h or* ***B****, transiently transfected with FXR dominant negative (FXR-DN) for 24 h or* ***C****, transfected with control siRNA or FXR siRNA for 24 h, and then treated as above reported. Thymidine incorporation assay was performed. The results represent the means ± S.D. of three different experiments each performed with triplicate samples, and expressed as percentage of growth vs control which was assumed to be 100%.*

It is well known that aromatase overexpression in tumor Leydig cells leads to a consequent excess of in situ estradiol production that sustains tumor cell growth and proliferation [30]. Since we demonstrated the ability of CDCA to down-regulate aromatase expression and activity in R2C cells, we wondered if CDCA

was able to antagonize the effect of an aromatizable androgen androst-4-ene-3,17-dione (AD) on estradiol/ERα signaling in R2C cells. To this aim we performed transient transfection experiment using XETL plasmid, which carries firefly luciferase sequences under the control of an estrogen response element upstream of the thymidine kinase promoter. As shown in Figure 16 we observed that the exposure to CDCA (50 μM) per se did not elicit any changes in luciferase activity but it completely reversed XETL activation induced by AD.

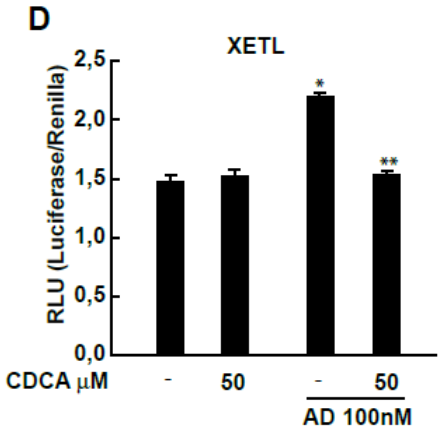

Figure 16. *Transient transfection experment with XETL promoter plasmid in R2C cells. Cells were treated with CDCA 50 μM in the presence or not of androst-4-ene-3,17-dione (AD) 100 nM for 24h. These results represent the means ± S.D. of three different experiments. In each experiment, the activities of the transfected plasmids were assayed in triplicate transfections. *p<0.01 with respect to the vehicle. **p<0.01 CDCA+AD treated vs AD alone.*

Moreover, we examined if CDCA was able to inhibit the effect of AD on R2C cell proliferation using two experimental approaches thymidine incorporation and anchorage independent soft agar growth assay. As expected, treatment with 100 nM of AD, through its conversion into estradiol, increased thymidine incorporation as well as the number of colonies present in soft agar (Figures 17A & B) concomitantly with an increased levels of cell cycle regulators ciclin D1 and cyclin E (Figure 17C). All these events were completely reversed by CDCA

exposure (Figures 17A, B & 17C). These data demonstrated that FXR ligand, through an inhibition of aromatase activity, is able to reduce the estrogen dependent tumor Leydig cells proliferation.

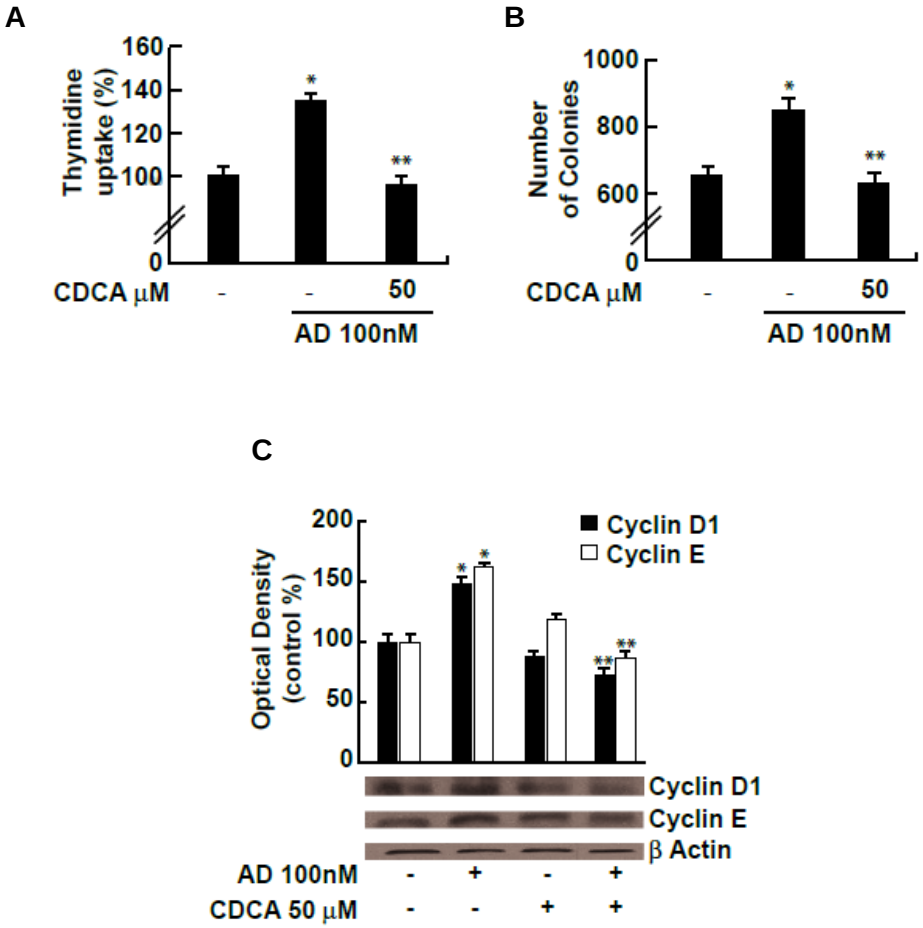

Figure 17. *CDCA inhibits the effect of AD on R2C cells **A**, R2C cells were treated with androst-4-ene-3,17-dione (AD) 100nM in the presence or not of CDCA 50 μM for 24h. Thymidine incorporation assay was performed. The results represent the means ± S.D. of three different experiments each performed with triplicate samples. *p<0.01 AD treated compared to vehicle. **p<0.01 CDCA+AD treated vs ADalone. **B**, R2C cells were seeded (10,000/well) in 0.5% agarose and the treated as described above. Cells were allowed to grow for 14 days and then the number of colonies >50μm were quantified and the results graphed. The results represent the means ± S.D. of three different experiments each performed with triplicate samples. *p<0.01 AD treated compared to vehicle. **p<0.01 CDCA+AD treated vs AD alone. **C**, Total proteins extracted from R2C cells treated with vehicle (-), Ad 100 nM, CDCA 50 μM and AD*CDCA for 24 h were used for immunoblot analysis of cyclin D1 and cyclin E. β-actin was used as a loading control. The histograms represent the means ± S.D. of three separate experiments in which band intensities were evaluated in terms of optical density arbitrary units and expressed as percentages of the control which was assumed to be 100%. *p<0.01 AD treated compared to vehicle. **p<0.01 CDCA+AD treated vs AD alone.*

DISCUSSION

FXR is highly expressed in the enterohepatic system where it drives bile acid absorption and secretion, lipid, glucid metabolism, and immunological response to intestinal bacterial overgrowth [51-55]. In hepatocytes, activation of FXR causes both feedback inhibition of cholesterol 7ahydroxylase (CYP7A1), the rate-limiting enzyme in bile acid biosynthesis from cholesterol, and activation of intestinal bile acid binding protein [56]. In addition, several observations suggest that FXR may also be involved in the control of steroid metabolism [25, 57]. Indeed, FXR activation results in the modulation of genes encoding androgen precursor-synthesizing enzymes, namely dehydroepiandrosterone sulfotransferase (SULT2A1), 5α-reductase and 3β-HSD (3β-hydroxysteroid dehydrogenase) in the liver [58, 59]. Recently, FXR was shown to inhibit androgen glucuronidation in prostatic cancer cell lines [60] and to suppress the activity of the aromatase in human breast cancer cells [25]. The enzyme aromatase coded by the gene CYP19, converts androgens in estrogens and is involved in the progression and growth of various estrogen hormonal-induced neoplasms.

For instance, overexpression of aromatase plays a significant role in the excessive estrogen production sustaining tumorogenesis in Leydig cells [30].

Here, we have documented that FXR is expressed in tissues of normal and tumor Fisher rat testis and in Leydig normal and tumor cell lines. In R2C cells, the FXR activators CDCA and GW4064, downregulate aromatase expression at both mRNA and protein level, together with the inhibition of its enzymatic activity.

One of the well-characterized mechanism by which FXR down-regulates gene expression is through induction of SHP [13] an atipica nuclear receptor lacking

both a DNA-binding domain and the NH2-terminal ligand independent activation domain [21]. This receptor interacts with other nuclear receptors, including Peroxisome Proliferator Activated Receptor (PPAR), RXR, Estrogen Receptor (ER) and Liver Receptor Homolog-1 (LRH-1), preventing their activation of gene transcription [13, 21]. In preadipocytes of cancerous breast tisuue, LRH-1 can regulate via an alternate promoter (II) the expression of aromatase induced by prostaglandin E2 [61, 62]. Moreover, SHP can inhibit LRH-1 induction of aromatase [63].

LRH-1 is most homologous to SF1, which is essential for sex differentiation and development of gonads [40], since they share a highly conserved DBD (DBD>90% identity) and a moderately conserved LBD (LBD 56% identity).

SHP is detected in the interstitial cells of the adult testis and its expression has been shown to be induced by FXR [47].

Our current study revealed that FXR activation does not induce SHP expression in Leydig tumor cells in which the inhibition of aromatase protein by CDCA occurs even when this nuclear receptor was knocked down. These results suggest that SHP is not required for the effect of FXR ligand to down-regulate aromatase expression, at least in R2C cells. On the basis of these observations, we focused our attention on the direct effect of FXR on the transcriptional activity of aromatase gene.

Distinctive tissues specific promoters are employed to direct the expression of aromatse mRNA driving from a single aromatase gene.

The promoter located immediately upstream of the transcriptional initiation site (PII) regulates aromatase expression in rat Leydig, Sertoli and germ cells and in

R2C Leydig tumor cells [35, 36]. A number of functional motifs have been identified in the PII aromatase promoter: three motifs resembling cAMP response elements (CRE) and an SF-1 binding site [39, 40].

We demonstrated by functional studies, using constructs containing different 5'-deleted regions of rat PII aromatase promoter, that CDCA treatment induces a decreased transcriptional activity. The observed inhibitory effect of CDCA was abrogated when a promoter fusion containing a mutated SF-1 element was employed. These results clearly suggest that the integrity of SF-1 sequence is a prerequisite for the down-regulatory effects of FXR ligand on aromatase promoter activity. These findings raise the possibility that FXR and SF-1 are competing for binding to a common site within this regulatory region. This assumption is further supported by the observation that FXR expression vector is able to abrogate the induction of SF-1 on human CYP17 promoter which contains multiple SF-1 response elements.

As a transcription factor, FXR binds to a specific consensus sequence (inverted repeat of 2 AGGTCA half-sites) either as a monomer or as a heterodimer with a common partner for NRs, as RXR to regulate the expression of various genes(4). Location of an AGGTCA sequence at the -90 position supports a possible binding of FXR to this promoter region, which we verified by EMSA experiments. Nuclear extracts from R2C cells treated with CDCA revealed an increase in DNA binding complex which was immunodepleted by both anti-SF-1 and anti-FXR antibodies suggesting how the two proteins are able to bind the AGGTCA sequence located in PII aromatase promoter. The specificity of the binding was proved by the attenuation, in the presence of anti-SF-1 and anti-FXR antibodies,

of the DNA complex observed using SF-1 and FXR transcribed and translated in a cell free system. In addition, the in vivo iinteraction between FXR and aromatase promoter was further supported by ChIP assay, where upon CDCA treatment we observed a reduced recruitment of RNA-POLII to this promoter addressing a negative transcriptional regulation mediated by FXR. All together these data suggest that FXR is able to compete with SF-1 in binding to a common sequence within the PII promoter of aromatase interfering negatively with its activity.

Finally, in our study we demonstrated that FXR activator CDCA induces growth inhibition in R2C cells which was reversed in the presence of FXR dominant negative as well as after knocking down FXR with a specific siRNA addressing a FXR dependency of this event.

However it is worth to mention, on the basis of our recent findings, that aromatase overexpression, in Leydig tumor cells, determines an excessive local estradiol production that is able to stimulate the expression of genes involved in cell cycle regulation sustaining cell proliferation [32].

Here, we evidenced the ability of CDCA to reverse the stimulatory effects of an aromatizable androgen androst-4-ene-3,17-dione(AD) at three different levels: 1) E2/ERα signaling; 2) an anchorage dependent and independent R2C cell growth proliferation; 3) expression of cell cycle regulators cyclin D1 and cyclin E.

The latter finding bring us to emphasize how the intrinsic property of FXR to inhibit R2C cell proliferation sound to be not linked to any substantial effect on cyclin D1 and cyclin E expression.

In conclusion, our results elucidate, for the first time, a new molecular mechanism through which FXR antagonizes estrogen signalling and inhibits Leydig tumor

growth and progression. addressing FXR ligands as potential pharmacological tools to be implemented in the novel strategies for testicular tumoral treatment. The identification of this molecular mechanism will be helpful in defining new therapeutic approaches for Leydig cell tumors.

REFERENCES

1. Forman BM, Goode E, Chen J, Oro AE, Bradley DJ, Perlmann T, Noonan DJ, Burka LT, McMorris T, Lamph WW, Evans RM, Weinberger C. (1995). Cell 81, 687–693

2. Seol W, Choi HS, Moore DD. (1995). Mol. Endocrinol. 9, 72–85

3. Maglich JM, Caravella JA, Lambert MH, Willson TM, Moore JT, Ramamurthy L. (2003). Nucleic Acids Res. 31, 4051–4058

4. Huber RM, Murphy K, Miao B, Link JR, Cunningham MR, Rupar MJ, Gunyuzlu PL, Haws TF, Kassam A, Powell F, Hollis GF, Young PR, Mukherjee R, Burn TC. (2002). Gene 290, 35–43

5. Zhang Y, Kast-Woelbern HR, Edwards PA. (2003). J. Biol. Chem. 278, 104–110

6. Otte K, Kranz H, Kober I, Thompson P, Hoefer M, Haubold B, Remmel B, Voss H, Kaiser C, Albers M, Cheruvallath Z, Jackson D, Casari G, Koegl M, Pääbo S, Mous J, Kremoser C, Deuschle U. (2003). Mol. Cell. Biol. 23, 864–872

7. Song CS, Echchgadda I, Baek BS, Ahn SC, Oh T, Roy AK, Chatterjee B. (2001). J Biol Chem 276, 42549-42556

8. Li J, Pircher PC, Schulman IG, Westin SK. (2005). J Biol Chem; 280:7427-7434

9. Ananthanarayanan M, Balasubramanian N, Makishima M, Mangelsdorf DJ, Suchy FJ. (2001). J Biol Chem; 276:28857-28865.

10. Song CS, Echchgadda I, Baek BS, Ahn SC, Oh T, Roy AK, Chatterjee B. (2001). J Biol Chem; 276:42549-42556.

11. Shibata M, Morizane T, Uchida T, Yamagami T, Onozuka Y, Nakano M, Mitamura K, Ueno Y. (1998). Lancet; 351:1773-1777.

12. Grober J, Zaghini I, Fujii H, Jones SA, Kliewer SA, Willson TM, Ono T, Besnard P. (1999). J Biol Chem; 274:29749-29754.

13. Goodwin B, Jones SA, Price RR, Watson MA, McKee DD, Moore LB, Galardi C, Wilson JG, Lewis MC, Roth ME, Maloney PR, Willson TM, Kliewer SA. (2000). Mol Cell; 6:517-526.

14. Pircher PC, Kitto JL, Petrowski ML, Tangirala RK, Bischoff ED, Schulman IG, Westin SK. (2003). J Biol Chem; 278:27703-27711.

15. Urizar NL, Dowhan DH, Moore DD. (2000). J Biol Chem; 275:39313-39317.

16. Huang W, Ma K, Zhang J, Qatanani M, Cuvillier J, Liu J, Dong B, Huang X, Moore DD. (2006). Science; 312:233-236.

17. Laffitte BA, Kast HR, Nguyen CM, Zavacki AM, Moore DD, Edwards PA. (2000). J Biol Chem; 275:10638-10647.

18. Anisfeld AM, Kast-Woelbern HR, Meyer ME, Jones SA, Zhang Y, Williams KJ, Willson T, Edwards PA. (2003). J Biol Chem; 278:20420-20428.

19. Kast HR, Goodwin B, Tarr PT, Jones SA, Anisfeld AM, Stoltz CM, Tontonoz P, Kliewer S, Willson TM, Edwards PA. (2002). J Biol Chem; 277:2908-2915.

20. Claudel T, Sturm E, Duez H, Torra IP, Sirvent A, Kosykh V, Fruchart JC, Dallongeville J, Hum DW, Kuipers F, Staels B. (2002). J Clin Invest; 109:961-971.

21. Seol W, Choi HS, Moore DD. (1996). Science 272, 1336-1339

22. Seol W, Hanstein B, Brown M, Moore DD. (1998). Mol Endocrinol 12, 1551-1557

23. Wang, Y. D., Chen, W. D., Moore, D. D. and Huang, W. D. (2008). Cell Research 18, 1087-1095

24. Journe, F., Laurent, G., Chaboteaux, C., Nonclercq, D., Durbecq, V., Larsimont, D., Body, J. J. (2008). Breast Cancer Res Treat 107, 49-61

25. Swales, K. E., Korbonits, M., Carpenter, R., Walsh, D. T., Warner, T. D., Bishop-Bailey, D. (2006). Cancer Res 66, 10120-10126

26. Modica S, Murzilli S, Salvatore L, Schmidt D R, Moschetta A. (2008). Cancer Res 68,9589-9594

27. Hawkins, C., Miaskowski, C. (1996). Oncol Nurs Forum 23, 1203-1211

28. Carroll, P. R., Whitmore, W. F. Jr., Herr, H. W., Morse, M. J., Sogani, P. C., Bajorunas, D., Fair, W. R., Chaganti, R. S. (1987). J Urol 137, 420-423

29. Bosland, M. C. (1996). Prog Clin Biol Res 394, 309-352

30. Fowler, K. A., Gill, K., Kirma, N., Dillehay, D. L., Tekmal, R. R. (2000). Am J Pathol 156, 347-353

31. Carpino, A., Rago, V., Pezzi, V., Carani, C., Andò, S. (2007). Eur. J. Endocrinol. 157, 239-44

32. Sirianni, R., Cimento, A., Malivindi, R., Mazzitelli, I., Andò, S., Pezzi, V. (2007). Cancer Res 67, 8368-8377

33. Aquila, S., Sisci, D., Gentile, M., Carpino, A., Middea, E., Catalano, S., Rago, V., Andò, S. (2003). Hum Reprod 18, 1650-1659

34. Inkster, S., Yue, W., Brodie, A. (1995). J Clin Endocrinol Metab 80, 1941-1947

35. Young, M., Lephart, E. D., McPhaul, M. J. (1997). J Steroid Biochem Mol Biol 63, 37–44

36. Lanzino, M., Catalano, S., Genissel, C., Ando', S., Carreau, S., Hamra, K., McPhaul, M. J. (2001). Biol Reprod 64, 1439-1443

37. Fitzpatrick, S. L., Richards, J. S. (1994). Mol Endocrinol 8, 1309–1319

38. Carlone, D. L., Richards, J. S. (1997). Mol Endocrinol 11, 292–304

39. Young, M., McPhaul, M. J. (1998). Endocrinology 139, 5082-5093

40. Parker, K. L., Shimmer, B. P. (1997). Endocr Rev 18, 361-377

41. Kocarek, T. A., Shenoy, S. D., Mercer-Haines, N. A., Runge-Morris, M. (2002). J Pharmacol Toxicol Methods 47, 177-187

42. Lephart, E. D. and Simpson, E .R. (1991). Methods Enzymol 206, 477–483

43. Anderws, N. C., and Faller, D. V. (1991). Nucleic Acids Res 19, 2499

44. Coleman, G. L., Barthold, W., Osbaldiston, G. W., Foster, S. J., Jonas, A. M. (1977). J Gerontol 32, 258–278

45. Jacobs, B.B., Huseby, R.A. (1967). J Natl Cancer Inst 39, 303–309

46. Nguyen, A., Bouscarel, B. (2008). Cellular Signalling 20, 2180-2197

47. Volle, D. H., Duggavathi, R., Magnier, B. C., Houten, S. M., Cummins, C. L., Lobaccaro, J.M., Verhoeven, G., Schoonjans, K., Auwerx, J. (2007). Genes Dev 21, 303-315

48. Pezzi V., Sirianni R., Chimento A., Maggiolini M., Bourguiba S., Delalande C., Carreau S., Andò S., Simpson E.R., Clyne C. (2004). Endocrinology 145, 2186-2169

49. Sugawara, T., Holt, J. A., Kiriakidou, M., Strauss, J. F. (1996). Biochemistry 35, 9052-9059

50. Hanley, N. A., Rainey, W. E., Wilson, D. I., Ball, S. G., Parker, K. L. (2001). Mol Endocrinol 15, 57-68

51. Makishima, M., Okamoto, A. Y., Repa, J. J., Tu, H., Learned, R. M., Luk, A., Hull, M.V., Lustig, K. D., Mangelsdorf, D. J., Shan, B. (1999). Science 284, 1362–3.

52. Kalaany, N.Y. and Mangelsdorf, D.J. (2006). Annu Rev Physiol 68, 159–191

53. Modica, S., Moschetta, A. (2006). FEBS Lett 580, 5492-5499

54. Jung, D., Inagaki, T., Gerard, R. D., Dawson, P. A., Kliewer, S. A., Mangelsdorf, D. J., Moschetta, A. (2007). J Lipid Res 48, 2693-2700

55. Inagaki, T., Moschetta, A., Lee, Y. K., Peng, L., Zhao, G., Downes, M., Yu, R. T., Shelton, J. M., Richardson, J. A., Repa, J. J., Mangelsdorf, D. J., Kliewer, S. A. (2006). Proc Natl Acad Sci U S A 103, 3920-3925

56. Chiang, J. Y. (2002). Endocr Rev 23, 443-463

57. Lee, F. Y., Lee, H., Hubbert, M. L., Edwards, P. A., Zhang, Y. (2006). Trends Biochem Sci 31,572-580

58. Pircher, P. C., Kitto, J. L., Petrowski, M. L., Tangirala, R. K., Bischoff, E. D., Schulman, I. G., Westin, S. K. (2003). J Biol Chem 278, 27703-27711

59. Miyata, M., Matsuda, Y., Tsuchiya, H., Kitada, H., Akase, T., Shimada, M., Nagata, K., Gonzalez, F. J., Yamazoe, Y. (2006). Drug Metab Pharmacokinet 21, 315-323

60. Kaeding, J., Bouchaert, E., Bélanger, J., Caron, P., Chouinard, S., Verreault, M., Larouche,O., Pelletier, G., Staels, B., Bélanger, A., Barbier, O. (2008). Biochem J 410, 245-253

61. Clyne, C. D., Speed, C. J., Zhou, J., Simpson, E. R. (2002). J Biol Chem 277, 20591-20597

62. Zhou, J., Suzuki, T., Kovacic, A., Saito, R., Miki, Y., Ishida, T., Moriya, T., Simpson, E.R., Sasano, H., Clyne, C.D. (2005). Cancer Res 65, 657-663

63. Kovacic, A., Speed, C. J., Simpson, E. R., Clyne, C. D. (2004). Mol Endocrinol 18, 252-259

Scientific Publications Performed during the Program

1. Catalano S., ***Malivindi R.***, Giordano C., Gu G., Panza S., Bonofiglio D., Lanzino M., Sisci D., Panno M.L., Andò S. *"Farnesoid X Receptor through its binding to Steroidogenic Factor 1 responsive element inhibits aromatase expression in tumor Leydig cells"*. The Journal Of Biological Chemistry 2009. In revision.

2. Catalano S., Barone I., Giordano C., Rizza P., Qi H., Gu G., ***Malivindi R.***, Bonofiglio D. and Andò S. *"Rapid estradiol/ERα signaling enhances aromatase enzymatic activity in breast cancer cells"*. Mol Endocrinol, 23(10):1634–1645, Oct 2009.

3. De Amicis F., Zupo S., Panno M.L., ***Malivindi R***., Giordano F., Barone I., Mauro L., Fuqua S.A.W., Andò S., *"Progesterone Receptor B recruits a repressor complex to a half-PRE site of the Estrogen Receptor α gene promoter"*. Mol Endocrinol., 23(4):454-65, Apr 2009.

4. Catalano S., Giordano C., Rizza P., Gu G., Barone I., Bonofiglio D., Giordano F., ***Malivindi R.***, Gaccione D., Lanzino M., De Amicis F., Andò S., *"Evidence that leptin through STAT and CREB signaling enhances cyclin D1 expression and promotes human endometrial cancer proliferation*". J Cell Physiol, 218(3):490-500, Mar2009.

5. Sirianni R., Chimento A., ***Malivindi R***., Mazzitelli I., Andò S., Pezzi V., *"Insulin-Like Growth Factor-I, Regulating Aromatase Expression through Steroidogenic Factor 1, Supports Estrogen-Dependent Tumor Leydig Cell Proliferation"*. Cancer Research, 67(17): 8368 – 8377, Sep 2007.

Comunications in National and International Conferences

1. Metzger D., Duteil D., Chambon C., Ali F., **Malivindi R.,** Zoll J. and Chambon P. *The Transcriptional Intermediary Factor TIF2 prevents mitochondrial uncoupling in skeletal muscle myocytes of adult mice*. EMBO Conference on Nuclear Receptors, Dubrovnik, Croatia, Sep 2009

2. Duteil D., Chambon C., Ali F., **Malivindi R.,** Zoll J., Chambon P. Metzger D. *The nuclear receptor coregulator TIF2 regulates energy homeostasis by controlling mitochondrial activity in skeletal muscle myocytes.* EMBO Conference on Nuclear Receptors, Dubrovnik, Croatia, Sep 2009

3. ***Malivindi R.***, Panza S., Gu G., Giordano C., Catalano S., Andò S. *"Inhibitory role of Farnesoid X Receptor ligand on aromatase expression in Leydig tumor cells"*. XII WORKSHOP on APOPTOSIS IN BIOLOGY AND MEDICINE. Parghelia (VV), Calabria, Italy, May, 2009

4. ***Malivindi R.***, Panza S., Gu G., Giordano C., Catalano S., Andò S. *"Inhibitory role of Farnesoid X Receptor ligand on aromatase expression in Leydig tumor cells"*. ASIP Annual Meeting, New Orleans (LA), April 2009

5. Andò S., ***Malivindi R***., Rizza P., Gu G., Catalano S., "*Inhibitory role of Farnesoid X Receptor ligands aromatase expression in Leydig tumor cells*". "90th Endocrine Society's Meeting", San Francisco, California, USA, 2008.

6. Andò S., ***Malivindi R***., Rizza P., Gu G., Catalano S., "*Farnesoid X Receptor ligand down-regulates aromatase expression in Leydig tumor cells"*. ASIP 2008 San Diego, California, USA, 2008

7. De Amicis F., Zupo S., ***Malivindi R.***, Ando' S., *"Evidences that progesterone receptor B decreases estrogen receptor gene expression through its interaction to a half-PRE site at estrogen receptor gene promoter"*. "30th San Antonio Breast Cancer Symposium", San Antonio, 2007.
8. De Amicis F., Zupo S., ***Malivindi R.***, Ando' S., *" Progesterone Receptor B recruits a repressor complex to a half-PRE site of the Estrogen Receptor α gene promoter"*. "X Congress AIBG", Torino, Italy, 2007.
9. Sirianni R., Chimento A., ***Malivindi R.***, Ando' S., Pezzi V., " *Cyclooxygenase-2 (COX-2) inhibit proliferation of tumor Leydig cells"*. "89th Endocrine Society's Meeting", Toronto, 2007.

FARNESOID X RECEPTOR, THROUGH THE BINDING WITH STEROIDOGENIC FACTOR 1 RESPONSIVE ELEMENT, INHIBITS AROMATASE EXPRESSION IN TUMOR LEYDIG CELLS

Stefania Catalano[1*], Rocco Malivindi[1*], Cinzia Giordano[1,3], Guowei Gu[1], Salvatore Panza[1], Daniela Bonofiglio[1], Marilena Lanzino[1], Diego Sisci[1], Maria Luisa Panno[2], Sebastiano Andò[2,3]

Departments of [1]Pharmaco-Biology and [2]Cell Biology, and [3]Centro Sanitario, University of Calabria 87030 Arcavacata di Rende (CS), Italy.

***** Stefania Catalano and Rocco Malivindi contributed equally to this work

Running head**:** FXR regulates aromatase expression in Tumor Leydig cells.

Address correspondence to:Prof. Sebastiano Andò, Department of Cell Biology University of Calabria, Arcavacata di Rende (CS) 87030, ITALY. Tel: +39 0984 496201, Fax: +39 0984 496203; E-mail: sebastiano.ando@unical.it

The Farnesoid X Receptor (FXR) is a member of the nuclear receptor superfamily that regulates bile acid homeostasis. It is expressed in the liver and the gastrointestinal tract, but also in several non-enterohepatic tissues including testis. Recently, FXR was identified as a negative modulator of the androgen-estrogen-converting aromatase enzyme in human breast cancer cells.

In the present study we detected the expression of FXR in Leydig normal and tumor cell lines and in rat testes tissue. We found, in rat Leydig tumor cells, R2C, that FXR activation by the primary bile acid chenodeoxycholic acid (CDCA) or a synthetic agonist GW4064, through a SHP-independent mechanism, down-regulates aromatase expression in terms of mRNA, protein levels and its enzymatic activity. Transient transfection experiment, using vector containing rat aromatase promoter PII, evidenced that CDCA reduces basal aromatase promoter activity. Mutagenesis studies, electrophoretic mobility shift and chromatin immunoprecipitation analysis reveal that FXR is able to compete with SF-1 in binding to a common sequence present in the aromatase promoter region interfering negatively with its activity. Finally, the FXR activator CDCA exerts anti-proliferative effects on tumor Leydig cells at least in part through an inhibition of estrogen-dependent cell growth.

In conclusion our findings demonstrate that FXR ligands as aromatase inhibitors may represent a promising new therapeutic approach for Leydig cell tumors.

The Farnesoid X Receptor (FXR, NR1H4) is a member of the nuclear receptor superfamily of ligand-dependent transcription factors, normally produced in the liver and the gastrointestinal tract, where it acts as a bile acid sensor (1-3). FXR regulates the expression of a wide variety of target genes involved in bile acid, lipid and glucose metabolism by binding either as monomer or as a heterodimer with the Retinoid X Receptor (RXR) to FXR response element (FXREs) (4-7). FXR induces the up-regulation of nuclear receptor SHP (Small Heterodimer Partner) which interacts with other nuclear receptors preventing their activation (8-10).

Recently, new functions of FXR beyond its roles in metabolism were discovered in several nonenterohepatic tissues, including its control in regulating cell growth and carcinogenesis (11-14). For instance, it has been demonstrated that FXR activation inhibits breast cancer cell proliferation and negatively regulates aromatase activity reducing local estrogen production which sustains tumor growth and progression (13).

Estrogen dependency is also a feature of testicular tumor which is the most frequent solid malignant tumour diagnosed in young men (20-40 years old) accounting for up to 20% of all malignancies diagnosed at this age. Ninety-five percent of all human testicular neoplasms arise from germinal cells whereas Leydig cell tumors are the most common tumors of the gonadal stroma (15). The molecular basis of testicular cell malignant transformation is poorly defined. It has been reported that estrogen serum levels are elevated in patients with testicular germ cell cancer as a consequence of increased local estrogen production reflecting an higher aromatase activity present in Sertoli and Leydig cells (16). Several studies on both rodents and humans indicate that prenatal, early post-natal and adult exposure to an excess of estrogens might have a central role in the mechanism leading to male reproductive tract malformations

such as testicular and prostatic tumors (17). The biological significance of estrogen-induced testicular tumorogenesis has been suggested by transgenic mice overexpressing aromatase and exhibiting enhancement of 17β-estradiol (E2) circulating levels (18). About half of these male mice were infertile and/or had enlarged testis and showed Leydig cell hyperplasia and Leydig cell tumors (18). Recently, we demonstrated aromatase and ERs expression in testis from patients affected by Leydigioma in which high estradiol levels in the presence of ERα could significantly contribute to tumor cell growth and progression (19). Besides, we also reported that one of the molecular mechanisms determining Leydig cell tumorogenesis is an excessive estrogen production that stimulates a short autocrine loop determining cell proliferation (20).

Aromatase activity is regulated primarly at the level of gene expression by tissue-specific promoters and is present in testicular somatic cells and along the maturative phases of male germ cells (21, 22). A promoter proximal to the translation start site, called promoter II (PII) regulates aromatase expression in fetal and adult testis, R2C and H540 rat Leydig tumor cells, and in purified preparations of rat Leydig, Sertoli, and germ cells (23, 24). Specific sequences seem to be mainly involved in aromatase expression: cyclic AMP (cAMP)-responsive element (CRE)-like sequences binding CREB/ATF protein families (25, 26) and a sequence containing an half-site binding nuclear receptors (AGGTCA) in position -90 binding steroidogenic factor 1 (SF-1) (27) which is essential for sex differentiation and development of gonads (28).

On the basis of all these observations, in this study we investigated in rat tumor Leydig cells, R2C whether FXR activation by specific ligand chenodeoxycholic acid (CDCA) or a synthetic agonist GW4064 may modulate aromatase expression and antagonize estrogen signalling, inhibiting testicular tumor growth and progression. We, for the first time, demonstrated that the molecular mechanism by which FXR ligands inhibit aromatase gene expression in R2C cells is mediated by a direct binding of FXR to SF-1 response element present in the aromatase promoter region.

Experimental Procedures

Reagents- Nutrient Mixture F-10 Ham, Dulbecco's Modified Eagle's Medium/Nutrient Mixture F-12 Ham (DMEM/F12), Dulbecco's Modified Eagle's Medium (DMEM), L-glutamine, penicillin, streptomycin, fetal bovine serum (FBS), horse serum (HS), phosphate-buffered saline, aprotinin, leupeptin, phenylmethylsulfonyl fluoride (PMSF), bovine serum albumin (BSA) and sodium orthovanadate were purchased by Sigma (Milan, Italy). TRIzol, Lipofectamine 2000 by Invitrogen (Carlsbad, CA, USA) and FuGENE 6 by Roche Applied Science (Indianapolis, IN, USA). TaqDNA polymerase, RETROscript kit, 100-bp DNA ladder, Dual Luciferase kit, TNT master mix and TK Renilla luciferase plasmid were provided by Promega (Madison, WI, USA). Antibodies against FXR, β-actin, GAPDH, Cyclin D1, Cyclin E and Lamin B by Santa Cruz Biotechnology (Santa Cruz, CA, USA), antibody against Aromatase by Serotec (Raleigh, NC, USA) and antibody against SF-1 kindly provided from Dr. K. Morohashi (National Institute Basic Biology, Myodaiji-cho, Okazaki, Japan). ECL system and Sephadex G-50 spin columns from Amersham Biosciences (Buckinghamshire, UK). [1β-^{3}H]androst-4-ene-3,17-dione, [γ^{32}P]ATP, and [^{3}H]thymidine from PerkinElmer (Wellesley, MA, USA). Salmon sperm DNA/protein A agarose by UBI (Chicago, IL, USA).

Plasmids- The plasmids containing different segments of the rat aromatase PII sequence ligated to a luciferase reporter gene [-1037/+94 (p-1037), -688/+94 (p-688) and -688/+94 mut (p-688m) (SF-1 site mutant)] were previously described (27). FXR responsive reporter gene (FXRE-IR1) and FXR-DN (dominant negative) expression plasmids were provided from Dr. T.A. Kocarek (Institute of Environmental Health Sciences, Wayne State University, USA) (29). FXR expression plasmid was provided from Dr. D.J. Mangelsdorf (Southwestern Medical Center, TX, USA). SF-1 expression plasmid and hCYP17 gene reporter were obtained from Dr. W. E. Rainey (Medical College of Georgia, USA). XETL plasmid is a construct containing an estrogen-responsive element from the *Xenopus* vitellogenin promoter, driving expression of the luciferase gene.

Cell Cultures and animals- Rat Leydig tumor cells (R2C) were cultured in Ham/F-10 supplemented with 15% HS, 2.5% FBS, and antibiotics. Mouse Leydig cells (TM3) were cultured in DMEM/F-12 supplemented with 5% HS, 2.5% FBS, and antibiotics. Human Cervix

tumor cells (HeLa) and Hepatoma cells (HepG2) were cultured in DMEM supplemented with 10% FBS, 1% L-glutamine and antibiotics. The cells were starved in serum free medium (SFM) 24 hours before treatments. Male Fisher 344 rats (a generous gift of Sgma-Tau), 6 (FRN) and 24 (FRT) months of age, were used for studies. Twenty-four-month-old animals presented spontaneously developed Leydig cell tumors, which were absent in younger animals. Testes of all animals were surgically removed by qualified, specialized animal care staff in accordance with the Guide for Care and Use of Laboratory Animals (NIH) and used for experiments.

Aromatase Activity Assay - The aromatase activity in subconfluent R2C cells culture medium was measured by the tritiated water release assay using 0.5 μM [1β-^{3}H]androst-4-ene-3,17-dione as substrate (30). The incubations were performed at 37°C for 2 h under an air/CO_2 (5%) atmosphere. The results obtained were expressed as pmol/h and normalized to mg of protein (pmol/h/mg protein).

Total RNA extraction and reverse transcription-PCR assay- Total RNA was extracted from R2C and TM3 cells using TRIzol reagent and the evaluation of genes expression was performed by the reverse transcription-PCR method using a RETROscript kit. The cDNAs obtained were amplified by PCR using the following primers: forward 5'-CAGCTATACTGAAGGAATCCACACTGT-3' and reverse 5'-AATCGTTTCAAAAGTGTAACCAGGA-3' (P450 aromatase) forward 5'-TTTCTACCCGCAACAACCGGAA-3' and reverse 5'-GTGACAAAGAAGCCGCGAATGG-3' (FXR), forward 5'-CAGCCACCAGACCCACCACAA-3' and reverse 5'-GAGGCACCGGACCCCATTCTA-3' (rat-SHP), forward 5'-CGTCCGACTATTCTGTATGC-3' and reverse 5'-CTTCCTCTAGCAGGATCTTC-3'(mouse-SHP) or forward 5'-GAAATCGCCAATGCCAACTC-3' and reverse 5'- ACCTTCAGGTACAGGCTGTG -3' (L19). The PCR was performed for 25 cycles for P450 aromatase (94°C 1 min, 58°C 1 min, 72°C 2 min), 35 cycles for FXR (94°C 1 min, 65°C 1 min, 72°C 2 min), 28 cycles for SHP (94°C 1 min, 65°C 1 min, 72°C 2 min) and 25 cycles for L19 (94°C 1 min, 60°C 1 min, and 72°C 2 min) in the presence of 1μl of first strand cDNA, 1 μM each of the primers, 0.5 mM dNTP, *Taq* DNA polymerase (2 units/tube) and 2.2 mM magnesium chloride in a final volume of 25 μl. DNA quantity in each lane was analyzed by scanning densitometry.

Immunoblot analysis- R2C, TM3, HepG2 cells or total tissue of FRNT and FRTT were lysed in 500 μl of 50 mM Tris-HCl, 150 mM NaCl, 1% NP-40, 0.5% sodium deoxycholate, 2 mM sodium fluoride, 2 mM EDTA, 0.1% SDS, containing a mixture of protease inhibitors (aprotinin, PMSF, sodium ortho-vanadate) for protein extraction. Nuclear extracts were prepared as previously described (31). Equal amount of proteins were resolved on 11% SDS-polyacrylamide gel, transferred to a nitrocellulose membrane and probed with FXR, Aromatase, Cyclin D1 and Cyclin E antibodies. To ensure equal loading all membranes were stripped and incubated with anti Lamin B antibody for nuclear extracts or anti-GADPH and anti-β-actin antibodies for total extracts. The antigen-antibody complex was detected by incubation of the membranes with peroxidase-coupled goat anti-mouse, goat anti-rabbit, or donkey anti-goat IgG and revealed using the ECL System. The bands of interest were quantified by Scion Image laser densitometry scanning program.

Immunofluorescence- R2C cells seeded on glass coverslips were treated with CDCA 50 and 100 μM for 24 h, washed with PBS and then fixed with 4% paraformaldehyde in PBS for 20 min at room temperature. Next, cells were permeabilized with 0.2% Triton X-100 in PBS for 5 min, blocked with 5% BSA for 30 min, and incubated overnight with anti-aromatase antibody (1:100) in PBS overnight at 4°C. The day after the cells were washed three times with PBS and incubated with the secondary antibody anti-mouse IgG-FITC (1:200) for 1 h at room temperature. To check the specificity of the immunolabelling the primary antibody was replaced by normal mouse serum (negative control). Immunofluorescence analysis was carried out on a OLYMPUS BX51 microscope using a 40x objective.

Transient transfection assay- R2C cells were transiently transfected using the FuGENE 6 reagent with FXR reporter gene (FXRE-IR1) or XETL plasmid. A set of experiments was performed transfecting rat aromatase PII constructs p-1037, p-688 and p-688m. HeLa cells were transiently cotransfected with CYP17 gene promoter and FXR or SF-1 expression plasmids. After transfection, R2C and Hela cells

were treated with CDCA 50 μM for 24 h. Empty vectors were used to ensure that DNA concentrations were constant in each transfection. TK Renilla luciferase plasmid was used to normalize the efficiency of the transfection. Firefly and Renilla luciferase activities were measured by Dual Luciferase kit. The firefly luciferase data for each sample were normalized based on the transfection efficiency measured by Renilla luciferase activity.

RNA interference (RNAi)- R2C cells were transfected with RNA duplex of stealth RNAi targeted rat SHP mRNA sequence 5'-ACUGAACUGCUUGAAGACAUGCUUU-3' (Invitrogen, Carlsbad, CA, USA), or with a stealth RNAi control to a final concentration of 50nM using Lipofectamine 2000 as recommended by the manufacturer. After 5 h the transfection medium was changed with SFM and 24 after transfection the cells were exposed to CDCA 50μM or 100μM for further 24 h. These transfected cells were used to examine the effects of silencing SHP gene expression on the aromatase mRNA and protein content.

Electrophoretic mobility shift assay (EMSA)- Nuclear extracts from R2C cells were prepared as previously described (31). The probe was generated by annealing single-stranded oligonucleotides, labeled with [γ^{32}P] ATP using T4 polynucleotide kinase, and purified using Sephadex G50 spin columns. The DNA sequences used as probe or as cold competitors are the following (nucleotide motifs of interest are underlined and mutations are shown as lowercase letters): SF-1, CAGGACCTGAGTCTCCCAAGGTCATCCTTGTTTGACTTGTA; mutated SF-1, TCTCCCAAtaTCATCCTTGT. *In vitro* transcribed and translated SF-1 and FXR proteins were synthesized using the T7 polymerase in the rabbit reticulocyte lysate system. The protein-binding reactions were carried out in 20μL of buffer [20 mmol/L HEPES (pH 8), 1 mmol/L EDTA, 50 mmol/L KCl, 10 mmol/L DTT, 10% glycerol, 1 mg/mL BSA, 50 μg/mL poly(dI/dC)] with 50,000 cpm of labeled probe, 20 μg of R2C nuclear protein or an appropriate amount of SF-1 or FXR proteins and 5 μg of poly (dI-dC). The mixtures were incubated at room temperature for 20 min in the presence or absence of unlabeled competitor oligonucleotides. For experiments involving anti-SF-1 and anti-FXR antibodies, the reaction mixture was incubated with these antibodies at 4°C for 12 h before addition of labeled probe. The entire reaction mixture was electrophoresed through a 6% polyacrylamide gel in 0.25x Tris borate-EDTA for 3 h at 150 V.

Chromatin immunoprecipitation and ReChip assays- R2C cells were treated with CDCA 50 μM for 1 h and then cross-linked with 1% formaldehyde and sonicated. Supernatants were immunocleared with salmon sperm DNA/protein A agarose for 1 h at 4°C. The precleared chromatin was immunoprecipitated with specific anti FXR or anti polymerase II antibodies and re immunoprecipitated with anti SF-1 antibody. A normal mouse serum IgG was used as negative control. Pellets were washed as reported, eluted with elution buffer (1% SDS, 0.1 M $NaHCO_3$) and digested with proteinase K. DNA was obtained by phenol/chloroform/isoamyl alcohol extractions and precipitated with ethanol; 3 μl of each sample were used for PCR amplification with the following primers flanking SF-1 sequence present in the P450arom PII promoter region: 5'-ATGCACGTCACTCTACCCACTCAA -3' and 5'-TAGCACGCAAAGCAGTAGTTTGGC -3'. The amplification products were analyzed in a 2% agarose gel and visualized by ethidium bromide staining.

[^{3}H]thymidine incorporation- R2C cells were treated with CDCA 50 and 100 μM for 24h and 48 h. For the last 6 hours, [^{3}H]thymidine (1 μCi/ml) was added to the culture medium. After rinsing with PBS, the cells were washed once with 10% and three times with 5% trichloroacetic acid, lysed by adding 0.1 N NaOH and then incubated for 30 min at 37 °C. Thymidine incorporation was determined by scintillation counting. In a set of experiment R2C cells were transiently transfected with FXR-DN expression plasmid 24 h before starting with the same treatments mentioned above.

Anchorage-independent soft agar growth assays- R2C cells were plated in 4 ml of Ham/F-10 with 0.5% agarose and 5% charcoal-stripped FBS, in 0.7% agarose base in six-well plates. Two days after plating, media containing hormonal treatments (androst-4-ene-3,17-dione, CDCA), was added to the top layer, and the appropriate media was replaced every two days. After 14 days, 150 μl of MTT was added to each well and allowed to incubate at 37° for 4 h. Plates were then placed at 4°C overnight and colonies > 50 μm diameter from triplicate assays were counted. Data are the mean colony number

of three plates and representative of two independent experiments.

Statistical Analysis- Each datum point represents the mean ± S.D. of three different experiments. Statistical analysis was performed using ANOVA followed by Newman-Keuls testing to determine differences in means. $P<0.05$ was considered as statistically significant.

RESULTS

FXR expression in normal and tumor testicular cells. We first aimed to evaluate, by Western Blotting analysis, the expression of FXR receptor in Leydig normal (TM3) and tumor (R2C) cell lines and in testes tissue from younger (FRNT) and older (FRTT) Fisher rats. The latter group have a high incidence of spontaneous Leydig cell neoplasma (32,33), a phenomenon not observed in younger animals. Immunoblot analysis revealed the presence of a FXR-immunoreactive protein band at ~ 60kDa in all samples examined, particularly, FXR receptor seems to be more expressed in R2C cells with respect to TM3 and in FRTT with respect to its control FRNT (Fig. 1A). Human hepatocyte cells (HepG2) were used as a positive control for FXR expression. In R2C cells, incubation for 24 h with CDCA 50 and 100 μM, a natural ligand of FXR, increased the level of the receptor at both mRNA and protein levels (Figs. 1B & 1C). Moreover, to assess the ability of CDCA to transactivate endogenous FXR, we transiently transfected R2C cells with FXR responsive reporter gene (FXRE-IR1). As reported in Figure1D, CDCA treatment for 24 h induced a significant enhancement in transcriptional activation of the reporter plasmid.

Inhibitory effects of FXR agonists on aromatase expression in R2C cells. Starting from previous findings showing that FXR activation represses aromatase expression in breast cancer cells (13) we investigated the ability of FXR agonists to modulate aromatase enzyme in R2C cells which have been shown to have high aromatase expression and activity (27). Treatment with CDCA 50 and 100 μM for 24 h showed a down-regulation of aromatase mRNA and protein content in a dose related manner (Figs. 2A & 2B). Because CDCA may also exert FXR-independent effects (34), the influence of GW4064, a synthetic FXR agonist, on aromatase gene was also investigated. We observed that GW4064 (3μM) reduced aromatase mRNA and protein levels to a similar order of magnitude as CDCA (Figs 2A & 2B). The down-regulatory effects of CDCA on the expression of aromatase was further confirmed by immunofluorescence analysis. The strong P450 aromatase immunoreactivity was detected in the cytoplasm as well as in the perinuclear region of untreated R2C cells and it was drastically decreased upon CDCA at the doses of 50 and 100 μM for 24 h (Fig. 2C). Next, we evaluated the effects of CDCA on aromatase enzymatic activity by tritiated water release assay. As reported in Figure 2D, exposure to CDCA 50 and 100 μM for 24 h reduced enzymatic activity in a dose dependent manner in R2C cells.

SHP is not involved in the down-regulatory effects induced by FXR ligand on aromatase. Induction of SHP expression is considered one of the canonical features of FXR transactivation. SHP has been shown to be expressed in the interstitial compartment of the adult testis, including steroidogenic Leydig cells (35).

We evidenced that SHP mRNA expression was significantly higher in R2C cells compared with very low levels detected in TM3 cell line, but administration of CDCA or GW4064 did not induce an increase of SHP mRNA in both cell lines (data not shown). However, to explore the role of SHP in CDCA-mediated repression of aromatase gene, we knocked SHP by siRNA. SHP mRNA expression was effectively silenced as revealed by RT-PCR after 24, 48 and 72 h of siRNA transfection (Fig. 3A). As shown in Figure 3B and 3C, silencing of the SHP gene failed to reverse the inhibition of aromatase expression induced by the specific FXR ligand in R2C cells ruling out any SHP involvement in the inhibitory effects of CDCA on aromatase expression.

CDCA down-regulates aromatase promoter activity through SF-1 site. The aforementioned observations led us to ascertain if the down-regulatory effects of CDCA on aromatase expression were due to its direct inhibitory influence in regulating aromatase gene transcriptional activity. Thus, we transiently transfected in R2C cells plasmids containing different segments of rat PII aromatase (Fig. 4A). A significant reduction of promoter activity was observed in cells transfected with p-1037 and p-688 exposed to CDCA 50 μM for 24 h. It is worth to note that construct p-688m bearing SF-1 mutated site displays significantly lower basal activity

compared with the p-688 plasmid while no inhibitory effects were noticeable upon CDCA treatment (Fig. 4B). This latter result highlights the importance of the SF-1 binding site in the regulation of aromatase expression in the R2C cells and suggests that the inhibitory effect of CDCA requires AGGTCA sequence motif.

To further demonstrate the functional interaction of FXR with SF-1 binding site, we transiently cotransfected Hela cells which do not express significant levels of SF-1 (36) with hCYP17 promoter construct containing multiple SF-1 response elements (37) with or without SF-1 plasmid in the presence of increasing amount of FXR expression plasmid. SF-1 expression vector strongly increased the CYP17 promoter activity, which was progressively reduced by FXR overexpression (Fig. 4C). We observed a similar results also in HeLa cells overexpressing FXR and treated with CDCA (data not shown). These data support the competitive role of FXR in binding SF-1 site.

FXR protein binds to SF-1 RE in vitro and in vivo. On the basis of the evidence that the inhibitory effect of CDCA on aromatase requires the crucial presence of SF-1 RE, EMSA experiments were performed using the SF-1 motif present in aromatase promoter as probe. We observed the formation of a complex in nuclear extract from R2C cells (Fig. 5A, *lane 1*), which was abrogated by 100 fold molar excess of unlabeled probe (Fig. 5A, *lane 2*) demonstrating the specificity of the DNA binding complex. This inhibition was not longer observed when mutated oligodeoxyribonucleotide was used as competitor (Fig. 5A, *lane 3*). CDCA 50 μM for 6 h induced an increase in DNA binding complex compared with control samples (Fig. 5A, *lane 4*). The inclusion of anti-SF-1 and anti-FXR antibodies in the reactions attenuated the specific bands suggesting the presence of SF-1 and FXR proteins in the complex (Fig. 5A, *lane 5 and 6*). Using SF-1 and FXR proteins transcribed and translated in vitro, we obtained complexes migrating at the same level as that of R2C nuclear extracts (Fig. 5A, *lane 7 and 8*).

The interaction of FXR with the aromatase gene promoter was further investigated by ChIP assay. Using specific antibody against FXR and RNA-POL II, formaldehyde cross-linked protein-chromatin complexes were immunoprecipitated from R2C cells cultured with or without CDCA 50 μM. The resulting genomic DNA precipitated by using anti-FXR was then reprecipitated with the anti SF-1 antibody. The results analyzed by PCR indicated that FXR was weakly constitutively bound to the aromatase promoter in untreated cells and this recruitment was increased upon CDCA treatment, which was correlated with a reduced association of RNA polymerase II (Fig. 5B). Interestingly, by Re-ChIP assay, we observed upon CDCA stimulation a significant reduction in SF-1 recruitment to the aromatase promoter (Fig. 5B).

CDCA inhibits R2C cell proliferation through FXR activation. Finally, we evaluated the effect of CDCA on the growth of R2C cells by measuring changes in the rate of DNA synthesis (3H thymidine incorporation). As shown in Figure 6A, treatment with CDCA for 24 and 48 h reduced R2C cells proliferation in a dose and time dependent manner. The specific involvement of FXR in the antiproliferative response of R2C cells to CDCA was demonstrated by the evidence that such inhibitory effects were completely reversed in the presence of FXR dominant negative plasmid (Fig. 6B).

It is well known that aromatase overexpression in tumor Leydig cells leads to a consequent excess of in situ estradiol production that sustains tumor cell growth and proliferation (18). Since we demonstrated the ability of CDCA to down-regulate aromatase expression and activity in R2C cells, we wondered if CDCA was able to antagonize the effect of an aromatizable androgen androst-4-ene-3,17-dione (AD) on estradiol/ERα signaling in R2C cells. To this aim we performed transient transfection experiment using XETL plasmid, which carries firefly luciferase sequences under the control of an estrogen response element upstream of the thymidine kinase promoter. As shown in Figure 6C we observed that the exposure to CDCA (50 μM) per se did not elicit any changes in luciferase activity but it completely reversed XETL activation induced by AD. Moreover, we examined if CDCA was able to inhibit the effect of AD on R2C cell proliferation using two experimental approaches thymidine incorporation and anchorage independent soft agar growth assay. As expected, treatment with 100 nM of AD, through its conversion into estradiol, increased thymidine incorporation as well as the number of colonies present in soft agar (Figs 6D & 6E) concomitantly with an increased levels of cell cycle regulators cyclin D1 and cyclin E (Fig. 6F). All these events were

completely reversed by CDCA exposure (Figs 6D & 6E & 6F). These data demonstrated that FXR ligand, through an inhibition of aromatase activity, is able to reduce the estrogen dependent tumor Leydig cells proliferation.

DISCUSSION

FXR is highly expressed in the enterohepatic system where it drives bile acid absorption and secretion, lipid, glucid metabolism, and immunological response to intestinal bacterial overgrowth (2,4,38-40). In hepatocytes, activation of FXR causes both feedback inhibition of cholesterol 7a-hydroxylase (CYP7A1), the rate-limiting enzyme in bile acid biosynthesis from cholesterol, and activation of intestinal bile acid-binding protein (41). In addition, several observations suggest that FXR may also be involved in the control of steroid metabolism (13,42). Indeed, FXR activation results in the modulation of genes encoding androgen precursor-synthesizing enzymes, namely dehydroepiandrosterone sulfotransferase (SULT2A1), 5α-reductase and 3β-HSD (3β-hydroxysteroid dehydrogenase) in the liver (43,44). Recently, FXR was shown to inhibit androgen glucuronidation in prostatic cancer cell lines (45) and to suppress the activity of the aromatase in human breast cancer cells (13). The enzyme aromatase coded by the gene CYP19, converts androgens in estrogens and is involved in the progression and growth of various estrogen hormonal-induced neoplasms. For instance, overexpression of aromatase plays a significant role in the excessive estrogen production sustaining tumorogenesis in Leydig cells (18).

Here, we have documented that FXR is expressed in tissues of normal and tumor Fisher rat testis and in Leydig normal and tumor cell lines. In R2C cells, the FXR activators CDCA and GW4064, downregulate aromatase expression at both mRNA and protein level, together with the inhibition of its enzymatic activity.

One of the well-characterized mechanism by which FXR down-regulates gene expression is through induction of SHP (10) an atypical nuclear receptor lacking both a DNA-binding domain and the NH2-terminal ligand-independent activation domain (8). This receptor interacts with other nuclear receptors, including Peroxisome Proliferator Activated Receptor (PPAR), RXR, Estrogen Receptor (ER) and Liver Receptor Homolog-1 (LRH-1), preventing their activation of gene transcription (8-10). In preadipocytes of cancerous breast tisuue, LRH-1 can regulate via an alternate promoter (II) the expression of aromatase induced by prostaglandin E2 (46, 47). Moreover, SHP can inhibit LRH-1 induction of aromatase (48). LRH-1 is most homologous to SF1, which is essential for sex differentiation and development of gonads (28), since they share a highly conserved DBD (DBD>90% identity) and a moderately conserved LBD (LBD 56% identity). SHP is detected in the interstitial cells of the adult testis and its expression has been shown to be induced by FXR (35).

Our current study revealed that FXR activation does not induce SHP expression in Leydig tumor cells in which the inhibition of aromatase protein by CDCA occurs even when this nuclear receptor was knocked down. These results suggest that SHP is not required for the effect of FXR ligand to down-regulate aromatase expression, at least in R2C cells. On the basis of these observations, we focused our attention on the direct effect of FXR on the transcriptional activity of aromatase gene.

Distinctive tissues specific promoters are employed to direct the expression of aromatse mRNA driving from a single aromatase gene. The promoter located immediately upstream of the transcriptional initiation site (PII) regulates aromatase expression in rat Leydig, Sertoli and germ cells and in R2C Leydig tumor cells (23,24). A number of functional motifs have been identified in the PII aromatase promoter: three motifs resembling cAMP response elements (CRE) and an SF-1 binding site (27,28).

We demonstrated by functional studies, using constructs containing different 5'-deleted regions of rat PII aromatase promoter, that CDCA treatment induces a decreased transcriptional activity. The observed inhibitory effect of CDCA was abrogated when a promoter fusion containing a mutated SF-1 element was employed. These results clearly suggest that the integrity of SF-1 sequence is a prerequisite for the down-regulatory effects of FXR ligand on aromatase promoter activity. These findings raise the possibility that FXR and SF-1 are competing for binding to a common site within this regulatory region. This assumption is further supported by the observation that FXR expression vector is able to abrogate the

induction of SF-1 on human CYP17 promoter which contains multiple SF-1 response elements.
As a transcription factor, FXR binds to a specific consensus sequence (inverted repeat of 2 AGGTCA half-sites) either as a monomer or as a heterodimer with a common partner for NRs, as RXR to regulate the expression of various genes (4).
Location of an AGGTCA sequence at the -90 position supports a possible binding of FXR to this promoter region, which we verified by EMSA experiments. Nuclear extracts from R2C cells treated with CDCA revealed an increase in DNA binding complex which was immunodepleted by both anti-SF-1 and anti-FXR antibodies suggesting how the two proteins are able to bind the AGGTCA sequence located in PII aromatase promoter. In addition, the *in vivo* iinteraction between FXR and aromatase promoter was further supported by ChIP assay, where upon CDCA treatment we observed a reduced recruitment of RNA-POLII to this promoter addressing a negative transcriptional regulation mediated by FXR. All together these data suggest that FXR is able to compete with SF-1 in binding to a common sequence within the PII promoter of aromatase interfering negatively with its activity.
Finally, in our study we demonstrated that FXR activator CDCA induces growth inhibition in R2C cells which was reversed in the presence of FXR dominant negative addressing a FXR dependency of this event.
However it is worth to mention, on the basis of our recent findings, that aromatase overexpression, in Leydig tumor cells, determines an excessive local estradiol production that is able to stimulate the expression of genes involved in cell cycle regulation sustaining cell proliferation (20).
Here, we evidenced the ability of CDCA to reverse the stimulatory effects of an aromatizable androgen androst-4-ene-3,17-dione (AD) at three different levels: 1) E2/ERα. signaling; 2) an anchorage dependent and independent R2C cell growth proliferation; 3) expression of cell cycle regulators cyclin D1 and cyclin E. The latter finding bring us to emphasize how the intrinsic property of FXR to inhibit R2C cell proliferation sound to be not linked to any substantial effect on cyclin D1 and cyclin E expression.
In conclusion, our results elucidate, for the first time, a new molecular mechanism through which FXR antagonizes estrogen signalling and inhibits Leydig tumor growth and progression addressing FXR ligands as potential pharmacological tools to be implemented in the novel strategies for testicular tumoral treatment.

REFERENCES

1. Forman, B. M., Goode, E., Chen, J., Oro, A. E., Bradley, D. J., Perlmann, T., Noonan, D. J., Burka, L. T., McMorris, T., Lamph, W. W., Evans, R. M., Weinberger, C. (1995) *Cell* **81**, 687–693
2. Makishima, M., Okamoto, A. Y., Repa, J. J., Tu, H., Learned, R. M., Luk, A., Hull, M.V., Lustig, K. D., Mangelsdorf, D. J., Shan, B. (1999) *Science* **284**, 1362–1365
3. Parks, D. J., Blanchard, S. G., Bledsoe, R. K., Chandra, G., Consler TG, Kliewer SA, Stimmel JB, Willson TM, Zavacki AM, Moore DD, Lehmann, J. M. (1999) *Science* **284**, 1365–1368
4. Kalaany, N.Y. and Mangelsdorf, D.J. (2006) *Annu Rev Physiol* **68**, 159–191
5. Song, C. S., Echchgadda, I., Beak, B. S., et al. (2001) *J Biol Chem* **276**, 42549-42556
6. Li, J., Pircher, P. C., Schulman, I. G., Westin, S. K. (2005) *J Biol Chem* **280**, 7427-7434
7. Ananthanarayanan, M., Balasubramanian, N., Makishima, M., Mangelsdorf, D. J., Suchy, F.J. (2001) *J Biol Chem* **276**, 28857-28865
8. Seol, W., Choi, H. S., Moore, D. D. (1996) *Science* **272**, 1336-1339
9. Seol, W., Hanstein, B., Brown, M., Moore, D. D. (1998) *Mol Endocrinol* **12,** 1551- 1557
10. Goodwin, B., Jones, S. A., Price, R. R., Watson, M. A., McKee, D. D., Moore, L. B., Galardi, C., Wilson, J. G., Lewis, M. C., Roth, M. E., Maloney, P. R., Willson, T. M., Kliewer, S. A. (2000) *Mol Cell Biol* **20**, 187-195
11. Wang, Y. D., Chen, W. D., Moore, D. D. and Huang, W. D. (2008) *Cell Research* **18**, 1087-1095

12. Journe, F., Laurent, G., Chaboteaux, C., Nonclercq, D., Durbecq, V., Larsimont, D., Body, J. J. (2008) *Breast Cancer Res Treat* **107**, 49-61
13. Swales, K. E., Korbonits, M., Carpenter, R., Walsh, D. T., Warner, T. D., Bishop-Bailey, D. (2006) *Cancer Res* **66**, 10120-10126
14. Modica, S., Murzilli, S., Salvatore, L., Schmidt, D. R., Moschetta, A. (2008) *Cancer Res* **68**, 9589-9594
15. Hawkins, C., Miaskowski, C. (1996) *Oncol Nurs Forum* **23**, 1203-1211
16. Carroll, P. R., Whitmore, W. F. Jr., Herr, H. W., Morse, M. J., Sogani, P. C., Bajorunas, D., Fair, W. R., Chaganti, R. S. (1987) *J Urol* **137**, 420-423
17. Bosland, M. C. (1996) *Prog Clin Biol Res* **394**, 309-352
18. Fowler, K. A., Gill, K., Kirma, N., Dillehay, D. L., Tekmal, R. R. (2000) *Am J Pathol* **156**, 347-353
19. Carpino, A., Rago, V., Pezzi, V., Carani, C., Andò, S. (2007) Eur. J. Endocrinol. **157**, 239-44
20. Sirianni, R., Cimento, A., Malivindi, R., Mazzitelli, I., Andò, S., Pezzi, V. (2007) *Cancer Res* **67**, 8368-8377
21. Aquila, S., Sisci, D., Gentile, M., Carpino, A., Middea, E., Catalano, S., Rago, V., Andò, S. (2003) *Hum Reprod* **18**, 1650-1659
22. Inkster, S., Yue, W., Brodie, A. (1995) *J Clin Endocrinol Metab* **80**, 1941-1947
23. Young, M., Lephart, E. D., McPhaul, M. J. (1997) *J Steroid Biochem Mol Biol* **63**, 37–44
24. Lanzino, M., Catalano, S., Genissel, C., Ando', S., Carreau, S., Hamra, K., McPhaul, M. J. (2001) *Biol Reprod* **64**, 1439-1443
25. Fitzpatrick, S. L., Richards, J. S. (1994) *Mol Endocrinol* **8**, 1309–1319
26. Carlone, D. L., Richards, J. S. (1997) *Mol Endocrinol* **11**, 292–304
27. Young, M., McPhaul, M. J. (1998) *Endocrinology* **139**, 5082-5093
28. Parker, K. L., Shimmer, B. P. (1997) *Endocr Rev* **18**, 361-377
29. Kocarek, T. A., Shenoy, S. D., Mercer-Haines, N. A., Runge-Morris, M. (2002) *J Pharmacol Toxicol Methods* **47**, 177-187
30. Lephart, E. D. and Simpson, E .R. (1991) *Methods Enzymol* **206**, 477–483
31. Anderws, N. C., and Faller, D. V. (1991) *Nucleic Acids Res* **19**, 2499
32. Coleman, G. L., Barthold, W., Osbaldiston, G. W., Foster, S. J., Jonas, A. M. (1977) *J Gerontol* **32**, 258–278
33. Jacobs, B.B., Huseby, R.A. (1967) *J Natl Cancer Inst* **39**, 303–309
34. Nguyen, A., Bouscarel, B. (2008) *Cellular Signalling* **20**, 2180-2197
35. Volle, D. H., Duggavathi, R., Magnier, B. C., Houten, S. M., Cummins, C. L., Lobaccaro, J. M., Verhoeven, G., Schoonjans, K., Auwerx, J. (2007) *Genes Dev* **21**, 303-315
36. Sugawara, T., Holt, J. A., Kiriakidou, M., Strauss, J. F. (1996) *Biochemistry* **35**, 9052-9059
37. Hanley, N. A., Rainey, W. E., Wilson, D. I., Ball, S. G., Parker, K. L. (2001) *Mol Endocrinol* **15**, 57-68
38. Modica, S., Moschetta, A. (2006) *FEBS Lett* **580**, 5492-5499
39. Jung, D., Inagaki, T., Gerard, R. D., Dawson, P. A., Kliewer, S. A., Mangelsdorf, D. J., Moschetta, A. (2007) *J Lipid Res* **48**, 2693-2700
40. Inagaki, T., Moschetta, A., Lee, Y. K., Peng, L., Zhao, G., Downes, M., Yu, R. T., Shelton, J. M., Richardson, J. A., Repa, J. J., Mangelsdorf, D. J., Kliewer, S. A. (2006) *Proc Natl Acad Sci U S A* **103**, 3920-3925
41. Chiang, J. Y. (2002) *Endocr Rev* **23**, 443-463
42. Lee, F. Y., Lee, H., Hubbert, M. L., Edwards, P. A., Zhang, Y. (2006) *Trends Biochem Sci* **31**, 572-580
43. Pircher, P. C., Kitto, J. L., Petrowski, M. L., Tangirala, R. K., Bischoff, E. D., Schulman, I. G., Westin, S. K. (2003) *J Biol Chem* **278**, 27703-27711
44. Miyata, M., Matsuda, Y., Tsuchiya, H., Kitada, H., Akase, T., Shimada, M., Nagata, K., Gonzalez, F. J., Yamazoe, Y. (2006) *Drug Metab Pharmacokinet* **21**, 315-323
45. Kaeding, J., Bouchaert, E., Bélanger, J., Caron, P., Chouinard, S., Verreault, M., Larouche, O., Pelletier, G., Staels, B., Bélanger, A., Barbier, O. (2008) *Biochem J* **410**, 245-253
46. Clyne, C. D., Speed, C. J., Zhou, J., Simpson, E. R. (2002) *J Biol Chem* **277**, 20591-20597

47. Zhou, J., Suzuki, T., Kovacic, A., Saito, R., Miki, Y., Ishida, T., Moriya, T., Simpson, E.R., Sasano, H., Clyne, C.D. (2005) *Cancer Res* **65**, 657-663
48. Kovacic, A., Speed, C. J., Simpson, E. R., Clyne, C. D. (2004) *Mol Endocrinol* **18**, 252-259

FOOTNOTES

We thank Dr T.A. Kocarek (Institute of Environmental Health Sciences, Wayne State University, USA), Dr. D.J. Mangelsdorf (Southwestern Medical Center, TX, USA) and Dr. W. E. Rainey (Medical College of Georgia, USA) for generously providing us with the FXR responsive reporter gene, FXR-DN, FXR, SF-1 and hCYP17 gene reporter plasmids respectively.
This work was supported by PRIN-MIUR and Associazione Italiana per la Ricerca sul Cancro (AIRC)

The abbreviation used are: FXR, Farnesoide X Receptor; RXR, Retinoid X Receptor; FXREs, FXR response element; SHP, Small Heterodimer Partner; E2, 17β-estradiol; CDCA, chenodeoxycholic acid; DMEM/F12, Dulbecco's Modified Eagle's Medium/Nutrient Mixture F-12 Ham; DMEM, Dulbecco's Modified Eagle's Medium; FBS, fetal bovine serum; HS, horse serum; PMSF, phenylmethylsulfonyl fluoride; BSA, bovine serum albumin; RNAi, RNA interference; EMSA, Electrophoretic mobility shift assay; FXRE-IR1,FXR responsive reporter gene; AD, androst-4-ene-3,17-dione; PPAR, Peroxisome Proliferator Activated Receptor; ER, Estrogen Receptor; LRH-1, Liver Receptor Homolog-1; CRE, cAMP response elements.

FIGURE LEGENDS

Fig. 1. FXR expression and activation in R2C cells. *A*, Western blot analysis of FXR was done on 50 μg of total proteins extracted from normal (TM3), tumor Leydig cells (R2C) and human hepatocytes cells (HepG2) or from tissues of normal (FRNT) and tumor (FRTT) Fisher rat testes. β-actin was used as a loading control. *B*, Total RNA was extracted from R2C cells treated with vehicle (-) or CDCA 50 and 100 μM for 24 h and reverse transcribed. cDNA was subjected to PCR using primers specific for FXR or L19 (ribosomal protein). NC: negative control, RNA sample without the addition of reverse transcriptase. The histograms represent the means ± S.D. of three separate experiments in which band intensities were evaluated in terms of optical density arbitrary units and expressed as percentages of the control, which was assumed to be 100%. *p<0.05, **p<0.01 compared to vehicle. *C*, Nuclear proteins were extracted from R2C cells treated with vehicle (-) or CDCA 50 and 100 μM for 24 h and then western blotting analysis was performed using anti-FXR antibody. Lamin B was used as loading control. The histograms represent the means ± S.D. of three separate experiments in which band intensities were evaluated in terms of optical density arbitrary units and expressed as percentages of the control, which was assumed to be 100%. *p<0.05 compared to vehicle. *D*, R2C cells were transiently transfected with FXR reporter gene (FXRE-IR1) and treated with vehicle (-) or CDCA 50 μM and 100 μM for 24 h. The values represent the means ± S.D. of three different experiments performed in triplicate. * p<0.01 compared to vehicle.

Fig. 2. Effects of CDCA on aromatase expression and activity in R2C cells. *A*, Total RNA was extracted from R2C cells treated with vehicle (-), CDCA 50 and 100 μM or GW4064 3 μM for 24 h and reverse transcribed. cDNA was subjected to PCR using primers specific for P450 aromatase or L19. NC: negative control, RNA sample without the addition of reverse transcriptase. The histograms represent the means ± S.D. of three separate experiments in which band intensities were evaluated in terms of optical density arbitrary units and expressed as percentages of the control which was assumed to be 100%. *p<0.05, **p<0.01 compared to vehicle. *B*, Total proteins extracted from R2C cells treated with vehicle (-), CDCA 50 and 100 μM or GW4064 3 μM for 24 h were used for immunoblot analysis of aromatase. GAPDH was used as a loading control. The histograms represent the means ± S.D. of three separate experiments in which band intensities were evaluated in terms of optical density arbitrary units and expressed as percentages of the control which was assumed to be 100%. *p<0.01 compared to vehicle. *C*, R2C cells were treated with vehicle (-) or CDCA 50 and 100 μM for 24 h and aromatase expression was determined by immunofluorescence analysis. DAPI staining was used to visualized the cell nucleus. Each experiment is representative of at last 4 tests. *D*,

R2C were cultured in the presence of vehicle (-) or 50 and 100 μM of CDCA for 24 h. Aromatase activity was performed as described in Materials and Methods. The results obtained were expressed as pmol [^{3}H] H_2O/h release and were normalized for mg protein (pmol/mg proteins/h). The values represent the means ± S.D. of three different experiments each performed with triplicate samples. *p<0.01 compared to vehicle.

Fig. 3. SHP is not involved in CDCA-mediated down-regulation of aromatase. *A*, SHP mRNA expression in R2C cells which were not transfected (–) or transfected with RNA interference (RNAi) targeted rat SHP mRNA sequence as reported in Materials and Methods for 24, 48 and 72 h. L19 was used as loading control. NC: negative control, RNA sample without the addition of reverse transcriptase. The histograms represent the means ± S.D. of three separate experiments in which band intensities were evaluated in terms of optical density arbitrary units and expressed as percentages of the control, which was assumed to be 100%. *p<0.01 compared to vehicle. *B*, R2C cells were transfected with control siRNA or SHP siRNA for 24 h, and then treated with vehicle (-) or CDCA 50 and 100 μM for 24 h. Total RNA was extracted and RT-PCR analysis was performed to evaluate the expression of aromatase. L19 was used as loading control. NC: negative control, RNA sample without the addition of reverse transcriptase. The histograms represent the means ± S.D. of three separate experiments in which band intensities were evaluated in terms of optical density arbitrary units and expressed as percentages of the control, which was assumed to be 100%. *p<0.01 compared to vehicle. *C*, In the same experimental condition of B, total proteins were extracted and western blotting analysis was performed. GAPDH was used as loading control. The histograms represent the means ± S.D. of three separate experiments in which band intensities were evaluated in terms of optical density arbitrary units and expressed as percentages of the control which was assumed to be 100%. * p<0.05, ** p<0.01 compared to vehicle.

Fig. 4. Functional interaction between FXR and SF-1 site. *A*, Schematic map of the P450arom proximal promoter PII constructs used in this study. All of the promoter constructs contain the same 3' boundary (+94). The 5' boundaries of the promoter fragments varied from -1037 to -688. Three putative CRE motifs (5'-CRE at -335; 3'-CRE at -231; XCRE at -169) are indicated as square. The AGGTCA site (SF-1 RE at-90) is indicated as rectangle. A mutated SF-1 binding site (SF-1 mut) is present in p-688m (black rectangle). *B*, Aromatase transcriptional activity of R2C cells transfected with promoter constructs are shown. After transfection, cells were treated in the presence of vehicle (-) or CDCA 50 μM for 24h. These results represent the means ± S.D. of three different experiments performed in triplicate. *p<0.01 with respect to the vehicle, **p<0.01 with respect to the the control of p688. *C*, HeLa cells were transiently cotransfected with CYP17 promoter and with SF-1 plasmid or empty vector (EV) in the presence of increasing amount of FXR expression plasmid. These results represent the means ± S.D. of three different experiments performed in triplicate. In each experiment, the activities of the transfected plasmids were assayed in triplicate transfections. *p<0.01 with respect to the EV, **p<0.01 with respect to the SF-1 alone.

Fig. 5. FXR binds to SF-1 site within aromatase promoter region. *A*, Nuclear extract from R2C cells were incubated with a double-stranded SF-1-specific sequence probe labeled with [γ^{32}P]ATP and subjected to electrophoresis in a 6% polyacrylamide gel (lane 1). Competition experiments were performed adding as competitor a 100-fold molar excess of unlabeled probe (lane 2) or a 100-fold molar excess of unlabeled oligonucleotide containing a mutated SF-1 RE (lane 3). Lane 4, nuclear extracts from CDCA (50 μM) treated R2C cells. Lanes 5 and 6, CDCA-treated nuclear extracts were incubated with anti-SF-1 or anti-FXR antibodies respectively. We used as positive controls transcribed and translated in vitro SF-1 (lane 7) and FXR (lane 8) proteins. Lane 9 contains probe alone. *B*, R2C cells were treated in the presence of vehicle (-) or CDCA 50 μM for 1 hour, then cross-linked with formaldehyde, and lysed. The precleared chromatin was immunoprecipitated with anti-FXR, and anti-RNA Pol II antibodies and normal mouse serum (NC) as negative control. Chromatin immunoprecipitated with the anti-FXR antibody was re-immunoprecipitated with anti-SF-1 antibody. The PII promoter sequence containing SF-1 site was detected by PCR with specific primers as detailed in the Materials and Methods. To determine input DNA, the PII promoter fragment was

amplified from 30 µl initial preparations of soluble chromatin before immunoprecipitations. Similar results were obtained in multiple independent experiments.

Fig. 6. CDCA effects on R2C cell proliferation. *A*, R2C cells were treated with vehicle (-) or CDCA 50 and 100 µM for 24 and 48 h or *B*, transiently transfected with FXR dominant negative (FXR-DN) for 24 h, and then treated as above reported. Thymidine incorporation assay was performed. The results represent the means ± S.D. of three different experiments each performed with triplicate samples, and expressed as percentage of growth vs control which was assumed to be 100%. *C*, R2C cells were transiently transfected with XETL promoter plasmid. Cells were treated with CDCA 50 µM in the presence or not of androst-4-ene-3,17-dione (AD) 100 nM for 24h. These results represent the means ± S.D. of three different experiments. In each experiment, the activities of the transfected plasmids were assayed in triplicate transfections. *$p<0.01$ with respect to the vehicle. **$p<0.01$ CDCA+AD treated vs AD alone. *D*, R2C cells were treated with androst-4-ene-3,17-dione (AD) 100nM in the presence or not of CDCA 50 µM for 24h. Thymidine incorporation assay was performed. The results represent the means ± S.D. of three different experiments each performed with triplicate samples. *$p<0.01$ AD treated compared to vehicle. **$p<0.01$ CDCA+AD treated vs AD alone. *E*, R2C cells were seeded (10,000/well) in 0.5% agarose and the treated as described above. Cells were allowed to grow for 14 days and then the number of colonies >50µm were quantified and the results graphed. The results represent the means ± S.D. of three different experiments each performed with triplicate samples. *$p<0.01$ AD treated compared to vehicle. **$p<0.01$ CDCA+AD treated vs AD alone. *F*, Total proteins extracted from R2C cells treated with vehicle (-), Ad 100 nM, CDCA 50 µM and AD*CDCA for 24 h were used for immunoblot analysis of cyclin D1 and cyclin E. β-actin was used as a loading control. The histograms represent the means ± S.D. of three separate experiments in which band intensities were evaluated in terms of optical density arbitrary units and expressed as percentages of the control which was assumed to be 100%. *$p<0.01$ AD treated compared to vehicle. **$p<0.01$ CDCA+AD treated vs AD alone.

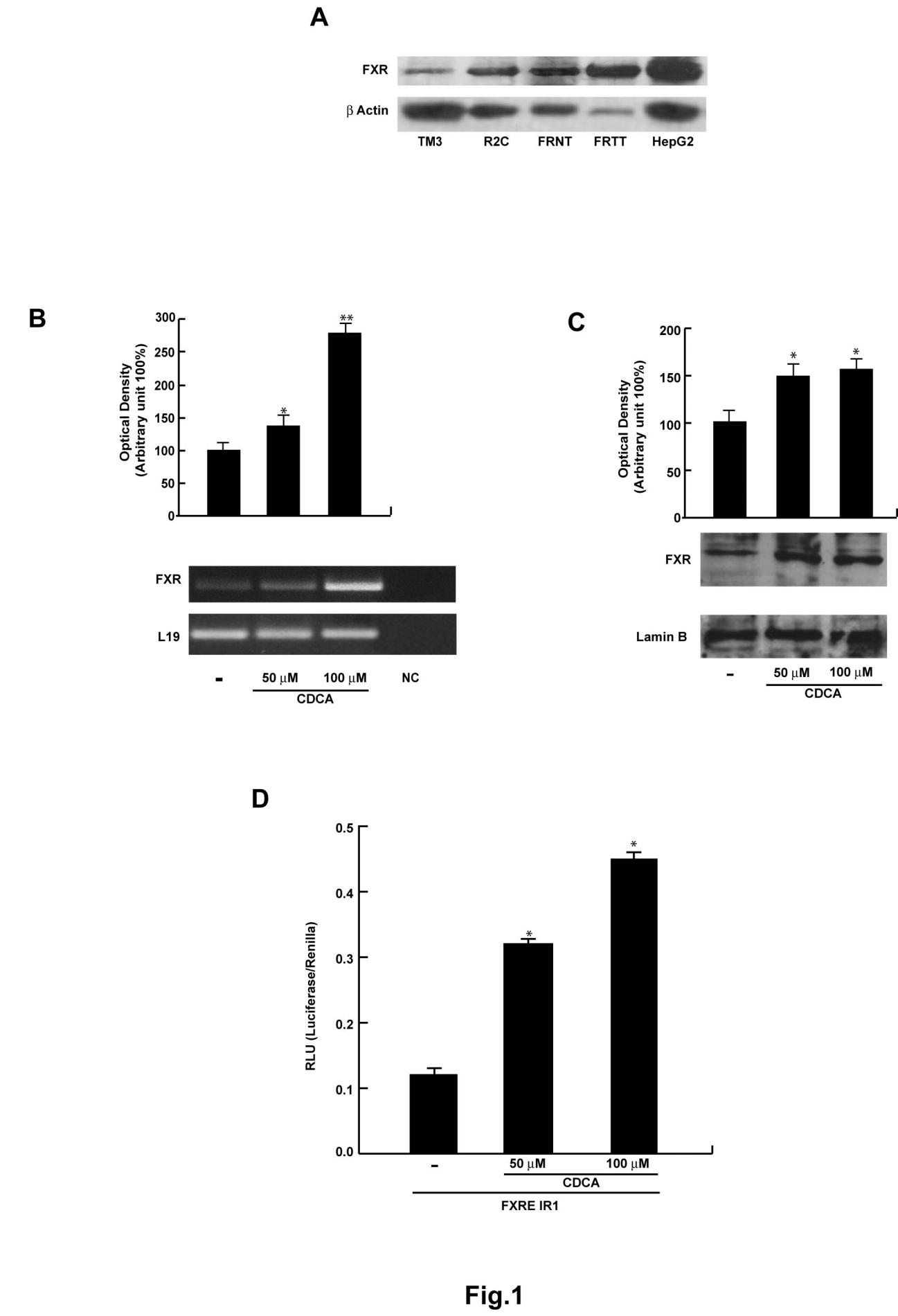
A
FXR
β Actin
TM3
R2C
FRNT
FRTT
HepG2
B
Optical Density
(Arbitrary unit 100%)
300
250
200
150
100
50
0
*
**
FXR
L19
-
50 μM
100 μM
NC
CDCA
C
Optical Density
(Arbitrary unit 100%)
200
150
100
50
0
*
*
FXR
Lamin B
-
50 μM
100 μM
CDCA
D
RLU (Luciferase/Renilla)
0.5
0.4
0.3
0.2
0.1
0.0
*
*
-
50 μM
100 μM
CDCA
FXRE IR1

Fig.1

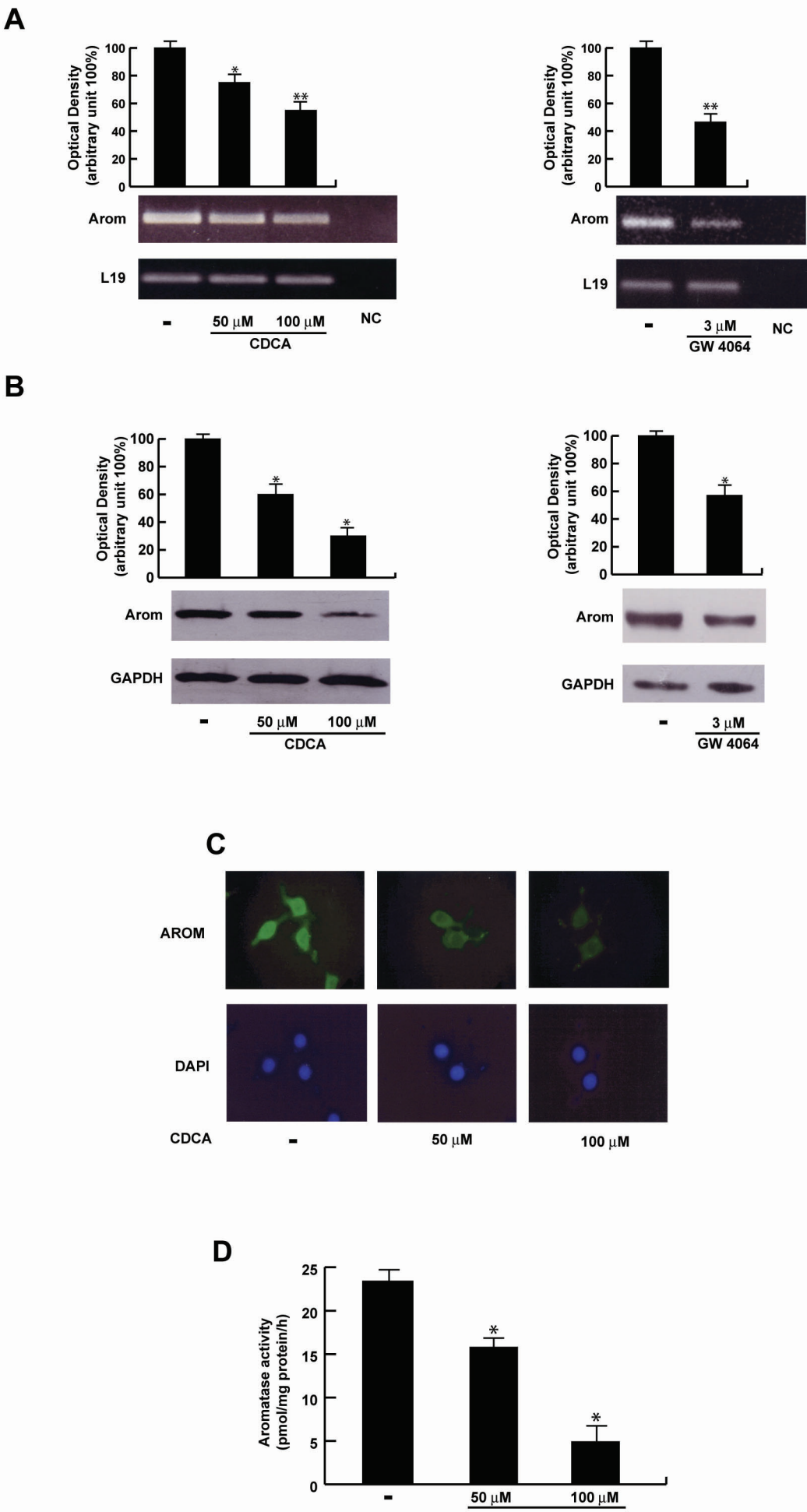
A
Optical Density (arbitrary unit 100%)
100
80
60
40
20
0
*
**
Arom
L19
-
50 μM
100 μM
CDCA
NC
Optical Density (arbitrary unit 100%)
100
80
60
40
20
0
**
Arom
L19
-
3 μM
GW 4064
NC
B
Optical Density (arbitrary unit 100%)
100
80
60
40
20
0
*
*
Arom
GAPDH
-
50 μM
100 μM
CDCA
Optical Density (arbitrary unit 100%)
100
80
60
40
20
0
*
Arom
GAPDH
-
3 μM
GW 4064
C
AROM
DAPI
CDCA
-
50 μM
100 μM
D
Aromatase activity (pmol/mg protein/h)
25
20
15
10
5
0
*
*
-
50 μM
100 μM
CDCA

Fig. 2

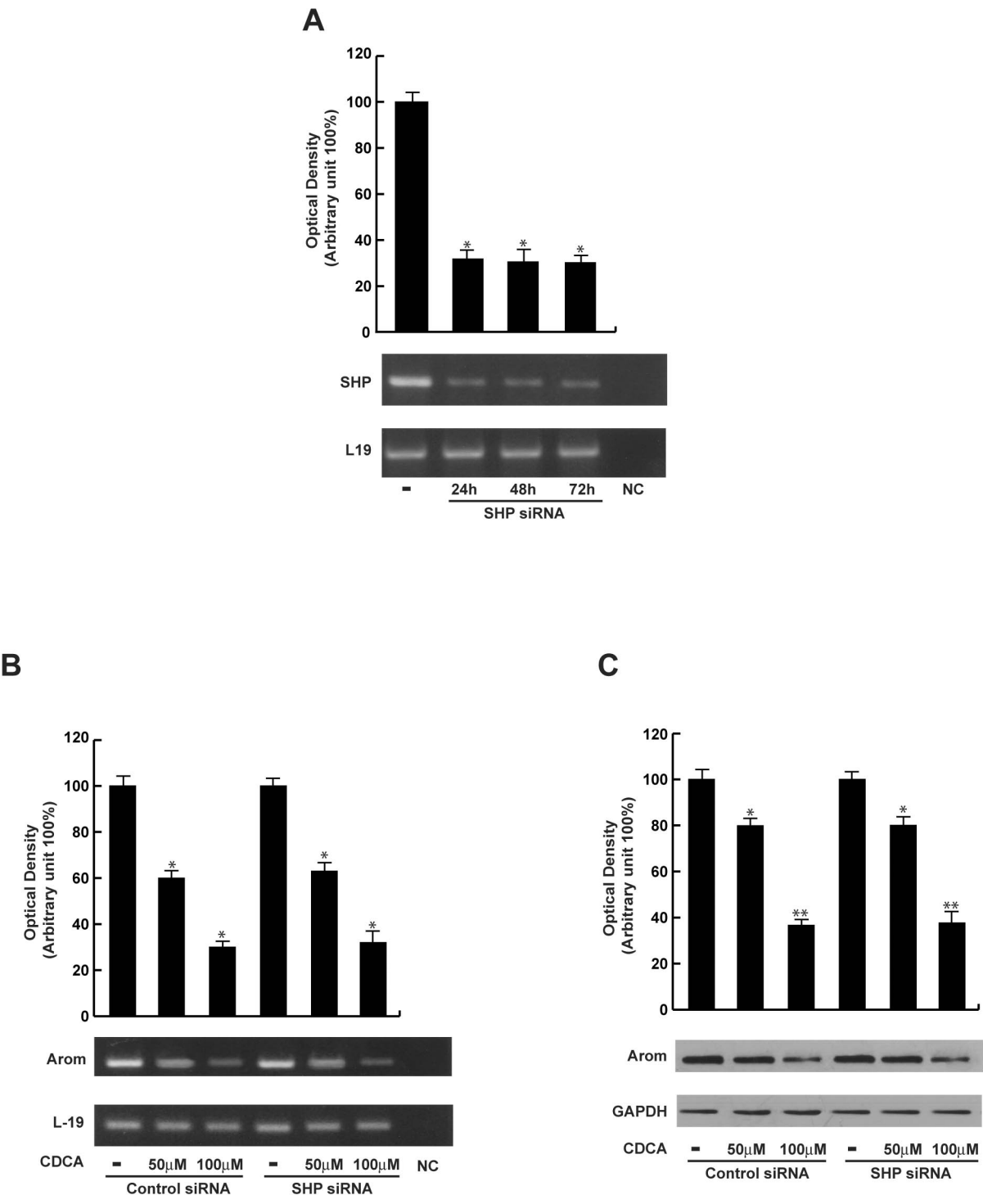
A
Optical Density (Arbitrary unit 100%)
120
100
80
60
40
20
0
*
*
*
SHP
L19
-
24h
48h
72h
NC
SHP siRNA
B
Optical Density (Arbitrary unit 100%)
120
100
80
60
40
20
0
*
*
*
*
*
Arom
L-19
CDCA
-
50μM
100μM
-
50μM
100μM
NC
Control siRNA
SHP siRNA
C
Optical Density (Arbitrary unit 100%)
120
100
80
60
40
20
0
*
*
**
*
**
Arom
GAPDH
CDCA
-
50μM
100μM
-
50μM
100μM
Control siRNA
SHP siRNA

Fig. 3

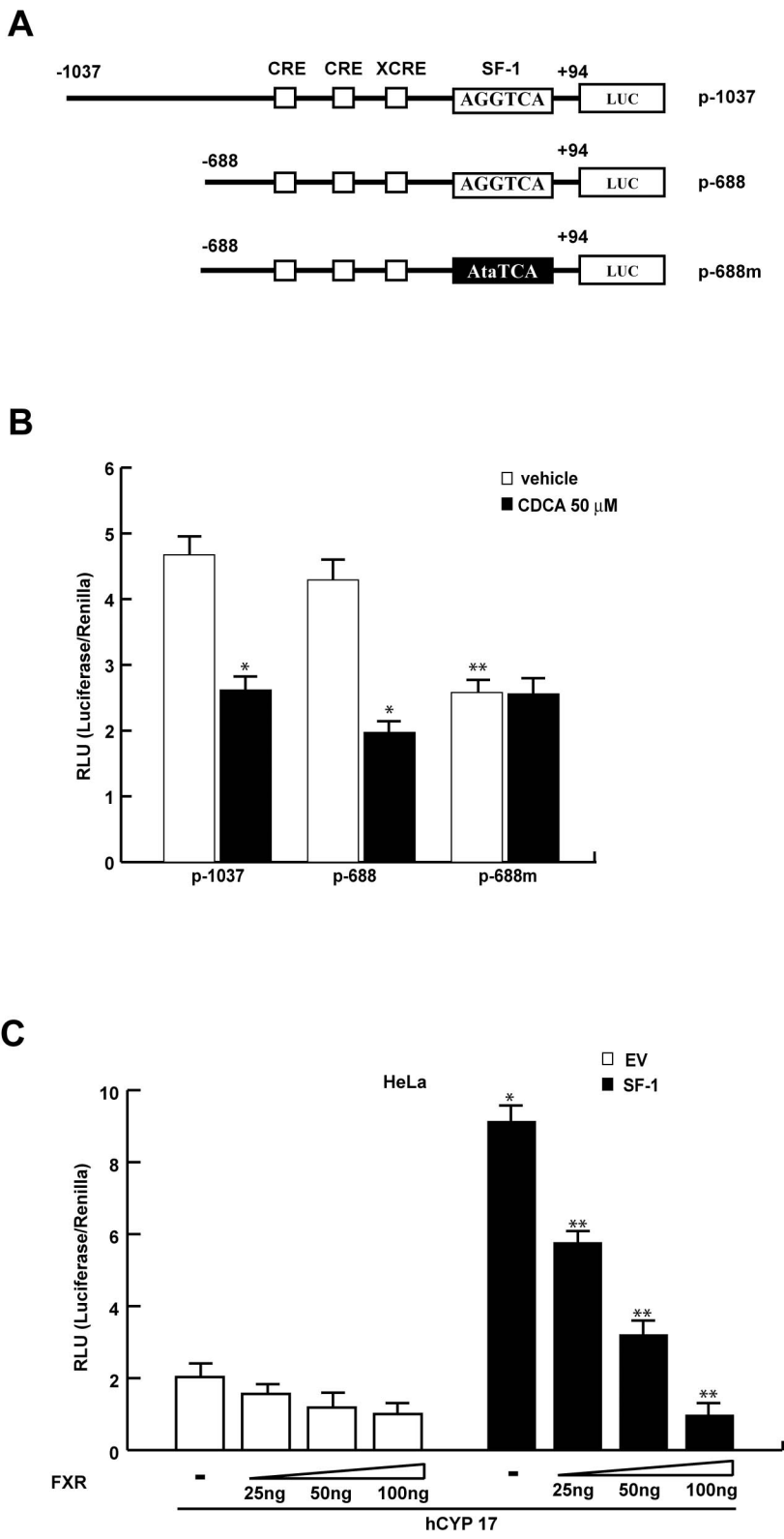
A
-1037
CRE
CRE
XCRE
SF-1
+94
AGGTCA
LUC
p-1037
-688
+94
AGGTCA
LUC
p-688
-688
+94
AtaTCA
LUC
p-688m
B
vehicle
CDCA 50 μM
RLU (Luciferase/Renilla)
0
1
2
3
4
5
6
*
*
**
p-1037
p-688
p-688m
C
HeLa
EV
SF-1
RLU (Luciferase/Renilla)
0
2
4
6
8
10
*
**
**
**
FXR
-
25ng
50ng
100ng
-
25ng
50ng
100ng
hCYP 17

Fig. 4

A

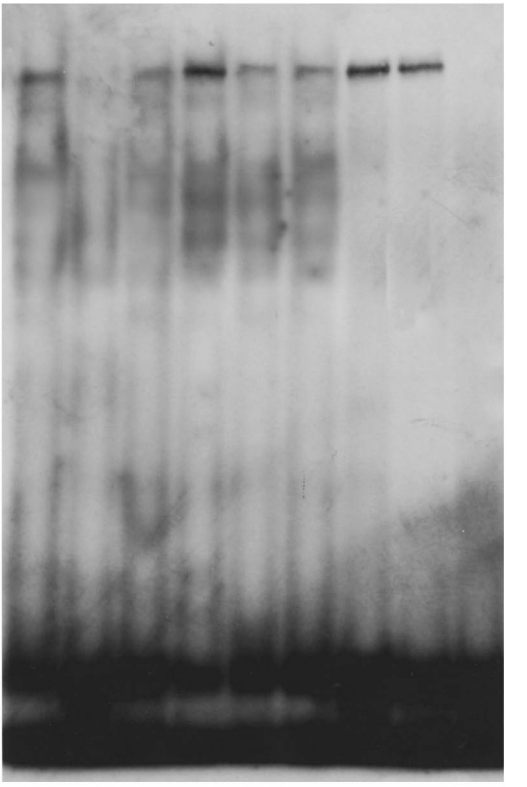

Nuclear extract	+	+	+	+	+	+	−	−	−
Competitor (100 fold excess)	−	+	Mut	−	−	−	−	−	−
CDCA 50 μM	−	−	−	+	+	+	−	−	−
Ab SF-1	−	−	−	−	+	−	−	−	−
Ab FXR	−	−	−	−	−	+	−	−	−
SF-1 protein	−	−	−	−	−	−	+	−	−
FXR protein	−	−	−	−	−	−	−	+	−

B

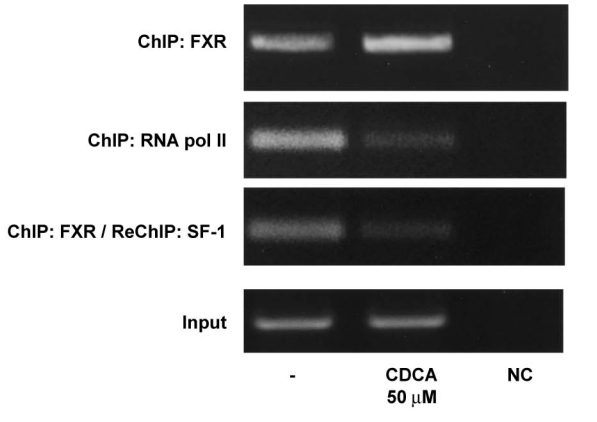

Fig. 5

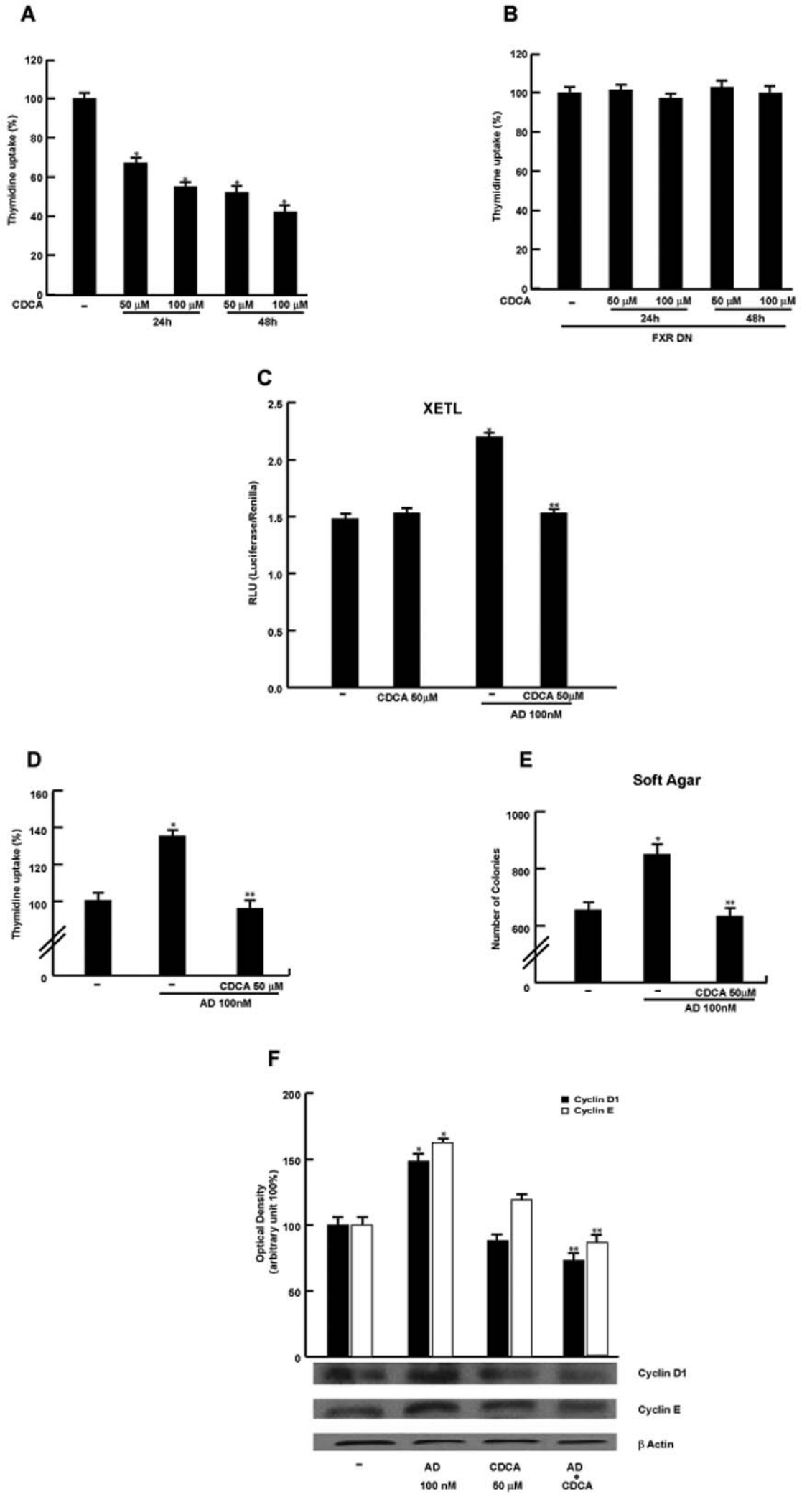
A
Thymidine uptake (%)
CDCA
–
50 μM
100 μM
50 μM
100 μM
24h
48h
B
Thymidine uptake (%)
CDCA
–
50 μM
100 μM
50 μM
100 μM
24h
48h
FXR DN
C
XETL
RLU (Luciferase/Renilla)
–
CDCA 50μM
–
CDCA 50μM
AD 100nM
D
Thymidine uptake (%)
–
–
CDCA 50 μM
AD 100nM
E
Soft Agar
Number of Colonies
–
–
CDCA 50μM
AD 100nM
F
Cyclin D1
Cyclin E
Optical Density (arbitrary unit 100%)
Cyclin D1
Cyclin E
β Actin
–
AD 100 nM
CDCA 50 μM
AD + CDCA

Fig. 6

Rapid Estradiol/ERα Signaling Enhances Aromatase Enzymatic Activity in Breast Cancer Cells

Stefania Catalano,* Ines Barone,* Cinzia Giordano, Pietro Rizza, Hongyan Qi, Guowei Gu, Rocco Malivindi, Daniela Bonofiglio, and Sebastiano Andò

Departments of Pharmaco-Biology (S.C., I.B., C.G., H.Q., G.G., R.M., D.B.) and Cell Biology (P.R., S.A.) and Centro Sanitario (C.G., S.A.), University of Calabria, 87030 Arcavacata di Rende (Cosenza), Italy

In situ estrogen production by aromatase conversion from androgens plays an important role in breast tumor promotion. Here, we show that 17β-estradiol (E_2) can rapidly enhance aromatase enzymatic activity through an increase of aromatase protein phosphorylation in breast cancer cell lines. *In vivo* labeling experiments and site-directed mutagenesis studies demonstrated that phosphorylation of the 361-tyrosine residue is crucial in the up-regulation of aromatase activity under E_2 exposure. Our results demonstrated a direct involvement of nonreceptor tyrosine-kinase c-Src in E_2-stimulated aromatase activity because inhibition of its signaling abrogated the up-regulatory effects induced by E_2 on aromatase activity as well as phosphorylation of aromatase protein. In addition, from our data it emerges that aromatase is a target of cross talk between growth factor receptors and estrogen receptor α signaling. These findings show, for the first time, that tyrosine phosphorylation processes play a key role in the rapid changes induced by E_2 in aromatase enzymatic activity, revealing the existence of a short nongenomic autocrine loop between E_2 and aromatase in breast cancer cells. **(*Molecular Endocrinology* 23: 1634–1645, 2009)**

Estrogens play a crucial role in the development and progression of breast cancer. The biosynthesis of estrogens from androgens is catalyzed by the enzyme complex termed "aromatase," which is composed of two polypeptides, an ubiquitous nonspecific flavoprotein, reduced nicotinamide adenine dinucleotide phosphate-cytochrome P450 reductase, and a specific microsomial form of cytochrome $P450_{arom}$ encoded by the cytochrome P450 (CYP)19 gene (1).

Aromatase expression in breast cancer tissue as well as in breast cancer cell lines has been shown by enzyme activity measurement, immunocytochemistry, and RT-PCR analysis (2–4). Cell culture (5) and nude mouse experiments (6) using aromatase-transfected MCF-7 cells have shown that aromatase expressed in breast cancer cells can promote tumor growth in both an autocrine and a paracrine manner. In addition, overexpression of aromatase in mammary gland of transgenic mice causes premalignant lesions, such as atypical ductal hyperplasia (7, 8). $P450_{arom}$ is found to be expressed at higher levels in cancer than in normal breast tissue (9, 10). Thus, induction of aromatase within the breast tumor can result in high levels of 17β-estradiol (E_2) production that, in turn, stimulate tumor growth. Indeed, intratumoral aromatase of breast carcinoma has been extensively studied for its potential clinical significance as a target for endocrine therapy using aromatase inhibitors (11, 12).

It is well known that aromatase is regulated at the transcriptional level through the alternative use of tissue-specific promoters (13, 14), whereas posttranscriptional regulation of this protein remains poorly understood. Balthazart *et al.* (15, 16) demonstrated that phosphatases modulate the activity of brain aromatase and that the phosphorylation status of the enzyme is critical for its activity. In addition, several studies have suggested that aromatase activity could be modulated at the posttrans-

ISSN Print 0888-8809 ISSN Online 1944-9917
Printed in U.S.A.

doi: 10.1210/me.2009-0039 Received January 23, 2009. Accepted June 19, 2009.
First Published Online June 25, 2009
* S.C. and I.B. contributed equally to this work.

Abbreviations: CHO, Chinese hamster ovary; CYP, cytochrome P450; E_2, 17β-estradiol; EGF, epidermal growth factor; EGFR, EGF receptor; ER, estrogen receptor; FBS, fetal bovine serum; GF-R, growth factor receptor; ICI, ICI 182,780; Mem-ECFP, membrane-enhanced cyan fluorescent protein; mERα, membrane ERα; NTA, nitrilotriacetic acid; PP2, 4-amino-5-(4-chlorophenyl)-7-(t.butyl)pyrazolo(3,4-d)pyramidine; RNAi, RNA interference; siRNA, small interfering RNA; TAM, tamoxifen; wt, wild type.

lation level in different cell types upon the addition of growth factors and kinase inhibitors (17–20). Recently, Miller *et al.* (21) demonstrated that aromatase serine (S) 118 is a potential phosphorylation site in mammalian cells, and mutation of S118 blocked phosphorylation and increased aromatase activity.

The classic effects of estrogens are mediated through binding to estrogen receptors (ERα and ERβ) and stimulation of transcription at nuclear levels. Recently, the nongenomic actions of estrogens have been reported through binding to membrane-associated ER (22, 23), which resides in or near the cell membrane and cross talks with the signal transduction pathways, including the c-Src/Ras/MAPK and cAMP pathway (24–26). Signaling from membrane ER induces posttranslational modification of many proteins. This includes the phosphorylation and regulation of enzymes, such as kinases or phosphatases, that impact cell physiology (27).

In the present study we demonstrated, in estrogen-dependent MCF-7 breast cancer epithelial cells, that 17β-estradiol (E_2) is able to rapidly up-regulate aromatase enzymatic activity, and this may occur through an enhanced tyrosine phosphorylation levels of aromatase protein. Our results provide a new insight into the regulation of aromatase through posttranscriptional modulation in human breast cancer cells.

Results

Rapid increase of aromatase activity induced by E_2 treatment

We first aimed to evaluate the effects of estrogens on aromatase activity by tritiated water assay in MCF-7 cells incubated for 10 and 120 min in the presence of 0.1, 1, and 10 nM of E_2. As reported in Fig. 1A, E_2 enhanced enzymatic activity at both times and doses investigated, even though to a higher extent under 1 and 10 nM E_2. The E_2 induction was also observed in MCF-7 cells transiently transfected with the aromatase gene (CYP19), that displayed a 6-fold increase in enzymatic activity (95.36 $\pm$ 0.92 fmol/h $\cdot$ mg protein) compared with parental MCF-7 cells (15.16 $\pm$ 0.47 fmol/h $\cdot$ mg protein) (Fig. 1B). To evaluate whether the E_2 effects on aromatase activity were transient, MCF-7 cells were treated with E_2 1 nM for different times (10 min; 6, 12, and 24 h; and 2, 4, and 6 d). We found that aromatase activity doubled upon E_2 exposure ranging from 10 min to 12 h and remained moderately high up to 6 d (data not shown). The ER antagonists, ICI 182,780 (ICI) and tamoxifen (TAM) were able to abrogate the up-regulation induced by E_2, whereas these treatments alone had no agonist activity (Fig. 1C). This suggests that estrogens can increase aromatase activity by binding to ERs.

It has been shown that the rapid actions of estrogen could be mediated by membrane-associated ER (22, 23). Thus, we cotransfected in ER-negative Chinese hamster ovary (CHO) cells CYP19 vector with ERα wild-type (wt) plasmid or membrane ERα (mERα) construct. The mERα construct consists solely of the AF-2/ligand binding domain (E) of ERα cloned into the membrane-enhanced cyan fluorescent protein (Mem-ECFP) vector that encodes a fusion protein called GAP-43 (N-terminal 20 amino acids of neuromodulin) containing a signal that targets this portion of the receptor to the plasma membrane (28, 29). This construct is a well-established mutant ERα able to discriminate the nongenomic to the genomic actions of E_2. As reported by Razandi *et al.* (30), expression of the E domain of ERα to the plasma membrane allowed the activation of ERK but did not result in the transactivation of an estrogen response element/luciferase reporter by E_2 treatment. As revealed in Fig. 1D, 1 and 10 nM E_2 for 10 min up-regulated enzymatic aromatase activity in CHO ectopically expressing mERα as well as ERα wt plasmids, suggesting that the expression of mERα is sufficient for E_2 induction.

We also evaluated the effects of E_2 on aromatase activity in ER-negative breast cancer cell line SKBR3 and in R2C rat Leydig tumor cells that express ERα and high levels of aromatase protein. No changes were observed in SKBR3 parental cells whereas E_2 treatment enhanced aromatase activity both in SKBR3, ectopically expressing ERα, and in R2C cells (Fig. 1, E and F). R2C cells displayed an elevated aromatase activity that is 1 order of magnitude higher than that detected in the other cell types investigated. This may probably explain the lack of E_2 dose-dependent stimulation of aromatase activity in the E_2 range concentration tested.

Because we observed an enhanced aromatase activity under E_2 treatment in a number of different cell lines, it could suggest that this regulation may underlie a general mechanism not related to cell specificity. However, this effect assumes a great importance in breast cancer cells, which are strongly dependent on estrogens for their growth.

E_2 increases tyrosine phosphorylation levels of aromatase protein

One mechanism by which E_2 might increase aromatase activity would be an enhancement in the transcription of aromatase mRNA and thus in the concentration of the enzyme. We performed RT-PCR and Western blotting analysis in MCF-7 cells treated with 1 nM E_2 for 10 and 120 min. We did not observe any change on aromatase

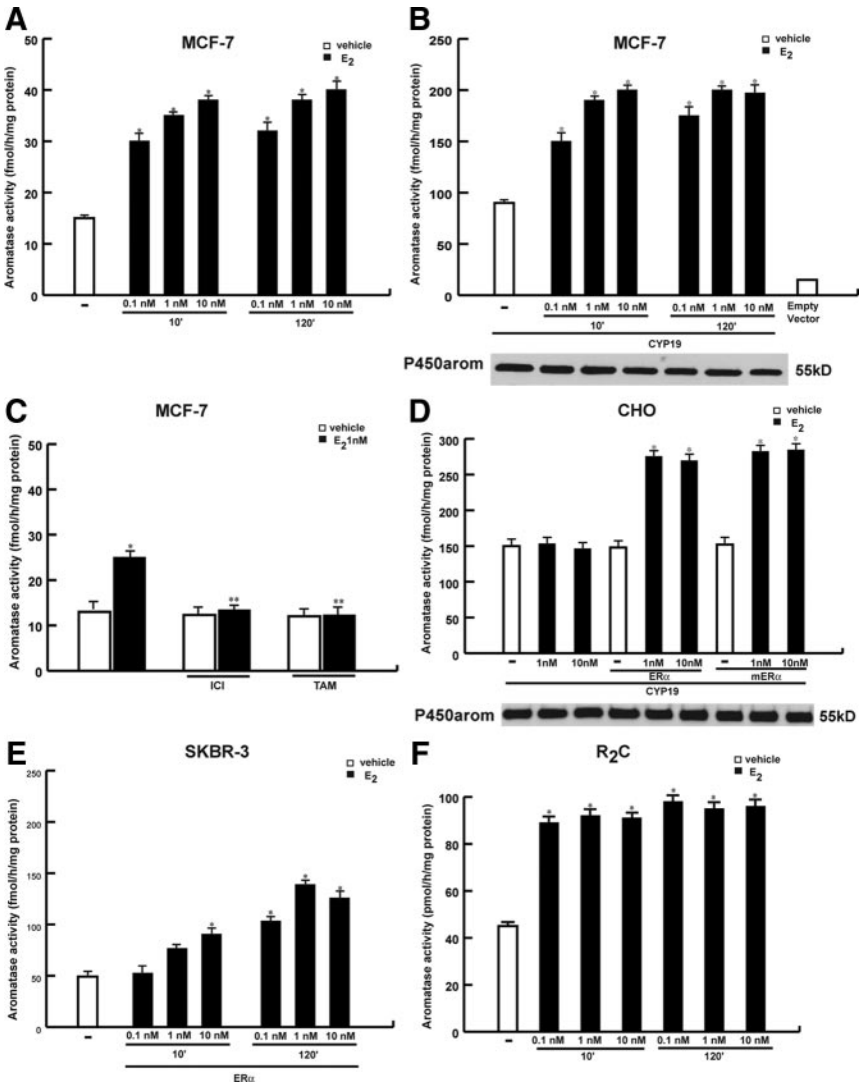

FIG. 1. Rapid effects of E_2 on aromatase activity. MCF-7 (A) or MCF-7 cells transiently transfected with CYP19 vector (B) were treated with vehicle (-) or 0.1, 1, and 10 nM E_2 for 10 and 120 min. Western blotting shows the expression of CYP19 vector used in the experiment. C, MCF-7 cells were pretreated with 1 μM ICI 182,780 (ICI) and 1 μM TAM for 30 min and then exposed or not to 1 nM E_2 for 10 min. D, CHO cells were transiently transfected with CYP19 vector and ERα wt or mERα or empty vector and treated with 1 and 10 nM E_2 for 10 min. Western blotting shows the expression of CYP19 vector used in the experiment. E, SKBR3 cells transiently transfected with ERα wt, and R2C cells (F) cells were treated as reported. Aromatase activity was performed as described in *Materials and Methods*. Empty vector: aromatase activity measured in cells transfected with pUC19 vector. The values represent the means $\pm$ SE of three different experiments, each performed with triplicate samples. *, $P < 0.01$ compared with vehicle; **, $P < 0.01$ compared with E_2-treated samples.

mRNA and protein level compared with the control (supplemental Fig. 1, A and B, published as supplemental data on The Endocrine Society's Journals Online web site at http://mend.endojournals.org). These results suggest that rapid changes in E_2-induced aromatase enzymatic activity are due to ERα action at the nongenomic level.

It is well known that the activity of many enzymes can be modulated rapidly by phosphorylation processes inducing conformational changes in the enzyme molecule. Previous analyses of the aromatase gene in a variety of mammalian and avian species demonstrated several consensus sites of phosphorylation on aromatase cDNA and deduced amino acid sequence (31–33). Thus, to evaluate the phosphorylation status of aromatase protein, we performed *in vivo* labeling experiment in MCF-7 cells transiently transfected with His_6-arom, a plasmid coding for the entire human aromatase sequence with six tandem histidine residues on the carboxyl terminus, as described in *Materials and Methods*. The His_6-tagged protein had the advantage to allow a higher yield of purified aromatase due to the specificity of Ni-NTA (nitrilotriacetic acid) agarose beads and avoid interference with the band of 55 kDa from heavy chains of antibodies used for immunoprecipitation. MCF-7 cells were transiently transfected with His_6-arom, metabolically labeled with radioactive orthophosphate and then treated with 1 and 10 nM E_2 for 10 min. Equal amounts of proteins were incubated with Ni-NTA agarose beads for isolation of recombinant $P450_{arom}$, and the eluates were run on SDS-PAGE. Autoradiography of the membrane revealed that aromatase protein was efficiently phosphorylated *in vivo* upon E_2 treatment (Fig. 2A). The membrane then was probed with an anti-aromatase antibody to visualize the input levels of the samples.

To determine which type of amino acid is phosphorylated, we performed Western blotting analysis with antibodies directed against phosphotyrosine and phosphoserine residues using cell lysates from MCF-7 cells transfected with His_6-arom and treated with 0.1, 1, and 10 nM E_2 for 10 min. Our results showed that E_2 was able to increase phosphotyrosine levels of purified aromatase protein, whereas no changes were detectable on serine phosphorylation status (Fig. 2B). This enhancement on tyrosine phosphorylation of aromatase was ERα-dependent because pretreatment with ICI reduced the E_2-associated tyrosine phosphorylation (Fig. 2C). We obtained similar results after pretreatment with TAM (data not shown). Moreover, in the presence of a specific inhibitor of tyrosine phosphatases, sodium orthovanadate, we observed an increase of aro-

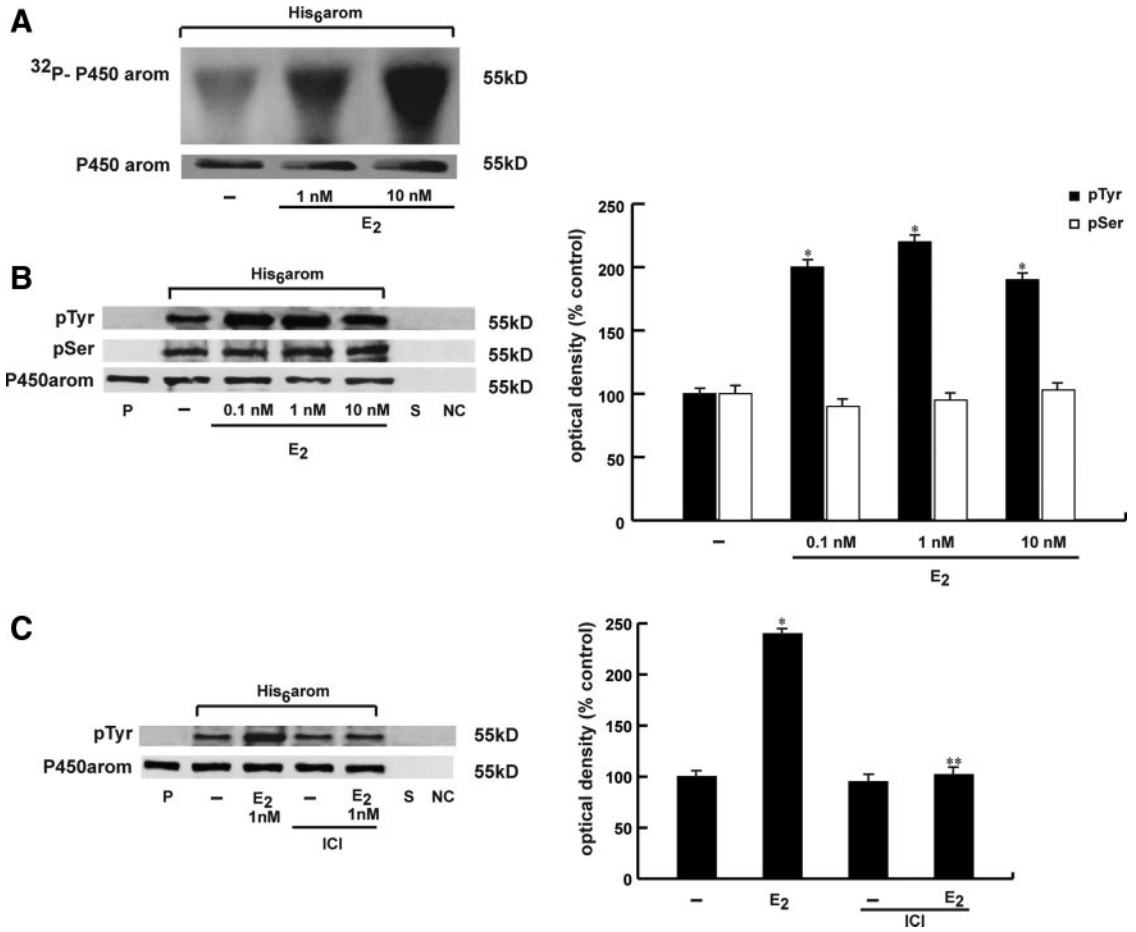

FIG. 2. Tyrosine phosphorylation levels of aromatase protein is enhanced by E_2. A, MCF-7 cells were transiently transfected with His_6-arom, labeled with [^{32}P]orthophosphate, and then treated with vehicle (-) or 1 and 10 nM E_2 for 10 min. Aromatase was purified using Ni-NTA agarose beads after which the complexes were resolved in SDS-PAGE. The *top panel* shows autoradiography of the SDS-PAGE, and the *bottom panel* shows immunoblot analysis with antiaromatase antibody ($P450_{arom}$) as a control for expressed protein. B, MCF-7 cells transiently transfected with His_6-arom were treated with vehicle (-) or 0.1, 1, and 10 nM E_2 for 10 min. Aromatase was purified using Ni-NTA agarose beads after which the complexes were resolved in SDS-PAGE. Immunoblotting was performed using the antiphosphotyrosine (pTyr) and antiphosphoserine (pSer) antibodies. C, MCF-7 cells transiently transfected with His_6-arom were pretreated with 1 μM ICI and then exposed or not to 1 nM E_2 for 10 min. To verify equal loading, the membrane was probed with antiaromatase antibody. Microsomal extracts from placenta (P) were used as positive control. As negative controls we used the supernatant removed after incubation with Ni-NTA agarose beads (S) and vector-transfected MCF-7 cell lysates incubated with Ni-NTA agarose beads (NC). The *side histograms* represent the means ± SE of three separate experiments in which band intensities were evaluated in terms of OD density arbitrary units and expressed as percentages of the control, which was assumed to be 100%. *, $P < 0.01$ compared with vehicle; **, $P < 0.01$ compared with E_2-treated samples. kD, Kilodaltons.

matase enzymatic activity as well as enhanced phosphotyrosine levels of purified aromatase protein, which were slightly increased by E_2 cotreatment (data not show).

All these data indicate that E_2 exposure is able to rapidly phosphorylate *in vivo* aromatase protein and increase tyrosine phosphorylation status of the enzyme.

Identification of tyrosine residue involved in the E_2 activation

Consensus phosphorylation sites of human aromatase protein were analyzed using the public domain software (netphos 2.0 server) available on the web site of the Center for Biological Sequence Analysis at http://www.cbs.dtu.dk. Based on a deduced amino acid sequence and on a previously encoded database of potential phosphorylation sites, this program identifies all serine, threonine, and tyrosine residues in the protein that could potentially be phosphorylated (34). The program also provides for each residue a phosphorylation score ranging from 0 to 1.0 the value of which was proportional to the probability that the residue could, in fact, be phosphorylated *in vivo*. A score equal or larger to 0.5 was considered to predict a likely phosphorylation consensus site (35). The netphos 2.0 program identified four of the 17 tyrosine residues. The residues located at positions 184 and 361 of the human aromatase sequence have the highest consensus scores (0.992 and 0.976, respectively). The position at 361 corresponds to the residue present in the steroid-binding domain, an important functional domain of human aromatase, and notably this residue and its immedi-

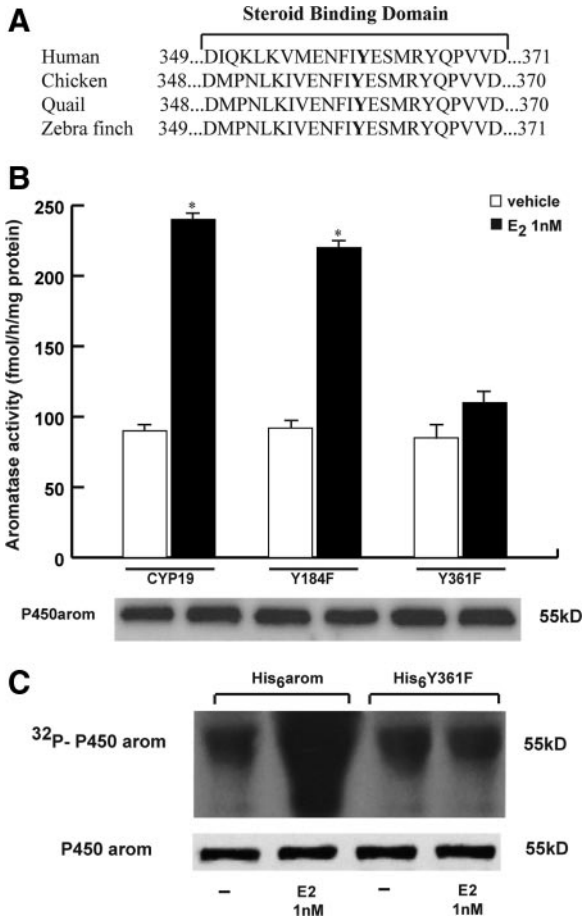

FIG. 3. Specific tyrosine residue involved in aromatase activation. A, Comparison of the amino acid sequences of steroid binding domain of aromatase in human, chicken, quail, and zebra finch. B, MCF-7 cells were transfected with CYP19 vector or Y184F or Y361F mutants, treated with vehicle or 1 nM E_2 for 10 min after which aromatase activity was performed. The values represent the means ± SE of three different experiments, each performed with triplicate samples. *, $P <$ 0.01 compared with vehicle. Western blotting shows the expression of DNA vectors used in the experiments. C, MCF-7 cells were transiently transfected with His_6-arom or His_6-Y361F, labeled with [^{32}P]orthophosphate, and then treated with vehicle (−) or 1 nM E_2 for 10 min. Aromatase was purified using Ni-NTA agarose beads after which the complexes were resolved in SDS-PAGE. The *top panel* shows autoradiography of the SDS-PAGE, and the *bottom panel* shows immunoblot analysis with antiaromatase antibody ($P450_{arom}$) as a control for expressed protein.

ate environment are well conserved across species (Fig. 3A). Thus, to address the location of the potential phosphorylation site within the aromatase protein, we mutated the conserved tyrosine (Y) at residue 361 as well as the one at 184 to phenylalanine (F) to create two different constructs, Y184F and Y361F. These plasmids were used in an aromatase enzymatic assay. We found that Y361F and Y184F mutation didn't affect the basal levels of aromatase activity. E_2 increased aromatase activity in cells transfected with Y184F mutant expression vector but had no effect in the presence of Y361F expression plasmid (Fig. 3B). To further confirm these results, we performed an *in vivo* labeling experiment in MCF-7 cells transiently transfected with either His_6-arom or His_6-Y361F constructs. We found that the His_6-Y361F mutated construct was not efficiently phosphorylated *in vivo* upon E_2 treatment (Fig. 3C). These data directly prove that phosphorylation of the 361 tyrosine residue is crucial in the upregulation of aromatase activity and its phosphorylation under E_2 stimulation. This last result led us to question which specific cellular kinase might be responsible for phosphorylation of aromatase at the Y361 site. The research for consensus sequences corresponding to the protein kinases pointed to the Y361 site as potentially phosphorylated by c-Src tyrosine kinase (with a consensus score higher than the critical value of 0.5). Taking into account that estrogen stimulation of breast cancer cells led to an immediate tyrosine phosphorylation and activation of the c-Src kinase (26, 36), we sought to determine whether c-Src might be the tyrosine kinase involved in the E_2 activation of aromatase protein. Thus, we performed Western blot analysis using the c-Src inhibitor, 4-amino-5-(4-chlorophenyl)-7-(t.butyl)pyrazolo(3,4-d)pyramidine (PP2), and as shown in Fig. 4A, PP2 reduced the E_2-associated tyrosine phosphorylation of the purified aromatase. In addition, PP2 treatment was able to abrogate the E_2-induced increase on aromatase enzymatic activity (Fig. 4B).

To further support the crucial role of c-Src, we examined whether knockdown of the c-Src gene would similarly reduce tyrosine aromatase phosphorylation. Transfection with pool of two small interfering RNA (siRNA) duplex specifically direct against human c-Src, reduced the expression of this protein (Fig. 4C). As shown in Fig. 4D, silencing of c-Src significantly decreased tyrosine phosphorylation of the purified aromatase induced by E_2.

We next examined the physical association between c-Src kinase and either wt or Y361F mutant aromatase proteins. To test this possibility, we transiently transfected MCF-7 cells with either His_6-arom or His_6-Y361F constructs. Equal amounts of proteins were incubated with Ni-NTA agarose beads for isolation of recombinant $P450_{arom}$ proteins followed by immunoblot for c-Src and $P450_{arom}$. Results obtained showed that both wt and Y361F mutant aromatase proteins were able to bind c-Src tyrosine kinase (Fig. 4E). We confirmed the formation of this protein complex by immunoprecipitation of c-Src and then detection of aromatase on Western blotting (data not shown).

Using *in vitro* recombinant c-Src kinase, we found that wt aromatase was more efficiently phosphorylated than Y361F mutant aromatase protein (Fig. 4F), addressing the importance of this residue of aromatase protein as phosphorylation substrate of c-Src.

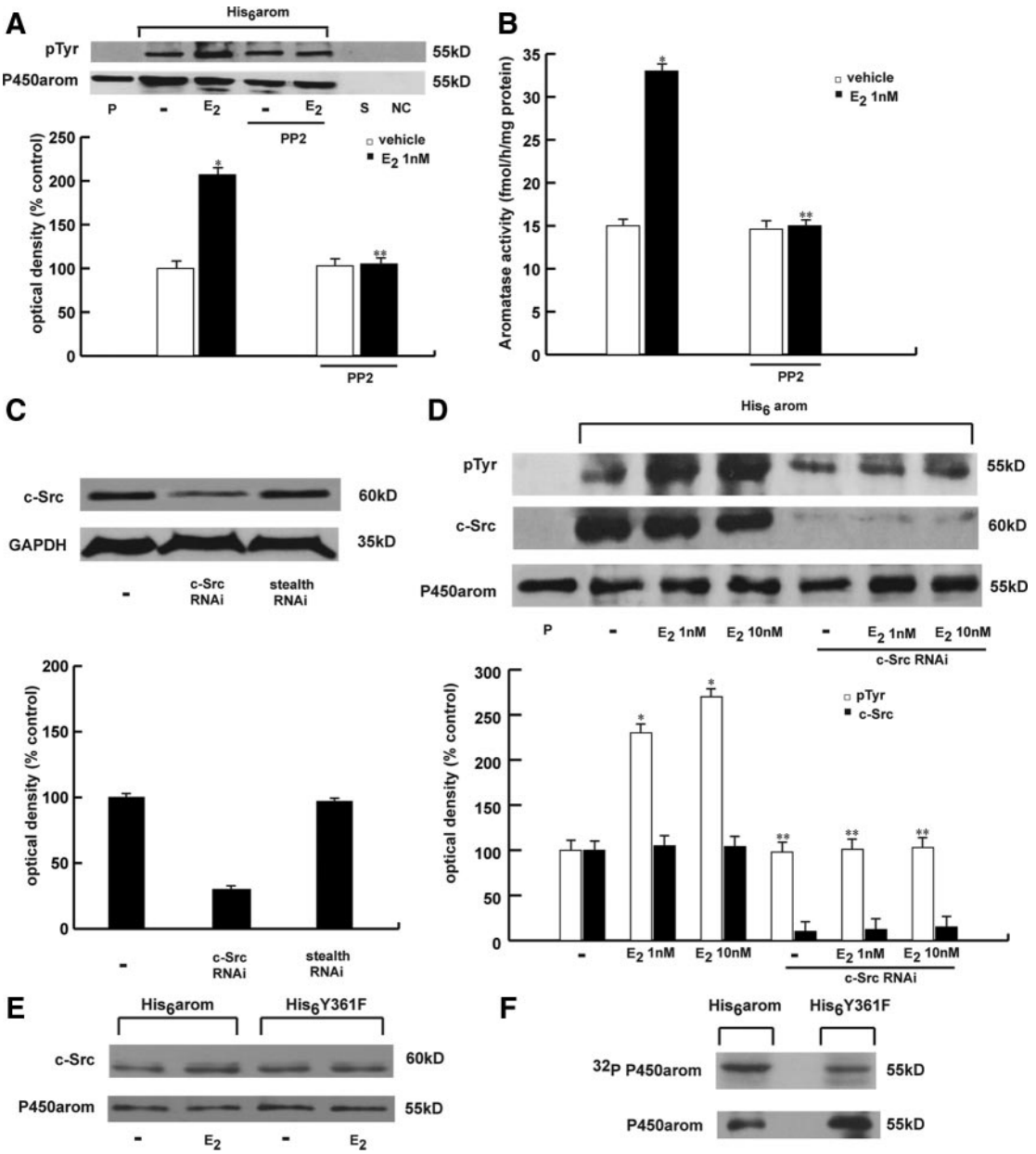

FIG. 4. c-Src signaling mediates E_2-induced aromatase activity. A, MCF-7 cells transiently transfected with His_6-arom were treated with vehicle (-) or 1 nM E_2 for 10 min, with or without pretreatment of PP2 (3 μM). The membrane was probed with antiphosphotyrosine (pTyr) antibody. To verify equal loading, the membrane was probed with antiaromatase antibody. Microsomal extracts from placenta (P) were used as positive control. As negative controls we used the supernatant removed after incubation with Ni-NTA agarose beads (S) and vector-transfected MCF-7 cell lysates incubated with Ni-NTA agarose beads (NC). The *histograms on the bottom* represent the means ± SE of three separate experiments in which band intensities were evaluated in terms of OD arbitrary units and expressed as percentages of the control, which was assumed to be 100%. *, $P < 0.01$ compared with vehicle; **, $P < 0.01$ compared with E_2-treated cells. B, MCF-7 cells were pretreated with or without PP2 (3 μM) before E_2 (1 nM) stimulation for 10 min, after which aromatase activity was performed. The values represent the means ± SE from triplicate assays. *, $P < 0.01$compared with vehicle; **, $P < 0.01$ compared with E_2-treated samples. C, c-Src protein expression (evaluated by Western blotting) in MCF-7 cells not transfected (-) or transfected with RNAi targeted human c-Src mRNA or with a stealth RNAi control as reported in *Materials and Methods*. Glyceraldehyde-3-phosphate dehydrogenase was used as loading control. The *histograms* represent the means ± SE of three separate experiments in which band intensities were evaluated in terms of OD arbitrary units and expressed as percentages of the control, which was assumed to be 100%. D, MCF-7 cells were not transfected or transfected with c-Src RNAi, then transfected with His_6-arom, and exposed to 1 and 10 nM E_2 for 10 min. The membrane was probed with antiphosphotyrosine (pTyr) or anti-c-Src antibodies. To verify equal loading, the membrane was probed with antiaromatase antibody. Microsomal extracts from placenta (P) were used as positive control. The *histograms* represent the means ± SE of three separate experiments in which band intensities were evaluated in terms of OD arbitrary units and expressed as percentages of the control, which was assumed to be 100%. *, $P < 0.01$ compared with vehicle; **, $P < 0.01$ compared with E_2-treated cells. E, MCF-7 cells were transfected with His_6-arom or His_6-Y361F vectors and then treated with E_2. Aromatase protein was purified using Ni-NTA agarose beads after which the complexes were resolved in SDS-PAGE. Immunoblotting was performed using the anti-c-Src and anti-aromatase ($P450_{arom}$) antibodies. F, MCF-7 cells were transfected with His_6-arom or His_6-Y361F vectors. *In vitro* c-Src kinase assay was performed on aromatase protein purified using Ni-NTA agarose beads using recombinant full-length human Src kinase. Autoradiography is shown in the *upper panel*, and input aromatase is shown in the *bottom panel*. kD, Kilodaltons.

Evidence that ERα, growth factor receptors (GF-Rs), c-Src, and aromatase interact in a multiprotein complex

Studies in breast cancer culture have highlighted an intimate cross talk between the endogenous membrane ER and GF-Rs signaling pathways (37–39). This process may involve the sequential activation of the cellular tyrosine kinase c-Src (26, 36, 40, 41). We wondered whether the cross talk between ERα and GF-Rs, through c-Src, could be involved in the rapid modulation of E_2-induced aromatase activity in breast cancer cells. To evaluate a direct protein-protein interaction among ERα, epidermal growth factor (EGF) receptor (EGFR), and aromatase, we performed coimmunoprecipitation studies. Particularly, MCF-7 cells transiently transfected with His_6-arom were lysated after which protein extracts were incubated with Ni-NTA agarose beads for isolation of recombinant $P450_{arom}$ (Fig. 5A, *left panel*). Equal amounts of the lysates were immunoprecipitated with ERα-specific antibody (Fig. 5A, *right panel*). The membranes were probed with anti-ERα, anti-EGFR, anti-c-Src, or antiaromatase antibodies. The results showed that ERα, EGFR, c-Src, and aromatase were in a multiprotein complex. Notably, the presence of c-Src is required for this complex formation because silencing of c-Src reduced the interaction of aromatase with ERα and EGFR (Fig. 5A).

Next, to determine whether EGFR stimulation leads to an increased production of E_2 via an up-regulation of aromatase enzymatic activity, MCF-7 cells were treated with 100 ng/ml EGF for 10 min. Our data demonstrated that EGF is able to enhance aromatase enzymatic activity as well as the tyrosine-phosphorylated status in the His_6-tagged purified aromatase protein to the same extent as E_2. Pretreatment with AG1478, a specific EGFR inhibitor, or ICI completely abrogated these effects (Fig. 5, B and C). The same results were obtained under treatment with IGF and AG1024, a monoclonal antibody specific to IGF-1R (data not shown).

These data indicate that the induction of aromatase enzymatic activity may involve the cross talk between E_2/ER and GF-Rs signaling.

Discussion

In the present study we demonstrate that short exposure to E_2 induces an increase of aromatase enzymatic activity, through an enhanced tyrosine phosphorylation level of the enzyme, in estrogen-dependent MCF-7 breast cancer epithelial cells.

Our results showed that the rapid effect induced by E_2 in enhancing aromatase activity was specifically mediated by the interaction of E_2 with ERα, because it was abrogated in the presence of ER antagonists, such as TAM and ICI. Moreover, when in ER-negative CHO cells overexpressing aromatase, we transfected the membrane ERα construct yielding the ligand-binding domain of the receptor exclusively localized to the cytoplasmic face of the membrane, we also reproduced the stimulatory effects of E_2 on aromatase activity. This underlines the ability of membrane ERα, which is unable to generate genomic response, in modulating aromatase activity. We also reproduced similar results in ER-negative breast cancer cells SKBR3, ectopically expressing ERα, and in R2C rat Leydig tumor cells, which display high aromatase expression. These latter results suggest that the rapid changes in aromatase activity may represent a general mechanism not related to cell specificity even though it assumes more relevance in breast cancer in which growth and progression are strongly estrogen dependent. Our data appear opposite to previous findings demonstrating that E_2 treatment reduced aromatase activity in breast cancer cells (42, 43). However, it is worthwhile to point out that they come from a different experimental design performed after a long-term E_2 exposure of MCF-7 cells either cultured long term in estrogen-deprived medium or stably transfected with the aromatase gene (MCF-7aro). For instance, Pasqualini and Chetrite (42) observed the maximal inhibition in aromatase activity (evaluated by quantification of ^{3}H-estradiol from cell incubated with [^{3}H]testosterone) at the nonphysiological dose of 50 μM in MCF-7aro. Instead, in our study, we evaluated aromatase activity by tritiated water release assay using as substrate [1β-^{3}H] androst-4-ene-3,17-dione (**Δ**4) in parental or transiently expressing aromatase MCF-7 cells. We demonstrated the maximal increase in aromatase enzymatic activity after a short time of exposure with low physiological doses of E_2.

The E_2 induced up-regulation of aromatase activity in MCF-7 cells was not correlated with any increase in the levels of aromatase mRNA and protein content, suggesting a posttranslational modulation of aromatase protein.

Posttranslational modification of enzymatic protein has been demonstrated for different members of the P450 enzyme family in vertebrates. For instance, cAMP-dependent protein kinase was essential for the activation of human and rat cholesterol 7α-hydroxylase (CYP7A) (44) as well as for phosphorylation of serine and threonine residues in human P450c17 (CYP17) (45, 46). Bovine P450scc (CYP11A1) has been identified as an active form phosphorylated by a protein kinase C (47), and similar activation of P450s through phosphorylation has been found in human liver enzymes such as CYP2E1 and CYP2B1 (48). Recently, phosphorylation of the cytochrome P450 aromatase has been proposed, even though

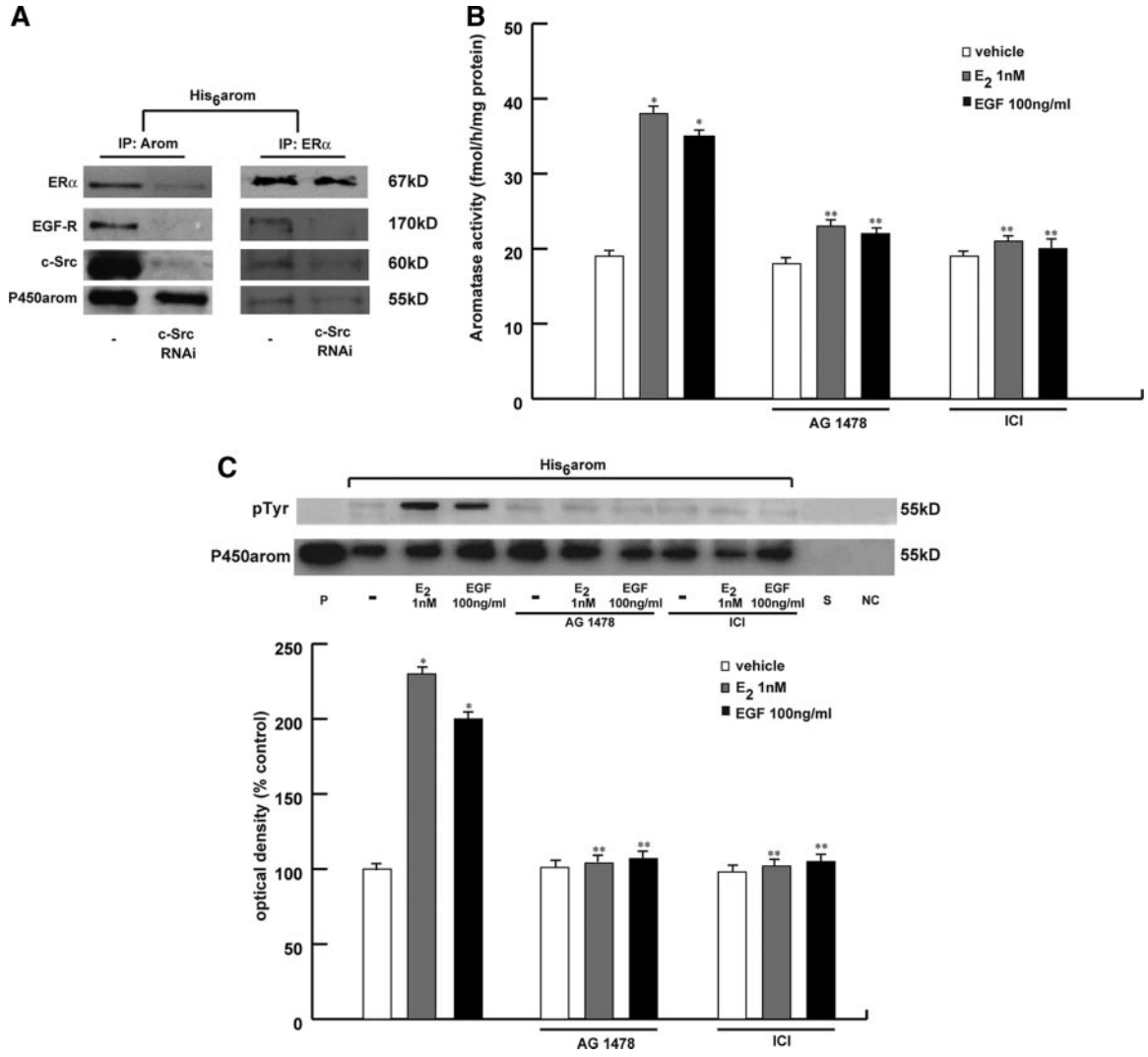

FIG. 5. Interaction between ERα and EGFR/c-Src in the aromatase activity induction. A, MCF-7 cells were not transfected (-) or transfected with c-Src RNAi and then transfected with His_6-arom vector. Aromatase protein was purified using Ni-NTA agarose beads after which the complexes were resolved in SDS-PAGE. In another set of experiments the same amount of cell lysate was immunoprecipitated (IP) with ERα antibody. Immunoblotting was performed using the anti-ERα, anti-EGFR, anti-c-Src, and antiaromatase antibodies. B, MCF-7 were pretreated with 10 μM AG1478 or 1 μM ICI for 30 min and then exposed to 1 nM E_2 or 100 ng/ml EGF. After 10 min, aromatase activity was performed. The values represent the means ± SE from triplicate assays. *, $P < 0.01$ compared with vehicle; **, $P < 0.01$ compared with E_2- or EGF-treated samples. C, MCF-7 cells transiently transfected with His_6-arom were pretreated with or without 10 μM AG1478 or 1 μM ICI for 30 min and then exposed to 1 nM E_2 or 100 ng/ml EGF for 10 min. The membrane was probed with antiphosphotyrosine (pTyr) antibody. To verify equal loading, the membrane was probed with antiaromatase antibody. P, Microsomal extracts from placenta. As negative controls we used the supernatant removed after incubation with Ni-NTA agarose beads (S) and vector-transfected MCF-7 cell lysates incubated with Ni-NTA agarose beads (NC). The *histograms* represent the means ± SE of three separate experiments in which band intensities were evaluated in terms of OD arbitrary units and expressed as percentages of the control, which was assumed to be 100%. *, $P < 0.01$ compared with vehicle; **, $P < 0.01$ compared with E_2- or EGF-treated samples. kD, Kilodaltons.

the specific kinases involved in this process are yet not well specified (16, 21). We demonstrated in MCF-7 cells that E_2 up-regulatory effects on aromatase activity resulted from a direct phosphorylation of enzymatic protein itself. Indeed, our *in vivo* labeling experiments showed, after E_2 treatment, a significant increase in phosphorylation of aromatase protein purified by Ni-NTA agarose beads. Particularly, we observed a specific enhancement of tyrosine phosphorylation levels of aromatase protein after E_2 exposure, whereas serine phosphorylation status remains unchanged. This suggests that the rapid nongenomic effects of the hormone specifically target tyrosine residues.

Site-directed mutagenesis experiments revealed that phosphorylation of the specific tyrosine residue, located at position 361 in the steroid-binding domain of aromatase protein, is crucial in the up-regulation of enzymatic activity after E_2 treatment. The 361-tyrosine residue of aromatase sequence is well conserved across species and represents a potential consensus site of

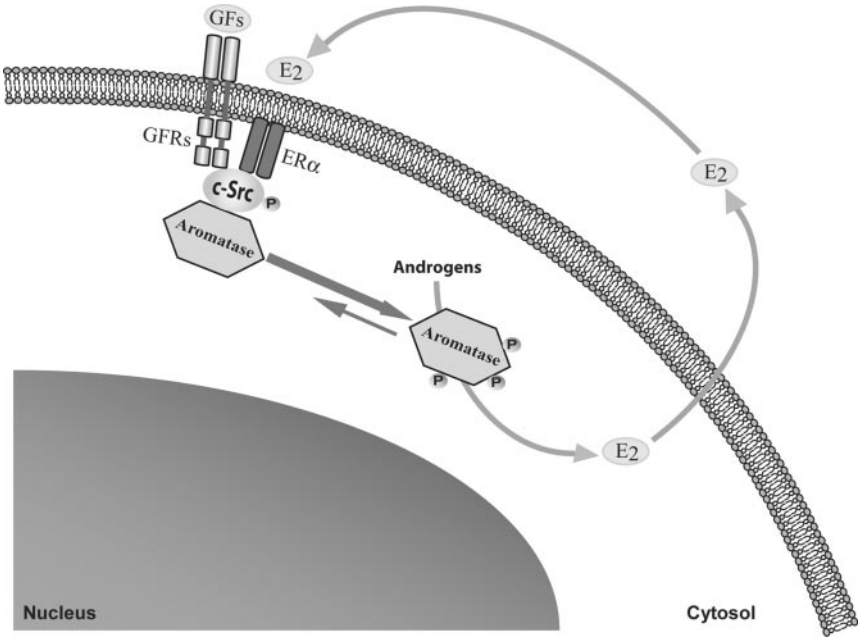

FIG. 6. Hypothetical model of the potential signaling transductional pathways through which E_2 and GFs (growth factors) may rapidly enhance aromatase activity in MCF-7 breast cancer cells. P, Placenta.

phosphorylation by an important nonreceptor tyrosine kinase c-Src (with a consensus score higher than the critical value of 0.5).

c-Src mediates signal transduction pathways implicated in proliferation, survival, cell adhesion, and migration (49). This kinase can be activated by many cell surface receptors and represents a crucial molecule downstream of ERα triggering estrogen rapid action (26, 36). In our study we demonstrated a direct interaction between c-Src and aromatase protein, and the involvement of this kinase in E_2-stimulated aromatase activity because blockade of c-Src activity completely reversed the E_2-induced increase of aromatase activity as well as reduced tyrosine phosphorylation of aromatase purified protein. Moreover, *in vitro* kinase activity assay using pure c-Src protein demonstrated that this kinase directly phosphorylates aromatase, and tyrosine located at the 361 site is involved in this event. Thus, we identified the phosphorylation of the critical residue 361 by c-Src kinase as a novel mechanism for regulating enzymatic activity and function of aromatase.

It is well known that ERα and GF-Rs utilize signaling pathways that intersect and directly interact at many levels. Estrogens have been shown to activate IGF-I receptor and EGFR (37–39), and it has been reported that E_2 upregulates aromatase expression via cross talk between ER and GF in breast cancer cells (17). A number of proteins, such as c-Src, Fak (focal adhesion kinase) MNAR (50), are reported to form a complex with ERs and to be involved in extranuclear functions of ERα. Our study shows the existence of a multipartite complex involving ERα, EGFR, c-Src, and aromatase. Silencing of c-Src by siRNA reduced the interaction of ERα and EGFR with aromatase, suggesting a key role of kinase active c-Src in the formation of this complex. In addition, treatment of MCF-7 cells with IGF-I and EGF increased, in a short time, aromatase activity as well as the tyrosine phosphorylation status of aromatase protein. Treatments with specific tyrosine kinase inhibitors of GF-Rs or with the antiestrogen ICI abrogated the GFs as well as the E_2 induction of aromatase activity. It has been largely demonstrated that c-Src is critical component of the bidirectional cross talk between ERα and GF-Rs (reviewed in Ref. 40). Thus, this may explain why, in the presence of antiestrogen or inhibitors of both GF-Rs tested, the up-regulatory effects on aromatase activity are not longer noticeable.

In summary, this study shows, for the first time, a new molecular mechanism by which E_2 rapidly increases aromatase activity through an enhanced tyrosine phosphorylation of the enzyme. We hypothesized that E_2, through an enhanced cross talk between GF-Rs, c-Src, and ER signaling, can phosphorylate and thus activate aromatase, resulting in a positive nongenomic autocrine loop between E_2 and aromatase in MCF-7 breast cancer cells (Fig. 6). All these data demonstrate that aromatase may be activated by different membrane cell signaling, which should be targeted in the novel therapeutic strategies for breast cancer treatment.

Materials and Methods

Cell cultures

MCF-7 and CHO cells were cultured in DMEM/F-12 medium containing 5% calf serum or 10% fetal bovine serum (FBS), respectively (Eurobio, Les Ullis Cedex, France). SKBR3 cells were cultured in RPMI 1640 medium supplemented with 10% FBS. R2C cells were cultured in Ham/F-10 supplemented with 15% HS, 2.5% FBS.

His_6-arom plasmid construction

His_6-arom plasmid construct was used to express the C-terminal 6×His-tagged form of human aromatase. The plasmid pUC19-arom containing the full-length of human aromatase gene (CYP19) was used as template. The 6×His epitope tag was inserted by two PCRs using the following primers: forward (5′-ATATAAGCTTATGGTTTTGGAAATGCTGA-3′) and two reverse (5′-ATGAT-

TABLE 1. Oligonucleotide Primers Used for Mutagenesis Studies

Mutant	Template	Primers	Sequence
Y184F	CYP19	Forward	5′-CCAATGAATCGGGCtttGTGGACGTGTTGACCC-3′
		Reverse	5′-GGGTCAACACGTCCACaaaGCCCGATTCATTGG-3′
Y361F	CYP19	Forward	5′-GAAAACTTCATTtttGAGAGCATGCGGTACCAGCCTGTCG-3′
		Reverse	5′-CGACAGGCTGGTACCGCAGCTCTCaaaAATGAAGTTTTCC-3′
His_6-Y361F	His_6-arom	Forward	5′-GAAAACTTCATTtttGAGAGCATGCGGTACCAGCCTGTCG-3′
		Reverse	5′-CGACAGGCTGGTACCGCAGCTCTCaaaAATGAAGTTTTCC-3′

GATGGTGTTCCAGACACCT-3′), (5′-ATATTCTAGACTAATGATGATGATGATGATGGTGTTCCAGA-3′). PCR product was subcloned into *Hin*dIII/*Xba*I sites of pcDNA3.1, and Hys_6-arom sequence was confirmed by nucleotide sequence analysis. We proved that the enzymatic activity of polyhistidine-containing recombinant protein was well preserved by measuring aromatase activity in MCF-7 cells transiently transfected with Hys_6-arom vector.

Site-directed mutagenesis

This step was performed with the QuikChange Site-Directed Mutagenesis kit (Stratagene, La Jolla, CA) according to manufacturer's standard method. The templates and the specific oligonucleotides used are summarized in Table 1.

Transient transfection

Transient transfection was performed using the FuGENE 6 (Roche, Indianapolis, IN) reagent with the mixture containing 1 μg/well of CYP19 or Y184F, Y361F mutants. A set of experiments was performed cotransfecting 1 μg/well of CYP19 and 1 μg/well of the membrane ERα construct (mERα) or ERα wt.

Aromatase activity assay

The aromatase activity in subconfluent MCF-7, SKBR3, CHO, and R2C cells culture medium was measured by the tritiated water release assay using 0.5 μM [1β-^{3}H]androst-4-ene-3,17-dione as substrate (51). The incubations were performed at 37 C for 3 h under an air-CO_2 (5%) atmosphere. The results obtained were expressed as fentomoles per h (MCF-7, CHO, and SKBR3) or picomoles per h (R2C) and normalized to mg of protein.

RT-PCR assay

Total cellular RNA was extracted from MCF-7 cells using TRIzol (Invitrogen, Carlsbad, CA). Aromatase mRNA was analyzed by the RT-PCR method as previously described (52).

Immunoblotting and immunoprecipitation analysis

Whole-cell lysates were prepared in lysing buffer [50 mmol/liter HEPES (pH 7.5), 150 mmol/liter NaCl, 1.5 mmol/liter $MgCl_2$, 1 mmol/liter EGTA, 10% glycerol, 1% Triton X-100, protease inhibitors (Sigma, Italy)]. Equal amounts of total protein were resolved on 11% SDS-PAGE, transferred onto a nitrocellulose membrane, and probed with antiserum against the human placental $P450_{arom}$ (Hauptman-Woodward Medical Research Institute, Buffalo, NY) or glyceraldehyde-3-phosphate dehydrogenase (Santa Cruz Biotechnology, Inc., Santa Cruz, CA). For immunoprecipitation studies, 300 μg of protein extracts was incubated with 1 μg of anti-ERα antibody (Santa Cruz) and 20 μl of protein A/G (Santa Cruz). The immunoprecipitated proteins were then subjected to Western blot analysis. Whole-cell lysates were used as input controls.

Detection of His_6-tagged aromatase protein by immunoblotting analysis

MCF7 cells were transiently transfected with His_6-arom or His_6-Y361F vectors and exposed to different treatments before lysis. Cellular proteins (300 μg) were incubated with Ni-NTA agarose beads (Invitrogen). Ni-NTA resin was used to isolate P450 aromatase tagged with six tandem histidine residues from cellular lysates. The beads containing bound proteins were washed in PBS buffer added with a mixture of protease inhibitors and analyzed by Western blot. Membrane was probed with a antibodies against human cytochrome $P450_{arom}$ (Serotec, Oxford, UK) or phosphotyrosine-containing proteins (pY99, Santa Cruz) or phosphoserine-containing proteins. For coimmunoprecipitation studies, membranes were probed with ERα, EGFR, and c-Src antibodies (Santa Cruz). Two set of controls were done in parallel: surnatant removed after the first centrifugation was added to one control and vector-transfected cell lysates plus Ni-NTA agarose beads was included in the other control. Microsomal extracts from placenta were used as positive control.

In vivo phosphorylation experiments

MCF-7 cells were transiently transfected with His_6-arom or His_6-Y361F construct, labeled for 2 h with [^{32}P]orthophosphate (PerkinElmer, Boston, MA) (0.5 mCi/ml in Krebs Ringer buffer, pH 7.4, containing 1% BSA), treated with E_2, washed with PBS, and immunoprecipitated with Ni-NTA agarose beads as described above. The supernatants were resolved onto 10% SDS-PAGE gel and transferred onto nitrocellulose membrane. Phosphorylated aromatase-purified protein was detected by autoradiography, and the aromatase protein level was determined by immunoblot of the same membrane with antiaromatase antibody.

In vitro c-Src kinase activity assay

C-Src kinase activity was measured by phosphorylation of aromatase protein specifically purified from lysates of MCF-7 cells transiently transfected with His_6-arom or His_6-Y361F constructs, as previously described. The washed Ni-NTA beads containing bound aromatase proteins were incubated with recombinant full-length human Src kinase (Cell Signaling Technology, Danvers, MA) in the presence of 10 μCi of [γ-^{32}P]ATP and 10 nmol/liter ATP in 40 μl kinase buffer at 30 C for 30 min. The reactions were stopped by the addition of sodium dodecyl sulfate loading buffer, and the samples were resolved by 10% SDS-PAGE. The phosphorylated aromatase protein bands were visualized by autoradiography.

c-Src knockdown by siRNA

MCF-7 cells were transfected with validated stealth RNA interference (RNAi) DuoPak (Invitrogen) targeted human c-Src or with a stealth RNAi control to a final concentration of 100 nM using Lipofectamine 2000 (Invitrogen) as recommended by the manufacturer. After 5 h the transfection medium was changed with serum free medium, transfected with His_6-arom vector, and then exposed to E_2. These transfected cells were used to immunoblotting analysis.

Statistical analysis

Each datum point represents the mean ± SE of three different experiments. Statistical analysis was performed using ANOVA followed by Newman-Keuls testing to determine differences in means. $P < 0.05$ was considered as statistically significant.

Acknowledgments

We thank Dr. E. R. Simpson and Dr. C. D. Clyne (Prince Henry's Institute of Medical Research, Clayton, Australia) and Dr. E. R. Levin (University of California, Irvine) for generously providing pUC19-arom and mERα plasmids, respectively.

Address all correspondence and requests for reprints to: Professor Sebastiano Andò, Department of Cell Biology University of Calabria, Arcavacata di Rende (CS) 87030, Italy. E-mail: sebastiano.ando@unical.it.

This work was supported by Associazione Italiana per la Ricerca sul Cancro (AIRC) grants in 2007 and 2008.

Disclosure Summary: All authors have nothing to declare.

References

1. **Simpson ER, Mahendroo MS, Means GD, Kilgore MW, Hinshelwood MM, Graham-Lorence S, Amarneh B, Ito Y, Fisher CR, Michael MD, Mendelson CR, Bulun SE** 1994 Aromatase cytocrome P450, the enzyme responsible for estrogen biosynthesis. Endocr Rev 15:342–355
2. **Sasano H, Nagura H, Harada N, Goukon Y, Kimura M** 1994 Immunolocalization of aromatase and other steroidogenic enzyme in human breast disorders. Hum Pathol 25:530–535
3. **Sourdaine P, Mullen P, White R, Telford J, Parker MG, Miller WR** 1996 Aromatase activity and CYP19 gene expression in breast cancers. J Steroid Biochem Mol Biol 59:191–198
4. **Maggiolini M, Carpino A, Bonofiglio D, Pezzi V, Rago V, Marsico S, Picard D, Andò S** 2001 The direct proliferative stimulus of dehydroepiandrosterone on MCF-7 breast cancer cells is potentiated by overexpression of aromatase. Mol Cell Endocrinol 184:163–171
5. **Sun XZ, Zhou D, Chen S** 1997 Autocrine and paracrine actions of breast tumor aromatase. A three-dimensional cell culture study involving aromatase transfected MCF-7 and T-47D cells. J Steroid Biochem Mol Biol 63:29–36
6. **Yue W, Zhou D, Chen S, Brodie A** 1994 A new nude mouse model for postmenopausal breast cancer using MCF-7 cells transfected with the human aromatase gene. Cancer Res 54:5092–5095
7. **Tekmal RR, Ramachandra N, Gubba S, Durgam VR, Mantione J, Toda K, Shizuta Y, Dillehay DL** 1996 Overexpression of int-5/aromatase in mammary glands of transgenic mice results in the induction of hyperplasia and nuclear abnormalities. Cancer Res 56:3180–3185
8. **Gill K, Kirma N, Tekmal RR** 2001 Overexpression of aromatase in transgenic male mice in the induction of gynecomastia and other biochemical changes in mammary glands. J Steroid Biochem Mol Biol 77:13–18
9. **Harada N** 1997 Aberrant expression of aromatase in breast cancer tissues. J Steroid Biochem Mol Biol 61:175–184
10. **Miller WR** 1997 Uptake and synthesis of steroid hormones by the breast. Endocr Relat Cancer 4:307–311
11. **Santen RJ, Yue W, Naftolin F, Mor G, Berstein L** 1999 The potential of aromatase inhibitors in breast cancer prevention. Endocr Relat Cancer 6:235–243
12. **Altundag K, Ibrahim NK** 2006 Aromatase inhibitors in breast cancer: an overview. Oncologist 11:553–562
13. **Simpson ER, Michael MD, Agarwal VR, Hinshelwood MM, Bulun SE, Zhao Y** 1997 Expression of the CYP19 (aromatase) gene: an unusual case of alternative promoter usage. FASEB J 11:29–36
14. **Bulun SE, Sebastian S, Takayama K, Suzuki T, Sasano H, Shozu M** 2003 The human CYP19 (aromatase P450) gene: update on physiologic roles and genomic organization of promoters. J Steroid Biochem Mol Biol 86:219–224
15. **Balthazart J, Baillien M, Ball GF** 2001 Phosphorylation processes mediate rapid changes of brain aromatase activity. J Steroid Biochem Mol Biol 79:261–277
16. **Balthazart J, Baillien M, Ball GF** 2006 Rapid control of brain aromatase activity by glutamatergic imputs. Endocrinology 147: 359–366
17. **Kinoshita Y, Chen S** 2003 Induction of aromatase (CYP19) expression in breast cancer cells through a nongenomic action of estrogen receptor α. Cancer Res 63:3546–3555
18. **Richards JA, Petrel TA, Brueggemeier RW** 2002 Signaling pathways regulating aromatase and cyclooxygenases in normal and malignant breast cells. J Steroid Biochem Mol Biol 80:203–212
19. **Shozu M, Sumitani H, Murakami K, Segawa T, Yang HJ, Inoue M** 2001 Regulation of aromatase activity in bone-derived cells: possible role of mitogen-activated protein kinase. J Steroid Biochem Mol Biol 79:61–65
20. **Yue W, Wang JP, Conaway MR, Li Y, Santen RJ** 2003 Adaptive hypersensitivity following long-term estrogen deprivation: involvement of multiple signal pathways. J Steroid Biochem Mol Biol 86: 65–274
21. **Miller WT, Shin I, Kagawa N, Evans DB, Waterman MR, Arteaga CL** 2008 Aromatase is phosphorylated *in situ* at Serine-118. J Steroid Biochem Mol Biol 112:95–101
22. **Razandi M, Pedram A, Park ST, Levin ER** 2003 Proximal events in signaling by plasma membrane estrogen receptors. J Biol Chem 24:2701–2712
23. **Hammes SR, Levin ER** 2007 Extranuclear steroid receptors: nature and actions. Endocr Rev 28:726–741
24. **Kato S, Endoh H, Masuhiro Y, Kitamoto T, Uchiyama S, Sasaki H, Masushige S, Gotoh Y, Nishida E, Kawashima H, Metzger D, Chambon P** 1995 Activation of the estrogen receptor through phosphorylation by mitogen-activated protein kinase. Science 270:1491–1494
25. **Migliaccio A, Di Domenico M, Castoria G, de Falco A, Bontempo P, Nola E, Auricchio F** 1996 Tyrosine kinase/p21 ras/MAP-kinase pathway activation by estradiol-receptor complex in MCF-7 cells. EMBO J 15:1292–1300
26. **Song RX, Zhang Z, Santen RJ** 2005 Estrogen rapid action via protein complex formation involving ERα and Src. Trends Endocrinol Metab 16:347–353
27. **Levin ER** 2005 Integration of the extra-nuclear and nuclear actions of estrogen. Mol Endocrinol 19:1951–1959
28. **Kousteni S, Bellido T, Plotkin LI, O'Brien CA, Bodenner DL, Han L, Han K, DiGregorio GB, Katzenellenbogen JA, Katzenellenbogen BS, Roberson PK, Weinstein RS, Jilka RL, Manolagas SC** 2001 Nongenotropic, sex-nonspecific signalling through the estrogen or androgen receptors: dissociation from transcriptional activity. Cell 104:719–730
29. **Razandi M, Pedram A, Rosen EM, Levin ER** 2004 BRCA 1 inhibits membrane estrogen and growth factor receptor signaling to cell proliferation in breast cancer. Mol Cell Biol 24:5900–5913
30. **Razandi M, Oh P, Pedram A, Schnitzer J, Levin ER** 2002 ERs

associate with and regulate the production of caveolin: implications for signalling and cellular actions. Mol Endocrinol 16:100–115
31. **Harada N** 1988 Cloning of a complete cDNA encoding human aromatase: immunochemical identification and sequence analysis. Biochem Biophys Res Commun 156:725–732
32. **McPhaul MJ, Noble JF, Simpson ER, Mendelson CR, Wilson JD** 1988 The expression of a functional cDNA encoding the chicken cytochrome P-450arom (aromatase) that catalyzes the formation of estrogen from androgen. J Biol Chem 263:16358–16363
33. **Shen P, Campagnoni CW, Kampf K, Schlinger BA, Arnold AP, Campagnoni AT** 1994 Isolation and characterization of a zebra finch aromatase cDNA: in situ hybridization reveals high aromatase expression in brain. Mol Brain Res 24:227–237
34. **Kennelly PJ, Krebs EG** 1991 Consensus sequences as substrate specificity determinants for protein kinases and protein phosphatases. J Biol Chem 266:15555–15558
35. **Blom N, Gammeltoft S, Brunak S** 1999 Sequence and structure based prediction of eukaryotic protein phosphorylation sites. J Mol Biol 294:1351–1362
36. **Migliaccio A, Castoria G, Di Domenico M, De Falco A, Bilancio A, Auricchio F** 2002 Src is an initial target of sex steroid hormone action. Ann NY Acad Sci 963:185–190
37. **Lee AV, Cui X, Oesterreich S** 2001 Cross-talk among estrogen receptor, epidermal growth factor, and insulin like growth factor signaling in breast cancer. Clin Cancer Res 7:4429s–4435s; discussion 4411s–4412s
38. **Stoll BA** 2002 Oestrogen/insulin-like growth factor-I receptor interaction in early breast cancer: clinical implications. Ann Oncol 13:191–196
39. **Levin ER** 2003 Bidirectional signaling between the estrogen receptor and the epidermal growth factor receptor. Mol Endocrinol 17:309–317
40. **Ishizawar R, Parsons SJ** 2004 c-Src and cooperating partners in human cancer. Cancer Cell 6:209–214
41. **Migliaccio A, Di Domenico M, Castoria G, Nanayakkara M, Lombardi M, de Falco A, Bilancio A, Varricchio L, Ciociola A, Auricchio F** 2005 Steroid receptor regulation of epidermal growth factor signaling through Src in breast and prostate cancer cells: steroid antagonist action. Cancer Res 65:10585–10593
42. **Pasqualini JR, Chetrite GS** 2006 Estradiol as an anti-aromatase agent in human breast cancer cells. J Steroid Biochem Mol Biol 98:12–17
43. **Yue W, Berstein LM, Wang JP, Clark GM, Hamilton CJ, Demers LM, Santen RJ** 2001 The potential role of estrogen in aromatase regulation in the breast. J Steroid Biochem Mol Biol 79:157–164
44. **Nguyen LB, Shefer S, Salen G, Chiang JY, Patel M** 1996 Cholesterol 7α-hydroxylase activities from human and rat liver are modulated in vitro post-translationally by phosphorylation-dephosphorylation. Hepatology 24:1468–1474
45. **Biason-Lauber A, Kempken B, Werder E, Forest MG, Einaudi S, Ranke MB, Matsuo N, Brunelli V, Schönle EJ, Zachmann M** 2000 17α-Hydroxylase/17,20-lyase deficiency as a model to study enzymatic activity regulation: role of phosphorylation. J Clin Endocrinol Metab 85:1226–1231
46. **Zhang LH, Rodriguez H, Ohno S, Miller WL** 1995 Serine phosphorylation of human P450c17 increases 17,20-lyase activity: implications for adrenarche and the polycystic ovary syndrome. Proc Natl Acad Sci USA 92:10619–10623
47. **Defaye G, Monnier N, Guidicelli C, Chambaz EM** 1982 Phosphorylation of purified mitochondrial cytochromes P450 (cholesterol desmolase and 11 β-hydroxylase) from bovine adrenal cortex. Mol Cell Endocrinol 27:157–168
48. **Oesch-Bartlomowicz B, Padma PR, Becker R, Richter B, Hengstler JG, Freeman JE, Wolf CR, Oesch F** 1998 Differential modulation of CYP2E1 activity by cAMP-dependent protein kinase upon Ser129 replacement. Exp Cell Res 242:294–302
49. **Thomas SM, Brugge JS** 1997 Cellular functions regulated by Src family kinases. Annu Rev Cell Dev Biol 13:513–609
50. **Wong CW, McNally C, NicKbarg E, Komm BS, Cheskis BJ** 2002 Estrogen receptor-interacting protein that modulates its nongenomic activity-crosstalk with Src/Erk phosphorylation cascade. Proc Natl Acad Sci USA 99:4783–14788
51. **Lephart ED, Simpson ER** 1991 Assay of aromatase activity. Methods Enzymol 206:477–483
52. **Catalano S, Marsico S, Giordano C, Mauro L, Rizza P, Panno ML, Andò S** 2003 Leptin enhances, via AP-1, expression of aromatase in the MCF-7 cell line. J Biol Chem 278:28668–28676

Progesterone Receptor B Recruits a Repressor Complex to a Half-PRE Site of the Estrogen Receptor α Gene Promoter

F. De Amicis, S. Zupo, M. L. Panno, R. Malivindi, F. Giordano, I. Barone, L. Mauro, S. A. W. Fuqua, and S. Andò

Department of Pharmaco-Biology (F.D., S.Z., R.M.), and Cellular Biology (M.L.P., F.G., L.M., S.A.) University of Calabria, Rende (Cosenza) Italy; Lester and Sue Smith Breast Center (I.B., S.A.W.F.), Baylor College of Medicine, Houston, Texas 77030

In the present study, we demonstrate that elevated levels of the progesterone receptor (PR)-B isoform in breast cancer cells induces down-regulation of estrogen receptor (ER) α mRNA and protein content, causing concomitant repression of the estrogen-regulated genes insulin receptor substrate 1, cyclin D1, and pS2, addressing a specific effect of PR/PR-B on ERα gene transcription. ERα gene promoter activity was drastically inhibited by PR-B overexpression. Promoter analysis revealed a transcriptionally responsive region containing a half-progesterone response element (PRE) site located at -1757 bp to -1752 bp. Mutation of the half-PRE down-regulated the effect induced by PR/PR-B overexpression. Moreover chromatin immunoprecipitation analyses revealed an increase of PR bound to the ERα-regulatory region encompassing the half-PRE site, and the recruitment of a corepressor complex containing nuclear receptor corepressor (NCoR) but not silencing mediator of retinoid and thyroid hormone receptor and DAX1, concomitantly with hypoacetylation of histone H4 and displacement of RNA polymerase II. Furthermore, NCoR ablation studies demonstrated the crucial involvement of NCoR in the down-regulatory effects due to PR-B overexpression on ERα protein and mRNA. We also demonstrated that the ERα regulation observed in MCF-7 cells depended on PR-B expression because PR-B knockdown partially abrogates the feedback inhibition of ERα levels after estrogenic stimulus. Our study provides evidence for a mechanism by which overexpressed PR-B is able to actively repress ERα gene expression. **(*Molecular Endocrinology* 23: 454–465, 2009)**

The sex steroid hormones, estradiol and progesterone (Pg), play important roles in normal mammary gland development, and it is thought that breast cancer progression is influenced by them and their receptors (1, 2). The level of these steroid hormone receptors is a prognostic factor for patients with breast cancer and has been used in clinical management as an indicator of endocrine responsiveness (3, 4). Although it is well accepted that enhanced expression of estrogen receptor α (ERα) is an early event in breast carcinogenesis, the role of progesterone receptor (PR) has been more controversial. Recent studies published on the largest retrospective analysis of early breast cancer treated with tamoxifen found that patients with ER+/PR+ tumors derived more benefit from adjuvant tamoxifen therapy than those patients with ER+/PR− tumors (5). Importantly, in multivariate analyses including lymph node involvement, tumor size, and age, PR status was independently associated with disease-free and overall survival (6).

PRs belong to the subfamily of classical nuclear steroid receptors, and human PR proteins exist as two isoforms, termed PR-A and PR-B, that are transcribed from a single gene under the control of separate promoters (7). Despite structural similarities, PR-A and PR-B regulate different subsets of genes and, although PR-B is transcriptionally more active, there are genes, known to be involved in breast cancer progression, that are uniquely regulated by the PR-A isoform (8, 9). *In vivo* the two PR isoforms are usually coexpressed at similar levels in normal

ISSN Print 0888-8809 ISSN Online 1944-9917
Printed in U.S.A.

doi: 10.1210/me.2008-0267 Received July 31, 2008. Accepted January 8, 2009.
First Published Online January 15, 2009

Abbreviations: AR, Androgen receptor; ARE, androgen-responsive element; ChIP, chromatin immunoprecipitation; DBD, DNA-binding domain; E2, Estradiol; ERα, estrogen receptor α; ERE, estrogen-responsive element; FCS, fetal calf serum; GAPDH, glyceraldehyde-3-phosphate dehydrogenase; LBD, ligand-binding domain; Pg, progesterone; Pol II, polymerase II; PR-A, progesterone receptor-A; PR-B, progesterone receptor-B; PRE, progesterone responsive element; NCoR, nuclear receptor corepressor; SDS, sodium dodecyl sulfate; siRNA, small interfering RNA; SMRT, silencing mediator of retinoic acid and thyroid hormone receptor; XETL, luciferase reporter plasmid containing ERE consensus.

cells, but their ratio varies dramatically in different tissues, in varying physiological states, and disease sites (10, 11). With regard to the mammary gland, 3:1 overexpression of PR-A over PR-B in transgenic mice results in extensive epithelial cell hyperplasia, excessive ductual branching, and disorganized basement membrane, all features associated with neoplasia. In contrast, overexpression of PR-B leads to premature ductal growth arrest and inadequate lobulo-alveolar differentiation (12, 13). Moreover the loss of coordinated PR-A and PR-B expression is thought to be an early event in carcinogenesis and is evident in premalignant breast lesions (14). A significant proportion of carcinomas express a predominance of the PR-A isoform, and elevated PR-A has been associated with poor clinical outcomes in endometrial cancer, indicating a direct association between PR-A isoform predominance and poor prognosis (15).

Although ER and PR are members of different steroid hormone receptor subfamilies and recognize distinct hormone response elements, there is considerable biological evidence for cross talk between their receptor-signaling pathways. For instance, progestins can suppress the stimulatory effects of estrogens in target cells; estrogen increases the expression of both c-*fos* and PR mRNA in uterine cells, and progestins block these effects (16, 17). This blockade appears to be mediated via the PRs, but it is unclear whether ER or some other component of the estrogen-ER signaling pathway is the target for repression. It is also known that liganded PRs can suppress E2-stimulated ER activity, with the magnitude of repression dependent on the PR isoform, progestin ligand, promoter, and cell type (18, 19). The exact molecular mechanisms regulating ERα expression in breast tumors are unclear, but studies suggest that they are partly at the level of transcription (20).

In the present study we examined whether alterations in the PR-B to PR-A ratio could affect response to E2 in ERα-positive breast cancer cells. We demonstrate that PR-B overexpression down-regulates ERα mRNA, protein content, and gene promoter activity, whereas PR-A isoform overexpression does not elicit these effects. Investigation of the ERα gene promoter nucleotide sequence, along with site-directed mutagenesis of a half-PRE region in the ERα promoter, and chromatin immunoprecipitation demonstrate that PR-B is able to negatively regulate expression of ERα by the recruitment of a corepressor transcriptional complex containing NCoR, but not silencing mediator of retinoic acid and thyroid hormone receptor (SMRT) and DAX1, causing hypoacetylation of histone H4, resulting in displacement of RNA polymerase II. Furthermore NCoR knockdown completely abrogated the down-regulatory effects on ERα protein and mRNA levels due to PR-B overexpression. PR-B ablation studies using small interfering RNA further demonstrated that endogenous PR-B levels are determinant in regulating ERα.

Results

Pg acting through PR-B decreases E2-induced cell proliferation in breast cancer cells

Reports about the effects of progestins on cell proliferation are contradictory, and there is debate about their actions in human breast tissue (21). In many instances, progestins can either inhibit or stimulate the growth of breast cancer cells (22).

To examine whether progestins affect estrogen-stimulated cell proliferation, we evaluated the effects of prolonged exposure to different concentrations of Pg (1 nM, 10 nM, 100 nM) on E2-stimulated proliferation of breast cancer cells. As expected after 6 d of E2 treatment, the numbers of MCF-7 cells, which express low levels of PR (Fig. 1A) were significantly increased, and Pg alone at all concentrations tested had no significant effect compared with the control experimental conditions. However Pg treatment at 10 nM caused the maximal inhibitory effects (48%) on the E2-induced cell proliferation (Fig. 1B). Similar results were obtained in ZR75, which express low levels of PR, and in T47D cells, which are known to express lower levels of ER but elevated levels of endogenous PR (23).

RU 486 is an antagonist of progestin action in human breast cancer cells, and it is known to bind with high affinity to PR (24). Under our control experimental conditions, 1 μM RU 486 did not affect the growth of MCF-7, ZR75, and T47D cells (Fig. 1C). However, the combination of 10 nM E2, 10 nM Pg, and 1 μM RU486 significantly reversed the inhibitory effects of Pg on E2-induced cell proliferation, suggesting that the inhibitory action was indeed mediated by PR.

It is largely documented that, in addition to their progestational effects, progestins, depending on dosage and tissue site, can also bind to the androgen receptor (AR) (25), which was also been described to antagonize ERα signaling in breast cancer (26). It is interesting to note that under our experimental conditions 1 μM OH-Fl, an AR antagonist (27), did not modify the down-regulatory response of Pg on E2 stimulated proliferation, indicating that AR was not involved in these effects.

To investigate the role of the endogenous PR isoforms in mediating the Pg-inhibitory effects, MCF-7 cells were transfected with an oligo PR-B small interfering RNA (siRNA). As shown in Fig. 1D, specific PR-B knockdown reversed the inhibitory effect on E2-induced cell proliferation produced by Pg cotreatment, demonstrating that this down-regulatory action is mediated by the endogenous PR-B isoform.

PR-B isoform overexpression represses the ERα transcriptional activity

The inhibitory action of Pg on breast cancer cell proliferation described in Fig. 1, required a priming treatment with E2 to induce elevated levels of both PR isoforms, which despite known structural similarities have markedly different transcriptional effects on progestin-responsive promoters (28–30).

To study whether changes in the relative expression levels of PR-B and -A isoforms could affect E2-induced signaling, and to identify the specific PR isoform involved in such modulatory action, we analyzed the effects of PR-A or PR-B overexpression on genomic activity induced by E2 treatment. To this aim a luciferase reporter plasmid containing a consensus estrogen-responsive element (ERE) sequence from the *Xenopus* vitellogenin promoter (XETL) was transiently cotransfected into MCF-7 and ZR75 cells, in the presence or absence of expression plasmids encoding either full-length PR-A or PR-B isoforms. Cells were treated with 10 nM E2 and/or 10 nM Pg, as indicated (Fig. 2, A and B) for 18 h. Treat-

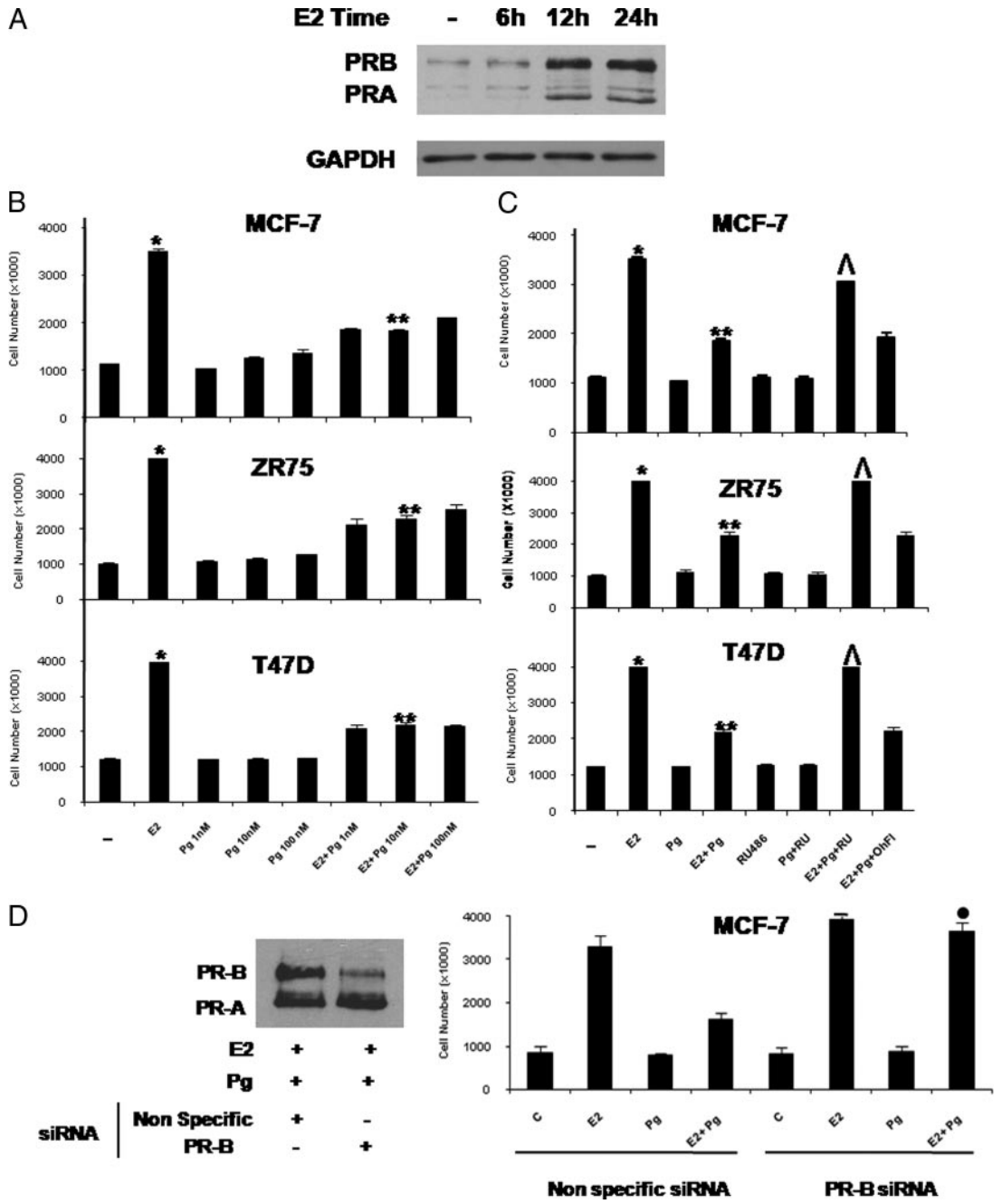

FIG. 1. Pg decreases the E2-induced cell proliferation in breast cancer cells. A, Immunoblot analysis of PR. MCF-7 cells were treated with vehicle (−) or 10 nM E2 at different time as indicated; GAPDH was used as loading control. Results are representative of three independent experiments. B, MCF-7, ZR75, and T47D cells were treated with vehicle (−) or 10 nM E2 and/or increasing amount of Pg (1 nM, 10 nM, 100 nM) in medium containing 5% charcoal-stripped fetal bovine serum (medium was refreshed and treatments were renewed every 2 d) and counted on d 6. C, MCF-7, ZR75, and T47D cells cultured in the experimental conditions described in panel B were also treated with vehicle (−) or 10 nM E2 and/or 10 nM Pg in combination with 1 μM RU or 1 μM OHFl and counted on d 6. D, MCF-7 cells were transfected with nonspecific siRNA or targeted against PR-B and cultured in the experimental conditions described in panel B. *Columns* indicate mean of three independent experiments done in triplicate; *bars* represent SD; *, $P < 0.001$ compared with vehicle; **, $P < 0.001$ compared with E2; ^, $P < 0.001$ compared with E2+Pg; ●, $P < 0.001$ *vs.* cells treated with E2+Pg transfected with nonspecific siRNA.

ment with E2 alone resulted, as expected, in a substantial increase in luciferase activity which was partially inhibited in the presence of transient overexpression of PR-B. Similar inhibition was seen in the presence of PR-B with a truncated ligand-binding domain (LBD) (PR-B 1-675 called mLBD PR-B), demonstrating that the inhibitory action of PR-B does not require ligand binding, whereas estrogen-induced transcriptional activity was not substantially affected in the presence of PR-A overexpression. A PR mutant with a disrupted DNA-binding domain (DBD) (Cys587 to Ala, called mDBD PR) was unable to induce any inhibitory effects on E2-mediated signaling, suggesting that PR-B effects occurred at the transcriptional level.

To investigate the role of the endogenous PR-B isoform in mediating such inhibitory action, cells were also transfected with an oligo PR-B siRNA. As shown in Fig. 2, the specific PR-B knockdown caused a relative increase on E2-induced XETL reporter activity.

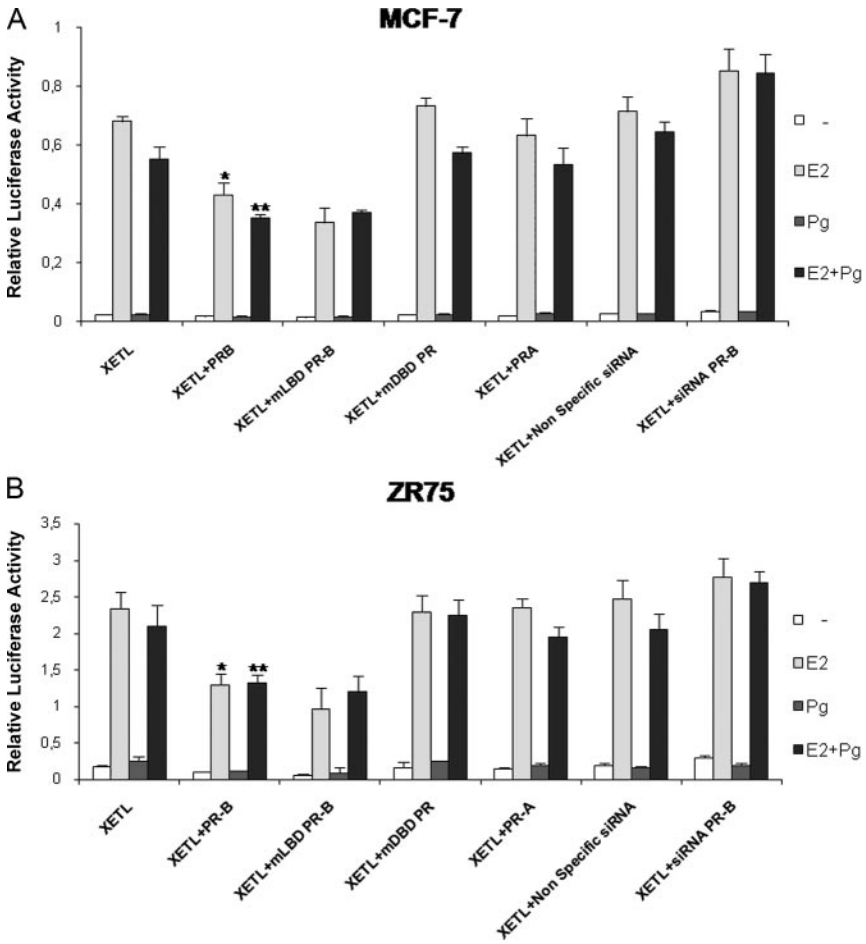

FIG. 2. PR-B overexpression down-regulates the E2-induced signal. ERE luciferase reporter assay. MCF-7 (panel A) and ZR75 (panel B) cells were transiently cotransfected with XETL in the presence or absence of full-length PR-B or mLBD PR or mDBD PR or PR-A expression plasmid, nonspecific siRNA, or targeted against PR-B. After transfection cells were treated with vehicle (−) or 10 nM E2 and/or 10 nM Pg, harvested after 18 h, and then luciferase activities were determined. *Columns* indicate mean of luciferase activities observed in three independent experiments; *bars* represent SD; *, $P < 0.001$ compared with XETL+E2; **, $P < 0.05$ compared with XETL+E2+Pg.

PR-B overexpression down-regulates ERα protein and mRNA

After demonstrating the inhibitory effects of PR-B overexpression on the ER-transcriptional activity, we next examined whether this action might be due to a decrease in the expression levels of ERα protein.

Previous studies provide strong evidence that ERα expression in breast cancer is regulated at both the transcriptional level by initially decreasing transcription of ERα and later via destabilization of ER mRNA (31, 32), as well as by posttranslational mechanisms (19, 20). Down-regulation of ERα expression in the presence of its own ligand is the feature of its transactivation; indeed, immunoblot analysis of lysates from MCF-7 and ZR75cells treated with 10 nM E2 and/or 10 nM Pg for 24 h showed that E2 treatment repressed the ERα expression levels whereas Pg alone had no effect (Fig. 3A). In contrast, however, PR-B over-expression caused a marked reduction in ERα content under control experimental conditions in the absence of treatment, as well as after ligand (E2 or Pg) exposures in both MCF-7 and ZR75 cells, and this inhibitory effect was still evident in cells transiently overexpressing mLBD PR-B.

To further investigate the molecular basis of PR-B-mediated regulation of ERα expression, we also examined the effects of PR-B overexpression on ERα mRNA levels in MCF-7 and ZR75 cells treated for 24 h with 10 nM E2 and/or 10 nM Pg. As shown in Fig. 3B and consistent with previous studies (33), E2 caused a decrease in the steady state level of ERα mRNA. We also found that PR-B or mLBD PR-B overexpression further decreased ERα mRNA levels. These results suggest that PR-B overexpression affects ERα signaling through direct effects on ERα content in a ligand-independent manner.

PR-B overexpression decreases the levels of ERα-regulated genes in MCF-7 cells

The effects of E2 hormone are known to be mediated by ER through its gene-regulatory activities. To confirm whether Pg could inhibit the effect of E2 by modifying the transcriptional activity of ERα, the mRNA levels of known estrogen target genes, such as insulin receptor substrate 1 (IRS1), cyclin D1, and pS2, were studied (Fig. 3C). As expected, after 24 h treatment, 10 nM E2 markedly increased the mRNA levels of all three of these genes in MCF-7 cells after standardization with a housekeeping gene (ribosomal protein 36B4).

To further explore whether overexpression of PR-B could affect the expression of estrogen-regulated gene, plasmids encoding full-length PR-B were transiently transfected into MCF-7 cells. After 24 h of ligand treatment, cells were harvested and RT-PCR experiments were performed to compare mRNA levels for IRS1, cyclin D1, and pS2. As depicted in Fig. 3C, PR-B overexpression represses mRNA levels of all estrogen-regulated genes tested, in the control experimental conditions in absence of treatment as well as after exposure to ligands. The inhibitory action observed on IRS1 mRNA levels was still evident when we overexpressed a PR-B with a truncated LBD (mLBD PR-B).

Similar results were obtained when Western blotting analysis was performed in the same experimental conditions (data not shown).

Overexpressed PR-B mediates down-regulation of ERα via a region between −2769 bp to −1000 bp of its promoter

To analyze how PR-B interferes with ERα gene transcription, the ERα promoter was investigated first with a bioinformatics approach using the National Center for Biotechnology Information Genome data base (www.ncbi.nlm.nih.gov). The region examined in this study covered from −4100 bp to +212 bp, and a half-progesterone response element (PRE) (−1757 bp to −1752 bp) was identified as within this region.

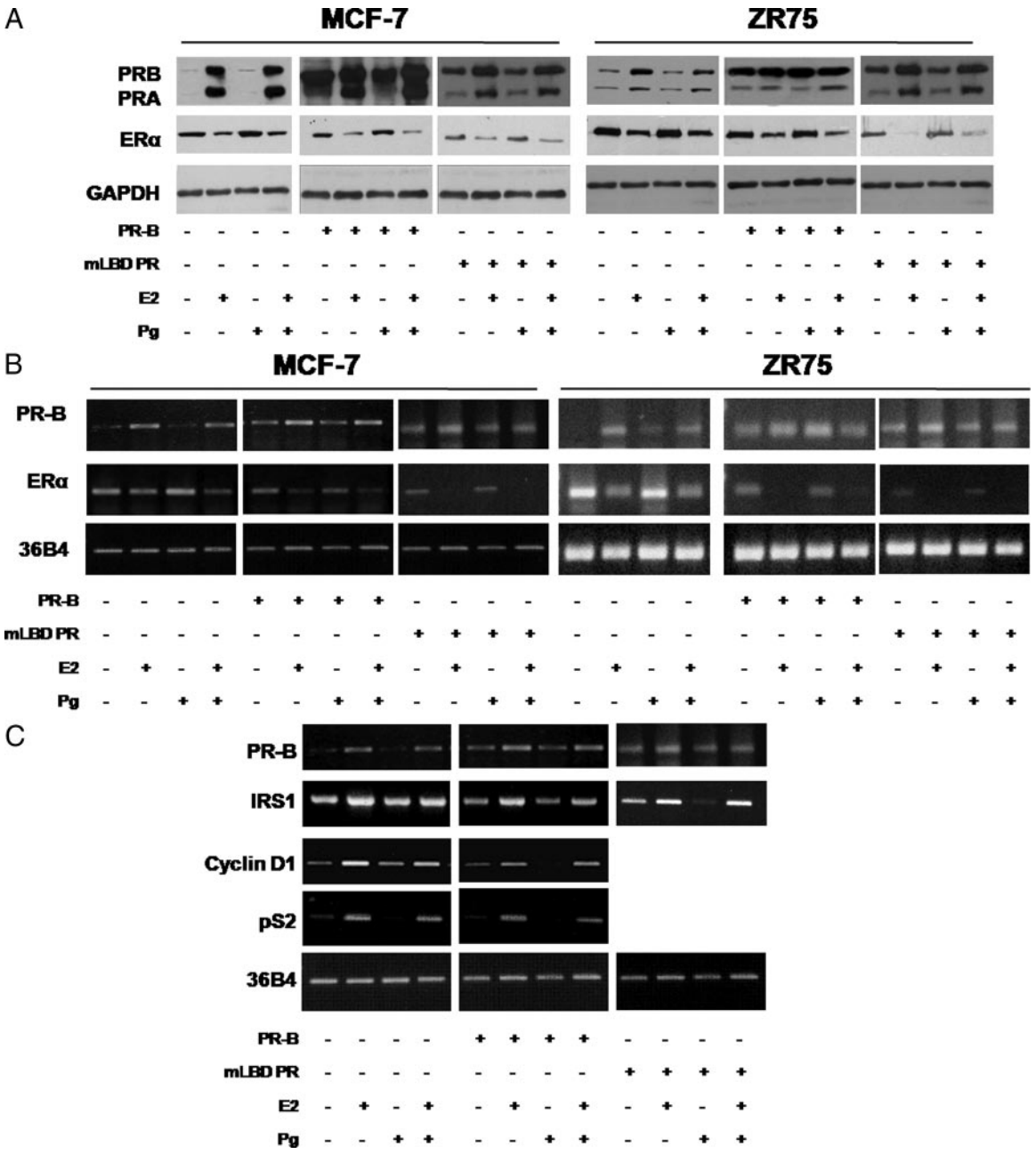

FIG. 3. PR-B overexpression decreases ERα protein, ERα mRNA, and estrogen-regulated genes mRNA. A, Immunoblot analysis of PR and ERα. MCF-7, ZR75, and cells transient overexpressing PR-B or mLBD PR were treated with vehicle (−) or 10 nM E2 and/or 10 nM Pg for 24 h; GAPDH was used as a loading control. *Columns*, represent mean of three separate experiments in which the band intensities were evaluated in terms of optical density arbitrary units and expressed as the percentage of the control assumed as 100%; *bars* represent SD. B, RT-PCR assay. mRNA expression of PR-B and ERα in MCF-7, ZR75, and cells transiently overexpressing PR-B or mLBD PR treated with vehicle (−) or 10 nM E2 and/or 10 nM Pg for 24 h; the housekeeping gene 36B4 was determined as a control. *Columns* indicate mean of three separate experiments; *bars,* represent SD. C, RT-PCR assay. mRNA expression of PR-B, IRS-1, cyclin D1, and pS2 in MCF-7 cells and MCF-7 transiently overexpressing PR-B or mLBD PR treated with vehicle (−) or 10 nM E2 and/or 10 nM Pg for 24 h; the housekeeping gene 36B4 was determined as a control. *Columns* indicate mean of three separate experiments; *bars,* represent SD.

To evaluate whether this region was a putative effector of PR action and involved in PR-mediated down-regulation of ERα expression, five overlapping ERα promoter deletion constructs, −245 bp to +212 bp (A), −735 bp to +212 bp (B), −1000 bp to +212 bp (C), −2769 bp to +212 bp (D), and −4100 bp to +212 bp (E), all relative to the first transcriptional ATG start site depicted in Fig. 4A, which had been subcloned into the luciferase reporter vector pGL3-basic, were analyzed in MCF-7 cells (34). Fragment A contains the region between −245 to −9 bp, known to posses low basal activity, as well as the two binding sites for AP2γ within the 5′-untranslated region (34). Fragment B extending to −735 bp includes a half-ERE at −420 bp. Fragment C includes two other half-EREs located at −860 and −888 bp, respectively. Fragments D and E include the P0 transcription start and the half-PRE that we identified in our NCBI genomic search; fragment E also contains the ER-EH0 enhancer (19). Plasmids containing these five ERα promoter fragments were

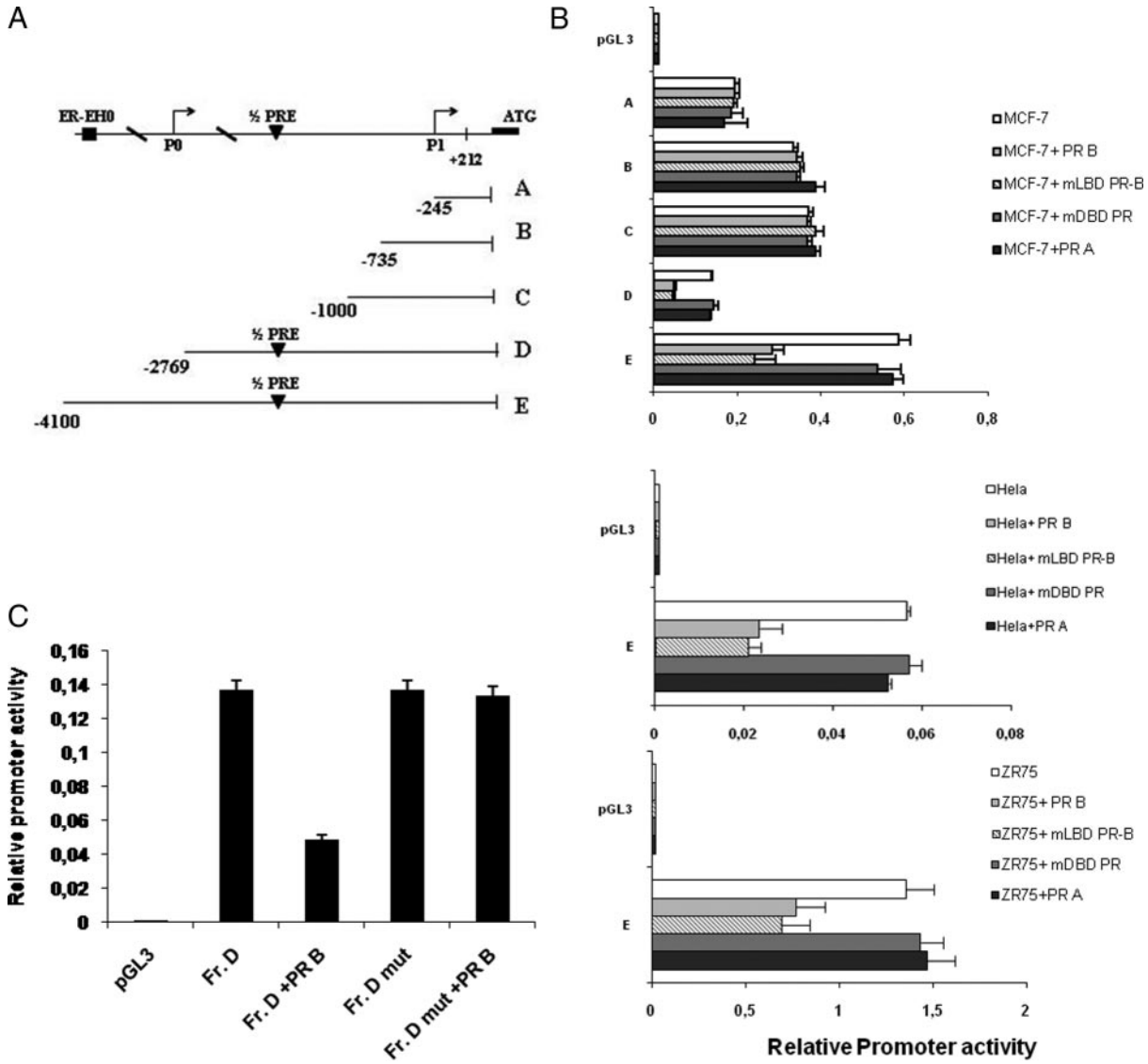

FIG. 4. ERα promoter activity is down-regulated by PR-B overexpression, and mutation of the half-PRE abrogates this effect. A, Schematic representation of deletion fragments of the ERα gene promoter. Fragments coordinates are expressed relative to the primary transcription start site. B, Promoter activity of the ERα 5′-flanking region. Constructs depicted in panel A were transiently cotransfected in MCF-7, Hela, and ZR75 cells in the presence or absence of full-length PR-B or mLBD PR, mDBD PR, or PR-A expression plasmid. After 24 h, cells were harvested, and luciferase activities were determined. *Columns* indicate mean of luciferase activities observed in three independent experiments; *bars* represent SD. C, Site-directed mutagenesis of the half-PRE site present in the fragment D promoter construct. Fragment D and fragment D mut promoter constructs were cotransfected into MCF-7 cells, and promoter activity was assessed in the absence or presence of full-length PR-B expression plasmid after 24 h. *Columns* represent mean of luciferase activities observed in three independent experiments; *bars* indicate SD. Fr., Fragment.

transiently transfected into MCF-7 cells, and the data are shown as relative promoter activity in luciferase units.

Consistent with our previous studies (34), fragment A exhibited high levels of activity (Fig. 4B), the activities of fragments B and C were slightly increased relative to A, whereas the activity of fragment D decreased. The highest level of control promoter activity was seen with fragment E. We found that PR-B overexpression had no effect on the promoter activity of fragments A, B, and C, all which lack the half-PRE site. In contrast PR-B reduced the activity of fragments D and E by 64% and 50%, respectively, indicating that the region between −2769 bp to −1000 bp was responsible for PR-B-mediated down-regulation of ERα activity. Similar results were obtained cotransfecting equal amounts of expression plasmids encoding PR-B with a truncated LBD (mLBD PR-B) [$]while different results were observed after cotransfection of equal amounts of expression plasmids encoding either the PR-A isoform or the PR mutant with a disrupted DBD (mDBD PR, Fig. 4B). To confirm the findings obtained on activity of fragment E, the experiments were repeated in ZR75 and Hela cells, and similar results were obtained.

The presence of a functional half-PRE site within the ERα promoter has not been reported previously, and our results suggest a transcriptional cross talk mechanism between the two receptor networks at the level of the ERα promoter.

Site-directed mutagenesis reveals a role for the half-PRE in fragment D of the ERα promoter

To evaluate the role of the potential half-PRE site present within ERα gene promoter from −1757 bp to −1752 bp, we

next used site-directed mutagenesis to alter this site. We changed 3 bp of the half-PRE to ensure that the altered binding site would not be recognizable by the PR (35). Transient transfections were performed in MCF-7 cells with multiple independent clones containing the desiderated mutation. Shown in a representative experiment, we found that the promoter activity of fragment D carrying the mutation in half-PRE site (Fr. D mut) was unaffected by PR-B overexpression (Fig. 4C). These results indicate that the half-PRE element in the ERα promoter is required for repression concomitant with PR-B overexpression.

The NCoR corepressor is recruited with PR-B to the ERα promoter

To demonstrate PR recruitment to the ERα gene promoter, we used ChIP assays. MCF-7 cells untreated or treated with E2 for 24 h to allow the expression of endogenous PR and MCF-7 cells ectopically overexpressing PR-B were exposed for 1 h with either control vehicle or 10 nM Pg, after which chromatin was cross-linked with formaldehyde, and protein-DNA complexes were immunoprecipitated with antibodies directed against PR, RNA polymerase II, acetyl histone H4-K16, or the corepressors NCoR, DAX-1, and SMRT. The PCR primers used in the ChIP assays encompass the half-PRE site we identified within the ERα promoter. Results obtained in MCF-7 cells overexpressing endogenous PR-B (treated with E2 for 24 h) or ectopic PR-B (Fig. 5A) demonstrate an enhanced recruitment of PR to the ERα promoter in the presence or absence of Pg treatment (*upper panel*); as a control we did not see recruitment to an unrelated ERα promoter region located upstream of the half-PRE site (*lower panel*).

To determine which PR isoform interacts with this region of the ERα promoter, MCF-7 cells were also transfected with a specific oligo PR-B siRNA to achieve efficient knockdown of PR-B as shown in Fig. 5B. PR recruitment to the half-PRE site of the ERα promoter was strongly reduced by PR-B siRNA expression, confirming the specific recruitment of this isoform to the ERα promoter (Fig. 5A).

Concomitant with the increased recruitment of PR-B to the promoter, we saw that acetyl histone H4-K16 was not recruited and RNA polymerase II was displaced from the ERα promoter, indicating that the chromatin in this region is probably in a less permissive environment for gene transcription. Among the different PR corepressors previously described (36, 37) and here tested, SMRT and DAX 1 were not detected under the examined experimental conditions. We only found NCoR to be recruited to the ERα promoter encompassing the half-PRE site, in a ligand-independent manner in MCF7 cells when endogenous or ectopic PR-B was overexpressed. These results highlight a possible new role of the NCoR corepressor in ERα regulation by PR-B.

To further assess whether endogenous NCoR could interact with PR, coimmunoprecipitation assays were performed. Nuclear extracts from control MCF-7 treated with E2 for 24 h, left untreated or transiently overexpressing PR-B, were coimmunoprecipitated with an anti-NCoR antibody and subjected to immunoblot analysis with an anti-PR antibody. As shown in Fig. 5C, a band of 114 kDa corresponding to PR-B was detected but only in MCF-7 cells overexpressing endogenous or ectopic PR-B.

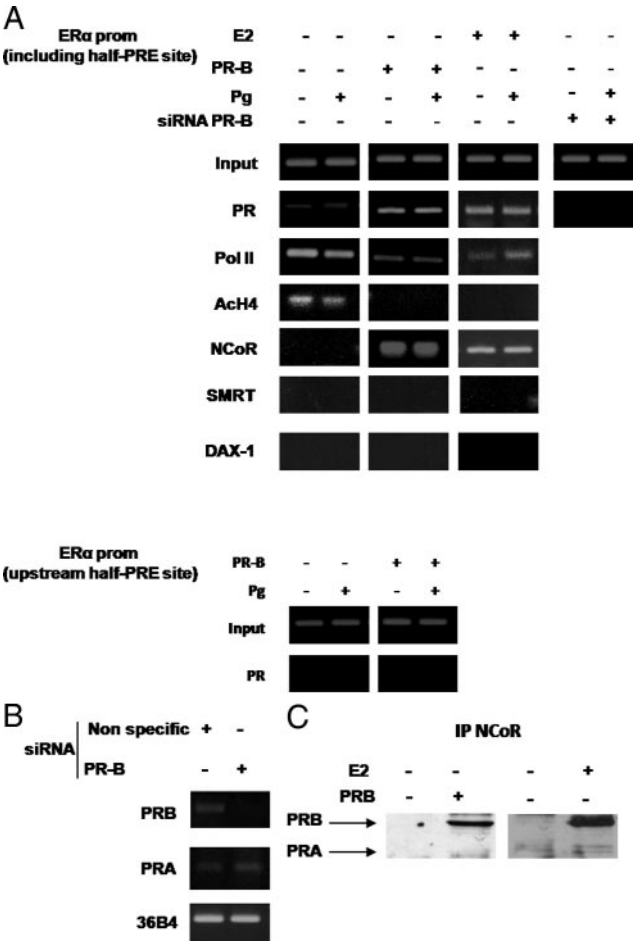

FIG. 5. The NCoR corepressor is recruited with PR-B to the ERα promoter. A, ChIP was performed on the PR-responsive region of the ERα promoter, and various antibodies are used as indicated (*upper panel*). Nonspecific region upstream of the half-PRE site in the ERα promoter was tested as negative control (*lower panel*). MCF-7 transiently overexpressing PR-B cells or siRNA PR-B and MCF-7 cells treated for 24 h with vehicle (−) or 10 nM E2 were treated for 1 h with vehicle (−) or 10 nM Pg. Results are representative of three independent experiments. B, Knockdown of PR-B. MCF-7 cells were transfected with nonspecific siRNA or targeted against PR-B. RNA was isolated, and the expression of PR-B was analyzed by RT-PCR; the housekeeping gene 36B4 and PR-A were determined as controls. C, Coimmunoprecipitation analysis. Nuclear extracts were prepared from MCF-7 cells treated for 24 h with vehicle (−) or 10 nM E2 and from MCF-7 cells transiently overexpressing PR-B. Immunoprecipitation assay was performed using anti-NCoR antibody. Immunoprecipitated (IP) proteins were resolved and subjected to immunoblotting with anti-PR antibody. Results are representative of three independent experiments. prom, Promoter.

Because NCoR bound to PR-B may physically interfere with binding of RNA polymerase II to the ERα promoter resulting in the observed ERα down-regulation (38), we performed NCoR siRNA knockdown experiments in MCF-7 and in MCF-7 PR-B overexpressing cells in combination with immunoblot analysis. Figure 6A shows that NCoR protein levels were greatly decreased by specific siRNA treatment compared with a nonspecific siRNA; importantly, NCoR knockdown reversed the ERα protein down-regulation that is induced by PR-B overexpression. Similar results were obtained at mRNA levels (Fig. 6B).

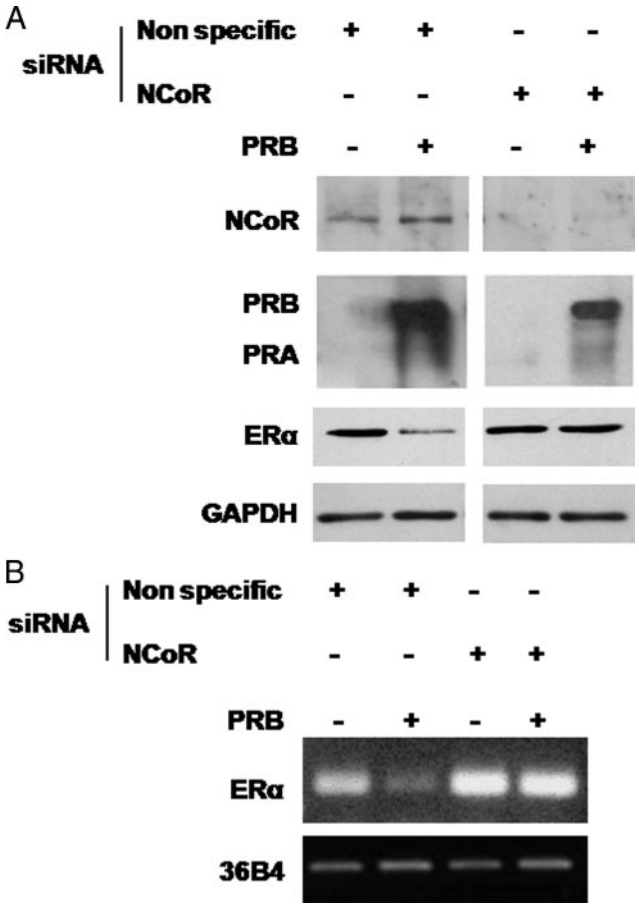

FIG. 6. NCoR knockdown reverses the down-regulation of ERα protein levels and mRNA induced by PR-B overexpression. A, Immunoblot analysis of NCoR, PR, and ERα. MCF-7 and MCF-7 cells transient overexpressing PR-B were transfected with nonspecific siRNA or targeted against NCoR; GAPDH was used as control. Results are representative of three independent experiments. B, RT-PCR assay. mRNA expression of ERα in MCF-7 cells and MCF-7 cells transiently overexpressing PR-B, transfected with nonspecific siRNA, or targeted against NCoR; the housekeeping gene 36B4 was determined as a control. Results are representative of three independent experiments.

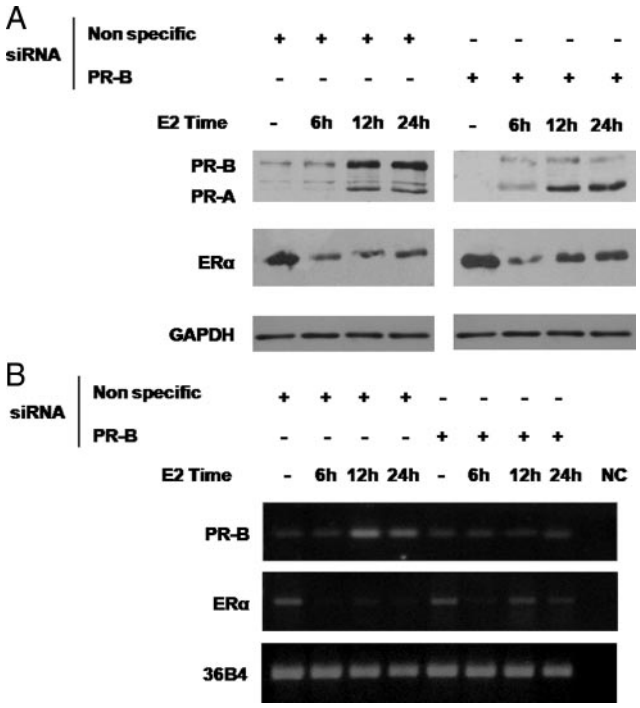

FIG. 7. PR-B knockdown partially reverses the down-regulation of ERα after E2 treatment. A, Immunoblot analysis of ERα and PR. MCF-7 cells were transfected with nonspecific siRNA or targeted against PR-B and treated with 10 nM E2 at different times as indicated; GAPDH was used as control. Results are representative of three independent experiments. B, RT-PCR assay. mRNA expression of PR-B and ERα. MCF-7 cells were transfected with nonspecific siRNA or targeted against PR-B and treated with 10 nM E2 at different times as indicated; the housekeeping gene 36B4 was determined as a control. Results are representative of three independent experiments. NC, Negative control.

Endogenous PR-B modulates ERα protein levels in MCF-7 cells

On the basis of all these findings we hypothesized that endogenous PR could be involved in ERα down-regulation upon E2 exposure. Therefore, we explored PR and ERα protein levels after 6 h, 12 h, and 24 h of E2 treatment in MCF-7 cells. As shown in Fig. 7A, ERα protein displayed a pattern of regulation consistent with previously published studies (20). Indeed, E2 caused a dramatic decrease in ERα levels starting from 6 h of treatment, and we observed an increase in PR expression after 12 h of treatment.

To ascertain a specific role for PR-B enhancement by E2 on the maintenance of ERα down-regulation, we also performed PR-B siRNA knockdown experiments in MCF-7 cells following 6 h, 12 h, and 24 h of E2 treatment. PR-B knockdown partially reversed the down-regulation of ERα protein levels starting from 12 h until 24 h of E2 treatment whereas it appears not to affect the early down-regulatory effects. Similar results were obtained at mRNA levels (Fig. 7B). These results suggest that the early down-regulatory effects induced by E2 on its own receptor occur independently of PR-B action, whereas the latter plays a specific role after prolonged E2 exposure.

Discussion

Approximately 75% of primary breast cancers express ERα, and more than half of these cancers coexpress PR. ER and PR are considered independent prognostic factors for early breast cancer therapeutic management although both are weak and lose their prognostic value after long-term follow-up.

Increased expression of ERα is an early event in breast carcinogenesis; in contrast, a decrease of PR levels is associated with breast cancer progression (39). PR is able to inhibit the growth of ER+ breast cancer cells in ovariectomized nude mice despite Pg deficiency, addressing a specific inhibitory role of PR independent of its natural ligand (40). It emerges from experimental models that ER+/PR+ breast cancers are well differentiated, presenting as low-risk, well-defined lesions whereas ER+/PR− metastatic tumors display a much more aggressive course after loss of PR compared with tumors retaining PR (39).

In humans, PR exists as two isoforms, called PR-A and PR-B, which exhibit distinct roles in regulating the effects of Pg that at physiological concentration is able to bind and activate both isoforms (41), and enhanced PR-A/PR-B ratio is coincident with a major breast cancer growth and progression (6, 42).

It is well documented that in hormone-dependent breast cancer cells, Pg may inhibit the induction of classical estrogen-regulated genes even though the molecular mechanisms underlying these effects remain to be fully elucidated (43, 44). Our study undertook to examine these molecular mechanisms.

We demonstrated that PR-B overexpression repressed ERα levels in breast cancer cells in a ligand-independent manner as it emerges from data obtained on cells transiently overexpressing PR-B truncated in LBD. This inhibitory effect is mediated by the recruitment of NCoR bound to PR-B on ERα promoter. Furthermore we demonstrated that PR-B overexpression, but not PR-A, inhibited ERα transactivation together with the expression of estrogen-dependent genes such as pS2, cyclin D1, and IRS1. These effects correlate well with the inhibition of E2-induced cell proliferation by Pg through endogenous PR-B isoform.

Our findings corroborate previous clinical studies (42, 45) illustrating that high PR-A/PR-B ratios in breast tumors predict shorter disease-free survival. The protective action of PR-B in breast cancer is further reinforced by studies showing that PR is inversely associated with HER-2/neu, the signaling of which is known to drive estrogen-independent breast cancer cell growth (46, 47).

Also of note are the findings that the levels of Her-2 are significantly higher in ER+/PR-A+ xenografts, than in ER+/PR-B+ xenografts (42). Thus, it remains an intriguing question as to whether a loss or a dysregulation of PR-B isoform expression could exert a direct effect on Her2 and in such a way it could perturb ERα signaling.

To clarify the molecular mechanisms through which PR-B may interfere with ERα gene transcription, we analyzed the ERα promoter sequence and identified a PRE half-site located at −1757 bp to −1752 bp. Functional experiments using five deletion constructs of the ERα promoter showed that the down-regulatory effects induced by PR-B overexpression on ERα promoter activity were through the half-site and were not detected in the deletion constructs lacking the half-PRE site. Moreover site-directed mutagenesis of the above region completely reversed down-regulation of ERα promoter activity. ChIP assay results further confirmed the specific recruitment of the PR-B isoform to the half-PRE site within the ERα gene promoter because recruitment was prevented in PR-B knockdown experiments. The inhibitory effects on the ERα promoter transcriptional machinery addressed the ability of PR-B to recruit corepressors interfering with ERα gene transcription.

Corepressors function as counterparts to coactivators revealing that nuclear receptor-mediated transcription is subjected to both positive and negative regulation. It has been reported that unliganded nuclear receptors, such as TR and RXR, can repress basal transcription in the absence of their cognate ligands, and these functions are mediated, at least in part, by the NCoR and SMRT (48). These two corepressors interact with unliganded nuclear receptors, through an elongated helix of sequence LXX I/H IXXX I/L, alternatively referred to as the CoRNR-box (49–51). It has been recently documented that NCoR and SMRT are also recruited by both ER and PR in the presence of ligand antagonist to regulate transcription of different genes (52, 53). For instance, our ChIP experiments showed that among potential corepressor molecules that are able to interact with PR, NCoR was the only one present on the PR-B/DNA complex regardless of its natural ligand. These results are consistent with evidence reporting that corepressors have different preferences and determinants for interactions with nuclear receptors and transcription factors at specific genes (54, 55). Moreover we show that formation of this bipartite complex leads to hypoacetylation of histone H4, which causes stabilization of nucleosome structure, limiting accessibility to the basal transcriptional machinery and thus repressing ERα gene expression.

All these data support a model in which elevated expression levels of PR-B increase the interaction of the receptor with NCoR on the half-PRE site of the ERα promoter, an event incompatible with PR-coactivator interactions. The crucial role of NCoR emerges from our data showing that silencing of this corepressor was able to reverse the down-regulation of ERα expression induced by PR-B overexpression.

E2 is known to down-regulate the levels of ERα in breast cancer cell line through an increased turnover of E2-bound receptor and via reduced transcription of its own gene (33). This down-regulation represents a classical feature of ERα transactivation. Our novel findings show that PR-B is a determinant of these down-regulatory effects, because PR-B knockdown attenuated the feedback inhibition of ERα levels after estrogenic stimulus. Therefore we propose that ERα modulation by E2 could be due to early events independent from PR expression, and later transcriptional events leading to PR-B overexpression, which in turn can produce a decrease in ERα transcription, via recruitment of a corepressor complex containing NCoR and displacing RNA polymerase II (Pol II). Thus we here demonstrate that the E2 enhanced PR-B is crucial in determining the concomitant ERα down-regulation. These results highlight the importance of tightly regulated expression of PR-A and PR-B, and we have provided new insights into the molecular mechanisms through which PR-B overexpression antagonizes ERα in breast cancer cells.

In conclusion we suggest that inhibition of ERα by PR-B is a critical regulatory pathway in ER-positive cells, and we speculate that dysregulation of this repression mechanism in breast cancer may have dramatic effects such as breast tumor progression. In other words we propose that unliganded PR-B and its ratio with PR-A influences breast cancer cell biology modulating ERα states. Because a large percentage of breast tumors are ER+/PR+ and might fall into a potential low-risk group (excess of PR-B) the antiestrogenic action of PR-B signaling could be exploited for innovative adjuvant strategies in breast cancer treatment.

Materials and Methods

Materials

DMEM/F-12, L-glutamine, Eagle's nonessential amino acids, penicillin, streptomycin, fetal calf serum, BSA, and PBS were purchased from Eurobio (Les Ullis Cedex, France). Triazol reagent was obtained from Invitrogen (Carlsbad, CA), and FuGENE 6 was from Roche Applied Science (Indianapolis, IN). Taq DNA polymerase, 100-bp DNA ladder, dual luciferase kit, thymidine kinase, and *Renilla* luciferase plasmid

were provided by Promega Corp. (Madison, WI). Aprotinin, leupeptin, phenylmethylsulfonyl fluoride, and sodium orthovanadate were purchased from Sigma (Milan, Italy).

Antobodies used in this study, anti-PR (H-190), anti-ERα, anti-glyceraldehyde-3-phosphate dehydrogenase (GAPDH), anti-Pol II, anti-NCoR, anti-SMRT, anti DAX-1, were purchased from Santa Cruz Biotechnology, Inc. (Santa Cruz, CA); antiacetyl histone4-K16, from Upstate Biotechnology (Lake Placid, NY); anti PR, from NeoMarkers (Labvision, Freemont, CA). Salmon sperm DNA was from Santa Cruz Biotechnology. Biotinylated horse antigoat IgG and ABC complex/horseradish peroxidase were provided by VECTOR Laboratories (Burlingame, CA). Chromogen, 3-diaminobenzidine tetrachloride dihydrate, was purchased from Bio-Optica (Milan, Italy). ECL System was purchased from Amersham Pharmacia (Buckinghamshire, UK). VCX500 ultrasonic processor was provided by Sonics (Newtown, CT).

Cell culture

Human breast cancer MCF-7 cells were gifts from Dr. B. Van der Burg (Utrecht, The Netherlands); ZR75 cells were kindly provided from Dr. A. Weisz (Naples, Italy); and T47D and human uterine cervix adenocarcinoma (HeLa) cells were obtained from the American Type Culture Collection (Manassas, VA). MCF-7 and HeLa cells were maintained in DMEM/F-12 medium containing 5% fetal calf serum (5% FCS), 1% L-glutamine, 1% Eagle's nonessential amino acids, and 1 mg/ml penicillin/streptomycin in a 5% CO_2 humidified atmosphere. Cells were cultured in phenol red-free DMEM, 0.5% BSA (0.5% BSA), and 2 mM L-glutamine (serum-free medium), for 48 h before each experiment. Hormone stimulation was performed in DMEM/F12 containing 5% charcoal-treated fetal calf serum to reduce the endogenous steroid concentration (56). ZR75.1 were maintained in complete DMEM supplemented with 10% fetal bovine serum and 250 ng/ml amphotericin B (Sigma, Milan, Italy), 1 mg/ml penicillin/streptomycin. T47D cells were routinely maintained in RPMI 1640 supplemented with 5% FCS, 1 μg/ml insulin (Sigma), 1 mg/ml penicillin /streptomycin (Sigma).

Proliferation assays

For quantitative proliferation assays, 10,000 cells were seeded in 24-well plates in regular growth medium. Cells were washed once they had attached, serum starved for 48 h, and then incubated in medium containing 5% charcoal-treated FCS with the indicated treatments; medium was renewed every 2 d (with treatments), and cells were trypsinized and counted in a hemocytometer on d 6.

Plasmid

The following plasmids were used: XETL (57), the wild-type human ERα (HEGO) (58), the full-length PR-B consisting of the full-length PR-B cDNA fused with the SV40 early promoter and expressed in the pSG5 vector (a gift from Dr. D. Picard, University of Genève, Switzerland); the PR-B 1-675 including the N-terminal fragment of PR-B (mLBD PR-B) (59); and the PR DNA-binding mutant C587A (mDBD PR) previously described by Faivre *et al.* (60) (both gifts from Dr. C. Lange, University of Minnesota Cancer Center, Minneapolis, MN), the full-length PR-A (7); and the deletion fragments of the ERα gene promoter (34). The *Renilla* luciferase expression vector pRL-TK (Promega, Milan, Italy) was used as a transfection standard.

Total RNA extraction and RT-PCR assay

Total cellular RNA was extracted from MCF-7 cells using Triazol reagent (Invitrogen, Carlsbad, CA). Reverse transcription was done using RETROscript kit (Ambion, Austin, TX). Primer sequences include: ERα forward, 5′-GGAGACATGAGAGCTGCCA-3′, and reverse, 5′-CCAGCAGCATGTCGACGATC-3′; PR-B forward, 5′-TAGTGAGGGGGCAGTGGAAC-3′, and reverse, 5′-AGGAGGGGGTTTCGGGAATA-3′; pS2 forward, 5′-TTCTATCCTAATACCATCGACG-3′, and reverse, 5′-TTTGAGTAGTCAAAGTCAGAGC-3′; cyclin D1 forward, 5′-TCTAAGATGAAGGAGACCATC-3′, and reverse, 5′-GCGGTAGTAGGACAGGAAGTTGTT-3′; IRS1 forward, 5′-AGGATATTTAATTTGCCTCGG-3′ and reverse, 5′-AAGCGTTTGTGCATGCTCTTG 3; rRNA 36B4, forward, 5′-CTCAACATCTCCCCCTTCTC-3′, and reverse, 5′-CAAATCCCATATCCTCGTCC-3′. Equal amounts of PCR product were electrophoresed on 1% agarose gels and visualized by ethidium bromide staining. To check for the presence of DNA contamination, an RT-PCR was performed without Moloney murine leukemia virus-reverse transcriptase (negative control).

Western blotting and immunoprecipitation

Cytoplasmic and nuclear fractions of cellular protein extract were obtained as previously described (26, 61). Proteins were resolved on an 8–10% sodium dodecyl sulfate (SDS)-polyacrylamide gel, transferred to a nitrocellulose membrane (Amersham Biosciences, Milan, Italy), and probed overnight at 4–C with the antibody indicated in the figure legends.

Transfections and luciferase assays

Cells (1×10^5) were plated into 24-well dishes with 500 μl of regular growth medium per well the day before transfection. The medium was replaced with that lacking serum on the day of transfection, which was done using Fugene 6 reagent as recommended by the manufacturer (Roche Diagnostics, Milan, Italy) with a mixture containing 0.5 μg of reporter plasmid, alone or in combination plasmids as indicated in the figure legends, and 5 ng of pRL-TK. Medium was renewed after which cells were treated for 24 h. Luciferase activity was measured with the Dual Luciferase kit (Promega) according to the manufacturer's recommendations. Firefly luciferase values were normalized to the internal transfection control provided by the *Renilla* luciferase activity. Empty vector was used to ensure that DNA concentration were constant in each transfection.

For RNA preparation, whole and nuclear cell extractions, and ChIP assays, cells were serum starved for 48 h, plated in medium containing 5% charcoal-treated fetal calf serum, and then transfected using the FuGENE 6 reagent, with an appropriate amount of the various plasmids as indicated in the figure legends. Cells were changed with fresh medium containing 5% charcoal-treated fetal calf serum for 48 h and then treated as indicated.

Lipid-mediated transfection of siRNA duplexes

RNA oligonucleotides directed against PR-B or NCoR were purchased from Invitrogen (Carlsbad, CA), and transfection was performed as described previously (38, 62). Cells were transfected using Lipofectamine 2000 reagent (Invitrogen) according to the manufacturer's instructions and then treated as indicated.

Site-directed mutagenesis

Mutagenesis was performed on Fragment D of the ERα promoter (34) using the QuikChange mutagenesis kit (Stratagene, La Jolla, CA) following the manufacturer's instructions. The sequence for the sense primer was: 5′-AGCAGGGAGATGAGGATTGC*TgaagT*CCATGGGGGTATGT-3′. The plasmids were then sequenced to confirm the mutation of the desired site.

ChIP assays

ChIP methodology was performed as described by Morelli *et al.* (63).

Cells were grown in 100-mm plates 90% confluent cultures, were shifted to serum-free medium for 48 h, and then treated for 1 h before harvesting for the assay. Then cells were washed twice with PBS and cross-linked with 1% formaldehyde at 37 C for 10 min. Next they were washed twice, collected, and resuspended in 200 μl of lysis buffer (1% SDS; 10 mM EDTA; 50 mM Tris-Cl, pH 8.1) and left on ice for 10 min. Lysates were sonicated four times for 10 sec at 30% of maximal power and collected by centrifugation at 4 C for 10 min at 14,000 rpm. Supernatants were collected and diluted in 1.3 ml of immunoprecipitation buffer (0.01% SDS; 1.1% Triton X-100; 1.2 mM EDTA; 16.7 mM Tris-Cl, pH 8.1; 16.7 mM NaCl) followed by immunoclearing with 80 μl of sonicated salmon sperm DNA/protein A-agarose for 1 h at 4 C. The

precleared chromatin was immunoprecipitated for 12 h either with PR, RNA Pol II, acetyl histone4-K16, NCoR, SMRT, and DAX-1 antibodies or with normal goat IgG as the negative control. After that, 60 μl of salmon sperm DNA/protein A-agarose was added, and precipitation was continued for 2 h at 4 C. Precipitates were washed sequentially for 5 min with the following buffers: Wash A (0.1% SDS; 1% Triton X-100; 2 mM EDTA; 20 mM Tris-Cl, pH 8.1; 150 mM NaCl); Wash B (0.1% SDS; 1% Triton X-100; 2 mM EDTA; 20 mM Tris-Cl, pH 8.1; 500 mM NaCl), and Wash C (0.25 M LiCl; 1% Nonidet P-40; 1% sodium deoxycholate; 1 mM EDTA; 10 mM Tris-Cl, pH 8.1), and then twice with TE buffer (10 mM Tris, 1 mM EDTA). The immune complexes were eluted with elution buffer (1% SDS, 0.1 M $NaHCO_3$), and then they were reverse cross-linked by heating at 65 C for 12 h and digested with 0.5 mg/ml proteinase K at 45 C for 1 h. DNA was obtained by phenol and phenol/chloroform extractions. Two microliters of 10 mg/ml yeast tRNA was added to each sample, and DNA was precipitated with ethanol for 12 h at −20 C and resuspended in 20 μl of TE buffer. Five microliters of each sample was used for PCR with the following ERα promoter primers: forward, 5′-ACGTTCTTGATCCAGCAGGGTA-3′ and reverse, 5′-ACCTGCCAAATTATATGCAAATGGCAG-3′ containing the half-PRE site; and forward, 5′-GTGGCCATTGTTGACCTACAG-3′ and reverse, 5′-CTGTAGGTCAACAATGGCCAC-3′ upstream the half-PRE site. The amplification products, obtained in 30 cycles, were analyzed in a 2% agarose gel and visualized by ethidium bromide staining.

Statistical analysis

Each datum point represents the mean SE of three different experiments. Data were analyzed by ANOVA test using the STATPAC computer program.

Acknowledgments

We thank Dr. D. Picard for the full-length PR-B plasmid and Dr. C. Lange for PR DNA-binding mutant plasmid and PR-B LBD truncated plasmid.

Address all correspondence and requests for reprints to: Professor Sebastiano Andò M.D., Department of Cellular Biology, University of Calabria, 87036 Rende (CS), Italy. E-mail: sebastiano.ando@unical.it.

This work was supported by Associazone Italiana Ricerca sul Cancro-2007 and Grant RO1 CA72038 from the National Institutes of Health/National Cancer Institute (to S.A.W.F.).

Disclosure Summary: All authors have nothing to declare.

References

1. **Clarke CL, Sutherland RL** 1990 Progestin regulation of cellular proliferation. Endocr Rev 11:266–330
2. **Dunnwald LK, Rossing MA, Li CI** 2007 Hormone receptor status, tumor characteristics, and prognosis: a prospective cohort of breast cancer patients. Breast Cancer Res 9:R6
3. **Fuqua SAW, Cui Y** 2004 Estrogen and progesterone receptor isoforms: clinical significance in breast cancer. Breast Cancer Res Treat 87:S3–S10
4. **Knight III WA, Osborne CK, Yochmowitz MG, McGuire WL** 1980 Steroid hormone receptors in management of human breast cancer. Ann Clin Res 12:202–207
5. **Kim HJ, Cui X, Hilsenbeck SG, Lee AV** 2006 Progesterone receptor loss correlates with human epidermal growth factor receptor 2 overexpression in estrogen receptor-positive breast cancer. Clin Cancer Res 12:1013s–1018s
6. **Bardou VJ, Arpino G, Elledge RM, Osborne CK, Clark GM** 2003 Progesterone receptor status significantly improves outcome prediction over estrogen receptor status alone for adjuvant endocrine therapy in two large breast cancer databases. J Clin Oncol 21:1973–1979
7. **Kastner P, Krust A, Turcotte B, Stropp U, Tora L, Gronemeyer H, Chambon P** 1990 Two distinct estrogen-regulated promoters generate transcripts encoding the two functionally different human progesterone receptor forms A and B. EMBO J 9:1603–1614
8. **Kraus WL, Katzenellenbogen BS** 1993 Regulation of progesterone receptor gene expression and growth in the rat uterus: modulation of estrogen actions by progesterone and sex steroid hormone antagonists. Endocrinology 132:2371–2379
9. **Richer JK, Jacobsen BM, Manning NG, Abel MG, Wolf DM, Horwitz KB** 2002 Differential gene regulation by the two progesterone receptor isoforms in human breast cancer cells. J Biol Chem 277:5209–5218
10. **Boyd-Leinen PA, Fournier D, Spelsberg TC** 1982 Nonfunctioning progesterone receptors in the developed oviducts from estrogen-withdrawn immature chicks and in aged nonlaying hens. Endocrinology 111:30–36
11. **Kato J, Hirata S, Nozawa A, Mouri N** 1993 The ontogeny of gene expression of progestin receptors in the female rat brain. J Steroid Biochem Mol Biol 47:173–182
12. **Shyamala G, Yang X, Cardiff RD, Dale E** 2000 Impact of progesterone receptor on cell-fate decisions during mammary gland development. Proc Natl Acad Sci USA 97:3044–3049
13. **Shyamala G, Yang X, Silberstein G, Barcellos-Hoff MH, Dale E** 1998 Transgenic mice carrying an imbalance in the native ratio of A to B forms of progesterone receptor exhibit developmental abnormalities in mammary glands. Proc Natl Acad Sci USA 20:696–701
14. **Mote PA, Bartow S, Tran N, Clarke CL** 2002 Loss of co-ordinate expression of progesterone receptors A and B is an early event in breast carcinogenesis. Breast Cancer Res Treat 72:163–172
15. **Arnett-Mansfield RL, de Fazio A, Wain GV, Jaworski RC, Byth K, Mote PA, Clarke CL** 2001 Relative expression of progesterone receptors A and B in endometrioid cancers of the endometrium. Cancer Res 61:4576–4582
16. **Loose-Mitchell DS, Chiappetta C, Stancel GM** 1988 Estrogen regulation of *c-fos* messenger ribonucleic acid. Mol Endocrinol 2:946–951
17. **Kirkland JL, Murthy L, Stancel GM** 1992 Progesterone inhibits the estrogen-induced expression of *c-fos* messenger ribonucleic acid in the uterus. Endocrinology 130:3223–3230
18. **Katzenellenbogen BS** 2000 Mechanisms of action and cross-talk between estrogen receptor and progesterone receptor pathways. J Soc Gynecol Investig 7:S33–S37
19. **Weigel RJ, deConinck EC** 1993 Transcriptional control of estrogen receptor in estrogen receptor negative breast carcinoma. Cancer Res 53:3472–3474
20. **Martin MB, Saceda M, Garcia-Morales P, Gottardis MM** 1994 Regulation of estrogen receptor expression. Breast Cancer Res Treat 31:183–189
21. **King RJ** 1993 William L. McGuire Memorial Symposium. Estrogen and progestin effects in human breast carcinogenesis. Breast Cancer Res Treat 27:3–15
22. **Mauvais-Jarvis P, Kuttenn F, Gompel A** 1986 Estradiol/progesterone interaction in normal and pathologic breast cells. Ann NY Acad Sci 464:152–167
23. **Graham JD, Roman SD, McGowan E, Sutherland RL, Clarke CL** 1995 Preferential stimulation of human progesterone receptor B expression by estrogen in T-47D human breast cancer cells. J Biol Chem 270:30693–30700
24. **Baulieu EE** 1989 Contragestion and other clinical applications of RU 486, an antiprogesterone at the receptor. Science 245:1351–1357
25. **Ghatge RP, Jacobsen BM, Schittone SA, Horwitz KB** 2005 The progestational and androgenic properties of medroxyprogesterone acetate: gene regulatory overlap with dihydrotestosterone in breast cancer cells. Breast Cancer Res 7:R1036–R1050
26. **Lanzino M, De Amicis F, McPhaul MJ, Marsico S, Panno ML, Andò S** 2005 Endogenous coactivator ARA70 interacts with estrogen receptor α (ERα) and modulates the functional ERα/androgen receptor interplay in MCF-7 cells. J Biol Chem 280:20421–20430
27. **Berrevoets CA, Umar A, Brinkmann AO** 2002 Antiandrogens: selective androgen receptor modulators. Mol Cell Endocrinol 198:97–103
28. **Sartorius CA, Melville MY, Hovland AR, Tung L, Takimoto GS, Horwitz KB** 1994 A third transactivation function (AF3) of human progesterone receptors located in the unique N-terminal segment of the B-isoform. Mol Endocrinol 8:1347–1360
29. **Meyer ME, Quirin-Stricker C, Lerouge T, Bocquel MT, Gronemeyer H** 1992 A limiting factor mediates the differential activation of promoters by the human progesterone receptor isoforms. J Biol Chem 267:10882–10887
30. **Vegeto E, Shahbaz MM, Wen DX, Goldman ME, O'Malley BW, McDonnell DP** 1993 Human progesterone receptor A form is a cell- and promoter-specific repressor of human progesterone receptor B function. Mol Endocrinol 7:1241–1243
31. **Saceda M, Lippman ME, Chambon P, Lindsey RL, Ponglikitmongkol M, Puente M, Martin MB** 1988 Regulation of the estrogen receptor in MCF-7 cells by estradiol. Mol Endocrinol 2:1157–1162
32. **Read LD, Greene GL, Katzenellenbogen BS** 1989 Regulation of estrogen receptor messenger ribonucleic acid and protein levels in human breast cancer cell lines by sex steroid hormones, their antagonists, and growth factors. Mol Endocrinol 3:295–304
33. **Pink JJ, Jordan VC** 1996 Models of estrogen receptor regulation by estrogens and antiestrogens in breast cancer cell lines. Cancer Res 56:2321–2330
34. **deGraffenried LA, Hilsenbeck SG, Fuqua SAW** 2002 Sp1 is essential for estrogen receptor α gene transcription. J Steroid Biochem Mol Biol 82:7–18
35. **Brayman MJ, Julian J, Mulac-Jericevic B, Conneely OM, Edwards DP, Carson**

DD 2006 Progesterone receptor isoforms A and B differentially regulate MUC1 expression in uterine epithelial cells. Mol Endocrinol 20:2278–2291
36. **Gao X, Loggie BW, Nawaz Z** 2002 The roles of sex steroid receptor coregulators in cancer. Mol Cancer 14:1–7
37. **Agoulnik IU, Krause WC, Bingman III WE, Rahman HT, Amrikachi M, Ayala GE, Weigel NL** 2003 Repressors of androgen and progesterone receptor action. J Biol Chem 278:31136–31148
38. **Dennis AP, Lonard DM, Nawaz Z, O'Malley BW** 2005 Inhibition of the 26S proteasome blocks progesterone receptor-dependent transcription through failed recruitment of RNA polymerase II. J Steroid Biochem Mol Biol 94:337–346
39. **Gross GE, Clark GM, Chamness GC, McGuire WL** 1984 Multiple progesterone receptor assays in human breast cancer. Cancer Res 44:836–840
40. **Sartorius CA, Shen T, Horwitz KB** 2003 Progesterone receptors A and B differentially affect the growth of estrogen-dependent human breast tumor xenografts. Breast Cancer Res Treat 79:287–299
41. **Nardulli AM, Katzenellenbogen BS** 1988 Progesterone receptor regulation in T47D human breast cancer cells: analysis by density labeling of progesterone receptor synthesis and degradation and their modulation by progestin. Endocrinology 122:1532–1540
42. **Hopp TA, Weiss HL, Hilsenbeck SG, Cui Y, Allred DC, Horwitz KB, Fuqua SA** 2004 Breast cancer patients with progesterone receptor PR-A-rich tumors have poorer disease-free survival rates. Clin Cancer Res 10:2751–2760
43. **Eden J** 2003 Progestins and breast cancer. Am J Obstet Gynecol 188:1123–1131
44. **Alexander IE, Shine J, Sutherland RL** 1990 Progestin regulation of estrogen receptor messenger RNA in human breast cancer cells. Mol Endocrinol 4:821–828
45. **Graham JD, Yeates C, Balleine RL, Harvey SS, Milliken JS, Bilous AM, Clarke CL** 1996 Progesterone receptor A and B protein expression in human breast cancer. J Steroid Biochem Mol Biol 56:93–98
46. **Huang HJ, Neven P, Drijkoningen M, Paridaens R, Wildiers H, Van Limbergen E, Berteloot P, Amant F, Christiaens MR, Vergote I** 2005 Association between HER-2/neu and the progesterone receptor in oestrogen-dependent breast cancer is age-related. Breast Cancer Res Treat 91:81–87
47. **Bamberger AM, Milde-Langosch K, Schulte HM, Löning T** 2000 Progesterone receptor isoforms, PR-B and PR-A, in breast cancer: correlations with clinicopathologic tumor parameters and expression of AP-1 factors. Horm Res 54:32–37
48. **Li X, Wong J, Tsai SY, Tsai MJ, O'Malley BW** 2003 Progesterone and glucocorticoid receptors recruit distinct coactivator complexes and promote distinct patterns of local chromatin modification. Mol Cell Biol 23:3763–3773
49. **Nagy L, Kao HY, Chakravarti D, Lin RJ, Hassig CA, Ayer DE Schreiber SL, Evans RM** 1997 Nuclear receptor repression mediated by a complex containing SMRT, mSin3A, and histone deacetylase. Cell 89:373–380
50. **Hu X, Lazar MA** 1999 The CoRNR motif controls the recruitment of corepressors by nuclear hormone receptors. Nature 402:93–96
51. **Webb P, Anderson CM, Valentine C, Nguyen P, Marimuthu A, West BL, Baxter JD, Kushner PJ** 2000 The nuclear receptor corepressor (N-CoR) contains three isoleucine motifs (I/LXXII) that serve as receptor interaction domains (IDs). Mol Endocrinol 14:1976–1985
52. **Giannoukos G, Szapary D, Smith CL, Meeker JE, Simons Jr SS** 2001 New antiprogestins with partial agonist activity: potential selective progesterone receptor modulators (SPRMs) and probes for receptor- and coregulator-induced changes in progesterone receptor induction properties. Mol Endocrinol 15:255–270
53. **Heldring N, Nilsson M, Buehrer B, Treuter E, Gustafsson JA** 2004 Identification of tamoxifen-induced coregulator interaction surfaces within the ligand-binding domain of estrogen receptors. Mol Cell Biol 24:3445–3459
54. **Hu X, Li Y, Lazar MA** 2001 Determinants of CoRNR-dependent repression complex assembly on nuclear hormone receptors. Mol Cell Biol 21:1747–1758
55. **Jepsen K, Rosenfeld MG** 2002 Biological roles and mechanistic actions of co-repressor complexes. J Cell Sci 115:689–698
56. **van der Burg B, Rutteman GR, Blankenstein MA, de Laat S W, van Zoelen EJ** 1988 Mitogenic stimulation of human breast cancer cells in a growth factor-defined medium: synergistic action of insulin and estrogen. J Cell Physiol 34:101–108
57. **Bunone G, Briand PA, Miksicek RJ, Picard D** 1996 Activation of the unliganded estrogen receptor by EGF involves the MAP kinase pathway and direct phosphorylation. EMBO J 15:2174–2183
58. **Tora L, Mullick A, Metzger D, Ponglikitmongkol M, Park I, Chambon P** 1989 The cloned human oestrogen receptor contains a mutation which alters its hormone binding properties. EMBO J 8:1981–1986
59. **Tung L, Abdel-Hafiz H, Shen T, Harvell DME, Nitao LK,. Richer JK, Sartorius CA, Takimoto G, Horwitz KB** 2006 Progesterone receptors (PR)-B and -A regulate transcription by different mechanisms: AF-3 exerts regulatory control over coactivator binding to PR-B. Mol Endocrinol 20:2656–2667
60. **Faivre EJ, Lange CA** 2007 Progesterone receptors upregulate Wnt-1 to induce epidermal growth factor receptor transactivation and c-Src-dependent sustained activation of Erk1/2 mitogen-activated protein kinase in breast cancer cells. Mol Cell Biol 27:466–480
61. **Fritsch M, Aluker M, Murdoch FE** 1999 Identification of a unique liganded estrogen receptor complex released from the nucleus by decavanadate. Biochemistry 38:6987–6996
62. **Hardy DB, Janowski BA, Corey DR, Mendelson CR** 2006 Progesterone receptor plays a major antiinflammatory role in human myometrial cells by antagonism of nuclear factor-κB activation of cyclooxygenase 2 expression. Mol Endocrinol 20:2724–2733
63. **Morelli C, Garofalo C, Sisci D, del Rincon S, Cascio S, Tu X, Vecchione A, Sauter ER, Miller Jr WH, Surmacz E** 2004 Nuclear insulin receptor substrate 1 interacts with estrogen receptor α at ERE promoters. Oncogene 23:7517–7526

Journal of Cellular Physiology

Evidence That Leptin Through STAT and CREB Signaling Enhances Cyclin D1 Expression and Promotes Human Endometrial Cancer Proliferation

STEFANIA CATALANO,[1,2] CINZIA GIORDANO,[1] PIETRO RIZZA,[3] GUOWEI GU,[1] INES BARONE,[1] DANIELA BONOFIGLIO,[1,2] FRANCESCA GIORDANO,[3] ROCCO MALIVINDI,[1] DONATELLA GACCIONE,[1] MARILENA LANZINO,[1] FRANCESCA DE AMICIS,[1] AND SEBASTIANO ANDÒ[2,3]*

[1]*Departments of Pharmaco-Biology, University of Calabria, Arcavacata di Rende (CS), Italy*

[2]*Departments of Centro Sanitario, University of Calabria, Arcavacata di Rende (CS), Italy*

[3]*Departments of Cell Biology, University of Calabria, Arcavacata di Rende(CS), Italy*

Obesity is a risk factor for endometrial cancer in pre- and post-menopausal women. Leptin, an adipocyte-derived hormone, in addition to the control weight homeostasis, is implicated in multiple biological actions. A recent study demonstrated that leptin promotes endometrial cancer growth and invasiveness through STAT/MAPK and Akt pathways, but the molecular mechanism involved in such processes still needs to be elucidated. In an attempt to understand the role of leptin in regulating endometrial cancer cells proliferation, we have demonstrated that leptin treatment reduced the numbers of cells in G0/G1-phase while increased cell population in S-phase. This effect is associated with an up-regulation of cyclin D1 together with a down-regulation of cyclin-dependent kinase inhibitor $p21^{WAF1/Cip1}$. Mutagenesis studies, eletrophoretic mobility shift, and chromatin immunoprecipitation analysis revealed that signal transducers and activators of transcription 3 (STAT3) and cyclic AMP-responsive element (CRE) binding protein motifs, within cyclin D1 promoter, were required for leptin-induced cyclin D1 expression in Ishikawa endometrial cancer cells. Silencing of STAT3 and CREB gene expression by RNA interference reversed the up-regulatory effect of leptin on cyclin D1 expression and cells proliferation. These results support the hypothesis that STAT3 and CREB play an important role in leptin signaling pathway that leads to the proliferation of Ishikawa cells, thus establishing a direct association between obesity and endometrial tumorogenesis.

J. Cell. Physiol. 218: 490–500, 2009.

Leptin, the product of the *ob* gene, mainly secreted by adipocytes, is involved in the control of body weight and its plasma levels strongly correlate to the body fat mass (Zhang et al., 1994; Ahima and Flier, 2000).

In addition to its regulatory role in energy metabolism, leptin is also implicated in the modulation of many other processes such as reproduction, lactation, hematopoiesis, immune responses, and cell proliferation (Ahima and Flier, 2000; Huang and Li, 2000; Brann et al., 2002). More interestingly, recent studies have demonstrated that leptin stimulates growth, migration, invasion, and angiogenesis in tumor cell models, suggesting that it is able to promote an aggressive cancer phenotype (Bouloumie et al., 1998; Somasundar et al., 2004b; Garofalo and Surmacz, 2006).

The activities of leptin are mediated through the transmembrane leptin receptor (ObR) present in a variety of tissues (Tartaglia, 1997), by activation of the Janus-activated kinase/signal transducers and activators of transcription (JAK/STAT) (Bahrenberg et al., 2002; Ahima and Osei, 2004) as well as mitogen-activated protein kinase (MAPK) and phosphatidylinositol 3-kinase/(PI-3K)/Akt pathways (Sweeney, 2002; Zabeau et al., 2003). Besides, induction of ObR can activate several genes involved in cell proliferation, such as c-fos, c-jun, jun B, and egr-1 (Sweeney, 2002; Zabeau et al., 2003).

Epidemiological studies have suggested a positive correlation between obesity and an increased risk of different cancers, including breast, prostate, colon, and endometrial (Calle and Kaaks, 2004; Garofalo and Surmacz, 2006; Somasundar et al., 2004a). There is convincing and consistent evidence from both case-control and cohort studies that obesity is tightly related to endometrial cancer in both pre- and post-menopausal women (Calle and Thun, 2004).

Endometrial cancer is the most common gynecological malignancy and the fourth most common malignancy in women in the developed world after breast, colorectal and lung cancer. The incidence is estimated at 15–20 per 100,000 women per year (Ryan et al., 2005).

Contract grant sponsor: AIRC.

*Correspondence to: Sebastiano Andò, Department of Cell Biology, University of Calabria, Arcavacata di Rende (CS) 87030, Italy. E-mail: sebastiano.ando@unical.it

Received 8 August 2008; Accepted 23 September 2008

Published online in Wiley InterScience (www.interscience.wiley.com.), 5 November 2008.
DOI: 10.1002/jcp.21622

Several studies demonstrated that serum–leptin levels among cases with endometrial cancer were significantly higher compared to controls (Petridou et al., 2002; Yuan et al., 2004). Expression of leptin and its functional receptor, short (ObRs) and long (ObRl) isoform has been shown in both cancer and non-cancer endometrium (Gonzalez et al., 2000; Kitawaki et al., 2000; Koda et al., 2007). The levels of ObRl were similar in cancer and normal tissue, but the short isoform was significantly decreased in malignant cells. Moreover, induction of the expression of this receptor resulted in inhibited proliferation of cancer cells due to delayed start of the mitotic S-phase, suggesting that loss of ObRs in the endometrial cancer might contribute to malignant progression (Yuan et al., 2004).

A recent report demonstrated that leptin promotes endometrial cancer growth and invasiveness through STAT/MAPK and Akt pathways. Particularly, treatment with leptin resulted in increased proliferation and induces invasion of ECC1 and Ishikawa cells (Sharma et al., 2006). However, the molecular mechanism by which leptin-induced endometrial cancer cell proliferation still needs to be elucidated.

In the last years, a large body of evidence has shown that disruption of cell cycle control mechanism is a common pathway in human cancer and overexpression of cyclin D1 is one of the most commonly observed alterations (Cordon-Cardo, 1995; Fu et al., 2004; Knudsen et al., 2006). Cyclin D1, an important cell cycle regulator is required for completion of the G1/S transition in normal mammalian cells (Fu et al., 2004). Moreover, its expression increases from normal endometrium to hyperplasia and carcinoma, suggesting that it may play a role in endometrial carcinogenesis (Ruhul-Quddus et al., 2002).

The aim of the present study was to explore the molecular mechanism eliciting the proliferative effect of leptin in endometrial cancer cell. We demonstrated that leptin enhances cyclin D1 expression through regulation of STAT binding site (GAS) and cyclic AMP-response element (CRE) located within its promoter.

Our findings have provided evidence for better understanding the association between obesity and endometrial cancer.

Materials and Methods

Materials

Dulbecco's modified Eagle's medium (DMEM), L-glutamine, Eagle's non-essential amino acids, penicillin, streptomycin, fetal bovine serum (FBS), bovine serum albumin (BSA), phosphate-buffered saline were purchased from Eurobio (Les Ullis Cedex, France). TRIzol and Lipofectamine 2,000 reagent by Invitrogen (Carlsbad, CA), FuGENE 6 by Roche Applied Science (Indianapolis, IN). TaqDNA polymerase, RETROscript kit, 100-bp DNA ladder, Dual Luciferase kit, and TK Renilla luciferase plasmid were provided by Promega (Madison, WI). Aprotinin, leupeptin, phenylmethylsulfonyl fluoride (PMSF), sodium orthovanadate, U0126, AG490, H89, and recombinant human leptin were purchased by Sigma (Milan, Italy). Antibodies against phospho p44/42 MAPK (Thr 202/Tyr 204) (#9101S), p44/42 MAPKinase (#9102), pCREB (Ser133), and CREB (48H2) were provided by Cell Signaling. Antibodies against cyclin D1 (M-20), GAPDH (FL-335), $p21^{WAF1/Cip1}$ (H164), pSTAT3 (B-7), STAT3 (F-2), and polymerase II (N20) by Santa Cruz Biotechnology (Santa Cruz, CA). An ECL system and Sephadex G-50 spin columns were purchased from Amersham Biosciences (Buckinghamshire, UK). [λ^{32}P]ATP and [^{3}H]thymidine from PerkinElmer Life Sciences (Wellesley, MA). RNase A (Calbiochem, La Jolla, CA).

Plasmids

The plasmids containing the human cyclin D1 promoter or its deletions (p−2966/+142, p−944/+142, p−848/+142, p−136/+142) were kindly provided by Prof A. Weisz (University of Naples, Italy). These fragments were inserted into the luciferase vector pXP2.

Site-directed mutagenesis

The cyclin D1 promoter plasmids bearing both STAT3 binding recognition (GAS) and cyclic AMP-responsive element (CRE) mutated sites (pGAS/CRE mut) were created by site-directed mutagenesis using QuickChange kit (Stratagene, La Jolla, CA). Briefly, this was based on a PCR reaction with two complementary oligonucleotide primers containing the mutation. The PCR was performed with the *Pfu* DNA polymerase during 16 cycles (30 sec at 95°C, 30 sec at 55°C, and 8 min at 68°C), using as template the human cyclin D1 promoter p−136/+142 and the following mutagenic primers (mutations are shown as lowercase letters): 5′-CGGACTACAGGGGAGTagcGTTGAAGTTGCAAAGTCC-TGGAG-3′ and 5′-CTCCAGGACTTTGCAACTTCAACgctAC-TCCCCTGTAGTCCG-3′ (GAS MUT); 5′-GATCTTTGCTTAA-CAACAGTAACtctACACGGACTACAGGGGAG -3′ and 5′-CTCCCCTGTAGTCCGTGTagaGTTACTGTTGTTAAG CAAAGATC-3′ (CRE MUT). The PCR products were then incubated with *Dpn*I which only digests the parental methylated cDNA and the constructed mutated expression vectors were confirmed by DNA sequencing.

Cell culture

Ishikawa human endometrial cancer cells were obtained from D. Picard (University of Geneva, Geneva, Switzerland). Ishikawa cells were maintained in DMEM without phenol red supplemented with 10% fetal bovine serum, 1% L-glutamine, and 1% penicillin/streptomycin. Cells were switched to medium without serum 48 h before each experiment.

DNA flow cytometry

Ishikawa cells were harvested, fixed, and stained with Propidium iodide (100 μg/ml) after treatment with RNase A (20 μg/ml). Stained cells were analyzed for DNA content by Flow Cytometry using FAC-Scan (Becton Dickingson and Co., Franklin Lakes, NJ).

Total RNA extraction and reverse transcription-PCR assay

Total cellular RNA was extracted from Ishikawa cells using Triazol reagent as suggested by the manufacturer. The evaluation of genes expression was performed by the reverse transcription-PCR method using a RETROscript kit as suggested by the manufacturer. The cDNAs obtained were amplified by PCR using the following primers: 5′-TCTAAGATGAAGGAGACCATC-3′ and 5′-GCGGTAGTAGGACAGGAAGTTGTT-3′ (cyclin D1); 5′-GCTTCATGCCAGCTACTTCC-3′ and 5′-CTGTGCTCACTTCAGGGTCA -3′ ($P21^{WAF1/Cip1}$); 5′-CTCAACATCTCCCCCTTCTC-3′ and 5′-CAAATCCCATATCCTCGTCC-3′ (36B4). The PCR was performed for 30 cycles for cyclin D1 (94°C for 1 min, 60°C for 1 min, and 72°C for 2 min), 30 cycles for p21 (94°C for 1 min, 58°C for 1 min, and 72°C for 2 min) and 15 cycles (94°C for 1 min, 58°C for 1 min, and 72°C for 2 min) to amplify 36B4 in the presence of 1 μl of first strand cDNA, 1 μM each of the primers mentioned above, 0.5 mM dNTP, *Taq* DNA polymerase (2 units/tube), and 2.2 mM magnesium chloride in a final volume of 25 μl. To check for the presence of DNA contamination, a reverse transcription-PCR was performed on 1 μg of total RNA without Moloney murine leukemia virus reverse transcriptase (the negative control). DNA quantity in each lane was analyzed by scanning densitometry.

Immunoblotting

Ishikawa cells were grown in 10 cm dishes to 50–60% confluence and lysed in 500 μl of 50 mM Tris–HCl, 150 mM NaCl, 1% NP-40, 0.5% sodium deoxycholate, 2 mM sodium fluoride, 2 mM EdTA, 0.1% SDS, and a mixture of protease inhibitors (aprotinin, PMSF,

and sodium ortho-vanadate). Equal amounts of total proteins were resolved on an 11% SDS–polyacrylamide gel, transferred to a nitrocellulose membrane and probed with the appropriated antibody. As internal control, all membranes were subsequently stripped (glycine 0.2 M, PH 2.6 for 30 min at room temperature) of the first antibody and reprobed with anti GADPH Ab. The antigen–antibody complex was detected by incubation of the membranes for 1 h at room temperature with peroxidase-coupled goat anti-mouse or anti-rabbit IgG and revealed using the ECL System. The blots were then exposed to film, and the bands of interest were quantified by Scion Image laser densitometry scanning program. The results obtained as optical density arbitrary values were transformed to percentages of the control (percent control) taking the samples from cells not treated as 100%.

Transient transfection assay

Ishikawa cells were starved with serum free medium for 24 h and then transfected using the FuGENE 6 reagent with the mixture containing 0.25 μg of human cyclin D1 promoter constructs. Twenty-four hours after transfection, the cells were untreated or treated with 1,000 ng/ml leptin for 6, 12, and 24 h. TK Renilla luciferase plasmid (10 ng per each well) was used. Firefly and Renilla luciferase activities were measured by Dual Luciferase kit. The firefly luciferase data for each sample were normalized based on the transfection efficiency measured by Renilla luciferase activity.

Electrophoretic mobility shift assay (EMSA)

Nuclear extracts from Ishikawa cells were prepared as previously described (Catalano et al., 2003). The probe was generated by annealing single-stranded oligonucleotides, labeled with [λ^{32}P] ATP and T4 polynucleotide kinase, and purified using Sephadex G50 spin columns. The DNA sequences used as probe or as cold competitors are the following (the nucleotide motifs of interest are underlined, and mutations are shown as lowercase letters): 5′-TTAACAACAGTAACGTCACACGGACTA-3′ and 5′-TAGTCCGTGTGACGTTACTGTTGTTAA-3′ (CRE); 5′-AGGGGAGTTTTGTT GAAGTTGCAAA-3′ and 5′-TTTGCAACTTCAACAAAACTCCCCT-3′ (GAS); 5′-C TTAACAACAGTAAttgCACACGGACTA-3′ and 5′-TAGTCCGTGTGcaaTT ACTGTTGTTAAG-3′ (CRE MUT); 5′-AGGGGAGTagcGTTGAAGTTGCAAA-3′ and 5′-TTTGCAAC TTCAACgctACTCCCCT-3′ (GAS MUT). In vitro transcribed and translated CREB protein was synthesized using the T7 polymerase in the rabbit reticulocyte lysate system. The protein-binding reactions were carried out in 20 μl of buffer [20 mmol/L HEPES (pH 8), 1 mmol/L EDTA, 50 mmol/L KCl, 10 mmol/L DTT, 10% glycerol, 1 mg/ml BSA, 50 μg/ml poly(dI/dC)] with 50,000 cpm of labeled probe, 20 μg of Ishikawa nuclear protein or an appropriate amount of CREB protein, and 5 μg of poly (dI-dC). The mixtures were incubated at room temperature for 20 min in the presence or absence of unlabeled competitor oligonucleotides. For experiments involving STAT3 and CREB antibodies, the reaction mixture was incubated with these antibodies at 4°C for 12 h before addition of labeled probe. The entire reaction mixture was electrophoresed through a 6% polyacrylamide gel in 0.25 × Tris borate–EDTA for 3 h at 150 V.

Chromatin immunoprecipitation assay (ChIP)

ChIP was performed as previously described (Morelli et al., 2004). Ishikawa cells were untreated or treated with 1,000 ng/ml leptin for 1 h. The cells were then cross-linked with 1% formaldehyde and sonicated. Supernatants were immunocleared with salmon sperm DNA/protein A and immunoprecipitated with specific anti-STAT3, anti-CREB and anti polymerase II antibodies or a normal mouse serum IgG as negative control. Pellets were washed as reported, eluted with elution buffer (1% SDS, 0.1 M $NaHCO_3$) and digested with proteinase K. DNA was obtained by phenol/chloroform/isoamyl alcohol extractions and precipitated with ethanol; 3 μl of each sample were used for PCR amplification with the following primers flanking GAS/CRE sequence present in the cyclin D1 promoter region: 5′-TGCGCCCGCCCCCGCCCCCCTC-3′ and 5′-TGTTCCATGGCTGGGGCTCTT-3′. The PCR conditions were 1 min at 94°C, 1 min at 65°C, and 2 min at 72°C. The amplification products obtained in 35 cycles were analyzed in a 2% agarose gel and visualized by Ethidium bromide staining.

RNA interference (RNAi)

Cells were plated in 6-well dishes with regular growth medium the day before transfection to 60–70% confluence. On the second day the medium was changed with SFM without P/S and cells were transfected with RNA duplex of stealth RNAi targeted human STAT3 mRNA sequence 5′-GCC UCA AGA UUG ACC UAG Att-3′ (Ambion, Austin, TX), with RNA duplex of validate RNAi targeted human CREB mRNA sequence 5′- GGC UAA CAA UGG UAC CGA Utt -3′ or with a stealth RNAi control (Ambion) to a final concentration of 50 nM using Lipofectamine 2000 as recommended by the manufacturer. After 5 h the transfection medium was changed with SFM in order to avoid Lipofectamine 2000 toxicity and cells were exposed to Leptin 1,000 ng/ml for 24 or 48 h. These transfected cells were used to examine the effects of silencing STAT3 and CREB gene expression on: (1) cyclin D1 protein content, (2) cellular proliferation by [^{3}H]thymidine incorporation.

[^{3}H]thymidine incorporation

Ishikawa cells were untreated or treated with leptin 1,000 ng/ml for 24 or 48 h. For the last 6 h, [^{3}H]thymidine (1 μCi/ml) was added to the culture medium. After rinsing with phosphate-buffered saline, the cells were washed once with 10% and three times with 5% trichloroacetic acid. The cells were lysed by adding 0.1 N NaOH and then incubated for 30 min at 37 °C. Thymidine incorporation was determined by scintillation counting.

Statistical analysis

Each datum point represents the mean ± SE of three different experiments. Statistical analysis was performed using ANOVA followed by Newman–Keuls testing to determine differences in means. $P < 0.05$ was considered as statistically significant.

Results

Leptin modulates cell cycle progression in endometrial cancer cells

Flow Cytometric analysis was used to investigate the role of leptin on Ishikawa cell cycle progression. Cells were synchronized by 48 h serum starvation and then induced to re-enter the cell cycle by treatment with hormone. Twenty-four hours leptin treatment reduced the percentage of cells in the G0/G1-phase of the cell cycle and increased the fraction of the cells in S-phase, compared with control group (Fig. 1).

Leptin enhances cyclin D1 and down-regulates $p21^{WAF1/Cip1}$ expression in Ishikawa cells

To characterize the molecular mechanism associated with the proliferative effects induced by leptin, we examined changes in the expression of genes involved in these processes. Since cyclin D1 is a critical modulator in the cell cycle G1/S transition and its overexpression is one of the most commonly observed alterations in human endometrial cancers (Lukas et al., 1994; Nikaido et al., 1996; Fu et al., 2004), we aimed to evaluate the potential ability of leptin to modulate cyclin D1 mRNA and protein content in Ishikawa human endometrial cancer cells. RT-PCR showed an increased mRNA expression of the cyclin D1 gene after treatment with leptin 1,000 ng/ml for 6, 12, and 24 h. Cyclin D1 mRNA expression was normalized using the human housekeeping gene 36B4 (Fig. 2A). The leptin-induced

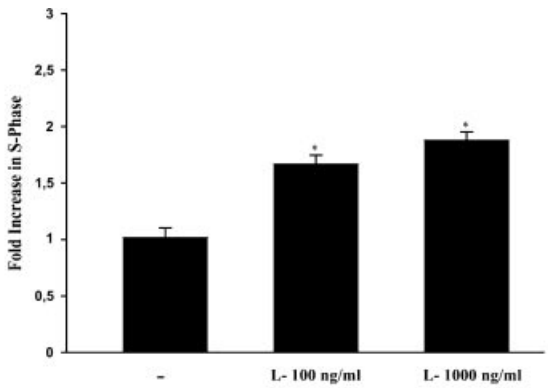

	S-Phase	G2/M	G0/G1
-	24 ± 2	22 ± 2,3	54 ± 1,6
L- 100 ng/ml	39 ± 1,9*	23 ± 1,7	38 ± 1,6*
L- 1000 ng/ml	44 ± 1,7*	24 ± 1,4	32 ± 1,2*

Fig. 1. Leptin increases the fraction of Ishikawa cells in S-phase of the cell cycle. Ishikawa cells were synchronized in serum-free media for 48 h and then exposed to 100 ng/ml and 1,000 ng/ml leptin (L) for 24 h or left untreated (–). The distribution of Ishikawa cells in the cycle was determined by Flow Cytometry using Propidium-iodide stained nuclei. The results indicate the fold-increase of Ishikawa cells in S-phase after serum starvation or leptin treatment. The histograms represent the mean ± SE of three separate experiments done in triplicate. The table shows the distribution of Ishikawa cells in the various phases of cell cycle. *$P < 0.01$ compared with untreated cells.

expression of cyclin D1 was evidenced at protein level, at all investigated times, by Western blotting analysis (Fig. 2B).

To study more properly the involvement of leptin in cell cycle G1/S transition phase, the expression of $p21^{WAF1/Cip1}$, the major cyclin-dependent-kinase inhibitor, was analyzed. As shown in Figure 2A and B $p21^{WAF1/Cip1}$ mRNA and protein levels decreased in leptin treated cells.

These observations indicate that leptin may promote G1/S-phase progression by stimulating expression of cyclin D1 and inhibiting the expression of $p21^{WAF1/Cip1}$.

Leptin-induced cyclin D1 expression is STAT, ERK, and PKA dependent in Ishikawa cells

Leptin exerts its biological functions through binding to its receptors that mediate a downstream signal by activating multiple signaling pathways (Sweeney, 2002; Ahima and Osei, 2004). To gain insight into the mechanism underlying the modulatory role of leptin on cyclin D1 expression in endometrial cancer cells, we examined the changes in signal transductional pathways involved in mediating leptin action. Cellular proteins were extracted from Ishikawa cells treated with 1,000 ng/ml of leptin at different times, and by Western blotting analysis we determined the status of STAT3 and ERK1/2 phosphorylation. As shown in Figure 3A, leptin significantly induced phosphorylation of STAT3 within 15 min of treatment while an increased phosphorylation of ERK was observed after 5 min of leptin stimulation (Fig. 3B). Besides, we also examined the effect of leptin on phosphorylated CREB/ATF-1, a downstream substrate of MAPK, but also an effector of PKA (Delghandi et al., 2005). The CREB Ab produces two bands and recognizes both CREB (upper band) and ATF-1 (lower band). Notably, leptin exposure for 15 min significantly induced phosphorylation of CREB/ATF1 (Fig. 3C), which was inhibited by pretreatment of these cells with PKA and ERK1/2 inhibitors, H89 and U0126 respectively (Fig. 3D).

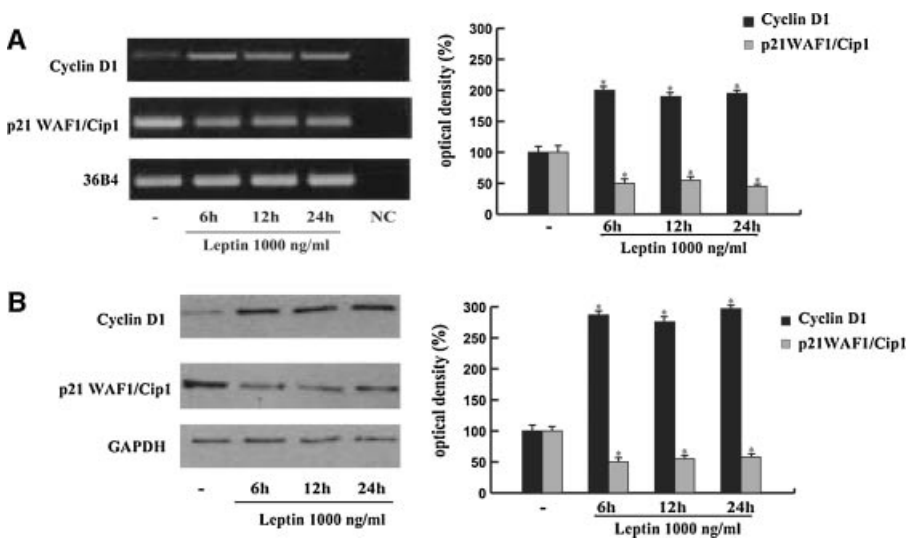

Fig. 2. Effects of Leptin on cyclin D1 and p $21^{WAF1/Cip1}$ expression in Ishikawa cells. Ishikawa cells were serum-starved for 48 h followed by treatment with 1,000 ng/ml leptin for 6, 12, and 24 h or left untreated (–). A: Total RNA was isolated from Ishikawa cells and reverse transcribed. cDNA was subjected to PCR using specific primers for cyclin D1, $p21^{WAF1/Cip1}$ or 36B4. NC: negative control, RNA sample without the addition of reverse transcriptase. 36B4 mRNA levels were determined as control. B: Protein extracts obtained from Ishikawa cells were resolved by SDS–PAGE and subjected to immunoblot analysis with rabbit antiserum against human cyclin D1 and $p21^{WAF1/Cip1}$. GAPDH served as loading control. The histograms represent the mean ± SE of three separate experiments in which band intensities were evaluated in terms of optical density arbitrary units and expressed as the percentage of the control assumed as 100%. *$P < 0.01$ compared to untreated cells.

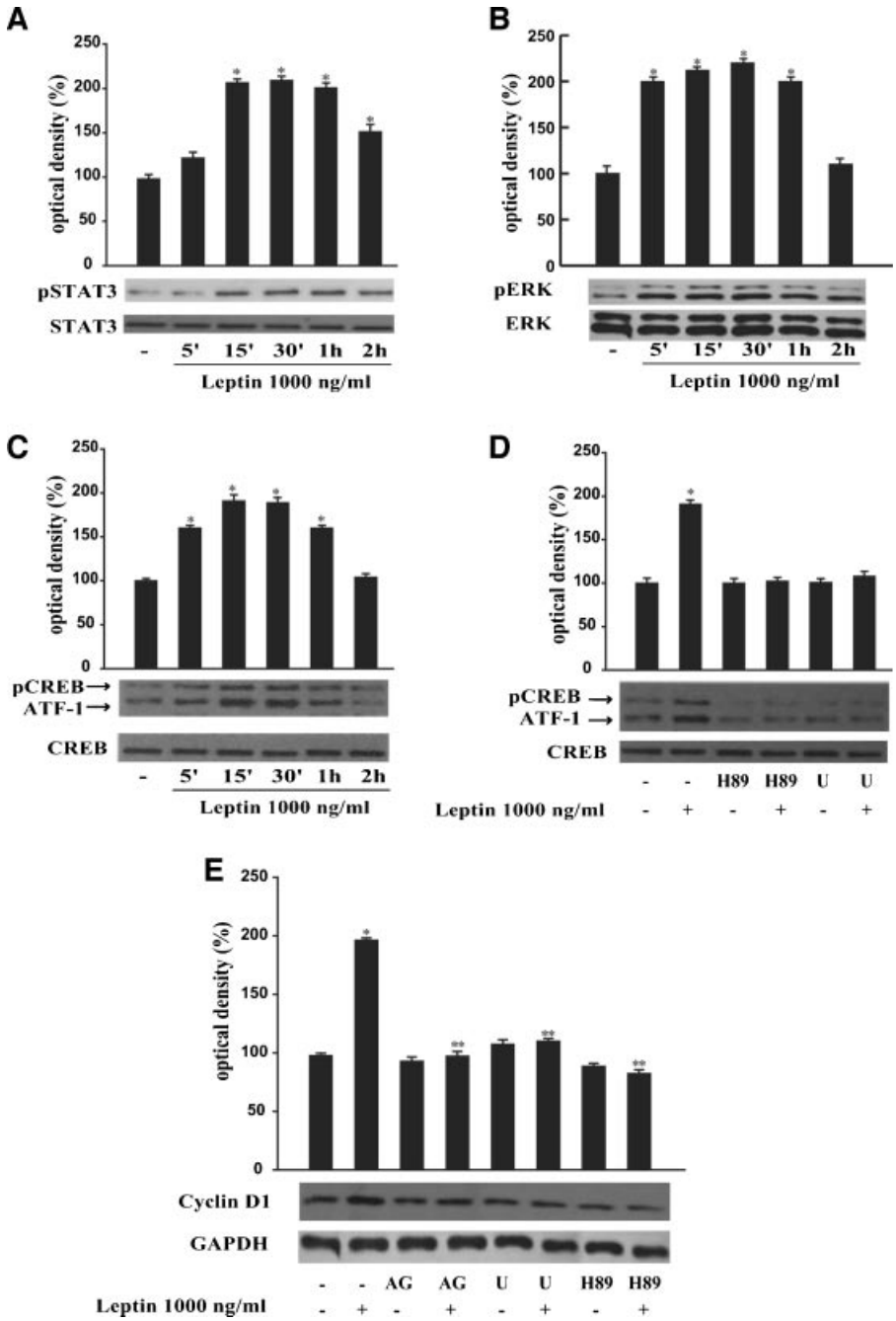

Fig. 3. Activation of leptin signalling in the up-regulation of cyclin D1 expression. Ishikawa cells were serum-starved for 48 h and then treated with 1,000 ng/ml leptin for various time intervals or left untreated (–). Protein extracts obtained from Ishikawa cells were resolved by SDS–PAGE and subjected to immunoblot analysis with specific antibodies against total or phosphorylated (p) forms of STAT3 (A), ERK (B), and CREB/ATF-1 (C). For combined treatment, cells were pretreated with H89 (10 μM) and U0126 (U) (10 μM) for 30 min followed by leptin treatment for 15 min. Equal amounts of protein were resolved by SDS–PAGE and subjected to immunoblot analysis and immunoblotted with specific antibodies against total or phosphorylated CREB/ATF1 (D). E: Ishikawa cells were serum-starved for 48 h and treated with 1,000 ng/ml leptin for 24 h or left untreated (–). For combined treatment, cells were pretreated with AG490 (AG) (20 μM), U0126 (U) (10 μM), and H89 (10 μM) for 30 min followed by leptin treatment. Specific antibodies against cyclin D1 and GAPDH were used. The histograms represent the mean ± SE of three separate experiments in which band intensities were evaluated in terms of optical density arbitrary units and expressed as the percentage of the control assumed as 100%. *$P < 0.01$ compared to untreated cells; **$P < 0.01$ compared to leptin treatment alone.

Leptin had no effect on total STAT3, ERK and CREB protein expression levels.

Next, to investigate the signal transduction pathways involved in leptin-induced cyclin D1 expression, chemical inhibitor of JAK/STAT (AG490), ERK1/2 (U0126), and PKA (H89) were added to serum-starved Ishikawa cells before treatment with 1,000 ng/ml of leptin for 24 h. Our results revealed that AG490, U0126, and H89 effectively prevent leptin induction of cyclin D1 expression (Fig. 3E).

Leptin transactivates cyclin D1 promoter in Ishikawa cells

The aforementioned observations prompted us to evaluate whether leptin signalling could affect cyclin D1 transcriptional activity. Thus, we transiently transfected Ishikawa cells with a luciferase reporter construct containing the upstream region of the cyclin D1 gene spanning from −2.966 to +142. As shown in Figure 4B, a significant increase in promoter activity was observed in the transfected cells exposed to leptin 1,000 ng/ml for 6, 12, and 24 h.

Cyclin D1 promoter contains multiple regulatory elements, including binding sites for AP-1, STATs, NF-kB, Oct-1, Sp1, CRE, and TCF/LEF (Allan et al., 2001; Natsume et al., 2003; Bartusel et al., 2005; Brockman and Schuler, 2005; Saxena et al., 2007b).

To delimit the *cis*-element involved in cyclin D1 transcriptional activation by leptin, we transiently transfected Ishikawa cells with plasmids containing a series of 5′ deleted segments of human cyclin D1 promoter. Schematic representation of constructs is shown in Figure 4A.

In transfection experiments performed using p−944/+142, p−848/+142, and p−136/+142 the responsiveness to leptin was still observed at all investigated time (Fig. 4B), suggesting that the region from −136 to +142 was required for the transactivation of cyclin D1 by leptin.

The nucleotide sequence analysis of this region evidenced a CRE and STAT3 binding motif (GAS) located at position −52 and −27 respectively, putative effectors of leptin signalling as previously demonstrated in other systems (Mauro et al., 2007; Saxena et al., 2007b). Thus, mutation analysis of both CRE and GAS sites on cyclin D1 promoter was carried out.

As shown in Figure 4D mutation of both GAS and CRE completely abolished leptin responsiveness of cyclin D1 promoter in Ishikawa cells demonstrating their involvement in the up-regulation of cyclin D1 induced by leptin.

Leptin increases STAT3-DNA and CREB-DNA binding activity to cyclin D1 promoter

To further investigate the specific role of GAS and CRE motifs in the transcriptional activation of cyclin D1 by leptin, we performed EMSA experiments.

Using synthetic oligodeoxyribonucleotides corresponding to the GAS and CRE motifs, we observed the formation of a complex in nuclear extract from Ishikawa cells (Fig. 5A and B, lane 1), which was abrogated by 100-fold molar excess of unlabeled probe (Fig. 5A and B, lane 2) demonstrating the specificity of the DNA binding complex. This inhibition was not longer observed when mutated oligodeoxyribonucleotides were used as competitor (Fig. 5A and B, lane 3). Leptin-induced both GAS and CRE activation compared with control samples at the same time-point (Fig. 5A and B, lane 4, 5, and 6). Incubation of anti-STAT3 with the nuclear extracts resulted in a greatly reduced band, indicating the presence of STAT3 protein in the complex (Fig. 5A, lane 7). Similarly, incubation of anti-CREB with the nuclear extracts resulted in reduced and supershifted band (Fig. 5B, lane 7). IgG did not affect either GAS or CRE complex formation (Fig. 5A and B, lane 8). Using transcribed and translated in vitro CREB protein, we obtained a complex migrating at the same level as that of Ishikawa nuclear extracts (Fig. 5B, lane 9).

Leptin enhances recruitment of STAT3 and CREB to the promoter region of cyclin D1

Although our findings clearly demonstrated the role of STAT3 and CREB in leptin mediated regulation of cyclin D1 promoter, we further sought to determine that STAT3 and CREB directly participate in leptin mediated cyclin D1 gene regulation using ChIP assay. Using specific antibody against STAT3, formaldehyde cross-linked protein-chromatin complexes were immunoprecipitated from Ishikawa cells cultured with or without leptin 1,000 ng/ml. The resulting precipitated genomic DNA was then analyzed by PCR using primers spanning the STAT3 binding element in the promoter region of cyclin D1. As shown in Figure 5C, ChIP analysis with anti-STAT3 antibody revealed that treatment with leptin for 1 h increased STAT3 recruitment to cyclin D1 promoter. Interestingly, we also observed upon leptin stimulation a significant increase in CREB recruitment to the cyclin D1 promoter as evidenced by ChIP analysis using anti-CREB antibody. In addition, the enhanced recruitment of STAT3 and CREB was correlated with greater association of polymerase II to the cyclin D1 regulatory region.

Our data suggest that cyclin D1 may be a target for leptin mediated growth stimulation of Ishikawa cells and the molecular mechanism may involve recruitment of STAT3 and CREB transcription factors.

STAT3 and CREB siRNAs prevent leptin-induced cyclin D1 expression and cell proliferation

We studied the effect of silencing STAT3 and CREB gene expression by siRNA on leptin-induced cyclin D1 expression and cellular proliferation in Ishikawa cells to better define the contribution of these two transcription factors. In preliminary experiment we evaluated, after 24 and 48 h of siRNA transfection, that STAT3 and CREB protein expression was effectively silenced as revealed by Western Blotting (Fig. 6A). As shown in Figure 6B, silencing of the STAT3 and CREB genes significantly decreased cyclin D1 activation induced by leptin, while no changes was observed after transfection of cells with scrambled dsRNA upon identical experimental conditions. We next determined the effect of STAT3 and CREB siRNA on growth stimulation by measuring changes in the rate of DNA synthesis (Thymidine incorporation). We confirmed, as previously demonstrated (Sharma et al., 2006), that treatment with leptin 1,000 ng/ml for 24 and 48 h induces proliferation of Ishikawa cells. The growth stimulatory effect of leptin was severely affected in Ishikawa cells with silenced STAT3 or CREB expression (Fig. 6C).

These results further support that STAT3 and CREB play an important role in leptin signaling pathway that leads to the proliferation of Ishikawa cells.

Discussion

Increasing epidemiologic data in humans as well as many in vitro investigative reports have linked obesity with various disease states and suggested a strong link between leptin and tumor progression (Garofalo and Surmacz, 2006). Indeed, several studies have described a mitogenic effect of leptin on gastric (Pai et al., 2005), breast (Hu et al., 2002; Catalano et al., 2003; Mauro et al., 2007), ovarian (Choi et al., 2004), and prostate cancer cells (Somasundar et al., 2004a). Recently, growth stimulatory effect of leptin in human endometrial cancer cells was proposed (Sharma et al., 2006), even though the molecular mechanism underlying this effect remains to be fully elucidated.

As first attempt, to provide new insight into the stimulatory action exerted by leptin on cell growth, we analyzed leptin signaling on cell cycle profile in Ishikawa endometrial cancer cells. Our results showed that leptin treatment was able to speed up cell cycle progression by reducing G0/G1 arrest with an increase of cell population in S-phase.

The cell cycle is regulated by the coordinate action of cyclin-dependent kinases (cdk), specific cyclin proteins and cdk inhibitors. Alterations of the mechanisms controlling cell cycle progression play a relevant role in the pathogenesis of different human neoplasia. Among the molecules involved in cell cycle regulation cyclin D1 abnormalities may contribute to such malignant transformation (Cordon-Cardo, 1995; Fu et al., 2004;

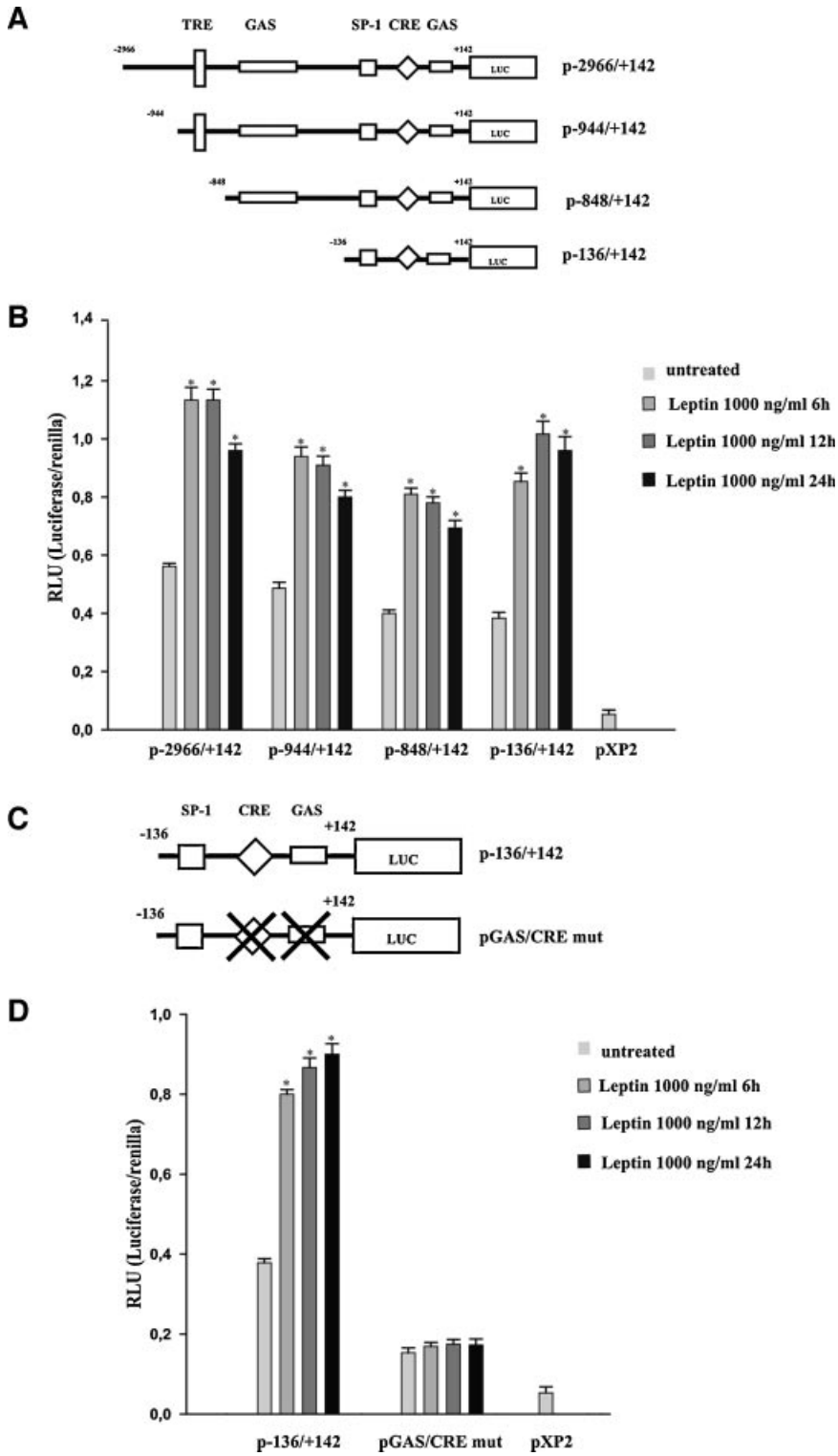

Fig. 4. Leptin transactivates cyclin D1 gene promoter through GAS and CRE motifs. A: Schematic representation of human cyclin D1 promoter fragments used in this study. All of the promoter constructs contain the same 3′ boundary (+142). The 5′ boundaries of the promoter fragments varied from −2 966 to −136. Each fragment was subcloned into the pXP2 vector. B: Transcriptional activity of Ishikawa cells with promoter constructs is shown. Ishikawa cells were serum-starved for 48 h, transfected for 24 h and left untreated or treated with 1,000 ng/ml leptin for 6, 12, and 24 h. C: Schematic representation of the mutated plasmid used in this study. D: Transcriptional activity of Ishikawa cells with promoter constructs is shown. Ishikawa cells were serum-starved for 24 h, transfected for 48 h and left untreated or treated with 1,000 ng/ml leptin for 6, 12, and 24 h. The values represent the mean ± SE of three separate experiments. In each experiment, the activities of the transfected plasmids were assayed in triplicate transfections. pXP2: basal activity measured in cells transfected with pXP2 basal vector $^{*}P < 0.01$ compared to untreated cells.

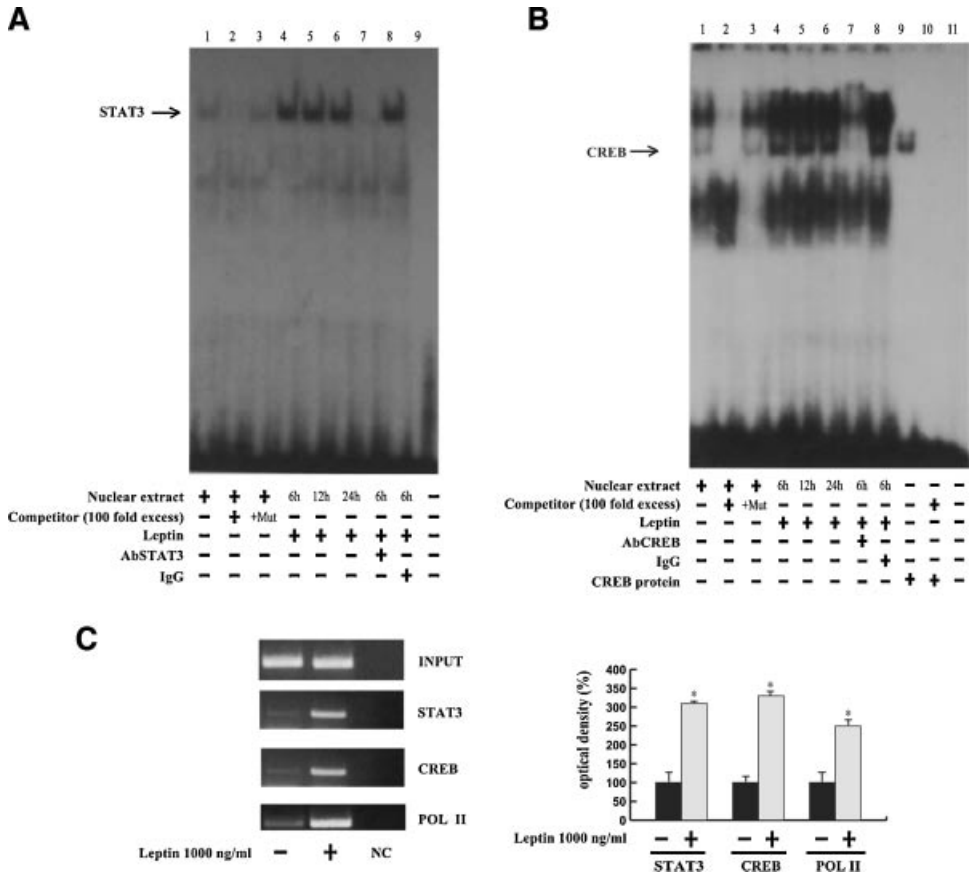

Fig. 5. Leptin induces activation of STAT3-DNA and CREB-DNA binding activity in Ishikawa cells. Nuclear extracts from Ishikawa cells were incubated with a double-stranded STAT3-specific (A) and CREB-specific (B) consensus sequence probe labeled with [λ32P] ATP and subjected to electrophoresis in a 6% polyacrylamide gel (lane 1). A: Competition experiments were done by adding as competitor a 100-fold molar excess of unlabeled probe (lane 2) or a 100-fold molar excess of unlabeled oligonucleotide containing a mutated GAS (lane 3). Ishikawa nuclear extracts treated with 1,000 ng/ml leptin for 6, 12, and 24 h incubated with probe (lane 4, 5, and 6). The specificity of the binding was tested by adding to the reaction mixture a STAT3 antibody (lane 7). IgG did not affect GAS complex formation (lane 8). Lane 9 contains probe alone. B: Competition experiments were done by adding as competitor a 100-fold molar excess of unlabeled probe (lane 2 and 10) or a 100-fold molar excess of unlabeled oligonucleotide containing a mutated CRE (lane 3). Ishikawa nuclear extracts treated with 1,000 ng/ml leptin for 6, 12, and 24 h incubated with probe (lane 4, 5, and 6). The specificity of the binding was tested by adding to the reaction mixture a CREB antibody (lane 7). IgG did not affect CRE complex formation (lane 8). We used as positive control a transcribed and translated in vitro CREB protein (lane 9). Lane 11 contains probe alone. (C) The cells were serum-starved for 48 h and left untreated (–) or treated with 1,000 ng/ml leptin for 1 h. The preacleared chromatin was immunoprecipitated with specific antibody anti-STAT3, anti-CREB, anti polymerase II antibodies, and with a normal mouse serum (NC) as negative control. Cyclin D1 promoter sequences containing GAS and CRE sites were detected by PCR with specific primers, as detailed in Materials and Methods Section. To determine input DNA, the cyclin D1 promoter fragment was amplified from 30 μl, purified soluble chromatin before immunoprecipitation. The histograms represent the mean ± SE of three separate experiments in which band intensities were evaluated in terms of optical density arbitrary units and expressed as percentages of the control, which was assumed to be 100%. *P < 0.01 compared to untreated cells.

Knudsen et al., 2006). Altered expression of cyclin D1 may result from rearrangement (Arnold et al., 1989), translocation (Withers et al., 1991), amplification and/or overexpression in head and neck, breast, squamous cell carcinomas, non-small cell lung cancer, colon and urinary bladder cancer (Hall and Peters, 1996). In addition, it has been reported that cyclin D1 overexpression in endometrial glands increases progressively in intensity and extent from normal endometrium to complex hyperplasia and carcinoma (Ruhul-Quddus et al., 2002).

Of interest, we found that leptin exposure up-regulates both cyclin D1 mRNA and protein levels at all the investigated times with a concomitant decrease of $p21^{WAF1/Cip1}$ expression. Our results are consistent with previous studies showing similar induction of cyclin D1 expression in human breast cancer cells (Okumura et al., 2002; Chen et al., 2006), in colon cancer HT-29 cell line (Rouet-Benzineb et al., 2004) as well as in human hepatocarcinoma cells (Chen et al., 2007; Saxena et al., 2007a).

Moreover, in our study, we demonstrated that leptin-stimulated cyclin D1 expression requires JAK/STAT, MAPK, and PKA activation, as it emerges by the observation that the chemical inhibitors of the above mentioned pathways completely reversed the increase of cyclin D1 protein levels.

It is worth noting that our findings recall previous reports indicating the involvement of JAK/STAT and MAPK signalling pathways in leptin mediated cell growth in diverse cellular contexts (Dieudonne et al., 2002; Choi et al., 2004; Sharma et al., 2006; Chen et al., 2007; Saxena et al., 2007a). For instance, recently, in Ishikawa endometrial cancer cells, leptin through ERK1/2 has been linked to cell proliferation (Sharma et al., 2006;), whereas in MCF-7 breast cancer cells,

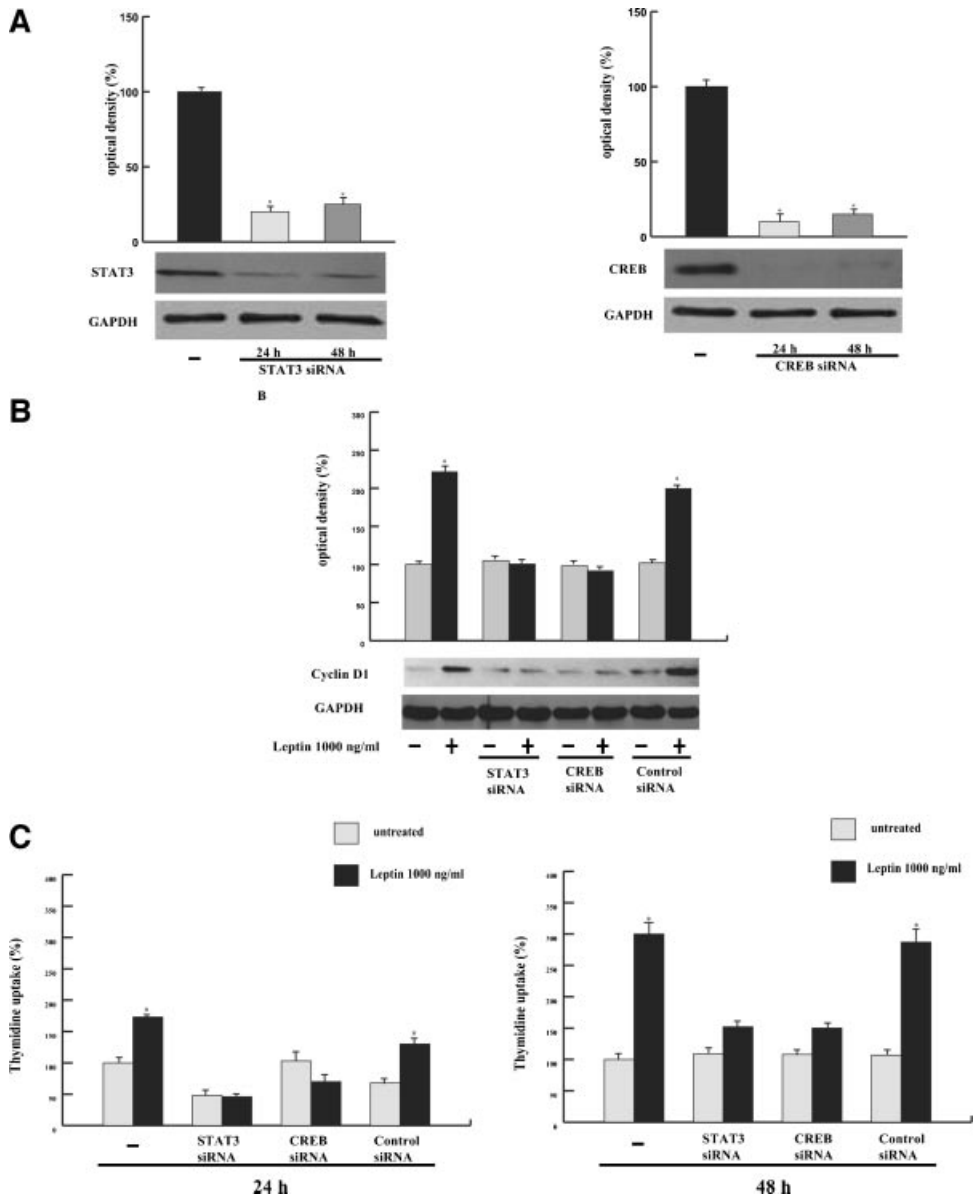

Fig. 6. The effect of STAT3 and CREB silencing on leptin-stimulated cyclin D1 and Ishikawa cells proliferation. A: STAT3 and CREB protein expression (evaluated by Western blotting) in Ishikawa cells not transfected (–) or transfected with RNA interference (RNAi) targeted human STAT3 or CREB mRNA sequence respectively as reported in Materials and Methods Section. GADPH was used as loading control. B: Ishikawa cells were transfected with STAT3, CREB, or control RNAi, and untreated (–) or treated with 1,000 ng/ml of leptin for 24 h. Total protein was extracted and Western blotting analysis was performed to evaluate the expression of cyclin D1. GADPH was used as loading control on the same stripped blot. C: Ishikawa cells were transfected with STAT3, CREB, control RNAi, or untransfected (–) and untreated or treated with 1,000 ng/ml of leptin for 24 and 48 h. Thymidine incorporation assay was performed. The data represent the mean ± SE of three separate experiments. *$P < 0.01$ compared to untreated cells.

we evidenced that leptin signaling via ERK1/2 was able to potentiate estrogen action and aromatase activity promoting breast cancer cell growth (Catalano et al., 2003; Catalano et al., 2004).

It was previously observed that stimulated Ras-MAPK pathway induces activation of CREB kinase, a member of the $p90^{RSK}$ family that corresponds to RSK2, and thereby phosphorylates CREB at Ser^{133} (Dalby et al., 1998). CREB, belongs to the ATF/CREB transcription family and interacts with CRE site in the cAMP-responsive gene promoter; although is a major downstream substrate of ERK1/2, it is also classically known as a PKA effector (Delghandi et al., 2005). The relationship of PKA and JAK/STAT-dependent intracellular mechanism of leptin action was previously suggested (Matsuoka et al., 1999) as well as the involvement of PKA in leptin-induced human ovarian proliferation (Sirotkin et al., 2007). These observations well fit with our results showing a significant increase of CREB/ATF-1 phosphorylation upon leptin exposure, which was completely abrogated by specific inhibitors of ERK1/2 and PKA signaling pathways demonstrating

that CREB is a target over which the above-mentioned pathways converge.

Therefore, in order to investigate the potential ability of leptin to modulate the cyclin D1 promoter gene, we performed transient transfection experiments in Ishikawa cells using deleted constructs of the cyclin D1 promoter gene. The results indicated that leptin signalling up-regulates the full-length promoter activity of cyclin D1. Moreover, we documented that the region spanning from −136 to +142, which contains CRE and GAS sites, was required for the responsiveness to leptin. Mutation analyses of the CRE and GAS sites on cyclin D1 promoter showed that both motifs were the mediators of cyclin D1 regulation by leptin since loss of both completely abolished leptin-induced promoter activation.

Other evidences strengthened our observation, since cyclin D1 has been reported to be transcriptionally regulated by STAT3 (Leslie et al., 2006) and CRE (Sabbah et al., 1999) in breast cancer cells. Moreover, GAS and CRE has been shown to be a potential target of leptin signaling. Indeed, a recent work, showed that leptin-activated STAT3 binds to its cognate sites in cyclin D1 promoter leading to hyperacetylation and overexpression of cyclin D1 gene through a recruitment of distinct co-activator complexes (Saxena et al., 2007b). On the other hand, our previous findings reported, in MCF-7 breast cancer cell line, activation of E-cadherin gene promoter by leptin through CRE site (Mauro et al., 2007).

Our EMSA experiments extended the aforementioned observations because nuclear extracts from Ishikawa cells treated with leptin showed an increased binding to the CRE and GAS sequences located in the cyclin D1 promoter region. These findings were supported by ChIP assay demonstrating the ability of leptin to enhance the recruitment of CREB and STAT3 to the promoter of cyclin D1. Finally, the relative contribution of these two transcription factors emerges from our data showing that silencing of STAT3 and CREB gene expression is able to reverse the up-regulatory effect of leptin on cyclin D1 expression and cell growth proliferation.

Taken together our results, for the first time, evidence that STAT3 and CREB are involved in leptin-mediated induction of cyclin D1 and clarify the role of leptin signaling in the progression of endometrial cancer, addressing it as a potential target of pharmacological therapy in obese women.

Acknowledgments

We thank Prof A. Weisz for generously providing human cyclin D1 promoter plasmids. We thank Dr Domenico Sturino for the English revision. This work was supported by AIRC grants 2006 and 2007.

Literature Cited

Ahima RS, Flier JS. 2000. Adipose tissue as an endocrine organ. Trends Endocrinology. Metabolism 11:327–332.
Ahima RS, Osei SY. 2004. Leptin signaling. Physiol Behav 81:223–241.
Allan AL, Albanese C, Pestell RG, LaMarre J. 2001. Activating transcription factor 3 induces DNA synthesis and expression of cyclin D1 in hepatocytes. J Biol Chem 276:27272–27280.
Arnold A, Kim HG, Gaz RD, Eddy RL, Fukurushima Y, Byers MG, Shows TB, Kronemberg HM. 1989. Molecular cloning and chromosomal mapping of DNA rearranged with the parathyroid hormone gene in parathyroid adenoma. J Clin Invest 83:2034–2040.
Bahrenberg G, Behrmann I, Barthel A, Hekerman P, Heinrich PC, Joost HG, Becker W, 2002. Identification of the critical sequence elements in the cytoplasmic domain of leptin receptor isoforms required for Janus kinase/signal transducer and activator of transcription activation by receptor heterodimers. Mol Endocrinol 16:859–872.
Bartusel T, Schubert S, Klempnauer KH. 2005. Regulation of the cyclin D1 and cyclin A1 promoters by B-Myb is mediated by Sp1 binding sites. Gene 351:171–180.
Bouloumie A, Drexler HC, Lafontan M, Busse R. 1998. Leptin, the product of Ob gene, promotes angiogenesis. Circ Res 83:1059–1066.
Brann DW, Wade MF, Dhandapani KM, Mahesh VB, Buchanan CD. 2002. Leptin and reproduction. Steroids 67:95–104.
Brockman JL, Schuler LA. 2005. Prolactin signals via Stat5 and Oct-1 to the proximal cyclin D1 promoter. Mol Cell Endocrinol 239:45–53.
Calle EE, Kaaks R. 2004. Overweight, obesity, and cancer: Epidemiological evidence and proposed mechanism. Nature Rev Cancer 4:579–591.
Calle EE, Thun MJ. 2004. Obesity and cancer. Oncogene 23:6365–6378.
Catalano S, Marsico S, Giordano C, Mauro L, Rizza P, Panno ML, Andò S. 2003. Leptin enhances, via AP-1, expression of aromatase in the MCF-7 cell line. J Biol Chem 278:28668–28676.
Catalano S, Mauro L, Marsico S, Giordano C, Rizza P, Rago V, Montanaro D, Maggiolini M, Panno ML, Andò S. 2004. Leptin induces, via ERK1/ERK2 signal, functional activation of estrogen receptor α in MCF-7 cells. J Biol Chem 279:19908–19915.
Chen C, Chang YC, Liu CL, Chang KJ, Guo IC. 2006. Leptin-induced growth of human ZR-75 breast cancer cells is associated with up-regulation of cyclin D1 and c-Myc and down-regulation of tumor suppressor p53 and $p21^{WAF1/Cip1}$. Breast Cancer Res Treat 98:121–132.
Chen C, Chang YC, Liu CL, Liu TP, Chang KJ, Guo IC. 2007. Leptin-induced proliferation and anti-apoptosis in human hepatocarcinoma cells by up-regulating cyclin D1 and down-regulating Bax via a janus kinase 2-linked pathway. Endocr Relat Cancer 14:513–529.
Choi JH, Park SH, Leung PC, Choi KC. 2004. Expression of leptin receptors and potential effects of leptin on the cell growth and activation of mitogen-activated protein kinases in ovarian cancer cells. J Clin Endocrinol Metab 90:207–210.
Cordon-Cardo C. 1995. Mutation of cell cycle regulators. Am J Pathol 147:545–560.
Dalby KN, Morrice N, Caudwell FB, Avruch J, Cohen P. 1998. Identification of regulatory phosphorylation sites in mitogen-activated protein kinase (MAPK)-activated protein kinase-1a/p90rsk that are inducible by MAPK. J Biol Chem 273:1496–1505.
Delghandi MP, Johannessen M, Moens U. 2005. The cAMP signalling pathway activates CREB through PKA, p38 and MSK1 in NIH 3T3 cells. Cell Signal 17:1343–1351.
Dieudonne MN, Machinal-Quelin F, Serazin-Leroy V, Leneveu MC, Pecquery R, Giudicelli Y. 2002. Leptin mediates a proliferative response in human MCF7 breast cancer cells. Biochem Biophys Res Commun 293:622–628.
Fu M, Wang C, Li Z, Sakamaki T, Pestell RG. 2004. Cyclin D1: Normal and abnormal functions. Endocrinology 145:5439–5447.
Garofalo C, Surmacz E. 2006. Leptin and cancer. J Cell Physiol 207:12–22.
Gonzalez RR, Caballero-Campo P, Jasper M, Mercader A, Devoto L, Pellicer A, Simon C. 2000. Leptin and leptin receptor are expressed in the human endometrium and endometrial leptin secretion is regulated by the human blastocyst. J Clin Endocrinol Metab 85:4883–4888.
Hall M, Peters G. 1996. Genetic alteration of cyclins, cyclin-dependent kinases, and CDK inhibitors in human cancer. Adv Cancer Res 68:67–108.
Hu X, Juneja SC, Maihle NJ, Cleary MP. 2002. Leptin a growth factor in normal and malignant breast cells and for normal mammary gland development. J Natl Cancer Inst 94:11704–11711.
Huang L, Li C. 2000. Leptin: A multifuncional hormone. Cell Res 10:81–92.
Kitawaki J, Koshiba H, Ishihara H, Kusuki I, Tsukamoto K, Honjo H. 2000. Expression of leptin receptor in human endometrium and fluctuation during the menstrual cycle. J Clin Endocrinol Metab 85:1946–1950.
Knudsen KE, Diehl JA, Haiman CA, Knudsen ES. 2006. Cyclin D1: Polymorphism, aberrant splicing and cancer risk. Oncogene 25:1620–1628.
Koda M, Sulkowska M, Wincewicz A, Kanczuga-Koda L, Musiatowicz B, Szymanska M, Sulkowski S. 2007. Expression of leptin, leptin receptor, and hypoxia-inducible factor 1 alpha in human endometrial cancer. Ann NY Acad Sci 1095:90–98.
Leslie K, Lang C, Devgan G, Azare J, Berishaj M, Gerald W, Kim YB, Paz K, Darnell JE, Albanese C, Sakamaki T, Pestell R, Bromberg J. 2006. Cyclin D1 is transcriptionally regulated by and required for transformation by activated signal transducer and activator of transcription 3. Cancer Res 66:2544–2552.
Lukas J, Pagano M, Staskovic Z, Draetta G, Bartek J. 1994. Cyclin D1 protein oscillates and is essential for cell cycle progression in human tumor cell lines. Oncogene 9:707–718.
Matsuoka T, Tahara M, Yokoi T, Masumoto N, Takeda T, Yamaguchi M, Tasaka K, Kurachi H, Murata Y. 1999. Tyrosine phosphorylation of STAT3 by leptin through leptin receptor in mouse metaphase 2 stage oocyte. Biochem Biophys Res Commun 256:480–484.
Mauro L, Catalano S, Bossi G, Morales S, Giordano C, Bartella V, Casaburi I, Andò S. 2007. Evidences that leptin up-regulates E-cadherin expression in breast cancer: Effects on tumor growth and progression. Cancer Res 67:3412–3421.
Morelli C, Garofalo C, Sisci D, del Rincon S, Cascio S, Tu X, Vecchione A, Sauter ER, Miller WH Jr, Surmacz E. 2004. Nuclear insulin receptor substrate 1 interacts with estrogen receptor alpha at ERE promoters. Oncogene 23:7517–7526.
Natsume H, Sasaki S, Kitagawa M, Kashiwabara Y, Matsushita A, Nakano K, Nishiyama K, Nagayama K, Misawa H, Masuda H, Nakamura H. 2003. Beta-catenin/Tcf-1-mediated transactivation of cyclin D1 promoter is negatively regulated by thyroid hormone. Biochem Biophys Res Commun 309:408–413.
Nikaido T, Li SF, Shiozawa T, Fujii S. 1996. Coabnormal expression of cyclin D1 and p53 protein in human uterine endometrial carcinomas. Cancer 78:1148–1153.
Okumura M, Yamamoto M, Sakuma H, Kojima T, Maruyama T, Jamali M, Cooper DR, Yasuda K. 2002. Leptin and high glucose stimulate cell proliferation in MCF-7 human breast cancer cells: Reciprocal involvement of PKC-alpha and PPAR expression. Biochimi Biophys Acta 1592:107–116.
Pai R, Lin C, Tran T, Tarnawski A. 2005. Leptin actives STAT and ERK2 patways and induces gastric cancer cell proliferation. Biochem Biophys Res Commun 331:984–992.
Petridou E, Belechri M, Dessypris N, Koukoulomatis P, Diakomanolis E, Spanos E, Trichopoulos D. 2002. Leptin and body mass index in relation to endometrial cancer risk. Ann Nutr Metab 46:147–151.
Rouet-Benzineb P, Aparicio T, Guilmeau S, Pouzet C, Descatoire V, Buyse M, Bado A. 2004. Leptin counteracts sodium butyrate-induced apoptosis in human colon cancer HT-29 cells via NF-kB signalling. J Biol Chem 279:16495–16502.
Ruhul-Quddus M, Latkovich P, Castellani WJ, James-Sung C, Steinhoff MM, Briggs RC, Miranda RN. 2002. Expression of cyclin D1 in normal, metaplastic, hyperplastic endometrium and endometrioid carcinoma suggests a role in endometrial carcinogenesis. Arch Pathol Lab Med 126:459–463.
Ryan AJ, Susil B, Jobling TW, Oehler MK. 2005. Endometrial cancer. Cell Tissue Res 322: 53–61.
Sabbah M, Courilleau D, Mester J, Redeuilh G. 1999. Estrogen induction of the cyclin D1 promoter: Involvement of a cAMP response-like element. Proc Natl Acad Sci USA 96:11217–11222.
Saxena NK, Sharma D, Ding X, Lin S, Marra F, Merlin D, Anania FA. 2007. Concomitant activation of the Jak/STAT, PI3K/Akt, and ERK signaling is involved in leptin-mediated promotion of invasion and migration of hepatocellular carcinoma cells. Cancer Res 67:2497–2507.
Saxena NK, Vertino PM, Anania FA, Sharma D. 2007. Leptin-induced growth stimulation of breast cancer cells involves recruitment of histone acetyltransferases and mediator complex to CYCLIN D1 promoter via activation of Stat3. J Biol Chem 282:13316–13335.

Sharma D, Saxena NK, Vertino PM, Anania FA. 2006. Leptin promotes the proliferative response and invasiveness in human endometrial cancer cells by activating multiple signal-transduction pathways. Endocr Relat Cancer 13:629–640.
Sirotkin AV, Mlynček M, Makarevich AV, Florkovičová I, Hetényi L. 2007. Leptin affects proliferation, apoptosis and protein kinase A-related peptides in human ovarian granulosa cells. Physiol Res [Epub ahead of print].
Somasundar P, McFadden DW, Hileman SM, Vona-Davis L. 2004a. Leptin is a growth factor in cancer. J Surg Res 116:337–349.
Somasundar P, Frankenberry KA, Skinner H, Vedula G, McFadden DW, Riggs D, Jackson B, Vangilder R, Hileman SM, Vona-Davis LC. 2004b. Prostate cancer cell proliferation is influenced by leptin. J Surg Res 118:71–82.
Sweeney G. 2002. Leptin signalling. Cell Signal 14:655–663.
Tartaglia LA. 1997. The leptin receptor. J Biol Chem 272:6093–6096.
Withers DA, Harvey RC, Faust JB, Melnyk O, Carey K, Meeker TC. 1991. Characterization of a candidate bcl-1 gene. Mol Cell Biol 11:4846–4853.
Yuan SS, Tsai KB, Chung YF, Chan TF, Yeh YT, Tsai LY, Su JH. 2004. Aberrant expression and possible involvement of the leptin receptor in endometrial cancer. Gynecol Oncol 92:769–775.
Zabeau L, Lavens D, Peelman F, Eyckerman S, Vandekerckhove J, Tavernier J. 2003. The ins and outs of leptin receptor activation. FEBS Lett 546:45–50.
Zhang Y, Proenca R, Maffei M, Barone M, Leopold L, Friedman JM. 1994. Positional cloning of the mouse obese gene and its human homologue. Nature 372:425–432.

Insulin-Like Growth Factor-I, Regulating Aromatase Expression through Steroidogenic Factor 1, Supports Estrogen-Dependent Tumor Leydig Cell Proliferation

Rosa Sirianni,[1] Adele Chimento,[1] Rocco Malivindi,[1] Ignazio Mazzitelli,[1] Sebastiano Andò,[2] and Vincenzo Pezzi[1]

Departments of [1]Pharmaco-Biology and [2]Cell Biology, University of Calabria, Arcavacata di Rende, Cosenza, Italy

Abstract

The aim of this study was to investigate the role of estrogens in Leydig cell tumor proliferation. We used R2C rat Leydig tumor cells and testicular samples from Fischer rats with a developed Leydig tumor. Both experimental models express high levels of aromatase and estrogen receptor α (ERα). Treatment with exogenous 17β-estradiol (E_2) induced proliferation of R2C cells and up-regulation of cell cycle regulators cyclin D1 and cyclin E, the expression of which was blocked by addition of antiestrogens. These observations led us to hypothesize an E_2/ERα–dependent mechanism for Leydig cell tumor proliferation. In determining the molecular mechanism responsible for aromatase overexpression, we found that total and phosphorylated levels of transcription factors cyclic AMP–responsive element binding protein and steroidogenic factor 1 (SF-1) were higher in tumor samples. Moreover, we found that tumor Leydig cells produce high levels of insulin-like growth factor I (IGF-I), which increased aromatase mRNA, protein, and activity as a consequence of increased total and phosphorylated SF-1 levels. Specific inhibitors of IGF-I receptor, protein kinase C, and phosphatidylinositol 3-kinase determined a reduction in SF-1 expression and in IGF-I–dependent SF-1 recruitment to the aromatase PII promoter. The same inhibitors also inhibited aromatase expression and activity and, consequently, R2C cell proliferation. We can conclude that one of the molecular mechanisms determining Leydig cell tumorigenesis is an excessive estrogen production that stimulates a short autocrine loop determining cell proliferation. In addition, cell-produced IGF-I amplifies estrogen signaling through an SF-1–dependent up-regulation of aromatase expression. The identification of this molecular mechanism will be helpful in defining new therapeutic approaches for Leydig cell tumors. [Cancer Res 2007;67(17):8368–77]

Introduction

The etiology and pathogenesis of human testicular tumors are poorly defined. It has been reported that serum estrogen levels are elevated in patients with testicular germ cell cancer as a consequence of increased local estrogen production reflecting higher aromatase activity present in Sertoli and Leydig cells (1). Ninety-five percent of all human testicular neoplasms arise from germinal cells whereas Leydig cell tumors are the most common tumors of the gonadal stroma (2).

In rodents, reproductive system tumors are uncommon in general, with the few exceptions of Leydig cell and ventral prostatic neoplasms in some rat strains (3) or non-inbred mice (4); however, analogously to the human (5), chronic administration of estrogens induces testicular tumors.

A useful model used to investigate whether excess estrogens might have a central role in the mechanism leading to testicular tumorigenesis are transgenic mice overexpressing aromatase and presenting enhancement of circulating 17β-estradiol (E_2) levels (6). About half of the male mice are infertile and/or have enlarged testis and show Leydig cell hyperplasia and Leydig cell tumors (6), whereas the female mice reveal mammary gland hyperplasia associated with an altered expression pattern of proteins involved in apoptosis, cell cycle, growth, and tumor suppression (7). Whereas the effects of estrogen on mammary gland tumorigenesis in human and rodents are well known, the role of aromatase overexpression and *in situ* estrogen production in testicular tumorigenesis has not been clearly defined. In this study, we have investigated the molecular mechanisms causing aromatase overexpression and the effect of estradiol (E_2) overproduction on rat Leydig cell tumor proliferation. As an experimental model, we used the R2C rat Leydig tumor cell line; to validate our *in vitro* data in an *in vivo* model, we used Leydig cell tumors from older Fisher rats characterized by an exceptionally high incidence of spontaneous neoplasm with aging (8).

Aromatase activity is regulated primarily at the level of gene expression and is present in testicular somatic cells and along the maturative phases of male germ cells (9, 10). The *CYP19* gene that encodes aromatase has at least eight unique promoters that are used in a tissue-specific manner (11). The proximal promoter II regulates aromatase expression in human fetal and adult testis, R2C and H540 rat Leydig tumor cells, and purified preparations of rat Leydig, Sertoli, and germ cells (12, 13). Specific sequences seem to be mainly involved in aromatase expression: a sequence that contains a half-site binding nuclear receptors (AGGTCA) in position −90 in the rat binding steroidogenic factor 1 (SF-1; ref. 14) and cyclic AMP (cAMP)–responsive element (CRE)–like sequences binding cAMP-responsive element binding protein (CREB)/activating transcription factor protein family members (15, 16) localized upstream at a more distal position, in the rat in positions −169 (TGCACGTCA), −335 (TGAACTCA), and −231 (TGAAATCA; ref. 17). Similar responsive elements (binding CRE and SF-1) have been reported for the steroidogenic acute regulatory (StAR) protein gene promoter (18) whose expression is regulated by insulin-like growth factor-I (IGF-I) signaling in Leydig cells. Because the StAR protein is involved in the transfer of cholesterol from the outer to the inner

Note: Supplementary data for this article are available at Cancer Research Online (http://cancerres.aacrjournals.org/).

R. Sirianni and A. Chimento contributed equally to this work.

Requests for reprints: Vincenzo Pezzi, Department of Pharmaco-Biology, Università della Calabria, 87036 Rende, Cosenza, Italy. Phone: 39-0984-493157; Fax: 39-0984-493271; E-mail: v.pezzi@unical.it.

doi:10.1158/0008-5472.CAN-06-4064

mitochondrial membrane, the rate-limiting and regulated step in steroidogenesis IGF-I plays an important role in the regulation of testicular steroid biosynthesis.

For these reasons, we investigated the role of IGF-I, a peptide also shown to have a role in testicular growth and development and in the control of Leydig cell number (19). IGF-I is produced locally in the testis, in Sertoli, Leydig, and peritubular cells derived from the immature rat testis and cultured *in vitro* (20, 21). The crucial role of IGF-I in the development and function of Leydig cells was highlighted by studies on *IGF-I* gene knockout mice (22, 23). The failure of adult Leydig cells to mature and the reduced capacity for testosterone production are caused by deregulated expression of testosterone biosynthetic and metabolizing enzymes (24). Expression levels of all mRNA species associated with testosterone biosynthesis are lower in the absence of IGF-I. However, this study did not investigate the effect of IGF-I on aromatase expression, although an effect could be supposed.

Starting from these findings, in this study we investigated whether a testicular overproduction of IGF-I could be one of the mechanisms determining aromatase overexpression in rat tumor Leydig cells through the activation of specific transcription factors. The elevated aromatase-dependent E_2 production in Leydig cells, through an autocrine/paracrine mechanism mediated by their own receptors, could contribute to the hormone dependence of testicular tumorigenesis by stimulating Leydig tumor cell proliferation.

Materials and Methods

Cell cultures and animals. TM3 cells (immature mouse Leydig cell line) were cultured in DMEM/F-12 supplemented with 5% horse serum (HS), 2.5% fetal bovine serum (FBS), and antibiotics (Invitrogen S.R.L.); R2C cells (rat Leydig tumor cell line) were cultured in Ham/F-10 supplemented with 15% HS, 2.5% FBS, and antibiotics (Invitrogen). Male Fischer 344 rats (a generous gift of Sigma-Tau), 6 (FRN) and 24 (FRT) months of age, were used for studies. Twenty-four-month-old animals presented spontaneously developed Leydig cell tumors, which were absent in younger animals. Testes of all animals were surgically removed by qualified, specialized animal care staff in accordance with the Guide for Care and Use of Laboratory Animals (NIH) and used for experiments.

Aromatase activity assay. The aromatase activity in subconfluent R2C cell culture medium was measured by tritiated water-release assay using 0.5 μmol/L [1β-^{3}H(N)]androst-4-ene-3,17-dione (DuPont NEN) as a substrate (25). Incubations were done at 37°C for 2 h under a 95%:5% air/CO_2 atmosphere. Obtained results were expressed as picomoles per hour (pmol/h) and normalized to milligrams of protein (pmol/h/mg protein).

RIA. Before the experiments, TM3 cells were maintained overnight in DMEM/F-12 and R2C cells in Ham/F-10 (medium only). The estradiol content of medium recovered from each well was determined against standards prepared in low-serum medium using a RIA kit (DSL 43100; Diagnostic System Laboratories). Results of the assay were normalized to the cellular protein content per well and expressed as picomoles per milligram of cell protein.

To measure IGF-I concentration in testicular extracts, testes were weighed, homogenated in 500 μL of 0.05 mol/L Tris/HCl (pH 7.6) plus protease inhibitors, and then submitted to ultrasonication followed by centrifugation, as previously published (26). IGF-I content in testicular extracts and in medium recovered from each well of R2C and TM3 cells was determined following extraction and assay protocols provided with the mouse/rat IGF-I RIA kit (DSL 2900; Diagnostic System Laboratories).

Chromatin immunoprecipitation. This assay was done using the chromatin immunoprecipitation assay kit from Upstate with minor modifications in the protocol. R2C cells were grown in 100-mm plates. Confluent cultures (90%) were treated for 24 h with AG1024 (Sigma), PD98059 (Calbiochem, VWR International S.R.L.), LY294002 (Calbiochem, VWR International), GF109203X (Calbiochem, VWR International), or for increasing times with 100 ng/mL IGF-I (Sigma), or left untreated. Following treatment, DNA/protein complexes were cross-linked with 1% formaldehyde at 37°C for 10 min. Next, cells were collected and resuspended in 400 μL of SDS lysis buffer (Upstate Technology) and left on ice for 10 min. Then, cells were sonicated four times for 10 s at 30% of maximal power and collected by centrifugation at 4°C for 10 min at 14,000 rpm. Ten microliters of the supernatants were kept as input (starting material, to normalize results) whereas 100 μL were diluted 1:10 in 900 μL of chromatin immunoprecipitation dilution buffer (Upstate Technology) and immunocleared with 80 μL of sonicated salmon sperm DNA/protein A agarose (Upstate) for 6 h at 4°C. Immunocomplex was formed using 1 μL of 1:5 dilution of specific anti–SF-1 antibody (provided by Prof. Ken-ichirou Morohashi, Division for Sex Differentiation, National Institute for Basic Biology, National Institutes of Natural Sciences, Myodaiji-cho, Okazaki, Japan) overnight at 4°C. Immunoprecipitation with salmon sperm DNA/protein A agarose was continued at 4°C until the following day. DNA/protein complexes were reverse cross-linked overnight at 65°C. Extracted DNA was resuspended in 20 μL of Tris-EDTA buffer. A 3-μL volume of each sample and input was used for PCR using CYP19 promoter II–specific primers. The PCR conditions were 1 min at 94°C, 1 min at 50°C, and 2 min at 72°C for 30 cycles using the following primers: forward, 5′-TCAAGGGTAGGAATTGGGAC-3′; reverse, 5′-GGTGCTGGAATGGACAGATG-3′. Amplification products were analyzed on a 1% agarose gel and visualized by ethidium bromide staining. In control samples, nonimmune rabbit immunoglobulin G was used instead of specific antibodies.

Real-time reverse transcription-PCR. Before the experiments, cells were maintained overnight in low-serum medium. Cells were then treated for the indicated times and RNA was extracted from cells using the TRizol RNA isolation system (Invitrogen). TRizol was also used to homogenize total tissue of normal (FRNT) and tumor (FRTT) Fisher rat testes for RNA extraction. Each RNA sample was treated with DNase I (Ambion), and purity and integrity of the RNA were confirmed spectroscopically and by gel electrophoresis before use. One microgram of total RNA was reverse transcribed in a final volume of 30 μL using the ImProm-II Reverse transcription system kit (Promega, Promega Italia S.R.L.); cDNA was diluted 1:3 in nuclease-free water, aliquoted, and stored at −20°C. Primers for the amplification were based on published sequences for the rat *CYP19*, rat *CREB*, and rat *SF-1* genes. The nucleotide sequences of the primers for *CYP19* were forward, 5′-GAGAAACTGGAAGACTGTATGGAT-3′, and reverse, 5′-ACTGATTCACGTTCTCCTTTGTCA-3′. For CREB amplification, we used the following primers: forward, 5′-AATATGCACAGACCACTGATGGA-3′, and reverse, 5′-TGCTGTGCGAATCTGGTATGTT-3′; for SF-1 amplification, primers have been previously published (27). PCR reactions were done in the iCycler iQ Detection System (Bio-Rad) using 0.1 μmol/L of each primer, in a total volume of 30-μL reaction mixture following the manufacturer's recommendations. SYBR Green Universal PCR Master Mix (Bio-Rad) with the dissociation protocol was used for gene amplification; negative controls contained water instead of first-strand cDNA. Each sample was normalized on the basis of its 18S rRNA content. The 18S quantification was done using a TaqMan rRNA Reagent kit (Applied Biosystems) following the method provided in the TaqMan rRNA Control Reagent kit (Applied Biosystems). The relative gene expression levels were normalized to a calibrator that was chosen to be the basal, untreated sample. Final results were expressed as *n*-fold differences in gene expression relative to 18S rRNA and calibrator, calculated using the $\Delta\Delta C_t$ method as follows:

$$n - \text{fold} = 2^{-(\Delta C_{\text{tsample}} - \Delta C_{\text{tcalibrator}})}$$

where ΔC_t values of the sample and calibrator were determined by subtracting the average C_t value of the 18S rRNA reference gene from the average C_t value of the different genes analyzed.

Western blot analysis. R2C and TM3 cells or total tissue of FRNT and FRTT were lysed in ice-cold radioimmunoprecipitation assay buffer containing protease inhibitors (20 mmol/L Tris, 150 mmol/L NaCl, 1% Igepal, 0.5% sodium deoxycholate, 1 mmol/L EDTA, 0.1% SDS, 1 mmol/L phenylmethylsulfonyl fluoride, 0.15 units/mL aprotinin, and 10 μmol/L leupeptin) for protein extraction. The protein content was determined by the Bradford method. The proteins were separated on 11% SDS-polyacrylamide gel and then electroblotted onto a nitrocellulose membrane. Blots were incubated overnight at 4°C with (*a*) antihuman *P*450 aromatase antibody (1:50; Serotec, MCA 2077), (*b*) anti-ERα (F-10) antibody (1:500; Santa Cruz Biotechnology), (*c*) anti-ERβ (H-150) antibody (1:1,000; Santa Cruz Biotechnology), (*d*) anti–cyclin D1 (M-20) antibody (1:1,000; Santa Cruz Biotechnology), (*e*) anti–cyclin E (M-20) antibody (1:1,000; Santa Cruz Biotechnology), (*f*) anti-CREB antibodies [48H2 (1:1,000; Cell Signaling Technology) and AHO0842 (1:1,000; Biosource, Inc.)]; (*g*) anti-pCREB Ser^{133} (87G3; 1:1,000; Cell Signaling Technology) or anti-pCREB $Ser^{129/133}$ (1:1,000; Biosource, Inc.), (*h*) anti–SF-1 (1:1,000; provided by Prof. Ken-ichirou Morohashi), (*i*) anti–pSF-1 (1:1,000; provided by Dr. Holly A. Ingraham, Department of Physiology, University of California, San Francisco, San Francisco, California), (*j*) anti-actin (C-2) antibody (1:1,000; Santa Cruz Biotechnology), and (*k*) anti–IGF-I receptor (IGF-IR; 1:800; Santa Cruz Biotechnology). Membranes were incubated with horseradish peroxidase–conjugated secondary antibodies (Amersham Pharmacia Biotech) and immunoreactive bands were visualized with the enhanced chemiluminescence Western blotting detection system (Amersham Biosciences). To ensure equal loading of proteins, membranes were stripped and incubated overnight with β-actin antiserum.

Cell proliferation assay. For proliferative analysis, a total of 1×10^5 cells were seeded onto 12-well plates in complete medium and allowed to grow for 2 days. Before the experiments, cells were maintained overnight in Ham/F-10 medium and were treated the next day with ICI 182780 (a gift from Astra-Zeneca), 4-hydroxytamoxifen (Sigma), and letrozole (a gift from Novartis Pharma AG) and E_2 (Sigma), or treated for 24 h with IGF-I alone or in combination with inhibitors, or incubated with an anti–IGF-I antibody (Santa Cruz Biotechnology). Control (basal) cells were treated with the same amount of vehicle alone (DMSO) that never exceeded the concentration of 0.01% (v/v). [^{3}H]Thymidine incorporation was evaluated after a 24-h incubation period with 1 μCi of [^{3}H]thymidine (Perkin-Elmer

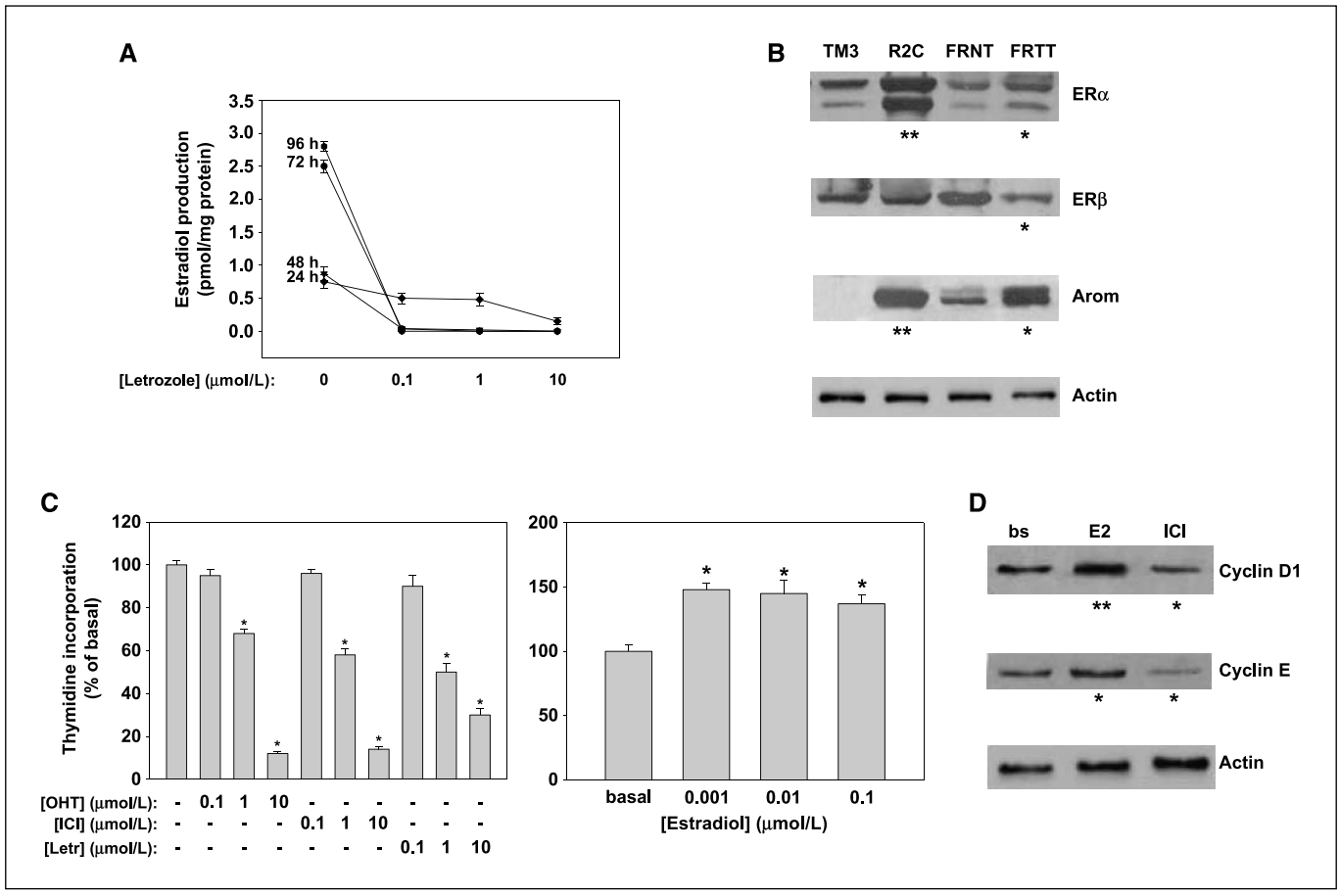

Figure 1. E_2 production and autocrine effects in R2C cells. *A,* cells were treated for the indicated times in HAM-F10 in the absence (0) or presence of aromatase inhibitor letrozole (0.1, 1, and 10 μmol/L). Every 24 h, before renewing treatment, cell culture medium was removed and analyzed for steroid content. E_2 content in R2C culture medium was determined by RIA and normalized to the cell culture well protein content. *Points,* mean from three separate cell culture wells; *bars,* SE. *B,* Western blot analyses of ERα, ERβ, and aromatase (*Arom*) were done on 50 μg of total proteins extracted from TM3 and R2C cells or from tissues of normal (FRNT) and tumor (FRTT) Fisher rat testes. Representative of three independent experiments. β-Actin was used as a loading control. *C,* R2C cell proliferation was evaluated by [^{3}H]thymidine incorporation analysis. Cells were treated for 96 h in HAM-F10 in the absence (−) or presence of antiestrogens hydroxytamoxifen (*OHT*) or ICI 182780 (*ICI*) or aromatase inhibitor letrozole (*Letr*) at the indicated concentrations or treated with estradiol (0.001–0.1 μmol/L) for 24 h after being cultured for 48 h in serum-free HAM-F10, removing and renewing cell culture medium every 24 h. *D,* R2C cells were cultured for 48 h in serum-free HAM-F10; every 24 h, cell culture medium was removed and renewed. Cells were then treated for 24 h in the absence (basal, *bs*) or presence of estradiol (1 nmol/L) and ICI 182780 (1 μmol/L) before extracting total proteins. Western blot analysis of cyclin D1 and cyclin E was done on 50 μg of total proteins extracted from R2C cells. β-Actin was used as a loading control. Protein expression in each lane was normalized to the β-actin content and expressed as fold over control represented by normal cells (*B*) or basal condition (*D*). Normalized absorbances were subjected to statistical analysis; statistically significant differences are indicated (*, $P < 0.05$; **, $P < 0.01$, compared with basal or control).

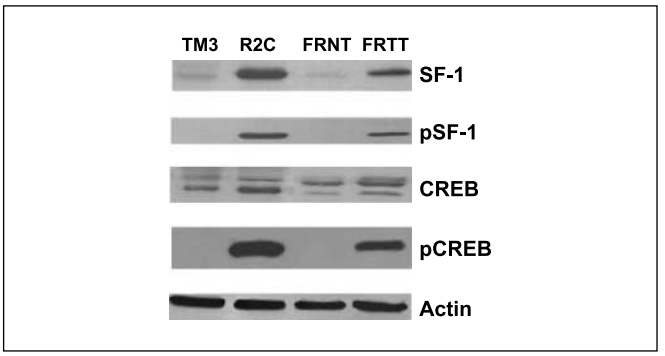

Figure 2. Expression of total and phosphorylated forms of SF-1 and CREB. Western blot analyses of SF-1, pSF-1, CREB, and pCREB were done on 50 μg of total proteins extracted from TM3 and R2C cells or from tissues of normal (FRNT) and tumor (FRTT) Fisher rat testes. Representative of three independent experiments with similar results. β-Actin was used as a loading control. Protein expression in each lane was normalized to the β-actin content.

Life Sciences) per well. Cells were washed once with 10% trichloroacetic acid, twice with 5% trichloroacetic acid, and lysed in 1 mL of 0.1 mol/L NaOH at 37°C for 30 min. The total suspension was added to 10 mL optifluor fluid and was counted in a scintillation counter.

Data analysis and statistical methods. Pooled results from triplicate experiments were analyzed by one-way ANOVA with Student-Newman-Keuls multiple comparison methods, using SigmaStat version 3.0 (SPSS).

Results

Estradiol induces Leydig cell tumor proliferation through an autocrine mechanism. We carried out our study using R2C Leydig tumor cells as model system. These cells have been shown to have high aromatase expression and activity (14). We also used another Leydig cell line, TM3, as a normal control and analyzed testes from older and younger Fischer rats. Aged animals have a high incidence of spontaneous Leydig cell neoplasm (8, 28), a phenomenon not observed in younger animals, allowing us to use them as a good *in vivo* model to confirm results obtained in cell lines. Our first step was to measure estradiol content in culture media of R2C and TM3 cells. Whereas E_2 levels in TM3 medium were extremely low (data not shown) in R2C cells, E_2 levels after 24 h were 0.5 pmol/mg protein and increased by 7-fold at 96 h (Fig. 1*A*). This production was dependent on high constitutive active aromatase activity because the presence of the aromatase inhibitor letrozole was able to decrease E_2 production at all doses and times tested (Fig. 1*A*). E_2 levels after 24-h treatment with letrozole were still detectable but were completely knocked down when we removed the medium after 24 h and renewed the treatment for an additional 24 h. The same effect was maintained at the other two time points investigated (Fig. 1*A*). Once estradiol is produced, it can exert its actions by binding to specific receptors, the estrogen receptors α and β (ERα and ERβ). Analysis of the two protein receptor isoforms in our models showed that tumor Leydig cells express both isoforms of ER (Fig. 1*B*). Particularly, the α isoform seems to be more expressed in R2C cells with respect to TM3 and in FRTT with respect to its control FRNT (Fig. 1*B*) in which ERβ, instead, is more expressed (Fig. 1*B*). In R2C as well as in FRTT, an increase in the ERα/ERβ ratio was observed (Supplementary Fig. S1*A*). Moreover, aromatase protein content is extremely high in tumor samples (Fig. 1*B*).

Our next experiments showed that ERs are required for proliferation through a short autocrine loop maintained by endogenous E_2 production in Leydig tumor cells. For instance, the use of both antiestrogens 4-hydroxytamoxifen and ICI 182780 and the use of the aromatase inhibitor letrozole determined a dose-dependent inhibition of cell proliferation (Fig. 1*C*). Among the different doses tested, the highest dose of 4-hydroxytamoxifen (10 μmol/L) was able to inhibit cell proliferation by 90%; 10 μmol/L ICI 182780, by 86%; and 10 μmol/L letrozole, by 70%. Moreover,

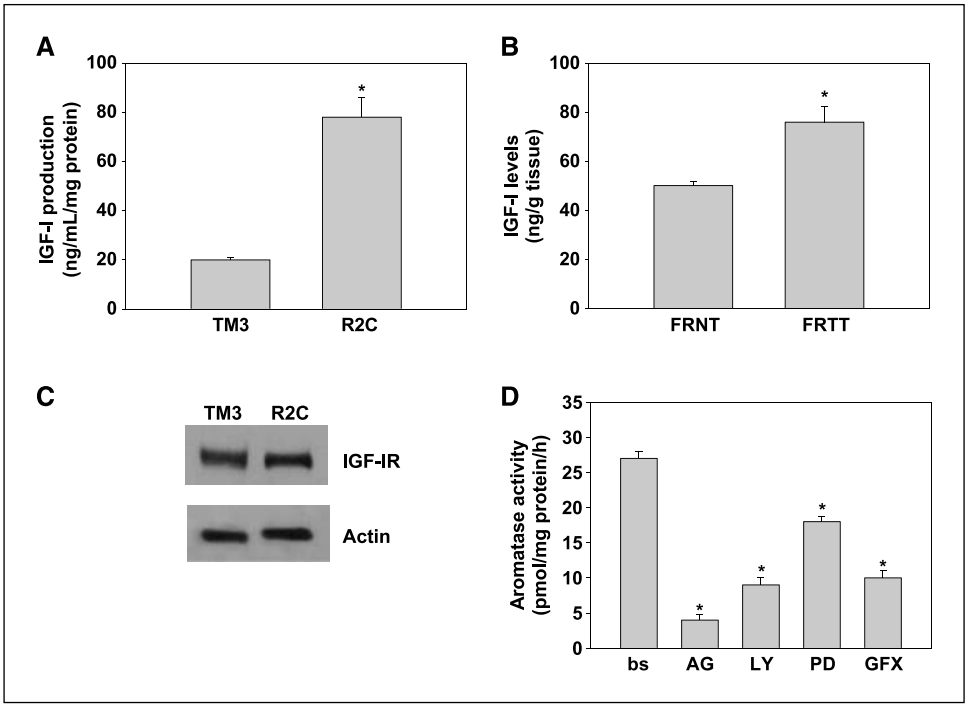

Figure 3. IGF-I production and autocrine effects in Leydig cells. *A,* TM3 and R2C cells were cultured for 24 h in serum-free medium and IGF-I levels in culture medium were determined by RIA. IGF-I levels were normalized to the cell culture well protein content. *Columns,* mean of three independent experiments each done in triplicate; *bars,* SE. *B,* total protein extracts from FRNT and FRTT were assayed for IGF-I content. IGF-I levels were normalized to the tissue weight. *Columns,* mean of three independent samples; *bars,* SE. *, $P < 0.01$, compared with control conditions, represented by TM3 cells or FRNT. *C,* Western blot analysis of IGF-IR in TM3 and R2C cells. β-Actin was used as a loading control. *D,* cells were treated with AG1024 (*AG*; 20 μmol/L), LY294002 (*LY*; 10 μmol/L), PD98059 (*PD*; 20 μmol/L), and GF109203X (*GFX*; 20 μmol/L). Aromatase activity was assessed by using the modified tritiated water method. Results obtained are expressed as picomoles of $[^3H]H_2O$ released per hour and normalized to the well protein content (pmol/h/mg protein). *Columns,* mean of three independent experiments each done in triplicate; *bars,* SE. *, $P < 0.01$, compared with basal.

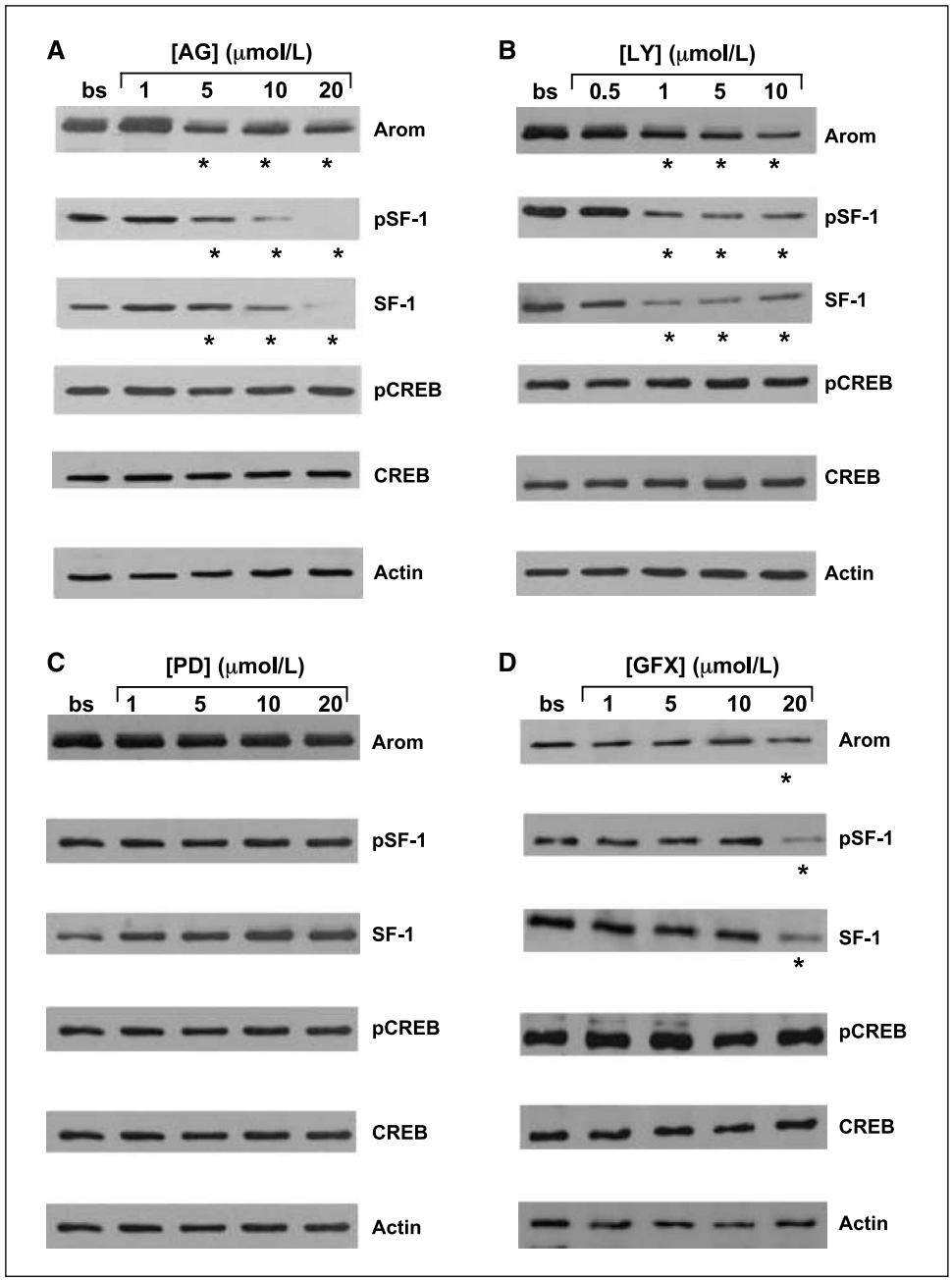

Figure 4. Effects of IGF-I pathway inhibitors on aromatase, SF-1, and CREB expression in R2C cells. *A* to *D,* Western blot analyses were done on 50 μg of total proteins extracted from R2C cells untreated (*bs*) or treated for 24 h with the indicated doses of AG1024 (*A*), LY294002 (*B*), PD98059 (*C*), and GF109203X (*D*). Representative of three independent experiments with similar results. β-Actin was used as a loading control. Normalized absorbances were subjected to statistical analysis; statistically significant differences are indicated (*, $P < 0.01$, compared with basal).

after starving cells for a prolonged time and changing the medium everyday to remove local E_2 production, we found that addition of 1, 10, and 100 nmol/L E_2 stimulated Leydig tumor cell proliferation (Fig. 1*C*), overcoming the inhibition induced by letrozole (Supplementary Fig. S1*B*). The stimulatory effect of E_2 was concomitant with increased levels of cell cycle regulators cyclin D1 and cyclin E, whose expression was inhibited by the pure antiestrogen ICI 182780 (Fig. 1*D*). All these results address how the classic E_2/ERα signaling may control Leydig cell tumor growth and proliferation similarly to what was observed in other estrogen-dependent tumors.

Aromatase overexpression is determined by constitutive activation of transcription factors SF-1 and CREB. Aromatase gene transcription in rat Leydig cells is driven by the PII promoter, which is mainly regulated through three CRE-like sites and one NRE site binding SF-1 and LRH-1 (14, 27). Constitutively active levels of CREB have previously been shown in R2C cells (29). Here, we confirmed these data and showed that FRTT have a high phosphorylated CREB status (Fig. 2), together with enhanced expression and phosphorylation of SF-1, with respect to FRNT (Fig. 2). Furthermore, we showed the presence of high expression levels of SF-1 with the phosporylated protein present in R2C but not in TM3 cells (Fig. 2).

IGF-I is produced by R2C cells and induces aromatase expression through phosphatidylinositol 3-kinase– and protein kinase C–mediated activation of SF-1. Starting from previous findings showing the ability of IGF-I to activate SF-1 and CREB, which leads to an increase in StAR transcription and then

steroidogenesis (18), we investigated the role of this factor in regulating aromatase. Determination of IGF-I content in TM3 and R2C culture medium by RIA revealed a significant difference in growth factor production, with R2C cells producing ~4-fold higher IGF-I amounts (Fig. 3*A*). Moreover, we measured IGF-I content in testicular tissues, revealing a significant difference between FRTT and FRNT (Fig. 3*B*). IGF-I exerts its actions by binding to specific receptors (IGF-IR); however, we did not reveal differences in IGF-IR expression between TM3 and R2C cells (Fig. 3*C*).

On binding to IGF-IR, IGF-I activates three major transductional pathways: Ras/Raf/mitogen-activated protein kinase (MAPK), phosphatidylinositol 3-kinase (PI3K)/AKT, and phospholipase C (PLC)/protein kinase C (PKC). To show the involvement of IGF-I transductional pathways in modulating aromatase expression in Leydig cell tumors, we used specific inhibitors of IGF-IR (AG1024), extracellular signal–regulated kinase (ERK)-1/2 (PD98059), PI3K (LY294002), and PKC (GF109203X). The IGF-IR inhibitor was able to inhibit aromatase activity by 85%; LY294002 determined 65% inhibition; PD98059, 35%; and GF109203X, 61% (Fig. 3*D*). A similar inhibitory pattern, except for PD98059, was observed also on aromatase mRNA (Supplementary Fig. S2*A*) and protein content (Fig. 4*A*–*D*). All of the different inhibitors, excluding PD98059, were able to reduce SF-1 mRNA (Supplementary Fig. S2*B*), whereas CREB remained unchanged (Supplementary Fig. S2*C*). Analysis of protein levels by Western blot confirmed the data from mRNA (Fig. 4*A*–*D*). Treatments with increasing doses of AG1024, LY294002, and GF109203X, but not PD98059, were able to induce a dose-dependent inhibition of total and phosphorylated levels of SF-1 without affecting CREB (Fig. 4*A*–*D*).

Addition of exogenous amounts of IGF-I was able to induce a significant increase of 2- and 3.8-fold in aromatase mRNA at 12 and 24 h, respectively (Fig. 5*A*). Aromatase protein levels under the same treatments reflected the mRNA data (Fig. 5*B*). Analysis of expression levels of total and phosphorylated forms of transcription factors SF-1 and CREB showed an increase in SF-1 and pSF-1 in the presence of IGF-I starting at 4 h, whereas no differences were observed for CREB at any of the investigated times (Fig. 5*B*). AG1024, LY294002, and GF109203X were able to inhibit IGF-I effects on CYP19 mRNA and protein levels (Fig. 5*C* and *D*) as a consequence of a decreased SF-1 expression (Fig. 5*D*).

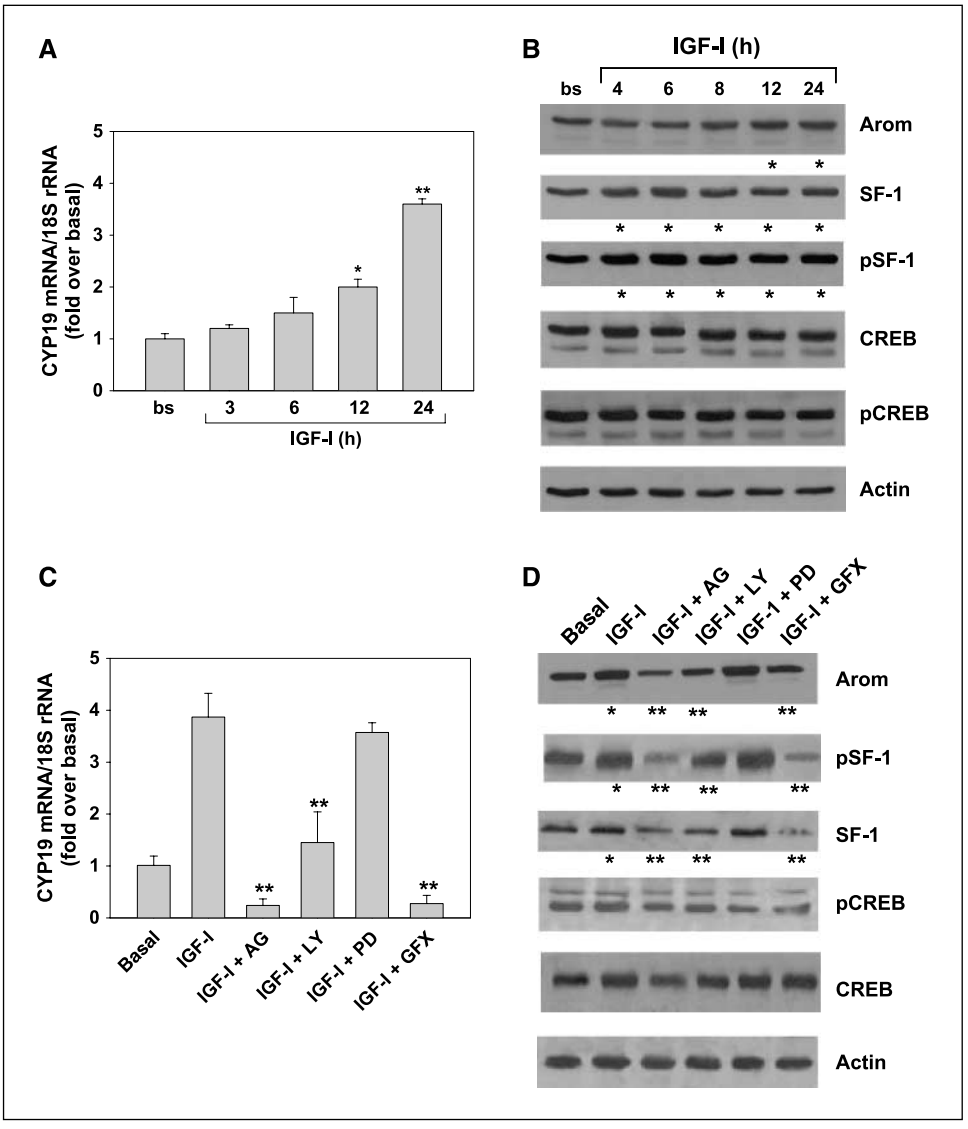

Figure 5. Effects of IGF-I on aromatase, SF-1, and CREB expression in R2C cells. Cells were treated in serum-free medium for the indicated times with IGF-I (100 ng/mL) or for 24 h with AG1024 (20 μmol/L), LY294002 (10 μmol/L), PD98059 (20 μmol/L), and GF109203X (20 μmol/L), alone or in combination with IGF-I (100 ng/mL). *A* and *C,* total RNA was extracted from R2C cells untreated or treated as indicated. Real-time reverse transcription-PCR was used to analyze CYP19 mRNA levels. *Columns,* mean of values from three separate RNA samples; *bars,* SE. Each sample was normalized to its 18S rRNA content. *, $P < 0.01$; **, $P < 0.001$, compared with basal. *B* and *D,* Western blot analyses were done on 50 μg of total proteins extracted from R2C cells untreated (basal) or treated as indicated. Representative of three independent experiments with similar results. β-Actin was used as a loading control. Normalized absorbances were subjected to statistical analysis; statistically significant differences are indicated (*, $P < 0.01$, compared with basal; **, $P < 0.01$, compared with IGF-I).

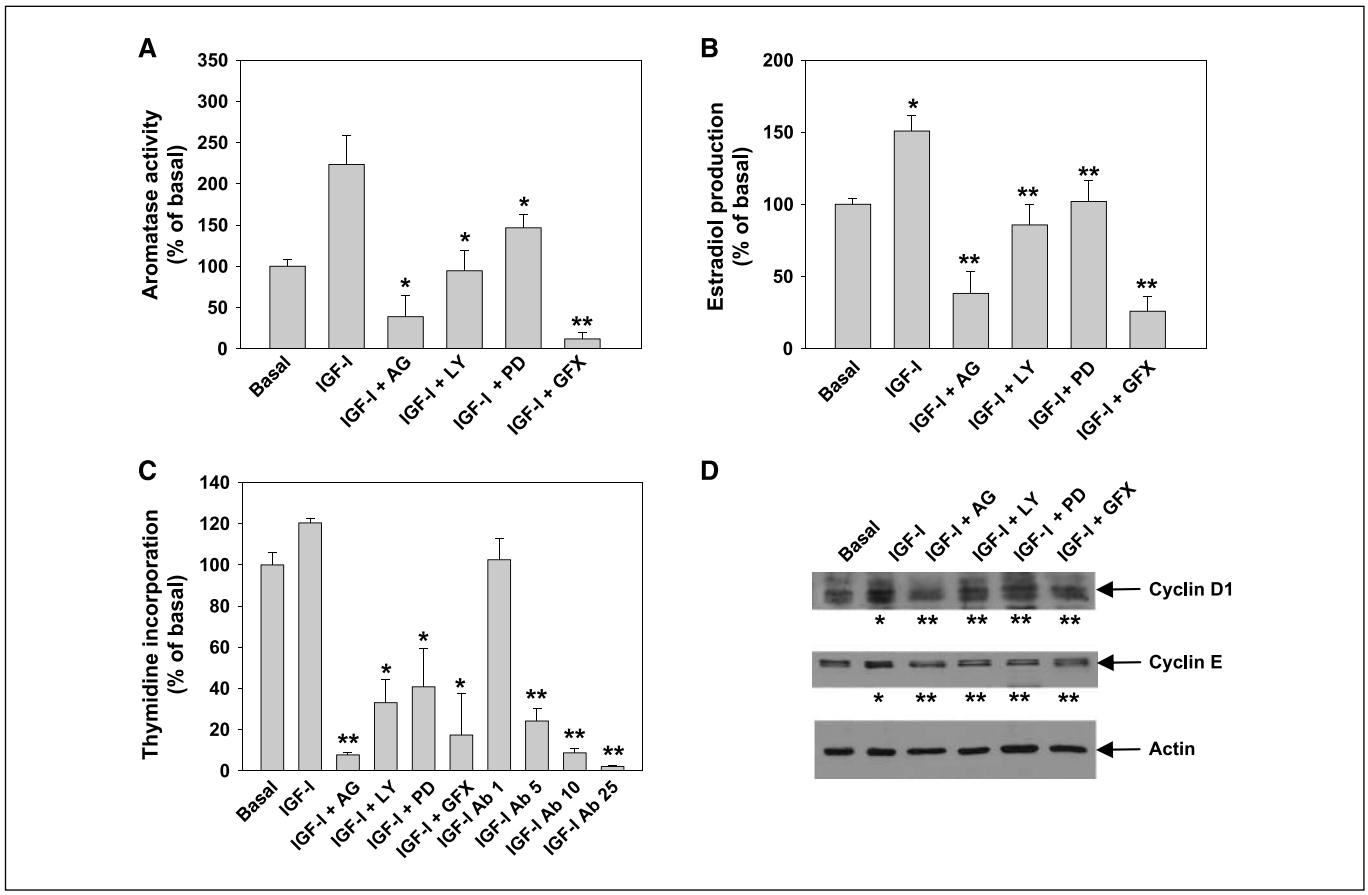

Figure 6. Effects of IGF-I and IGF-I pathway inhibitors on estradiol production and R2C cell proliferation. Cells were treated in serum-free medium for 24 h with IGF-I (100 ng/mL) alone or in combination with AG1024 (20 μmol/L), LY294002 (10 μmol/L), PD98059 (20 μmol/L), and GF109203X (20 μmol/L). *A,* aromatase activity is expressed as percent of basal. *Columns,* mean of three independent experiments each done in triplicate; *bars,* SE. *, $P < 0.01$; **, $P < 0.001$, compared with IGF-I. *B,* R2C cells were maintained for 48 h in serum-free medium, before being treated for 24 h. E_2 content in R2C culture medium was determined by RIA and normalized to the cell culture well protein content. *Columns,* mean percent of basal; *bars,* SE. *, $P < 0.05$, compared with basal; **, $P < 0.01$, compared with IGF-I. *C,* R2C cell proliferation was evaluated by [^{3}H]thymidine incorporation analysis. Cells were maintained for 24 h in serum-free medium and treated for 24 h as indicated. IGF-I antibody (*IGF-I Ab*) was added to the medium at 1, 5, 10, and 25 μg/mL. *Columns,* mean percent of untreated (basal) cells (100%) from three independent experiments each done in triplicate; *bars,* SE. *, $P < 0.01$; **, $P < 0.001$, compared with IGF-I. *D,* Western blot analyses were done on 50 μg of total proteins extracted from R2C cells treated as indicated. Representative of three independent experiments with similar results. β-Actin was used as a loading control. Normalized absorbances were subjected to statistical analysis; statistically significant differences are indicated (*, $P < 0.01$, compared with basal; **, $P < 0.01$, compared with IGF-I).

We also carried out chromatin immunoprecipitation assays to investigate how IGF-I influences binding of transcription factors to the aromatase PII promoter. The increase in SF-1 protein content that was seen under IGF-I treatment reflected an increase in SF-1 binding to the PII promoter (Supplementary Fig. S3*A*). Moreover, we evidenced how in basal conditions (Supplementary Fig. S3*B*), as well as after IGF-I treatment (Supplementary Fig. S3*C*), all the different inhibitors, but not PD98059, reduced SF-1 binding.

IGF-I–induced estradiol production modulates R2C cell proliferation. Treatment with IGF-I induces aromatase activity and estradiol production, which are decreased by AG1024, LY294002, and GF109203X, as well as by PD98059 (Fig. 6*A* and *B*). The observed changes in estradiol production modified R2C cell proliferative behavior (Fig. 6*C*). In addition, the use of an anti–IGF-I antibody in immunoneutralization experiments caused a dose-dependent inhibition in tritiated thymidine incorporation (Fig. 6*C*). The ability of IGF-I to stimulate, and that of the inhibitors to block, cell proliferation was linked to an alteration in cyclin D1 and cyclin E expression (Fig. 6*D*).

Discussion

The current study aimed to explain the molecular mechanism responsible for aromatase overexpression in tumor Leydig cells leading to a consequent excess of *in situ* estradiol production that sustains tumor cell growth and proliferation.

The mammalian testis is capable of estrogen synthesis, which is regulated by different factors at different ages. In mature animals, aromatization of testosterone to estradiol is enhanced by luteinizing hormone (LH)/chorionic gonadotropin (CG) and not by follicle-stimulating hormone. The site of this synthesis seems to be age dependent, at least in some species such as the rat (30). Leydig cells are an elective target site of LH/CG that controls testosterone biosynthesis as well as its conversion to estradiol through aromatase activity. Alterations in local estrogen synthesis may have significant consequences in malignancy of these cells. In the present study, we observed that R2C cells release a conspicuous amount of E_2 from cellular storage in a time-dependent manner. In this condition, E_2 production (1,300 ± 230 pg/10^6 cells/24 h) is significantly higher compared with E_2 levels produced by TM3 cells and by primary rat Leydig cell cultures (246 pg/10^6

3β-hydroxysteroid dehydrogenase–positive cells/24 h; ref. 31). E_2 synthesis by R2C cells was abrogated by treatment with letrozole, addressing how steroid production is dependent on high constitutive aromatase activity. A strong increase in aromatase expression was observed in R2C cells compared with the normal cell line TM3 control, as well as in FRTT compared with FRNT. These findings agree with a previous study on human tissues showing that the increase in estrogen synthesis, as a consequence of a more intense aromatase activity, is higher in the Leydig cell tumor fraction than in normal tissues surrounding the tumor of the same patient (32).

Mediators of the physiologic effects of estrogens are ERα and ERβ. An enhanced expression of ERα, resulting in an increased ERα/ERβ ratio, was observed in R2C compared with TM3 cell line, as well as in FRTT compared with FRNT. This is in agreement with previous reports showing that transgenic mice overexpressing aromatase have an enhanced occurrence of breast and Leydig cell tumors together with an enhanced expression of ERα in the tumor tissue (6). The latter findings reasonably address how a short estrogen autocrine loop may be involved in breast and testicular tumorigenesis in the presence of an excess of locally produced estradiol. Indeed, an arrest of cell growth was observed following abrogation of local E_2 production with letrozole or after addition of ERα inhibitors ICI 182780 or 4-hydroxytamoxifen. Besides, only after changing the medium everyday along with prolonged R2C starvation, abolishing local steroid production, did we observe how exogenous E_2 was able to display proliferative effects.

One mechanism through which estrogens induce cell proliferation is by increasing protein levels of G_1 regulatory cyclins A, B1, D1, D3, and E in target cells (33). In our study, we showed that the expression of two of the most important regulators of Leydig cell cycle, cyclin D1 and cyclin E, can be increased by E_2 and down-regulated by treatment with antiestrogens. These data further confirm that aromatase overexpression and the consequent E_2 production may be the cause of altered cell cycle regulation of Leydig tumor cells.

In an attempt to explain the molecular mechanism determining aromatase overexpression in our tumor cell line, we focused our attention on the expression levels of transcription factors identified as crucial regulators of aromatase gene expression, CREB and SF-1. In the adult testis, SF-1 is predominantly expressed in Leydig cells (34). The increase of total and/or phosphorylated protein can potentiate SF-1 transcriptional activity (35). In R2C cells and in FRTT, compared with the normal controls, we found higher phosphorylated SF-1 protein levels as a consequence of elevated protein content. Total CREB levels were similar in all samples but highly phosphorylated in tumor samples. Starting from these observations, we investigated which pathways might be involved in the activation of these transcription factors.

The most important signal regulating Leydig cell function is the binding of LH to the LH receptor (LHR; ref. 36). Several observations indicate that constitutively active mutants of LHRs could be involved in Leydig cell transformation (37). It has been shown that the LH/LHR signaling pathway is constitutively active in the R2C tumor Leydig cell line and makes the phenotype of these cells constitutively steroidogenic (38). For instance, in the presence of a specific protein kinase A (PKA) inhibitor, constitutive syntheses of *Star* mRNA and steroids were significantly inhibited (39). These observations fit well with our findings indicating how the presence of PKA inhibitor determined a strong decrease in aromatase activity, together with a drop in CREB phosphorylation (data not shown). Here, we show that the presence of a specific PKC inhibitor had no effects on CREB phosphorylation while SF-1 dropped dramatically.

It has been shown that CREB in mouse Leydig cells can be phosphorylated also through the PKC pathway activated by IGF-I (38). In this work, we have revealed that R2C tumor Leydig cells release higher levels of IGF-I in the culture medium with respect to TM3 cells, and the concentration of IGF-I in FRTT is increased with respect to FRNT. However, the exposure to IGF-I as well as to the treatment with inhibitors of IGF-I signaling did not affect the CREB phosphorylative status but decreased SF-1 phosphorylation, postulating separate mechanisms that control CREB and SF-1 activation in modulating aromatase activity.

It has been suggested that IGF-I can influence Leydig cell survival and proliferation (40, 41). Moreover, it has been shown that IGF-I up-regulates aromatase expression in primary cultures of rat Leydig cells through a cAMP-independent mechanism (42). Our findings led us to suppose that the elevated IGF-I levels derived from tumor Leydig cells *in vivo* and *in vitro* contribute to enhance aromatase expression through an autocrine mechanism activating SF-1. The important role played by IGF-I in Leydig cell tumorigenesis is further supported by the substantially unchanged IGF-IR expression level between TM3 and R2C cells. Binding of IGF-I to its receptor causes receptor autophosphorylation and the activation of an intrinsic tyrosine kinase that acts on various substrates, leading to activation of multiple signaling pathways including the PI3K/AKT and MAPK cascades. In addition, it has been shown that IGF-I can activate the PLC/PKC pathway (18). We treated R2C cells with specific inhibitors of IGF-I signaling (AG1024), ERK1/2 (PD98059), PI3K (LY294002), and PKC (GF109203X) in the presence or absence of IGF-I and revealed that addition of IGF-I itself was able to increase aromatase expression, activity, and estradiol production, whereas all the inhibitors determined a reduction of enzyme activity and estradiol release.

For instance, the inhibition of IGF-I signaling through inhibition of either the PI3K/AKT or PLC/PKC pathway was able to block SF-1 expression and protein phosphorylation. In particular, treatment with AG1024 blocked SF-1 phosphorylation more efficiently than the separate treatment with PI3K or PKC alone, addressing how both pathways may synergize in up-regulating SF-1 activity. In the presence of PD98059, SF-1 expression remained unchanged as did aromatase mRNA and protein levels. Importantly, aromatase activity and estradiol production seemed to be decreased in the presence of PD98059, suggesting a potential stimulatory role of ERK1/2 on the enzyme at a posttranscriptional level. Furthermore, we observed that SF-1 binding to the aromatase promoter II is enhanced by IGF-I and reduced by AG1024, LY294002, and GF109203X, but not by PD98059, indicating the central role of this transcription factor in regulating aromatase gene transcription in tumor Leydig cells. This is the first report of a direct link between SF-1 transcription and the IGF-I signaling pathway in regulating aromatase expression.

The observed changes in estradiol production due to IGF-I determined an effect on R2C cell proliferative behavior. In fact, inhibitors of IGF-I signaling or the use of an anti–IGF-I antibody in immunoneutralization experiments blocked thymidine incorporation. Moreover, IGF-I up-regulates cyclins D1 and E whereas IGF-I signaling inhibitors decrease the same factors, analogously to the antiestrogen ICI 182780.

From our findings emerges a double mechanism inducing enhanced expression of aromatase: (*a*) constitutive activation of the LH/cAMP/PKA pathway, which determines CREB activation; (*b*) enhanced IGF-I signaling potentiating SF-1 action. The enhanced activity of SF-1 in inducing aromatase expression may be maintained by the lack of DAX-1 (dosage-sensitive sex reversal, adrenal hypoplasia congenita, critical region on the X chromosome, gene 1) expression in R2C cells (29). DAX-1 is a specific corepressor of SF-1 (43, 44) and inhibits StAR expression and steroidogenesis by 40% to 60% when overexpressed in R2C cells (29). The lack of DAX-1 expression in R2C cells may be due to constitutively active PKA signaling because in a mouse Leydig cell line, a marked decrease of DAX-1 mRNA occurred within 3 h after addition of LH and forskolin (45). Then, the activation of LH/LHR/PKA pathway at the same time decreases DAX-1 expression and promotes SF-1 activity. A further demonstration of the role of DAX-1 in regulating *P*450 aromatase expression comes from the observations that in TM3 cells, IGF-I induces SF-1 expression but is unable to induce aromatase expression because DAX-1 is highly expressed (data not shown). Finally, the finding that in DAX-1 knockout mice aromatase is overexpressed selectively in Leydig cells (46) underscores the importance of this type of transcription factor in local testicular estrogen production *in vivo*.

It remains to be explained which molecular mechanism(s) is responsible for the elevated IGF-I production in Leydig tumor cells. *In vivo*, the administration of human CG increases IGF-I mRNA levels in rat Leydig cells (47). LH deprival determines a decrease in bromodeoxyuridine incorporation as well as a decrease in IGF-I and IGF-IR mRNA levels (48). These observations suggest the possibility that LH can mediate its proliferative effects also by regulating IGF-I and its receptor in Leydig cells and that the altered LH/LHR–activated pathway in R2C cells could be the cause of IGF-I overproduction. Moreover, the observation that in murine Leydig cells IGF-I is able to increase LHR mRNA stability (49), together with data showing that the presence of an anti–IGF-I antibody reduces the steroidogenic responsiveness to LH/human CG (50), also suggests the possibility of IGF-I action in sustaining LH/LHR signaling. Aromatase overexpression seems to be induced by the combined enhancement of LH/LHR and IGF-I signaling. Particularly, LH/LHR signaling determines a constitutive active CREB phosphorylation on aromatase gene promoter whereas IGF-I overproduction stimulates SF-1 binding on the same promoter through an autocrine mechanism. In other words, from this study, it emerges that the reproducibility of data between our *in vivo* and *in vitro* models is linked to an enhanced PKA activity, together with increased E_2/ERα and IGF-I signaling.

In conclusion, in this study we showed that in Leydig tumor cells, aromatase overexpression determines an excessive local estradiol production that is able to stimulate the expression of genes involved in cell cycle regulation sustaining cell proliferation. Aromatase overexpression seems to be concomitant with an enhanced IGF-I signaling in R2C cells as well as in our *in vivo* model, supporting the hypothesis of a cooperation between estrogen and IGF-I in Leydig cell tumorigenesis, which is also observed in other tumor tissues. The observation that antiestrogens and aromatase inhibitors as well as IGF-I signaling blockers are able to reduce R2C proliferation is indicative of possible applications of these drugs as new adjuvant therapeutic tools for the treatment of testicular cancer.

Acknowledgments

Received 11/2/2006; revised 5/9/2007; accepted 6/20/2007.

Grant support: PRIN-MIUR grant no. 2004067227 and Associazione Italiana per la Ricerca sul Cancro (AIRC).

The costs of publication of this article were defrayed in part by the payment of page charges. This article must therefore be hereby marked *advertisement* in accordance with 18 U.S.C. Section 1734 solely to indicate this fact.

We thank Dr. V. Cunsulo (Biogemina Italia S.R.L., Catania-Italy) for generously providing us with the RIA kits, Dr. Ken-ichirou Morohashi and Dr. Holly A. Ingraham for providing us respectively with anti–SF-1 and anti–pSF-1 antibodies, and Dr. Soluzzo Cavalcanti for his technical and scientific contribution.

References

1. Carroll PR, Whitmore WF, Jr., Herr HW, et al. Endocrine and exocrine profiles of men with testicular tumors before orchiectomy. J Urol 1987;137:420–3.
2. Hawkins C, Miaskowski C. Testicular cancer: a review. Oncol Nurs Forum 1996;23:1203–11.
3. Mostofi FK, Sesterhenn IA, Bresler VM. Pathology of tumours in laboratory animals. Tumours of the rat. Tumours of the testis. IARC Sci Publ 1990;99:399–419.
4. Horn HA, Stewart HL. A review of some spontaneous tumors in noninbred mice. J Natl Cancer Inst 1952;13: 591–603.
5. Bosland MC. Hormonal factors in carcinogenesis of the prostate and testis in humans and in animal models. Prog Clin Biol Res 1996;394:309–52.
6. Fowler KA, Gill K, Kirma N, Dillehay DL, Tekmal RR. Overexpression of aromatase leads to development of testicular Leydig cell tumors: an *in vivo* model for hormone-mediated testicular cancer. Am J Pathol 2000; 156:347–53.
7. Kirma N, Gill K, Mandava U, Tekmal RR. Overexpression of aromatase leads to hyperplasia and changes in the expression of genes involved in apoptosis, cell cycle, growth, and tumor suppressor functions in the mammary glands of transgenic mice. Cancer Res 2001;61:1910–8.
8. Coleman GL, Barthold W, Osbaldiston GW, Foster SJ, Jonas AM. Pathological changes during aging in barrier-reared Fischer 344 male rats. J Gerontol 1977;32:258–78.
9. Aquila S, Sisci D, Gentile M, et al. Towards a physiological role for cytochrome *P*450 aromatase in ejaculated human sperm. Hum Reprod 2003;18:1650–9.
10. Inkster S, Yue W, Brodie A. Human testicular aromatase: immunocytochemical and biochemical studies. J Clin Endocrinol Metab 1995;80:1941–7.
11. Simpson ER, Mahendroo MS, Means GD, et al. Aromatase cytochrome *P*450, the enzyme responsible for estrogen biosynthesis. Endocr Rev 1994;15:342–55.
12. Young M, Lephart ED, McPhaul MJ. Expression of aromatase cytochrome *P*450 in rat H540 Leydig tumor cells. J Steroid Biochem Mol Biol 1997;63:37–44.
13. Lanzino M, Catalano S, Genissel C, et al. Aromatase messenger RNA is derived from the proximal promoter of the aromatase gene in Leydig, Sertoli, and germ cells of the rat testis. Biol Reprod 2001;64:1439–43.
14. Young M, McPhaul MJ. A Steroidogenic actor-1-binding site and cyclic adenosine 3′,5′-monophosphate response element-like elements are required for the activity of the rat aromatase promoter in rat Leydig tumor cell lines. Endocrinology 1998;139:5082–93.
15. Fitzpatrick SL, Richards JS. Identification of a cyclic adenosine 3′,5′-monophosphate-response element in the rat aromatase promoter that is required for transcriptional activation in rat granulosa cells and R2C Leydig cells. Mol Endocrinol 1994;8:1309–19.
16. Carlone DL, Richards JS. Functional interactions, phosphorylation, and levels of 3′,5′-cyclic adenosine monophosphate-regulatory element binding protein and Steroidogenic Factor-1 mediate hormone-regulated and constitutive expression of aromatase in gonadal cells. Mol Endocrinol 1997;11:292–304.
17. Fitzpatrick SL, Richards JS. *cis*-acting elements of the rat aromatase promoter required for cyclic adenosine 3′,5′-monophosphate induction in ovarian granulosa cells and constitutive expression in R2C Leydig cells. Mol Endocrinol 1993;7:341–54.
18. Manna PR, Chandrala SP, King SR, et al. Molecular mechanisms of insulin-like growth factor-I mediated regulation of the steroidogenic acute regulatory protein in mouse Leydig cells. Mol Endocrinol 2006;20:362–78.
19. Saez JM. Leydig cells: endocrine, paracrine, and autocrine regulation. Endocr Rev 1994;15:574–626.
20. Casella SJ, Smith EP, van Wyk JJ, et al. Isolation of rat testis cDNAs encoding an insulin-like growth factor I precursor. DNA 1987;6:325–30.
21. Zhou J, Bondy C. Anatomy of the insulin-like growth factor system in the human testis. Fertil Steril 1993;60: 897–904.
22. Baker J, Hardy MP, Zhou J, et al. Effects of an Igf1 gene null mutation on mouse reproduction. Mol Endocrinol 1996;10:903–18.
23. Liu JP, Baker J, Perkins AS, Robertson EJ, Efstratiadis A. Mice carrying null mutations of the genes encoding insulin-like growth factor I (Igf-1) and type 1 IGF receptor (Igf1r). Cell 1993;75:59–72.
24. Wang GM, O'Shaughnessy PJ, Chubb C, Robaire B, Hardy MP. Effects of insulin-like growth factor i on steroidogenic enzyme expression levels in mouse Leydig cells. Endocrinology 2003;144:5058–64.

25. Lephart ED, Simpson ER. Assay of aromatase activity. Methods Enzymol 1991;206:477–83.

26. Wolanska M, Bankowski E. An accumulation of insulin-like growth factor I (IGF-I) in human myometrium and uterine leiomyomas in various stages of tumour growth. Eur Cytokine Netw 2004;15:359–63.

27. Pezzi V, Sirianni R, Chimento A, et al. Differential expression of steroidogenic factor-1/adrenal 4 binding protein and liver receptor homolog-1 (LRH-1)/fetoprotein transcription factor in the rat testis: LRH-1 as a potential regulator of testicular aromatase expression. Endocrinology 2004;145:2186–96.

28. Jacobs BB, Huseby RA. Neoplasms occurring in aged Fischer rats, with special reference to testicular, uterine and thyroid tumors. J Natl Cancer Inst 1967;39:303–9.

29. Jo Y, Stocco DM. Regulation of steroidogenesis and steroidogenic acute regulatory protein in R2C cells by DAX-1 (dosage-sensitive sex reversal, adrenal hypoplasia congenita, critical region on the X chromosome, gene-1). Endocrinology 2004;145:5629–37.

30. Pomerantz D. Developmental changes in the ability of follicle stimulating hormone to stimulate estrogen synthesis *in vivo* by the testis of the rat. Biol Reprod 1980;23:948–54.

31. Genissel C, Carreau S. Regulation of the aromatase gene expression in mature rat Leydig cells. Mol Cell Endocrinol 2001;178:141–6.

32. Valensi P, Coussieu C, Pauwles A, et al. Feminizing Leydig cell tumor: endocrine and incubation studies. J Endocrinol Invest 1987;10:187–93.

33. Prall OWJ, Sarcevic B, Musgrove EA, Watts CKW, Sutherland RL. Estrogen-induced activation of Cdk4 and Cdk2 during G_1-S phase progression is accompanied by increased cyclin D1 expression and decreased cyclin-dependent kinase inhibitor association with cyclin E-Cdk2. J Biol Chem 1997;272:10882–94.

34. Hatano O, Takayama K, Imai T, et al. Sex-dependent expression of a transcription factor, Ad4BP, regulating steroidogenic P-450 genes in the gonads during prenatal and postnatal rat development. Development 1994;120:2787–97.

35. Desclozeaux M, Krylova IN, Horn F, Fletterick RJ, Ingraham HA. Phosphorylation and intramolecular stabilization of the ligand binding domain in the nuclear receptor steroidogenic factor 1. Mol Cell Biol 2002;22:7193–203.

36. Dufau ML, Winters CA, Hattori M, et al. Hormonal regulation of androgen production by the Leydig cell. J Steroid Biochem 1984;20:161–73.

37. Ascoli M. Potential Leydig cell mitogenic signals generated by the wild-type and constitutively active mutants of the lutropin/choriogonadotropin receptor (LHR). Mol Cell Endocrinol 2007;260–262:244–8.

38. Jo Y, King SR, Khan SA, Stocco DM. Involvement of protein kinase C and cyclic adenosine 3′,5′-monophosphate-dependent kinase in steroidogenic acute regulatory protein expression and steroid biosynthesis in Leydig cells. Biol Reprod 2005;73:244–55.

39. Rao RM, Jo Y, Leers-Sucheta S, et al. Differential regulation of steroid hormone biosynthesis in R2C and MA-10 Leydig tumor cells: role of SR-B1-mediated selective cholesteryl ester transport. Biol Reprod 2003;68:114–21.

40. Colon E, Zaman F, Axelson M, et al. Insulin-like growth factor-I is an important antiapoptotic factor for rat Leydig cells during postnatal development. Endocrinology 2007;148:128–39.

41. Wang G, Hardy MP. Development of Leydig cells in the insulin-like growth factor-I (IGF-I) knockout mouse: effects of IGF-I replacement and gonadotropic stimulation. Biol Reprod 2004;70:632–9.

42. Rigaudiere N, Grizard G, Boucher D. Aromatase activity in purified Leydig cells from adult rat. Comparative effects of insulin, IGF-I, and hCG. Acta Endocrinol Copenh 1989;121:677–85.

43. Bae DS, Schaefer ML, Partan BW, Muglia L. Characterization of the mouse DAX-1 gene reveals evolutionary conservation of a unique amino-terminal motif and widespread expression in mouse tissue. Endocrinology 1996;137:3921–7.

44. Osman H, Murigande C, Nadakal A, Capponi AM. Repression of DAX-1 and induction of SF-1 expression. Two mechanisms contributing to the activation of aldosterone biosynthesis in adrenal glomerulosa cells. J Biol Chem 2002;277:41259–67.

45. Song KH, Park YY, Park KC, et al. The atypical orphan nuclear receptor DAX-1 interacts with orphan nuclear receptor Nur77 and represses its transactivation. Mol Endocrinol 2004;18:1929–40.

46. Wang ZJ, Jeffs B, Ito M, et al. Aromatase (Cyp19) expression is up-regulated by targeted disruption of Dax1. Proc Natl Acad Sci U S A 2001;98:7988–93.

47. Moore A, Chen CL, Davis JR, Morris ID. Insulin-like growth factor-I mRNA expression in the interstitial cells of the rat testis. J Mol Endocrinol 1993;11:319–24.

48. Sriraman V, Rao VS, Sairam MR, Rao AJ. Effect of deprival of LH on Leydig cell proliferation: involvement of PCNA, cyclin D3 and IGF-1. Mol Cell Endocrinol 2000;162:113–20.

49. Zhang FP, El-Hafnawy T, Huhtaniemi I. Regulation of luteinizing hormone receptor gene expression by insulin-like growth factor-I in an immortalized murine Leydig tumor cell line (BLT-1). Biol Reprod 1998;59:1116–23.

50. Le Roy C, Lejeune H, Chuzel F, Saez JM, Langlois D. Autocrine regulation of Leydig cell differentiated functions by insulin-like growth factor I and transforming growth factor β. J Steroid Biochem Mol Biol 1999;69:379–84.